

MODIFICATION OF FUSED FILAMENT FABRICATION PRINTER TO PRINT
HIGH TEMPERATURE THERMOPLASTICS TO IMPROVE Z-STRENGTH

by

Robert Philip Brushaber, B.S.

A thesis proposal submitted to the Graduate Council of
Texas State University in partial fulfillment
of the requirements for the degree of
Master of Science
with a Major in Engineering
August 2020

Committee Members:

Jitendra S. Tate, Chair

Namwon Kim, Co-Chair

Michael L. Dingus

COPYRIGHT

by

Robert Philip Brushaber

2020

FAIR USE AND AUTHOR'S PERMISSION STATEMENT

Fair Use

This work is protected by the Copyright Laws of the United States (Public Law 94-553, section 107). Consistent with fair use as defined in the Copyright Laws, brief quotations from this material are allowed with proper acknowledgement. Use of this material for financial gain without the author's express written permission is not allowed.

Duplication Permission

As the copyright holder of this work I, Robert Philip Brushaber, authorize duplication of this work, in whole or in part, for educational or scholarly purposes only.

ACKNOWLEDGEMENTS

I would like to thank Texas Research Institute Austin, Inc. for providing me with the funding and flexible work schedule to pursue my Masters Degree in Mechanical and Manufacturing Engineering at Texas State University.

I would also like to thank Dr. Jitendra Tate for providing wisdom and inspiration. I think of Dr. Tate not only as a teacher but a great colleague and friend.

Last but not least I would like to thank my family and wonderful wife, Jennifer Brushaber for their faith in my perseverance. I couldn't have taken this journey without your support and love.

TABLE OF CONTENTS

	Page
ACKNOWLEDGEMENTS.....	iv
LIST OF TABLES.....	viii
LIST OF FIGURES.....	xiii
LIST OF ABBREVIATIONS.....	xxiv
ABSTRACT.....	xxvii
CHAPTER	
I. INTRODUCTION.....	1
II. BACKGROUND.....	4
Z Strength Problem.....	8
Non-Isothermal Process.....	10
FFF Relationship to Thermoplastic Welding.....	13
Non-Traditional Methods for Improving Strength.....	17
Fused Filament Fabrication (FFF) Additive Manufacturing (AM).....	22
III. PRESENTATION OF WORK.....	25
FFF Printer Modifications.....	25
Printing with Omega Infrared Heat Lamp.....	49
IV. RESULTS.....	73
PLA Testing.....	78
PLA Flat (XY) Tensile Specimens at Room Temperature (22°C).....	79
PLA Flat (XY) Tensile Specimens with 60°C Heat Lamp.....	81
PLA Flat (XY± 45° Infill) Tensile Specimens at Room Temperature (22°C).....	83
PLA 60°C Tensile Flat (XZ) ±45° Infill Specimen with Heat Lamp at 60°C.....	85

PLA on Edge (XZ) Tensile Specimens at Room Temperature (22°C).....	87
PLA on Edge (XZ) Tensile Specimens with Heat Lamp at 60°C	90
PLA Upright (ZX) Tensile Properties at Room Temperature (22°C) ...	92
PLA Upright (ZX) Tensile Specimens Printed with Heat Lamp at 60°C	95
PLA Tensile Properties Summary with and without Heat Lamp	98
PLA Flexural Flat (XY) Specimen at Room Temperature (22°C)	101
PLA Flexural Flat (XY) Specimen Printed with Heat Lamp at 60°C ...	103
PLA Flexural on Edge (XZ) Specimen at Room Temperature (22°C)..	105
PLA Flexural on Edge (XZ) Specimen with Heat Lamp at 60°C	107
PLA Flexural Upright (ZX) Specimen at Room Temperature (22°C) ..	109
PLA Flexural Upright (ZX) Specimen with Heat Lamp at 60°C	111
PLA Flexural Summary	114
PLA Properties with the Heat Lamp at 60°C compared to Injection Molded PLA.....	116
PEKK Testing.....	118
PEKK Flat (XY) Tensile Specimens	120
PEKK Flat (XY) ±45° Infill Tensile Specimens.....	123
PEKK on Edge (XZ) Tensile Specimens.....	126
PEKK Upright (ZX) Tensile Specimens.....	129
PEKK Tensile Testing Summary.....	132
PEKK Flat (XY) Flexural Specimens.....	135
PEKK Flexural on Edge (XZ) Specimen.....	138
PEKK Upright (ZX) Flexural Specimens	141
PEKK Flexural Testing Summary	144
FFF PEKK with the Heat Lamp at 120°C compared to Injection Molded PEKK.....	147
PEI Ultem 1010 Testing.....	149
PEI Ultem 1010 Flat (XY) Tensile Specimens.....	151
PEI Ultem 1010 on Edge (XZ) Tensile Specimens	154
PEI Ultem 1010 Upright (ZX) Tensile Specimens	157
PEI Ultem 1010 Tensile Testing Summary	160
PEI Ultem 1010 Flat (XY) Flexural Specimens	163
PEI Ultem 1010 on Edge (XZ) Flexural Specimens.....	166
PEI Ultem 1010 Upright (ZX) Flexural Specimens	168
PEI Ultem 1010 Flexural Summary.....	171
FFF PEI with the Heat Lamp at 120°C compared to Injection Molded PEI	174
PEEK Testing.....	176
PEEK Flat (XY) Tensile Specimens.....	177

PEEK on Edge (XZ) Tensile Specimens	181
PEEK Tensile Testing Summary	184
PEEK Flat (XY) Flexural Test Specimens	187
PEEK on Edge (XZ) Flexural Specimens.....	190
PEEK Flexural Testing Summary.....	192
FFF PEEK with the Heat Lamp at 120°C compared to Injection	
Molded PEEK	194
Density and Porosity	196
Material Property Comparison.....	198
V. CONCLUSIONS.....	201
LITERATURE CITED	207

LIST OF TABLES

Table	Page
1. Proper 3D Printing Requires Optimization of a Number of Parameters to Fully Utilize the Capabilities of both the Process and the Material	7
2. Material Printing Parameters.	50
3. Injection Molding Material Properties	74
4. PLA 22°C Tensile Flat (XY) Specimen Dimensions.	80
5. PLA Flat (XY) Tensile Properties at Room Temperature (22°C).	80
6. PLA 60°C Tensile Flat (XY) Specimen Dimensions.	82
7. PLA Flat (XY) Tensile Properties with Heat Lamp at 60°C	82
8. PLA 22°C Tensile Flat (XZ) ±45° Infill Specimen Dimensions	84
9. PLA Flat (XY ± 45° Infill) Tensile Properties at Room Temperature 22°C.....	84
10. PLA 60°C Tensile Flat (XZ) ±45° Infill Specimen Dimensions	85
11. PLA Flat (XY ± 45° Infill) Tensile Properties with Heat Lamp at 60°C	85
12. PLA 22°C Tensile on Edge (XZ) Specimen Dimensions	88
13. PLA on Edge (XZ) Tensile Properties at Room Temperature (22°C).....	89
14. PLA 60°C Tensile on Edge (XZ) Specimen Dimensions	91
15. PLA on Edge (XZ) Tensile Properties with Heat Lamp at 60°C.....	91
16. PLA 22°C Tensile Upright (ZX) Specimen Dimensions.....	94
17. PLA Upright (ZX) Tensile Properties at Room Temperature (22°C)	94
18. PLA 60°C Tensile Upright (ZX) Specimen Dimensions.....	97

19.	PLA Upright (ZX) Tensile Properties with Heat Lamp at 60°C	97
20.	Summary of PLA Tensile Properties with and without the Heat Lamp	98
21.	PLA 22°C Flexural Flat (XY) Specimen Dimensions.....	101
22.	PLA Flat (XY) Flexural Properties at Room Temperature (22°C).....	102
23.	PLA 60°C Flexural Flat (XY) Specimen Dimensions.....	103
24.	PLA Flat (XY) Flexural Properties with Heat Lamp at 60°C.....	103
25.	PLA 22°C Flexural on Edge (XZ) Specimen Dimensions	105
26.	PLA on Edge (XZ) Flexural Properties at Room Temperature (22°C)	105
27.	PLA 60°C Flexural on Edge (XZ) Specimen Dimensions	107
28.	PLA on Edge (XZ) Flexural Properties with Heat Lamp at 60°C	107
29.	PLA 22°C Flexural Upright (ZX) Specimen Dimensions	109
30.	PLA Upright (ZX) Flexural Properties at Room Temperature (22°C)	109
31.	PLA 60°C Flexural Upright (ZX) Specimen Dimensions	113
32.	PLA Upright (ZX) Flexural Properties with Heat Lamp at 60°C.....	113
33.	Summary of PLA Flexural Properties with and without the Heat Lamp.....	114
34.	Comparison of Injection Molded PLA to FFF with the Heat Lamp at 60°C.....	116
35.	PEKK Tensile Flat (XY) Specimen Dimensions.....	122
36.	PEKK Flat (XY) Tensile Properties with 120°C Heat Lamp	122
37.	PEKK Tensile Flat (XZ) ±45° Infill Specimen Dimensions	124
38.	PEKK Flat (XY) ±45° Infill Tensile Properties with 120°C Heat Lamp	125
39.	PEKK Tensile on Edge (XZ) Specimen Dimensions	127

40.	PEKK on Edge (XZ) Tensile Properties with Heat Lamp at 120°C.....	128
41.	PEKK Tensile Upright (ZX) Specimen Dimensions.....	131
42.	PEKK Upright (ZX) Tensile Properties with Heat Lamp at 120°C	131
43.	Tensile Testing Summary PEKK on Lulzbot Taz 5 with 120°C Heat Lamp	132
44.	Published Tensile Testing Data for FDM PEKK from Stratasys Antero 800 NA-F900 with T20D Tip.....	132
45.	Published Tensile Testing Data for FDM PEKK from Stratasys Antero 800 NA-Fortus 450mc with T20D Tip.....	132
46.	PEKK Flexural Flat (XY) Specimen Dimensions	136
47.	PEKK Flat (XY) Flexural Properties with 120°C Heat Lamp.....	137
48.	PEKK Flexural on Edge (XZ) Specimen Dimensions.....	139
49.	PEKK on Edge (XZ) Flexural Properties with Heat Lamp at 120°C	140
50.	PEKK Flexural Upright (ZX) Specimen Dimensions	142
51.	PEKK Upright (ZX) Flexural Properties with Heat Lamp at 120°C.....	143
52.	Flexural Testing Summary PEKK on Lulzbot Taz 5 with 120°C Heat Lamp	144
53.	Published Flexural Testing Data for FFF PEKK from Stratasys Antero 800 NA-F900 with T20D Tip.....	144
54.	Published Flexural Testing Data for FFF PEKK from Stratasys Antero 800 NA-Fortus 450mc with T20D Tip.....	144
55.	Comparison of Injection Molded PEKK to FFF with the Heat Lamp at 120°C	147
56.	PEI Tensile Flat (XY) Specimen Dimensions	152
57.	PEI Ultem 1010 Flat (XY) Tensile Properties with 120°C Heat Lamp.....	153

58. PEI Tensile on Edge (XZ) Specimen Dimensions.....	155
59. PEI Ultem 1010 on Edge (XZ) Tensile Properties with Heat Lamp at 120°C	156
60. PEI Tensile Upright (ZX) Specimen Dimensions	158
61. PEI Ultem 1010 Upright (ZX) Tensile Properties with Heat Lamp at 120°C, Specimens 4 to 6 had Grip Failures	159
62. Tensile Testing Summary PEI on Lulzbot Taz 5 with 120°C Heat Lamp	160
63. Published Tensile Testing Data for FFF Ultem 1010 Stratasys Fortus 900mc with T14 Tip	160
64. PEI Flexural Flat (XY) Specimen Dimensions.....	164
65. PEI Ultem 1010 Flat (XY) Flexural Properties with 120°C Heat Lamp.....	165
66. PEI Flexural on Edge (XZ) Specimen Dimensions	167
67. PEI Ultem 1010 on Edge (XZ) Flexural Properties with Heat Lamp at 120°C...	167
68. PEI Flexural Upright (ZX) Specimen Dimensions.....	169
69. PEI Ultem 1010 Upright (ZX) Flexural Properties with Heat Lamp at 120°C ...	170
70. Flexural Testing Summary PEI on Lulzbot Taz 5 with 120°C Heat Lamp.....	171
71. Published Flexural Testing Data for Stratasys FDM Ultem 1010 printed with a Fortus 900mc with T14 Tip.....	171
72. Comparison of Injection Molded PEI to FFF with the Heat Lamp at 120°C	174
73. PEEK Tensile Flat (XY) Specimen Dimensions.	180
74. PEEK Flat (XY) Tensile Properties with 120°C Heat Lamp.....	180
75. PEEK Tensile on Edge (XZ) Specimen Dimensions.....	182
76. PEEK on Edge (XZ) Tensile Properties with Heat Lamp at 120°C	183

77.	Tensile Testing Summary PEEK on Lulzbot Taz 5 with 120°C Heat Lamp	184
78.	Published Tensile Testing Data for PEEK 3DXTech ThermaX.....	184
79.	Published Tensile Testing Data for PEEK FFF Printing from South Dakota State University.....	184
80.	PEEK Flexural Flat (XY) Specimen Dimensions.....	188
81.	PEEK Flat (XY) Flexural Properties with 120°C Heat Lamp	188
82.	PEEK Flexural on Edge (XZ) Specimen Dimensions	191
83.	PEEK on Edge (XZ) Flexural Properties with Heat Lamp at 120°C.....	191
84.	Flexural Testing Summary PEEK on Lulzbot Taz 5 with 120°C Heat Lamp.....	192
85.	Published Flexural Testing Data for PEEK 3DXTech Thermax.....	192
86.	Published Flexural Testing Data for PEEK FFF Printing from South Dakota State University.....	192
87.	Comparison of Injection Molded PEEK to FFF with the Heat Lamp at 120°C	194
88.	PLA Density and Porosity	197
89.	PEKK Density and Porosity	197
90.	PEI Density and Porosity	197
91.	PEEK Density and Porosity	197

LIST OF FIGURES

Figure	Page
1. Diagram of the Fused Filament Fabrication (FFF) Process.....	3
2. Build Direction Orientations.....	9
3. Lulzbot TAZ 5 FFF 3D Printer.....	26
4. V6 All-Metal Hot End and Plated Copper Heater Block.....	29
5. Volcano Nozzle to Extend the Length of the Nozzle past the Infrared Light.....	30
6. Hot End Cooling Fan with Insulation to Protect it from the heat from the Infrared Light.....	31
7. Printer Heated Bed.....	32
8. Different Reflector Types on Omega Infrared Emitters	34
9. Omega Infrared Emitter with a Gold I reflector that points the Infrared Light Straight Down	35
10. Omega Infrared Emitters are typically used for Welding and Riveting Plastics	35
11. Looking up at the Infrared Heat Lamp and the Bottom of the Nozzle.	36
12. Looking at the Side of the Heat Lamp and the Nozzle	36
13. 120 Volt Power Supply.....	37
14. Z Height Home Adjustment Extension.....	38
15. Omega Infrared Heat Lamp Printed Mount.....	38
16. Installed Omega Infrared Heat Lamp Mount.....	39
17. Shorter Corner Bracket to Hold Print Bed to allow Clearance for the Light.....	39

18.	Lulzbot Taz 5 Enclosure	40
19.	Printed Mounting Bracket for Enclosure	41
20.	Installed Mounting Bracket for Enclosure.....	41
21.	Inside View of Enclosure.....	42
22.	Insulated Fan to block the heat from the Infrared Heat Lamp.....	43
23.	Desiccant Dryer for Filament while Printing.....	44
24.	Hairspray used to Stick Parts to Print Bed.....	45
25.	Glue Sticks to Stick Parts to Print Bed	46
26.	PEI Sheet to Stick Parts to Print Bed.....	46
27.	Label of PEI Sheet	47
28.	Kapton Polyimide Tape to Stick Parts to Print Bed.....	47
29.	Label of Kapton Polyimide Tape	48
30.	Print Orientation.....	50
31.	Printing Upright (ZX) PLA Tensile Specimens.....	52
32.	Printed Flat (XY) PLA Tensile Specimens.....	52
33.	Printed PLA Tensile Specimens on the Edge (XZ)	53
34.	Printed PLA Flexural Specimens on the Edge (XZ).....	53
35.	Printed PLA Flexural Specimens Vertical.....	54
36.	The first attempt at printing the Upright PLA Flexural Specimens.....	55
37.	Printing the Upright PLA Flexural Test Specimens with the Heat Lamp	55
38.	Printing PEKK Tensile Specimens on the Edge (XZ).....	57

39.	Printing PEKK Tensile Specimens on the Edge (XZ) Image 2	58
40.	Printing PEKK Tensile Specimens on Edge (XZ) Image 3	58
41.	First Attempt at Printing PEEK Tensile Specimens Flat (XY)	59
42.	Printed Flat (XY) PEKK Tensile Specimens.....	59
43.	Printing PEKK Upright (ZX) Tensile Specimens.....	60
44.	Printing PEKK Upright (ZX) Flexural Specimens Image 1	61
45.	Printing PEKK Upright (ZX) Flexural Specimens Image 2	62
46.	Printing PEKK on Edge (XZ) Flexural Specimen.....	63
47.	Printing PEI Upright (ZX) Tensile Specimens	65
48.	Finished PEI Upright (ZX) Tensile Specimens	65
49.	Printing PEI on Edge (XZ) Tensile Specimens	66
50.	Printing PEI Flat (XY) Flexural Specimens	66
51.	First Attempt at Printing PEEK Tensile Specimens on the Edge (XZ).....	69
52.	First Attempt at Printing PEEK Upright (ZX) Tensile Specimens.....	70
53.	First Attempt at Printing PEEK Upright (ZX) Tensile Specimens that Broke off and had no Bonding between Layers	70
54.	Second Attempt at Printing PEEK Upright (ZX) Tensile Specimens with Warping at the Print Bed	71
55.	Second Attempt at Printing PEEK Upright (ZX) Tensile Specimens that broke off because of Poor Bonding between Layers	71
56.	Printing of PEEK Flat (XY) Flexural Specimen.....	72
57.	Printing of PEEK on Edge (XZ) Flexural Specimen.....	72

58.	Tensile Curves Explanation	74
59.	4505 Series Instron Test Frame used for Tensile and Flexural Testing	76
60.	Axial extensometer model 3542 from Epsilon that was used to Measure the Tensile Strain	77
61.	Tensile Testing Setup.....	77
62.	Flexural Testing Setup	78
63.	Tensile Test Specimens, Flat (XY), Upright (ZX), on Edge (XZ), and Flat $\pm 45^\circ$ Infill (XY)	78
64.	PLA Flat (XY) Tensile Specimens	79
65.	PLA Flat (XY) Tensile Properties at Room Temperature 22°C Stress vs. Strain Plot.....	80
66.	PLA Flat (XY) Tensile Specimens after Testing.....	81
67.	PLA Flat (XY) Tensile Properties with Heat Lamp at 60°C Stress vs. Strain Plot.....	82
68.	PLA Flat (XY $\pm 45^\circ$ Infill) Tensile Specimens after Testing.....	83
69.	PLA Flat (XY $\pm 45^\circ$ Infill) Tensile Properties at Room Temperature 22°C Stress vs. Strain Plot	84
70.	PLA Flat (XY $\pm 45^\circ$ Infill) Tensile Properties with Heat Lamp at 60°C Stress vs. Strain Plot	86
71.	PLA on Edge (XZ) Tensile Specimens before Testing and Removing the Printing Supports	87
72.	PLA on Edge (XZ) Tensile Specimens after Testing	88
73.	PLA on Edge (XZ) Tensile Properties at Room Temperature 22°C Stress vs. Strain Plot.....	89
74.	PLA on Edge (XZ) Tensile Specimens with Heat Lamp at 60°C after Testing..	90

75. PLA on Edge (XZ) Tensile Properties with Heat Lamp at 60°C Stress vs. Strain Plot.....	91
76. PLA Upright (ZX) Tensile Specimens Printed at Room Temperature before Testing.....	92
77. PLA Upright (ZX) Tensile Specimens Printed at Room Temperature after Testing.....	93
78. PLA Upright (ZX) Tensile Properties at Room Temperature 22°C Stress vs. Strain Plot.....	94
79. PLA Upright (ZX) Tensile Specimens Printed with Heat Lamp at 60°C before Testing	95
80. Upright (ZX) Tensile Specimens Printed with Heat Lamp at 60°C after Testing.....	96
81. PLA Upright (ZX) Tensile Properties with Heat Lamp at 60°C Stress vs. Strain Plot.....	97
82. PLA Tensile Strength Summary	98
83. PLA Tensile Modulus Summary	99
84. PLA % Elongation at Break Summary	99
85. PLA % Elongation at Yield Summary.....	100
86. PLA Flat (XY) Flexural Specimens.....	101
87. PLA Flat (XY) Flexural Properties at Room Temperature 22°C Stress vs. Strain Plot.....	102
88. PLA Flat (XY) Flexural Properties with Heat Lamp at 60°C Stress vs. Strain Plot.....	104
89. PLA on Edge (XZ) Flexural Properties at Room Temperature 22°C Stress vs. Strain Plot.....	106

90. PLA on Edge (XZ) Flexural Properties with Heat Lamp at 60°C Stress vs. Strain Plot.....	108
91. PLA Upright (ZX) Flexural Properties at Room Temperature 22°C Stress vs. Strain Plot.....	110
92. PLA Upright (ZX) Flexural Specimens before Testing.....	111
93. PLA Upright (ZX) Flexural Specimens after Testing.....	112
94. PLA Upright (ZX) Flexural Properties with Heat Lamp at 60°C Stress vs. Strain Plot.....	113
95. PLA Flexural Strength Summary.....	114
96. PLA Flexural Modulus Summary.....	115
97. PLA Flexural Strain at Maximum Stress Summary	115
98. Comparison of Injection Molded PLA to FFF Strength with the Heat Lamp at 60°C	116
99. Comparison of Injection Molded PLA to FFF Modulus with the Heat Lamp at 60°C	117
100. Annealing PEKK Specimens	118
101. PEKK Tensile Specimens	119
102. Testing PEKK Tensile Specimen.....	119
103. PEKK Flat (XY) Tensile Specimens before Testing	120
104. PEKK Flat (XY) Tensile Specimens after Testing	121
105. PEKK Flat (XY) Tensile Properties with 120°C Heat Lamp Stress vs. Strain Plot.....	122
106. PEKK Flat (XY) ±45° Infill Tensile Specimens before Testing	123
107. PEKK Flat (XY) ±45° Infill Tensile Specimens after Testing	124

108. PEKK on Edge (XZ) $\pm 45^\circ$ Infill Tensile Properties with Heat Lamp at 120°C Stress vs. Strain Plot	125
109. PEKK on Edge (XZ) Tensile Specimens before Testing.....	126
110. PEKK on Edge (XZ) Tensile Specimens before Testing.....	127
111. PEKK on Edge (XZ) Tensile Properties with Heat Lamp at 120°C Stress vs. Strain Plot.....	128
112. PEKK Upright (ZX) Tensile Specimens before Testing	129
113. PEKK Upright (ZX) Tensile Specimens after Testing	130
114. PEKK on Upright (ZX) Tensile Properties with Heat Lamp at 120°C Stress vs. Strain Plot.....	131
115. PEKK FFF Tensile Strength Printing with Lulzbot 5 with Heat Lamp at 120°C compared to Stratasys FDM Printers	133
116. PEKK FFF Tensile Modulus Printing with Lulzbot 5 with Heat Lamp at 120°C compared to Stratasys FDM Printers	133
117. PEKK FFF % Elongation Printing with Lulzbot 5 with Heat Lamp at 120°C compared to Stratasys FDM Printers	134
118. Flexural Testing of PEKK Specimen.....	135
119. PEKK Flat (XY) Flexural Specimens before Testing.....	135
120. PEKK Flat (XY) Flexural Specimens after Testing	136
121. PEKK Flat (XY) Flexural Properties with 120°C Heat Lamp Stress vs. Strain Plot.....	137
122. PEKK on Edge (XZ) Flexural Specimens before Testing.....	138
123. PEKK on Edge (XZ) Flexural Specimens after Testing	139
124. PEKK on Edge (XZ) Flexural Properties with Heat Lamp at 120°C Stress vs. Strain Plot.....	140

125. PEKK Upright (ZX) Flexural Specimens	141
126. PEKK Upright (ZX) Flexural Specimens after Testing.....	142
127. PEKK on Upright (ZX) Flexural Properties with Heat Lamp at 120°C Stress vs. Strain Plot.....	143
128. PEKK FFF Flexural Strength Printing with Lulzbot 5 with Heat Lamp at 120°C compared to Stratasys FDM Printers.....	145
129. PEKK FFF Flexural Modulus Printing with Lulzbot 5 with Heat Lamp at 120°C compared to Stratasys FDM Printers.....	145
130. PEKK FFF Flexural Strain at Break Printing with Lulzbot 5 with Heat Lamp at 120°C compared to Stratasys FDM Printers.....	146
131. Comparison of Injection Molded PEKK Strength to FFF with the Heat Lamp at 120°C	148
132. Comparison of Injection Molded PEKK Modulus to FFF with the Heat Lamp at 120°C	148
133. PEI Tensile and Flexural Test Specimens	149
134. PEI Tensile Testing.....	150
135. PEI Ultem 1010 Flat (XY) Tensile Specimens before Testing.....	151
136. PEI Ultem 1010 Flat (XY) Tensile Specimens after Testing	152
137. PEI Ultem 1010 Flat (XY) Tensile Properties with 120°C Heat Lamp Stress vs. Strain Plot.....	153
138. PEI Ultem 1010 on Edge (XZ) Tensile Specimens before Testing.....	154
139. PEI Ultem 1010 on Edge (XZ) Tensile Specimens after Testing.....	155
140. PEI Ultem 1010 on Edge (XZ) Tensile Properties with Heat Lamp at 120°C Stress vs. Strain Plot	156
141. PEI Ultem 1010 Upright (ZX) Tensile Specimens before Testing.....	157

142. PEI Ultem 1010 Upright (ZX) Tensile Specimens after Testing.....	158
143. PEI Ultem 1010 Upright (ZX) Tensile Properties with Heat Lamp at 120°C Stress vs. Strain Plot	159
144. PEI FFF Tensile Strength Printing with Lulzbot 5 with Heat Lamp at 120°C compared to Stratasys FDM Printers	161
145. PEI FFF Tensile Modulus Printing with Lulzbot 5 with Heat Lamp at 120°C compared to Stratasys FDM Printers	161
146. PEI FFF % Elongation Printing with Lulzbot 5 with Heat Lamp at 120°C compared to Stratasys FDM Printers	162
147. PEI Flexural Testing	163
148. PEI Ultem 1010 Flat (XY) Flexural Specimens before Testing.....	163
149. PEI Ultem 1010 Flat (XY) Flexural Specimens after Testing.....	164
150. PEI Ultem 1010 Flat (XY) Flexural Properties with 120°C Heat Lamp Stress vs. Strain Plot.....	165
151. PEI Ultem 1010 on Edge (XZ) Flexural Specimens.....	166
152. PEI Ultem 1010 on Edge (XZ) Flexural Properties with Heat Lamp at 120°C Stress vs. Strain Plot	167
153. PEI Ultem 1010 Upright (ZX) Flexural Specimens before Testing	168
154. PEI Ultem 1010 Upright (ZX) Flexural Specimens after Testing.....	169
155. PEI Ultem 1010 Upright (ZX) Flexural Properties with Heat Lamp at 120°C Stress vs. Strain Plot	170
156. PEI FFF Flexural Strength Printing with Lulzbot 5 with Heat Lamp at 120°C compared to Stratasys FDM Printers	172
157. PEI FFF Flexural Modulus Printing with Lulzbot 5 with Heat Lamp at 120°C compared to Stratasys FDM Printers	172

158. PEI FFF Flexural Strain Printing with Lulzbot 5 with Heat Lamp at 120°C compared to Stratasys FDM Printers	173
159. Comparison of Injection Molded PEI Strength to FFF with the Heat Lamp at 120°C	174
160. Comparison of Injection Molded PEI Modulus to FFF with the Heat Lamp at 120°C	175
161. PEEK Test Specimen Annealing	176
162. PEEK Flat (XY) Tensile Specimens before Testing.....	177
163. PEEK Flat (XY) Tensile Specimen after Testing	178
164. PEEK Flat (XY) Tensile Specimens after Testing	179
165. PEEK Flat (XY) Tensile Properties with 120°C Heat Lamp Stress vs. Strain Plot.....	180
166. PEEK on Edge (XZ) Tensile Specimens before Testing.....	181
167. PEEK on Edge (XZ) Tensile Specimens after Testing.....	182
168. PEEK on Edge (XZ) Tensile Properties with Heat Lamp at 120°C Stress vs. Strain Plot.....	183
169. PEEK FFF Tensile Strength Printing with Lulzbot 5 with Heat Lamp at 120°C compared to Published Data	185
170. PEEK FFF Tensile Modulus Printing with Lulzbot 5 with Heat Lamp at 120°C compared to Published Data	185
171. PEEK FFF % Elongation Printing with Lulzbot 5 with Heat Lamp at 120°C compared to Published Data	186
172. Flexural Testing of PEEK.....	187
173. PEEK Flat (XY) Flexural Test Specimens before Testing	187
174. PEEK Flat (XY) Flexural Test Specimens after Testing	188

175. PEEK Flat (XY) Flexural Properties with 120°C Heat Lamp Stress vs. Strain Plot.....	189
176. PEEK on Edge (XZ) Flexural Specimens.....	190
177. PEEK on Edge (XZ) Flexural Properties with Heat Lamp at 120°C Stress vs. Strain Plot.....	191
178. PEEK FFF Flexural Strength Printing with Lulzbot 5 with Heat Lamp at 120°C compared to Published Data	193
179. PEEK FFF Flexural Modulus Printing with Lulzbot 5 with Heat Lamp at 120°C compared to Published Data	193
180. Comparison of Injection Molded PEEK Strength to FFF with the Heat Lamp at 120°C	194
181. Comparison of Injection Molded PEEK Modulus to FFF with the Heat Lamp at 120°C	195
182. Measuring the Weight in Water to Calculate Density	196
183. Tensile Testing Comparison	198
184. Percent Elongation Comparison	199
185. Tensile Modulus Comparison	199
186. Flexural Strength Comparison	200
187. Flexural Modulus Comparison	200

LIST OF ABBREVIATIONS

Abbreviation	Description
ABS	Acrylonitrile Butadiene Styrene
AM	Additive Manufacturing
ASTM	American Society for Testing and Materials
BAAM	Big Area Additive Manufacturing
C	Concentration of Diffusion Material
°C	Degrees Celsius
CAD	Computer Aided Design
cm	Centimeter
CO ₂	Carbon Dioxide
DBD	Dielectric Barrier Discharge
D _m	Mass Diffusion
D _o	Diffusivity constant of system
FDM	Fused Deposition Modeling
FFF	Fused Filament Fabrication
G Code	G Programming Language
GPa	Gigapascal
GUI	Graphical User Interface
H	Convection Constant
H-code	Hex Code

IDE	Integrated Development Environment
Inc	Incorporated
IR	Infrared
ISO	International Standards Organization
K	Bonding Potential Coefficient
K	Toughness of Interface Material
K_{∞}	Maximum Toughness
kHz	Kilohertz
kW	Kilowatt
LLC	Limited Liability Corporation
ME	Material Extrusion
mm	Millimeter
MPa	Megapascal
Nd:YAG	Transmission Welding
PDHS	Pre-Deposition Heating System
PEEK	Polyetheretherketone
PEI	Polyetherimide
PEKK	Polyetherketoneketone
PID	Proportional Integral Derivative
PLA	Polylactic Acid
Q	Activation Energy of the Diffusion Material

R	Gas constant
RP	Rapid Prototypes
S	Second
SD	Standard Deviation
STL	Sterolithography
T	Interface Temperature
T	Time that T is Greater than T _g
T _c	Critical Bonding Temperature
T _e	Envelope Temperature
T _g	Glass Transition Temperature
T _n	Nozzle Temperature
T(τ)	Dependent Interface Temperature
USB	Universal Serial Bus
V	Volts
Vs.	Versus
W	Watt
X	Diffusion distance
3D	Three Dimensional

ABSTRACT

A fused filament fabrication (FFF) desk top three dimensional printer was modified with a pre-deposition heating method using an infrared heat lamp in an omega shape around the printing nozzle to print high temperature materials and improve the tensile and flexural properties. The FFF additive manufacturing (AM) process is inherently a non-isothermal thermoplastic welding process that leads to anisotropic material properties. A non-traditional method to improve the strength using an infrared quartz heater as a pre-deposition heating system was developed and tested. The tensile and flexural properties of polylactic acid (PLA), polyetheretherketone (PEEK), polyetherketoneketone (PEKK) and polyetherimide (PEI) were evaluated. The goal of developing the desktop 3D printer to print high temperature materials equivalent to high end printers was achieved. The testing concluded that the printer modifications were successful in improving the material properties of low temperature PLA and that it gives the functionality to print high temperature materials such as PEKK and PEI. However, the modifications did not improve the “Z” strength anisotropy problem. PEKK was the easiest high temperature material to print. Overall, the material properties were comparable to material printed with high end printers and to some of the injection molded properties.

I. INTRODUCTION

ISO/ASTM 52900:2015(E) defines Additive Manufacturing (AM) as a “process of joining materials to make parts from 3D model data, usually layer upon layer, as opposed to subtractive manufacturing and formative manufacturing technologies” [1]. Additive manufacturing (AM) started in 1986 with Charles Hull’s patent for stereolithography [2]. Stereolithography is an AM technology that uses ultra violet light to cure polymers in a layer by layer process. The first forms of AM were used to create Rapid Prototypes (RP) to visualize the parts that would closely resemble the final parts for a quick evaluation. The use of on demand high resolution RP reduced the product development cycle and the costs of making the actual part to evaluate the prototype [3]

AM classifications are liquid, solid, or powder based. Materials have ranged from plastics and metals to concrete and tissue [3]. Material Extrusion (ME) based 3D printing is a liquid processes that has become a tool for research and developmental in a wide range of engineering disciplines [4]. ISO/ASTM 52900:2015(E) defines ME as an “additive manufacturing process in which material is selectively dispensed through a nozzle or orifice” [1].

Fused Deposition Modeling (FDM) is an ME process that was invented by S. Scott Crump founder of Stratasys, Inc. in 1989 [5]. FDM is a trademarked term by Stratasys. Stratasys FDM printers control print settings, feedstock material, and the print chamber environment to optimize the process parameters for consistency of part dimensional accuracy, surface roughness, and strength [4, 6]. Stratasys does not allow the end user to change the print settings or filament materials without the risk of voiding their warranty on the AM printer. With the expiration of Stratasys patent in 2009, low

cost open source FDM printers have been introduced to the market and have become an important part of the AM revolution taking place [4].

The term Fused Filament Fabrication (FFF) has replaced the Stratasys trademarked FDM term. Since the expiration of the Stratasys patent, new low cost FFF printer designs use inexpensive microprocessors, simple thermoplastic filament extrusion heads, and gantries that move in a three dimensional pattern relative to the build plate [7]. Open-source low cost 3D printers have become affordable solutions to consumers that are easy and safe to use and maintain while producing high quality parts [3]. FFF technology has quickly become a capable, flexible, and cost-effective option in the AM industry for creating complex 3D geometries [8]. It is currently the most widely used technique for polymer AM in the consumer/hobbyist field [9].

The FFF process begins with a thermoplastic filament being pulled by rollers into hot end that melts the filament. The melted thermoplastic is then extruded through a nozzle onto the heated printer bed. The extruded material is placed in precise paths called “roads” by controlling the movements in the x-y plane. After the layer of roads has been deposited the z direction is moved to start the next layer [10]. The FFF printing process part is fabricated from a precise sequence of successive layers producing a three dimensional part of user-defined shape. There are numerous FFF printer designs that use the same process of pushing a solid thermoplastic filament through a heated extrusion nozzle that deposits a three dimensional pattern onto a build plate [7].

The two most commonly used materials FFF are Polylactic Acid (PLA) and Acrylonitrile Butadiene Styrene (ABS) because they are inexpensive, have low melting temperatures and produce parts with acceptable geometrical tolerances for general use

[3]. Open-Source printers typically have a minimum geometric tolerance of not more than 0.1 mm [11]. Figure 1 shows a diagram of the FFF process.

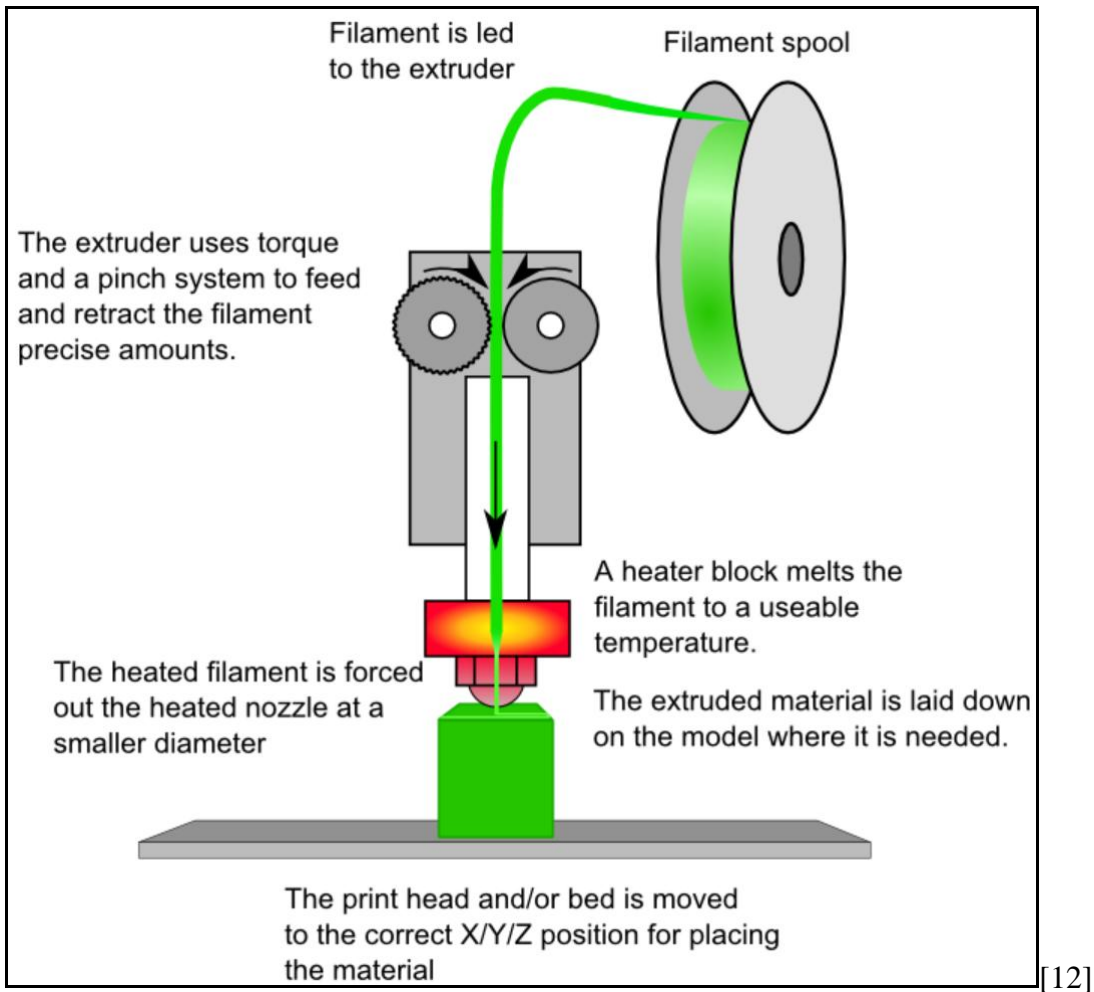


Figure 1. Diagram of the Fused Filament Fabrication (FFF) Process

II. BACKGROUND

Micromechanics have been used to define the mechanical properties of 3D printed parts by defining the properties as a representative unit cell. The unit cell is described as a bundle of fibers aligned in the XZ direction. The properties are represented as orthotropic mechanical properties with orthonogonal planes of symmetry in the X, Y, and Z directions. The extruded fiber is in-plane X-Y bonding and the layers are out-of-plane Z bonding. To characterize the principle mechanical properties of the unit cell tensile specimens are printed with the tensile axis in the X, Y, or Z direction. The FFF process has poor interlayer and intralayer bond strength that is due to the incomplete polymer chain entanglement that forms across the interfacial boundary of the printed layers. Processing methods are needed to address the mechanical anisotropy issue that limits the functional use of FFF parts for production parts [6].

There isn't a single standard for measuring interlayer properties of FFF printed parts. The most often used technique that is easily compared to industry-standard mechanical tests is uniaxial tensile tests of dog bone samples [13]. A problem with this technique as related to FFF printed samples have sharp interfaces between the adjacent layers that are not repeatable and can affect the cross sectional area measurements. The tensile strength is measuring the fracture mechanics and the critical flaws in the specimen. FFF parts are a collection of interfaces that aren't fully welded where the weakest weld will be the weakest link in the chain. The tensile sample is not the estimate of the interlaminar fracture behavior of the material but the collective behavior of all the welds. The dog bone tensile test will give a general understanding of the strength but not a complete understanding of the true fracture mechanics [6].

As open-source FFF printers are becoming more common there is a growing need to optimize the mechanical properties to allow the 3D printed parts to be used as functional parts and not just prototypes to demonstrate the form and function. Some functional applications will also require materials to withstand higher temperatures [6]. To mature the open-source FFF from rapid prototyping into a rapid manufacturing tool where parts are used for end use the processing and material characteristics need to improve the material property uniformity and be able to use high performance materials [8]. These open-source FFF technologies have impacted industries where low volume and personalized production are needed with features that cannot be made with traditional subtractive manufacturing [7]. The complexity of manufacturing is not a cost driver in AM like it is with standard subtractive machining of parts [3].

Advances need to be made in the open-source FFF technology to be adopted as a manufacturing tool. An approach that is capable of controlling the temperatures at the layer interfaces when the filament is deposited may increase the desired isotropy of the mechanical properties with a balance between the material property and dimensional tolerance. To evolve FFF into the production of engineering applications where dynamic loads or multi-direction static loads are present the properties need to be predictable and uniform to reach high levels of standard [4].

There are many parameters in the FFF process that will impact the material properties of the final part. The raster orientation (angle between layers) and the build direction (direction normal to the build plane) are geometrical parameters that change the material properties [14]. The strength in directions of the build plane can be optimized by raster strategy. However, the Z direction normal to the build plane strength of the FFF

part is dependent on the thermal history across layers as well as the rheology-dependent microstructures of the printed layers [8, 15-18].

The FFF process has interdependent processing parameters where each parameter in the FFF process will have different effects on different properties of the part. By optimizing a set of parameters for one property other properties can be affected. There is always a balance between dimensional accuracy and mechanical properties [4]. To achieve the best dimensional accuracy and surface finish lower extruder temperatures are used which will also reduce the part strength [19].

Printer parameters (both those associated with the printer and the part design) will need to be optimized for each individual material, as described in Table 1.

Table 1. Proper 3D Printing Requires Optimization of a Number of Parameters to Fully Utilize the Capabilities of both the Process and the Material

Build Parameters	Affects
Hot End Extrusion Temperature	Too low and material will not extrude. Too high and material will come out too low in viscosity and will not maintain shape after extrusion
Build Plate Temperature	Chosen to ensure material will not warp and determines the cooling rate through the component into the build plate
Cooling Fan Parameters	Provides local cooling immediately after deposition onto part. If too much cooling is applied, the material will warp; too little, and the material will be low in viscosity and cannot hold its shape or support more material
I/R Heating Parameters	Must be cycled on/off appropriately to maintain needed heating/cooling rates through different sections of the component being fabricated
Part Fill Pattern	Determines thermal load, degree of anisotropy
Layer Thickness	Determines level of detail, printing time, and amount of thermal load applied at any time (thicker layers put more heat into a component for a specific time)
Extrusion Parameters	Filament retraction, overlap, appropriate infill, etc. greatly affect part quality in many different ways
Print Speed	Faster print speeds result in faster manufacturing time, slower print speeds result in higher detail, heating/cooling also affected by print speed
Build Plate Adhesion	Different materials require different substances to best adhere to the build plate, not warp, and not become detached during print
Design Parameters	Affects
Part Orientation	Affects anisotropic material properties, means to support/scaffold part, and heating/cooling
Use and Type of Scaffolding	Ensure complex shapes can be successfully printed, but scaffolding must be able to be removed prior to use
Cooling Time (Post Build)	Determination of appropriate cooling time/rate post build to ensure dimensional accuracy is maintained
Environmental Conditions	Ideally low humidity and appropriate room temperature to ensure correct heat transfer (or lack thereof) from the build chamber

Z Strength Problem

The rate of crystallization of polymers will affect the mechanical strength of the part. Semi-crystalline polymers need the proper growth of its semi-crystalline structure, which is impaired by a low rate of crystallization when using open-source FFF printers. Open-source FFF printers can have a non-uniform thermal distribution of heat which causes improper curing of the printed layers of material that will affect the mechanical properties. The curing rate can be improved by in-process temperature variations to cure the joints among the beads. The control parameters that affect mechanical properties of polymers such as tensile, impact and flexural strength can be controlled by variations in the control parameters such as infill percentage, printing speed, bed temperature, build orientation, layer thickness (height), extruding temperature, hatch spacing, etc. The crystallization rate can be improved with heat treatments during processing or annealing heat treatments after printing [11].

The “Z Strength Problem” of weak interlayer bonding strength has a trade off of strength versus dimensional tolerance accuracy. This low welding strength does not produce isotropic full strength polymer production parts using FFF [20]. The anisotropic material properties of FFF parts depends on the part geometry and the process parameters. This is a result from the weak interlayer Z bonding of the polymer molecules and the aligning of the polymer chains with the direction of the polymer flow out from the extrusion head [21]. Figure 2 shows the build direction orientations that are possible with FFF.

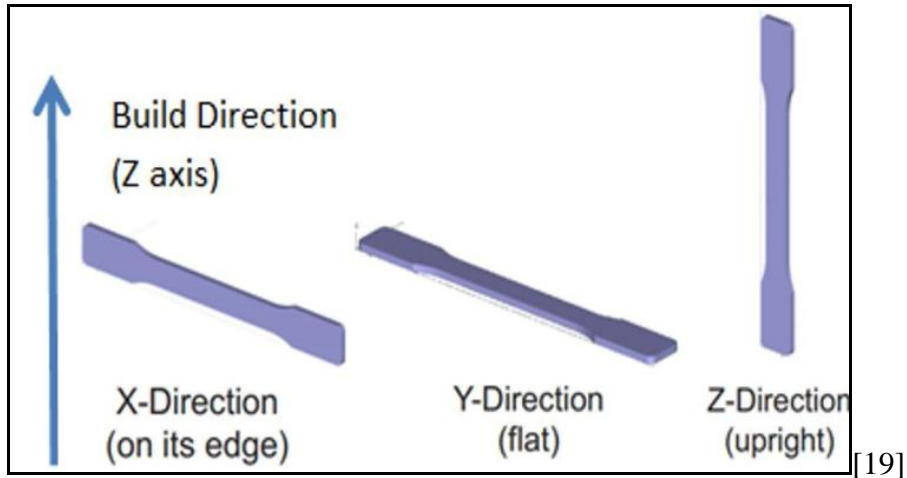


Figure 2. Build Direction Orientations

The tensile strength of parts in the Z direction typically falls in the range of 10–65% of that in the direction along the filaments depending on process conditions and materials [17]. A “Strength Isotropy Factor” is defined as the ratio of the tensile strength of FFF parts in the normal-to-layer direction to the strength in the directions along-the-filament. With a value range of 0 to 1, 0 has no strength in the normal-to-layer direction and 1 has the same strength along the layer and in the Z direction. The FFF process produces parts with a strength isotropy factor in the range of 0.1 to 0.65. When the process parameters are optimized for the part and the build volume is heated the strength isotropy factor can reach 0.65 [4]. Parts fabricated using FFF in large Big Area Additive Manufacturing (BAAM) at Oak Ridge National Labs using ABS reinforced with 20% chopped carbon fiber; the tensile strength in the z-direction has been determined to be about 85% lower than the corresponding in-plane strength. The mechanical anisotropy will also happen on small scale FFF processes [22]. New processing methods are needed to address the anisotropic property weakness in FFF parts to be used as full strength functioning parts comparable to the isotropic properties that are obtained using injection molding.

Non-Isothermal Process

There is a challenge to get the best interlayer adhesion from the thermodynamics of heating the feedstock and kinetics of bonding the polymer interfaces in polymer processing using FFF [6]. This is attributed to poor bonding between printed layers when the lower layers cool below the glass transition temperature (T_g) before the next layer is deposited [22]. Heat and time play a role in the polymer diffusion and welding across the interface of the layers. There is a trade off that has to be considered for the dimensional tolerance that can be affected [6]. FFF produced parts have lower mechanical strength in the Z direction because the inter-layer strength is affected by the non-isothermal process inherent with FFF [7].

The bonding mechanism between layers is a thermal fusion and polymer inter-diffusion process that will depend on the thermal energy of the semi-molten polymer and the amount of area that contact between the layers [9, 23]. When the extruded material comes in contact with the previously deposited layer below, it cools by transferring thermal energy into the layers while also heating the layers and the interface between the two layers. The development of inter-layer weld strength at interface of these hot and cold layers will experience different non-isothermal conditions which results in varying degrees of polymer interdiffusion [7]. The longer the time when the temperature of the deposited filament is above the glass transition temperature the greater the intermolecular diffusion will be across the interface and the mechanical strength at the interface will be greater [9, 23].

Experiments have been performed to optimize the FFF process parameters such as temperature, print path strategy, layer height, and over extrusion to remove defects

between printed tracks. The more time that the polymer chains on the two sides of an FFF layer interface go through three stages of wetting, diffusion, and randomization before the interface of the polymer heals the closer the mechanical property in the interlayer direction will be to the isotropic properties of the polymer. Increasing the time that the interface stays above the glass transition temperature can improve the healing process [8]. The physics of the inter-layer bonding process during FFF and its relation to the effect of process parameters on the bond formation between a “hot” polymer filament and a “cold” existing polymer surface has been investigated [18]. When the lower layers cool below the glass transition temperature (T_g) before the next layer is deposited there is poor bonding between the printed layers [22]. Es-Said studied the effects on the mechanical properties of parts printed using FFF as a result of varying time between the successive printing layers which allowed for more interlayer cooling. The temperature of the top layer was measured after each layer deposition. An increase in the time between deposited layers results in a decrease in the yield strength between printing layers. Larger parts will inherently have more time between layers printing which reduces the mechanical strength in the Z direction [21].

Uneven cooling between the layers can warp the part; produce poor layer adhesion, and delaminations. Enclosures around the print envelope can be used to control the heat loss but interlayer cooling will still occur. As the amount of time between printed layers increases the more the previous layer will cool will affect the ability of the layers to adhere resulting in poorer material properties since the process of interlayer bonding is thermally driven [24]. The cooling between successively deposited layers effects the compressive and shear strength of FFF parts with a 12% and 25% decrease

over the wait times up to 20 seconds. The cooling in between layers will be present in parts with larger feature sizes resulting in weaker interlayer bonds produced. To minimize the effects the already deposited layer cooling heated enclosures or other pre-deposition heat sources have been studied. By adding these printer features the effects of interlayer cooling can be reduced but they cannot achieve the temperatures required to mitigate the reduction in strength all together. The parts will not hold their geometrical tolerances during printing at the temperatures that would be required to mitigate these effects [14].

Polymer welding has been studied under isothermal conditions around the glass transition temperature. In the thermoplastic welding process temperature control and how long the polymer spends at each temperature is a critical parameter in the repeatability of the process [7]. The temperatures of the nozzle and the build environment are the critical factors affecting the bond strength between layers [18]. The build environment temperature will have a more significant effect on the bond strength. However, if the build environment temperature is too high the part dimensional and structural accuracy goes down when build envelope temperature increases beyond a certain point [4]. Also, printing at higher nozzle temperatures will increase the part strength isotropy but reduce part dimensional tolerances [8].

FFF Relationship to Thermoplastic Welding

Kim and Wool developed a theoretical background for isothermal welding (healing) of polymer interfaces. Their model has been used to study the polymer welding process during FFF [15]. De Gennes has described this reptation model of polymer motion in a four step process for polymer crack healing as surface rearrangement, surface approach, wetting, diffusion and randomization [16]. In the FFF process where the extrusion of the hot layer meets the cool layer below it the wetting of the interface between the layers and the randomization of the polymer entanglements play the largest role in the Z strength [6]. Sun and Bellhumeur describe the FFF printing heat transfer process of the hot extruded layer heating the layer below and cooling the deposited layer. They conducted sintering experiments on ABS to evaluate the neck growth profile between the particles [25]. Seppala and Migler used thermography of the printed layers while they were being deposited to determine the weld times using rheology data and time-temperature superposition shift factors to correlate the models with the interlayer fracture strength [7].

The physical phenomenon that governs the issues with the FFF process mechanical property anisotropy is a result of the effect of macroscopic thermal mechanical properties from the thermal history of the layer interface and the microscopic effect of the polymer microstructure and the mass transfer across the interfaces [8]. The polymer welding process of polymer interfaces has been widely studied and modeled. De Gennes developed the reptation model of polymer motion in the crack healing process as steps that consist of surface rearrangement, surface approach, wetting, diffusion, and randomization [16]. Kim and Wool expanded on this reptation model by outlining a

theory of healing at the polymer-polymer interfaces during isothermal welding. The steps of the reptation model that are the most relevant to the FFF process of the hot layer being extruded onto a cold layer are polymer interface wetting and polymer entanglement randomization [15]. Sun and Bellehumeur applied the Kim and Wool model to the AM process by modeling the heat transfer process of the hot top layer being cooled by the layers below it during the sintering process on ABS to model the dimensionless neck growth profiles between the polymer particles [25]. Seppala and Migler studied this reptation model of polymer motion by using thermography of the AM printed layers to determine equivalent weld times by using rheology data and time-temperature superposition shift factors to correlate the models to their measurements of the interlayer fracture strength [7].

The critical factors for good bonding are the interface temperature and the time the interface temperature is above the critical temperature. The longer the time the greater the strength of the material bond will be. The envelope temperature, T_e , and the convection constant, h , within the envelope are the process parameters that are most critical to the interlayer bond strength. These parameters control the rate of cooling of a newly deposited layer that will become the substrate for the next layer. The envelope temperature affects the bond strength more than the nozzle temperature, T_n . The nozzle temperature does play a role in bond strength as it controls the amount of energy transferred to the previous layer. The interlayer bond strength will also vary due to the size of the part being fabricated because larger parts will require more time between layers than small parts will. This will allow the previous layer more time to cool between layers and resulting in a weaker interlayer strength [10].

The FFF process is an extension of thermoplastic welding where molecular bonding occurs by the interpenetration of molecular chains across a bonding interface. As the interpenetration increases the bonding interface disappears and bond strength increases. The welding process is a type of mass diffusion that is thermally activated at temperatures above a critical temperature, T_c . Rodriguez et al. use the glass transition temperature, T_g , as the critical temperature [10, 13]. Rodriguez *et al.* and Yan *et al.* studied the bond strength to characterize and optimize interlayer strength processing parameters that are needed to developing strong material bonds [10,13,18]. Yan et al. have described this mass diffusion process using the following Arrhenius form of the diffusion equation [10, 18]:

$$dm = -D_0 e^{-Q/RT} \frac{dc}{dx} dt$$

Where: D_0 = Diffusivity constant of the system
 T = Interface temperature
 Q = Activation energy of the diffusion material
 c = Concentration of diffusion material
 x = Diffusion distance
 R = Gas constant [10]

The concentration gradient dc/dx is difficult to accurately measure the interface diffusion bonding. Yan *et al.* introduced variable called bonding potential (ψ), to model the bonding interface status, which is defined as follows [10,18]:

$$\psi = \int_0^{\infty} \xi(T) \cdot e^{-k/t} dt$$

$$\xi(T) = \begin{cases} 1 & T \geq T_c \\ 0 & T < T_c \end{cases}$$

Where: T_c = Critical bonding temperature
 k = Bonding potential coefficient (units in temperature)
 T = Interface temperature [10]

A higher bonding potential increases the degree of bonding which results in a stronger bond. A finite difference method was used to calculate the bonding potential for the different processing surrounding envelope temperatures and nozzle temperatures. Tensile tests were performed to correlate the bonding potential with the tensile strength. Rodriguez *et al.* characterized the molecular diffusion using the De Gennes reptation model as having three stages: wetting, diffusion, and randomization. At temperatures greater than T_g the wetting process removes the irregularities on the polymer surface to allow the molecular chains to move freely across the surface instantaneously [10,13,16]. Rodriguez *et al.* derived an expression for the instantaneous wetting where the toughness of the bond is proportional to the monomer segment interpenetration depth across the interface and a time-dependant interface temperature. A finite element model was used to calculate the time-dependent interface temperature $T(\tau)$ and equation (4) to predict the interlayer toughness of FDM parts [10].

$$\frac{K(t)}{K_x} = \frac{K_0(T)}{K_x} + \left[\frac{1}{t} \int_0^t \left(\frac{\tau}{C \exp\left(\frac{Q}{RT(\tau)}\right)} \right) d\tau \right]^{1/4}$$

Where:

- K = toughness of interface material
- K_x = maximum toughness (equal to the toughness of the virgin material)
- $K_0(T)$ = toughness that occurs due to surface wetting only (no interdiffusion)
- T = interface temperature
- t = time that T is greater than T_g
- Q = material activation energy
- R = gas constant
- C = pre-exponential factor, assumed constant

[10]

Non-Traditional Methods for Improving Strength

Traditional approaches to thermal control and process optimization have only shown small improvements in strength in the Z direction. Optimized printing process parameters that have shown improvement in the strength on part geometries are typically specific to that particular part, process, and material. The advantage of FFF printing is the ability to print one-off parts. The computer programs to optimize the print settings for one-off parts currently do not exist. Non-traditional methods have been explored to solve the Z strength problem. These non-traditional methods include: layer preheating, annealing, mechanical mixing, surface modifications, and adhesives [6].

To improve the transverse direction properties of FFF part strength the amount of material bonding between the layers needs to be increased. A deposition process improvement system that re-heats the substrate material immediately preceding deposition called a pre-deposition heating system (PDHS) needs to be designed implemented, and tested. To test the system the material properties in the axial and transverse directions need to be measured as well as the parts dimensional accuracy. The heating process needs to be designed to raise the interface temperature above the glass transition temperature where bonding occurs. The heat source needs to be limited to not provide excessive heat that can cause degradation and material instability that will lead to a loss of properties. If the temperature is maintaining the part at too high of a temperature the material may lose dimensional accuracy by not solidifying enough to support additional layers. The PDHS needs to not contact the previously printed layer to not disrupt the shape of the material. The desired temperature is to heat the previously printed layer locally to the glass transition temperature of the material. If the entire part

was heated to the glass transition temperature the dimensional accuracy would be degraded. Plastic welding technologies that meet the no-contact requirement are laser welding, ultrasonic welding, infrared heating and forced air welding [10].

Different techniques have been developed to improve the interlayer bond strength in FFF printed materials by introducing additional PDHS methods to the interfaces either as an in-process technique. The objective of the PDHS is to increase the mass transfer on the interface by increasing the temperature dependent diffusivity [8].

In 2007, Partain et al at Montana State University reported the use of localized pre-deposition heating using forced air with FFF [10]. The non-traditional method was used to raise the previous layer surface temperature to the glass transition temperature to increase the time for wetting, diffusion, and randomization that is described in the DeGennes's reptation model [16]. A forced air polymer welding kit was placed on the printer pointed just ahead of the printing nozzle to raise the layer above the glass transition temperature of the polymer. This method was chosen because it did not contact the part which could affect the dimensional accuracy. However, the forced air still blew on the part too much which resulted in changes to the part shape and poor mechanical properties. This hot air pre-deposition heating approach during the printing was inconclusive. An advantage of forced air heating systems is that they are simple and low-cost. A disadvantage it that they are not as controlled or localized to a single point [10].

In 2016, Hsu et al at Arizona State University reported the use of localized pre-deposition heating using an infrared laser with FFF [4]. Typical laser welding systems used for polymers are CO₂ and transmission welding (Nd:YAG). The transmission welding system requires a transparent and colored pairing of materials which will not

work for this application [10]. A CO₂ laser pre-deposition heating system used a custom laser and optics system built onto an open-source Lulzbot Mini platform. The laser was mounted on the printer to heat the layer in front of the printing nozzle as it travels. The laser scanning speed was coupled with the printing speed. It was observed that there was evaporation of the of the polymer filament when the print speed was slow by a trench that was created on the surface. If the extruded material was not enough to fill the trench a void was created that acts as a stress concentration in the part during the flexural testing. With the correct printing speed of 4 mm/s and laser power of 1W the laser increased the interface temperature which increased the time for diffusion of materials. The interlayer tensile strength was increased by 50% to 48.3 Mpa and the flexural strength reached 80% of the flexural strength of injection molded ABS. The localized heating to the glass transition temperature allowed the part to maintain the geometrical accuracy by not heating the entire part. Entire build envelope heating methods are typically limited to about half of the polymer's T_g to maintain the parts geometrical accuracy. The laser heating method showed to be a feasible solution. A computer program would be needed to control the laser position in real time for all geometries [4]. An advantage of the laser welding pre-deposition heating system is that it can precisely deliver a controlled amount of heat to a localized point. The disadvantage of laser welding is the costly customization of the complex hardware that is required (optics, cooling system, power source, etc) [10].

In 2017, Kishore et al at Oak Ridge National Labs reported on using Infrared heating lamps as a pre-deposition heating method to apply heat to the previously printed layer just prior to deposition of the current layer to increase the interlayer bond strength in their Big Area Additive Manufacturing (BAAM) system [23]. BAAM prints parts on

the order of several meters. The extended time to print a layer results in the surface temperature of the previous layer being below the T_g of the polymer. The BAAM process has not resulted in functional parts because of the anisotropic nature of the parts from the weaker strength in the Z direction. ABS filled with 20 % chopped carbon fiber has z-direction tensile strength that is 85 % lower than the corresponding strength in the x-y build plane [16, 20]. By raising the surface temperature of the previously deposited layer above the glass transition temperature (T_g) with infrared heating lamps for sufficient periods of time the bonding between layers is enhanced [22]. The heating efficiency of the IR lamps is dependent on the standoff distance, view angle, power density, and travel speed [23]. 500 W and 1kW lamps were used at distances ranging from 1 cm to 8cm standoff distances from the layer with a print speed of 3.8cm/s [22]. A 6.35 cm long 1 kW lamp (model number 5306B-02-1000-01-00 Strip IR® Infrared Heaters, obtained from Research Inc.) was positioned directly over the layer at a standoff distance of 1 cm [23]. Improvements were made in the interlayer tensile strength by preheating the previous layer to above the T_g with a large infrared lamp [22]. Infrared preheating with lamps is a useful technique when the layer cools below the glass transition temperature before depositing the next layer. However the part can't be above T_g for too long of a time due to reduced geometrical resolution and increased surface roughness. This method was able to increase the interlayer bond temperature which more than doubled the Z-strength of the printed part under certain printing conditions [23].

Ultrasonic Vibrations have been used to increase the Z Strength for FFF [8]. A transducer and horn assembly creates ultrasonic waves are used to vibrate and melt the material together at the bond line interface [10]. A 34.4 kHz ultrasonic vibration resulted

in an increase of 10% of the Z strength ABS. The ultrasonic vibrations relaxed the stretched polymer chains in the interface regions which allowed more diffusion in the polymers. ASTM F88 peel test was used to measure the Z strength [8]. Ultrasonic Welding usually will require the parts to be held together with clamps during the welding process. In FFF there isn't a way to clamp the layers together because the top layer is semi-molten [10].

Additives on the surface to enhance localized heating of filaments have been studied to promote polymer diffusion. An electrically responsive nanomaterial ink coating was applied as a surface treatment on the filament to locally target the interface of the FFF printed parts and apply a post processing electromagnetic energy to heat and weld the filaments together. A dielectric barrier discharge (DBD) plasma electromagnetic applicator disk that was excited with high potential radio frequency energy was mounted concentrically around the extrusion nozzle to induce in-situ welding of the layers. The electric current passing through the nanomaterial coating resulted in heating of the layers and thermal welding of the filament layers. The Z strength was increased close to that of injection molded parts [6].

None of the pre-deposition heating methods meets isotropic strengths. Each of these non-traditional proof-of-concept techniques has shown improvements to solve the Z strength problem. A method to produce isotropic strength properties is still needed that can work for a range of engineering-grade materials to be adopted for commercial applications [6].

Fused Filament Fabrication (FFF) Additive Manufacturing (AM)

Models are generated using a Computer Aided Design (CAD) program such as Solidworks [26]. Pre-generated models can also be downloaded from online communities such as Thingiverse and Youmagine [27,28]. The models are then exported to the STL file format and imported into an open source slicer program such as Cura. Cura allows the user to prepare and convert the CAD model into a G code for 3D printing. The slicer is a planning software package that slices the model into layers for fabrication and creates the tool paths and processing parameters. The slices are determined by the processing parameters that are entered by the user and dependent on the nozzle size and materials that are used to fabricate the part. The user has the ability to set the printing parameters of the part such as layer height, deposition speed, raster angles, etc [29]. Printron Pronterface is a graphical user interface (GUI) that lets you control the printer from a computer and a USB cord connected to the printer [30].

The TAZ 5 requires the appropriate settings and some calibrations to get good print quality. The print bed needs to be leveled. This is verified by printing a layer that goes across the entire build plate such as a large circle or square. The print level is adjusted by turning set screws in each corner. The Z height also needs to be calibrated by turning the Z height home screw by turning it up or down. The Z height can be calibrated when it is in its home position using a sheet of paper to gauge distance between the bed and nozzle. By having the print bed level and the Z height calibrated the adhesion to the print bed will be better which will prevent warping during printing [31].

Sometimes a brim of one layer in thickness is added around the print on the first layer to add surface area in contact with the build plate which can help improve adhesion.

A skirt is the first thing that is printed around the part. The skirt is a one nozzle diameter wide loop of filament laid around the outside circumference of the part to be printed. This acts as a prime of the extruder head to ensure the flow of the material is consistent before it begins to print the part [31].

The width of the filament line that is laid down needs to be proportional to the nozzle diameter size. The wall thickness should be a multiple of the nozzle diameter to print with accurate dimensions. The layer thickness needs to also be a multiple of the layer thickness from the bottom to the top of the part being printed. Thinner layer thickness will produce a better quality part. The thicker the layers will produce the part faster but can't be thicker than the nozzle diameter [31].

Slower printing generally produces higher quality parts. The speed can be affected by the layer height, wall thickness, degree of infill and the speed of the print head. Cura allows the user to set all of these parameters related to the printing. Cura is also used to adjust the model for printing such as the orientation, position, and scale. Supports are generated in Cura to hold up any overhang that is not supported by the print bed [31].

Cura then converts the model into a numerical control programming language called G-Code. The G code is the instructions for the 3D printer tool paths to create the part one layer at a time. The G-code also controls the processing parameters set in Cura such as the print speed and flow of the polymer through the nozzle. The G-code can be loaded into open source software such as Printrun to prepare the printer and visualize the printing on a screen while it is printing [31].

Arduino is an integrated development environment (IDE) software that is used to

change the firmware on the TAZ 5. The firmware is constantly updated and revised. Arduino allows for the alteration of the code and uploading of that code to the main board. The code is written in C++ and consists of many files that defines and controls all the functions of the TAZ 5 from the stepper motor, heater temperatures, and user interface controls. The files are represented by different tabs in Arduino and can be edited to reconfigure the specific settings. The edited firmware is then uploaded the Taz 5 main board through a USB connection [31].

III. PRESENTATION OF WORK

FFF Printer Modifications

The system that was adapted is a Lulzbot TAZ 5 FFF 3D printer that is shown in Figure 3. The LulzBot TAZ 5 was chosen as the FFF 3D Printer because of the low cost (~\$2,200) and none of the additions to the LulzBot TAZ 6 are needed for changing it to print high temperature materials. The standard TAZ 5 has a maximum hot end temperature of 260°C, maximum print bead temperature of 100°C and the ambient temperature within the build area are a few degrees higher than the ambient room temperature [31]. The TAZ 5 is the perfect generation for converting to printing high temperature materials because it has all the things that the TAZ needed but it does not have the things that you don't need for the high temperature printing. The TAZ 6 has a box with the power supply built into it which is beside the print bead. It is better to have the power supply away from the high temperature so it will not overheat. The TAZ 5 has the improved aluminum high precision Z axis features that were not on the fully 3D printed TAZ 4.

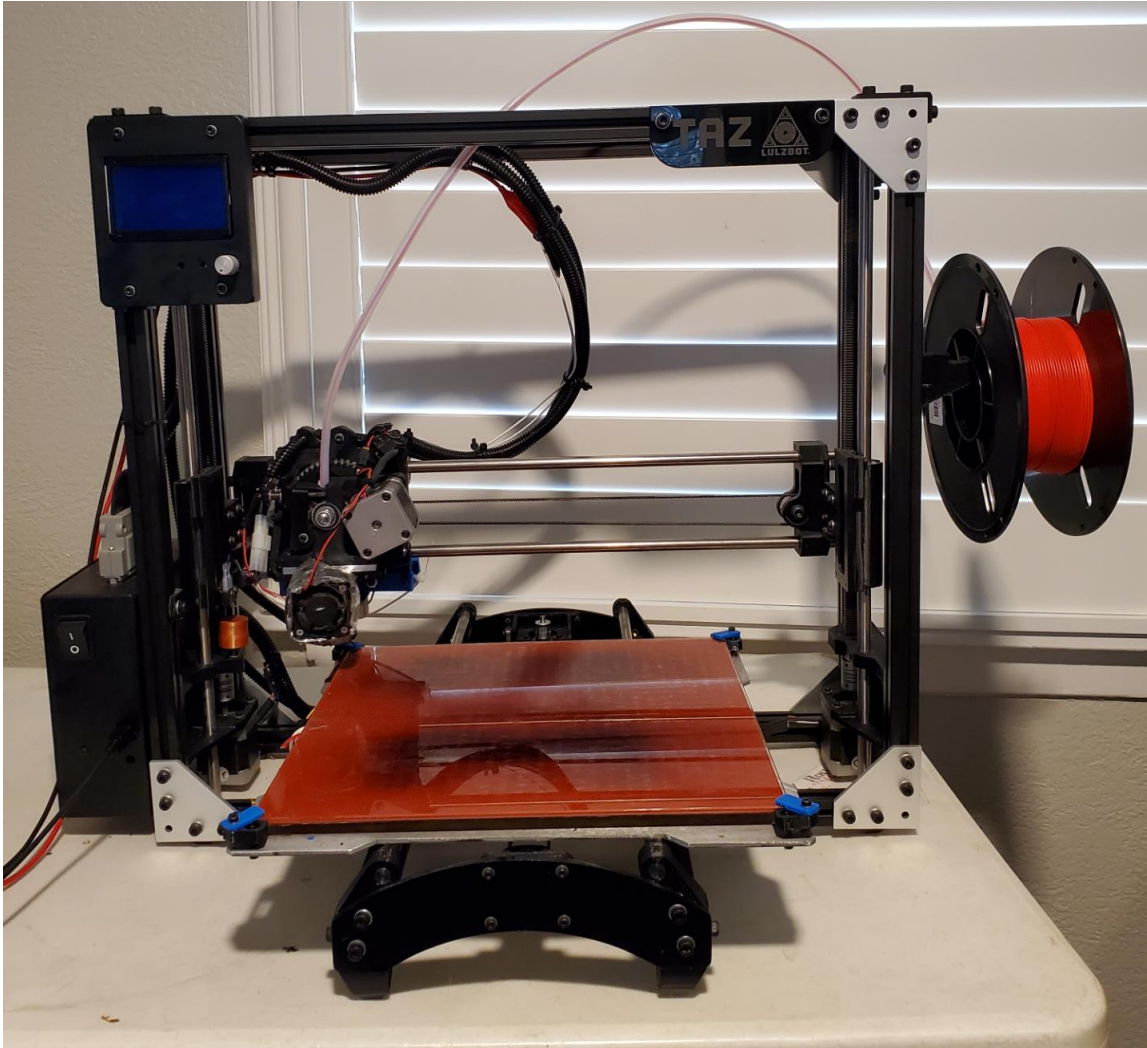


Figure 3. Lulzbot TAZ 5 FFF 3D Printer

The approach to addressing the problem was a structured breakdown, analysis, and implementation for the conversion of the TAZ 5 to print high temperature materials. The methodology was to divide the main goals into individual tasks to develop the capacity to print high temperature materials using FFF. The TAZ 5 FFF 3D printer was characterized in detail from a systems and process stand point. The aspects that constrained it regarding 3D printing with high temperature materials were identified and the printer was adapted with hardware and software changes.

The first objective was to characterize the TAZ 5 capabilities and to identify the

constraints for high temperature printing. The second objective was to develop the hardware and software modification that would be needed to enable high temperature material printing. The final objective was to perform printing investigations to develop the system and analyze the results.

These objectives were then divided into tasks that were either software related or hardware related. The tasks were carried out and implemented while assessing if the completion of each task had been achieved. After each objective was completed the next one would start. Once all the tasks had been completed of the objectives the TAZ 5 conversion process was completed to start test printing high temperature materials. The process for each task is detailed below.

The off-the-shelf TAZ 5 uses 3mm filament. However, the high temperature material filament diameter is 1.75mm. The filament feeder had to be modified to accept the 1.75 mm filament. To make this conversion on the hot end a piece of nylon tubing was put in that is sleeved to 1.75 mm from 3 mm. There was an issue with that tubing slide up a little bit which would create a gap at the bottom. When the fan went off it would get soft in the hot end which would plug up everything and jam the filament. The nylon sleeve was pushed all the way down. Then it had to be flared on the top so that it would not slide up. The flare also made it easier to get the filament down into the hot end. The fan was then set to have it on all the time at 100%.

To aligning everything up a piece of wire that is 1.75mm has to be run down the middle to make sure everything is aligned when we tighten the screws down. The wire is pushed down the throat and it makes everything align so that when the filament is inserted it goes in smoothly without restrictions. The filament has to be wiggled a little

bit when it gets inserted at the top of the middle of the plate to get it in.

To modify the hot end a high temperature heater cartridge kit (E-HEATER-HT-24V-65W-KIT), V6 Plated Copper Heater Block (V6-BLOCK-CARTRIDGE-COPPER), V6 All-Metal Hot End (C6-175-24V), V6 PT100 Upgrade Kit (V6-KIT-PT100), and a V6 Plated Copper Nozzle 1.75mm x 0.80mm (V6-Nozzle-COP-175-800) were procured from E3D Online. The hot end hardware had to be modified to a PT 100 temperature sensor to accurately measure the temperature of the E3D V6 Hotend. The PT100 is able to measure temperatures up to 500°C which is higher than a thermistor or thermocouple can read. The E3d V6 Hotend is a 65 watt high quality high end heater shown in Figure 4. The all metal 1.75 mm filament hotend has a heat sink that thermally isolates the hot end from the rest of the print head. It is wired to run off the mother board amplifier. It comes into the amplifier board and then goes to the analog port number 3 with stock connector styles. Custom length wires had to be made for the connections. The stock end for the PT100 did not have a long enough line and had to create a custom plug to extend to the mother board. The hot end temperatures can get quickly to as high as 500°C. The E3 hot end is all solid copper which allows it to get up to temperature and holds the temperature better than the aluminum ones.

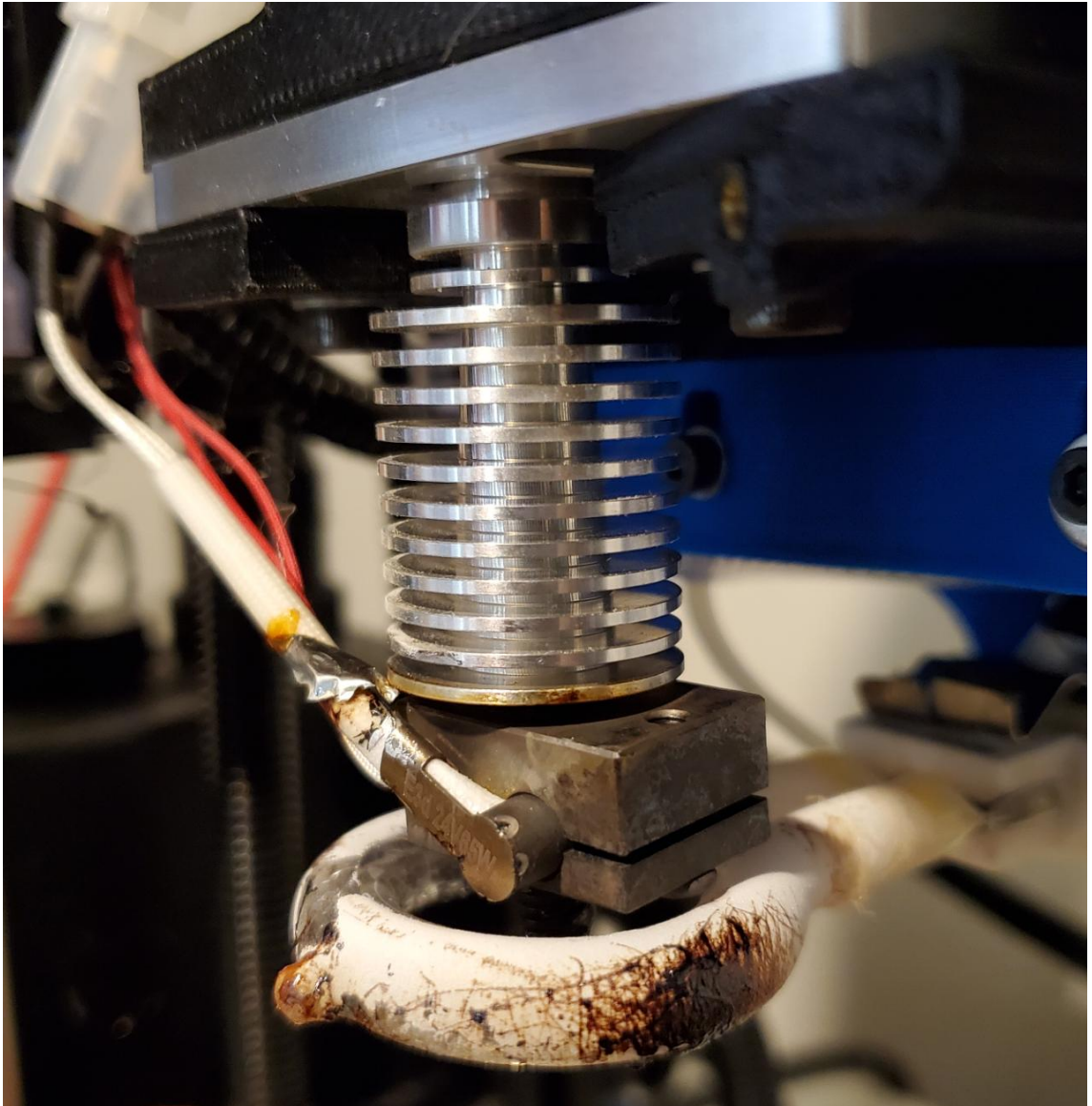


Figure 4. V6 All-Metal Hot End and Plated Copper Heater Block

A 0.8 mm hardened steel nozzle shown in Figure 5 was added so it will last a while because if abrasive material is used it will start wallowing it out. To take the nozzle on and off a wrench is used on the nozzle and to grip the heater block so that everything is not loosened up. The extruder goes all the way down and is spaced so that the brass heatbreak tube goes all the way into the block but it meets the tube so that there is not a gap. When removing the nozzle the rest of the assembly is held in place so that nothing turns. The nozzle needs to be tightened to the tube inside of the hot end and not

the heater base. If it is bottoming out on the heater and not touching the tube it will be loose or the polymer will squirt out at the heater and not the nozzle. The high temperature hot end limits the speed that the filament can be pushed thorough because printing fast with so much material the hot end can't heat it up fast enough.



[32]

Figure 5. Volcano Nozzle to Extend the Length of the Nozzle past the Infrared Light

The cooling fan on the hotend had to be modified to a high performance fans when it is running twice as hot as the stock set up as shown in Figure 6. An adapter had to be printed to go from a 30mm fan to a larger 40 mm fan. The fan is used to keep the heat sink on the heater cool. Two wire male plugs had to be connected to the fan wires to connect it to the mother board. The fan is ran off the secondary fan circuit and set to run all the time to cool as much as it can. If the fan is not running something is wrong and it will plug up the hotend, the fan is always on.



Figure 6. Hot End Cooling Fan with Insulation to Protect it from the heat from the Infrared Light

The heater on the print bead shown in Figure 7 was left stock because the mother board can only supply 5 amps before blowing it out. The stock TAZ firmware was reducing the power to the heated bed by 20 to 30%. The range is from 0 to 255 set on a 32 bit. It was set at 209 and then bumped up to 250 which is a little below the full max 5 amps. A Proportional-Integral-Derivative (PID) control was ran at a higher temperature of 110°C on the bed. It can easily get up to 110°C to 120°C. The bottom of the bed was insulated with double sided insulating material and kapton tape all around it to stick it on the bottom. This helps to maintain the temperature and get up to temperature quicker. The insulation will also prevent the heater from heating up the aluminum bed. If the heater on the bed is taken too much higher than 120°C the adhesive could degrade

between the heater and the bed. Once the heated bed was taken up to 120°C with the Poly-Ether-Imide (PEI) bonded to the bed bubbles formed in the adhesive bond line. The PEI was replaced and worked fine at 100°C. When printing high temperature Polyether-Ether-Ketone (PEEK) material with the pre-deposition heater it bonded to the PEI and peeled it up. Printing to the glass plate with Kapton Tape was an option that was explored. The Kapton Polyamide Tape was found to be the best option for high temperature materials.

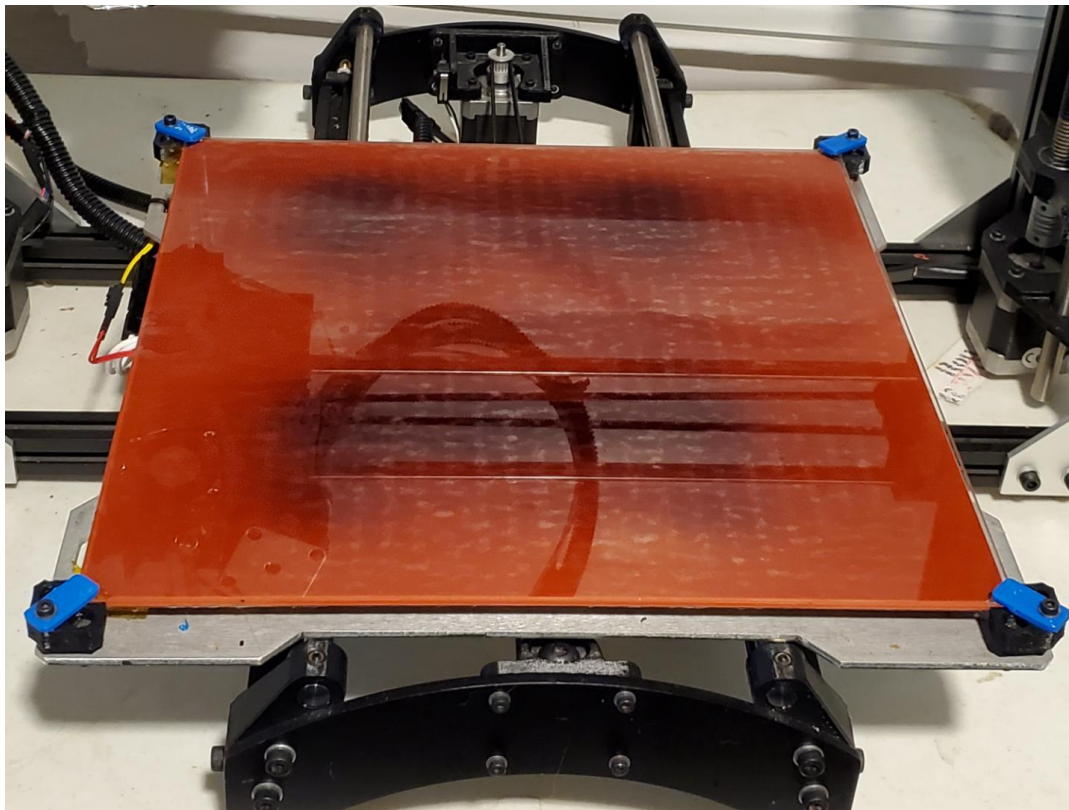


Figure 7. Printer Heated Bed

The firmware had to be updated to make everything work off the correct ports. The Arduino IDE is the program used to configure the firmware on the TAZ 5. The newest Arduino 1.8 version could not be used because the firmware on the TAZ 5 is older and not compatible with the libraries on the controllers that are used. Arduino version 1.0.6 had to be used to interface to configure the files that are in the firmware.

The firmware library contains different files and each file controls different things. The hex code (H-code) files need to be modified to configure the motherboard to give a wider range of optimal temperatures. The hotend was limited to 450°C to limit it so that it does not get out of the range of the PT100 temperature controller. There is a file for every pin on the motherboard controller file that has to be reconfigured to reassign the PT100 temperature controller. The analog inputs had to be modified to tell it what we are using. The stock ports that are referenced had to be modified the analog port instead of the thermistors that came with it. The only other files that had to be modified are the configuration.H and the configuration.advanced.H. Pronterface software was used to run the PID codes that give the new temperature tables had to be added to the firmware.

Once everything was modified in the firmware the TAZ 5 had to be calibrated. A PID temperature adjustment was made so that the firmware can ramp the temperature up to a point and then level it off. There are three numerical setting to adjust the ramp up and how much power it puts into it so that it comes right into the temperature. The PID was set to a 350°C which is in the range for some high temperature materials. The accuracy of this temperature was verified with a calibrated external digital thermometer inserted into the hot end.

The pre-deposition heating system methodology is to use quartz heat lamps as shown in Figures 8 to 12. The best place to put the heat lamps directly around the nozzle. Quartz heaters come in a variety of shapes. A more directional and tight heat lamp that can direct a large amount of heat but not put off too much heat to soften or melt the plastics parts on the TAZ 5 was needed. The quartz type heaters have a reflector on the back to direct the heat towards the printing area. A circular shape heater was chosen that

could go around the printing nozzle so that any direction that was being printed would be receiving the heat. The idea is to provide the heat in a directional way right at the print head prior to the layer being deposited to get the previous layer to the glass transition temperature. Omega shaped shortwave infrared lamps were purchased from Anderson Thermal Devices, Inc. and Heraeus Noblelight America LLC. The infrared lights have either a ceramic or gold reflector to target the heat where it is needed. The configurations for the reflectors are to shine the heat directly downward, inward, or to a 45 degree down and inward. The configuration that points the heat down and in to a 45 degree was chosen as this would be directed at the point of the material extrusion. These omega infrared emitters are typically used for joining, welding or riveting of plastics. The product that was chosen has a 39 mm outside diameter, uses up to 250 W power, and 115 V. The configuration was a Gold III part number 80008214 from Heraeus and CB051153845C/QD from Anderson Thermal Devices with a ceramic reflector. The ceramic reflector has the benefit of lower cost and higher operating temperatures [33, 34]. A 120V power supply with adjustable power outage was used to control the heat lamp as shown in Figure 13.

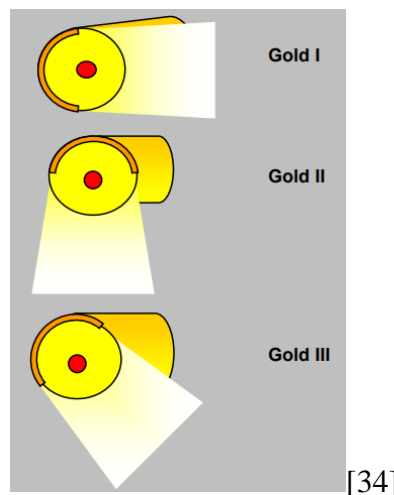
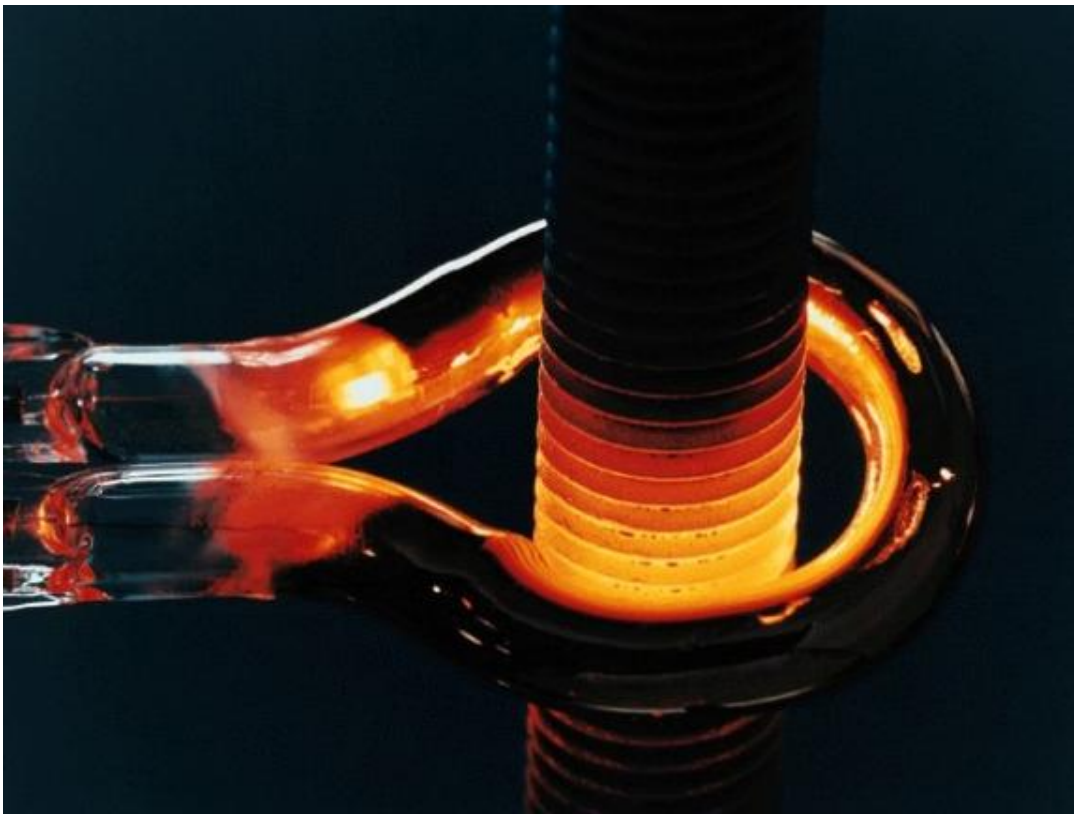


Figure 8. Different Reflector Types on Omega Infrared Emitters



[34]

Figure 9. Omega Infrared Emitter with a Gold I reflector that points the Infrared Light Straight Down



[35]

Figure 10. Omega Infrared Emitters are typically used for Welding and Riveting Plastics. They can also be used for Bending Tubes and Drawing Plastics



Figure 11. Looking up at the Infrared Heat Lamp and the Bottom of the Nozzle



Figure 12. Looking at the Side of the Heat Lamp and the Nozzle

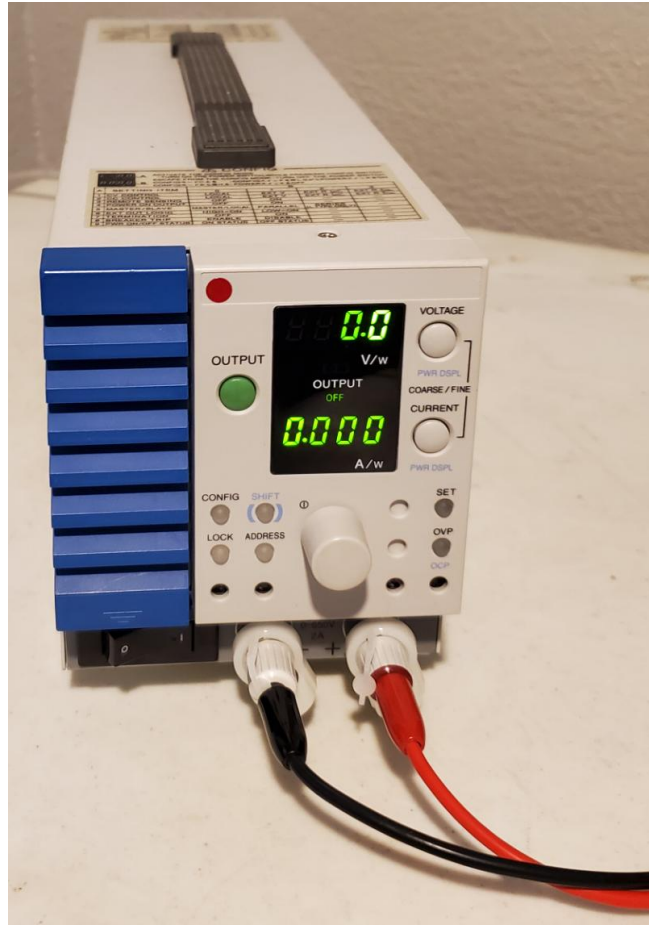


Figure 13. 120 Volt Power Supply

To allow the omega shaped quartz infrared heater to fit around the printing nozzle and still be above the print bed an extended nozzle had to be installed. A hardened steel volcano nozzle shown in Figure 5 was installed that has a longer thread was used to extend the nozzle down. The Z height of the print head had to be extended up to accommodate the nozzle and infrared light. The z height adjustment screw was not long enough. A part had to be printed to extend the height of the screw as shown in Figure 14. A part was printed to mount the light to the printer head as shown in Figure 15 and 16. The corner brackets were too tall to not run into the light when it was in the home position. Shorter corner brackets had to be printed to make room for the light as shown in Figure 17.

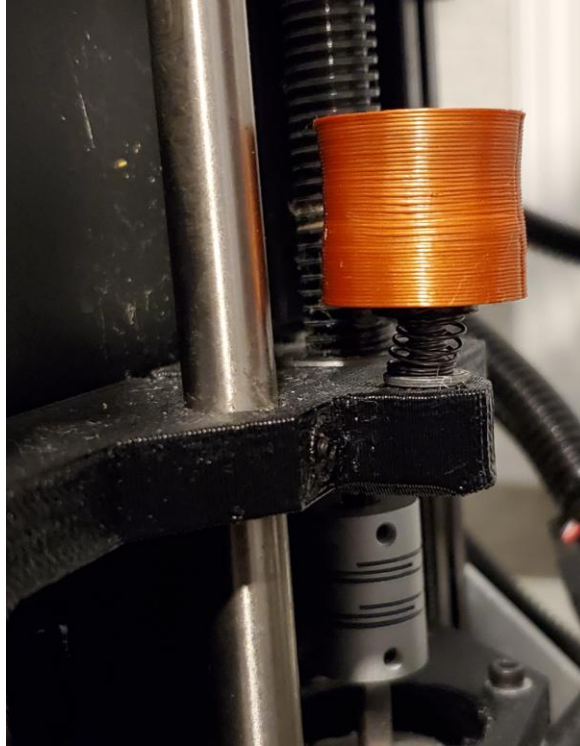


Figure 14. Z Height Home Adjustment Extension

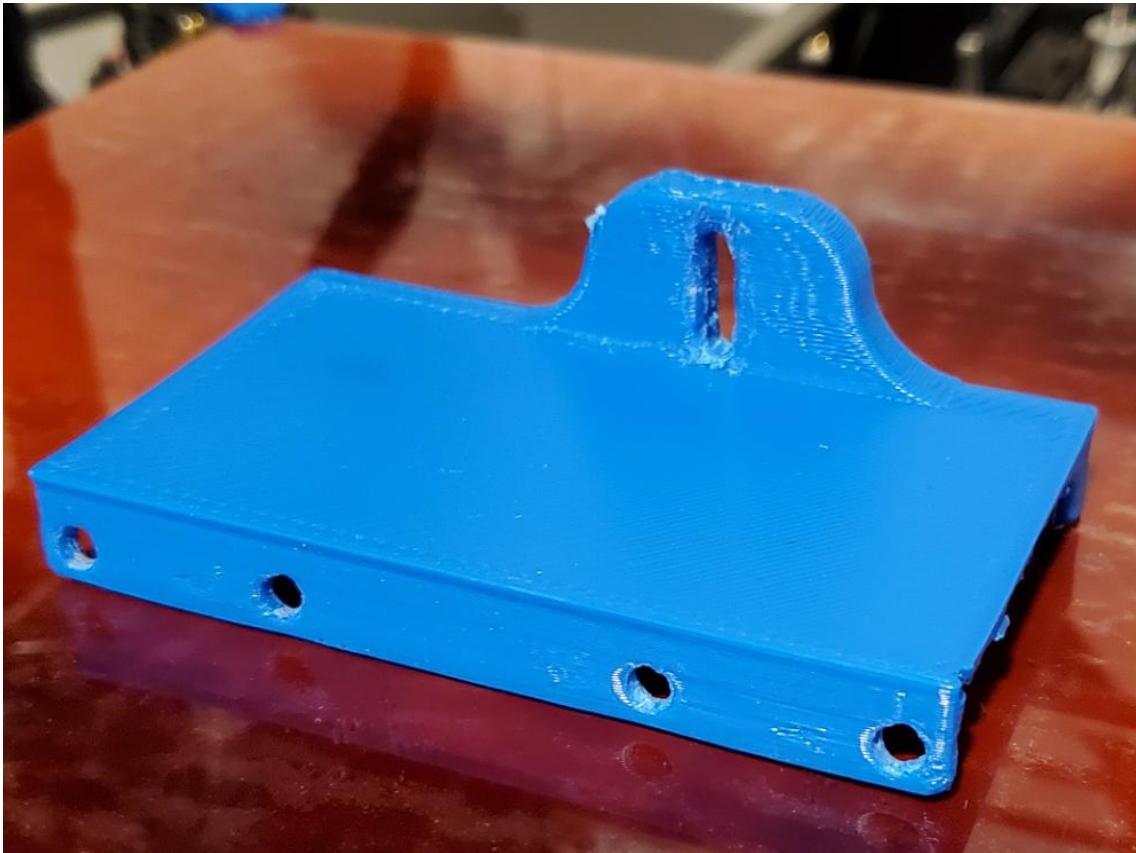


Figure 15. Omega Infrared Heat Lamp Printed Mount

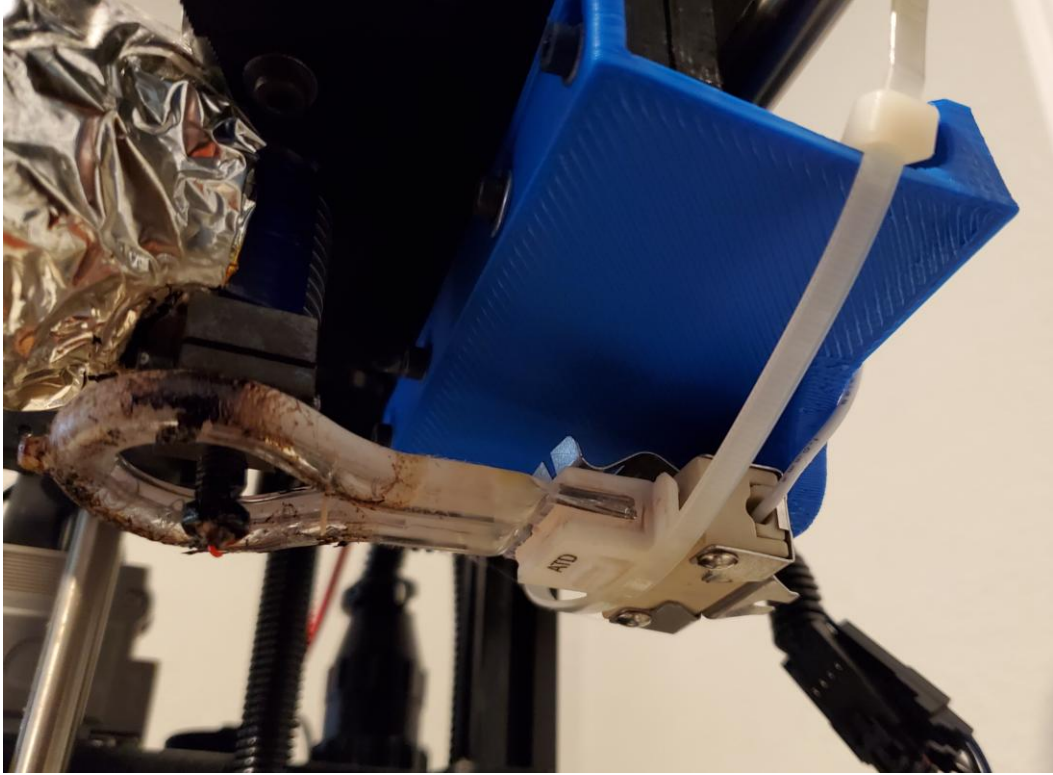


Figure 16. Installed Omega Infrared Heat Lamp Mount

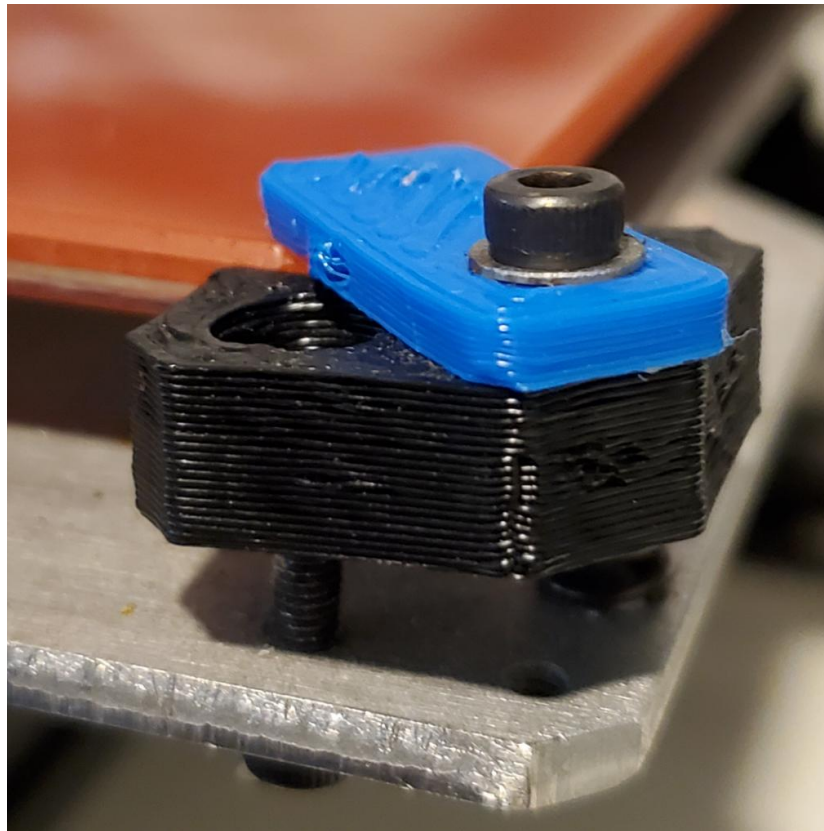


Figure 17. Shorter Corner Bracket to Hold Print Bed to allow Clearance for the Light

An enclosure for the printer was purchased to stabilize the environment from any breeze or changes in the room temperature as shown in Figure 18. With an enclosure the design is creating an environment that heats up slightly when the print bed, heater block, and infrared light are on. The hottest that the environment temperature achieved is 44°C. The idea is to have the directional heat raise the temperature of the previous layer to around the glass transition temperature and not the whole part. A mounting part had to be printed to hold the enclosure up as shown in Figure 19 to 21.



Figure 18. Lulzbot Taz 5 Enclosure

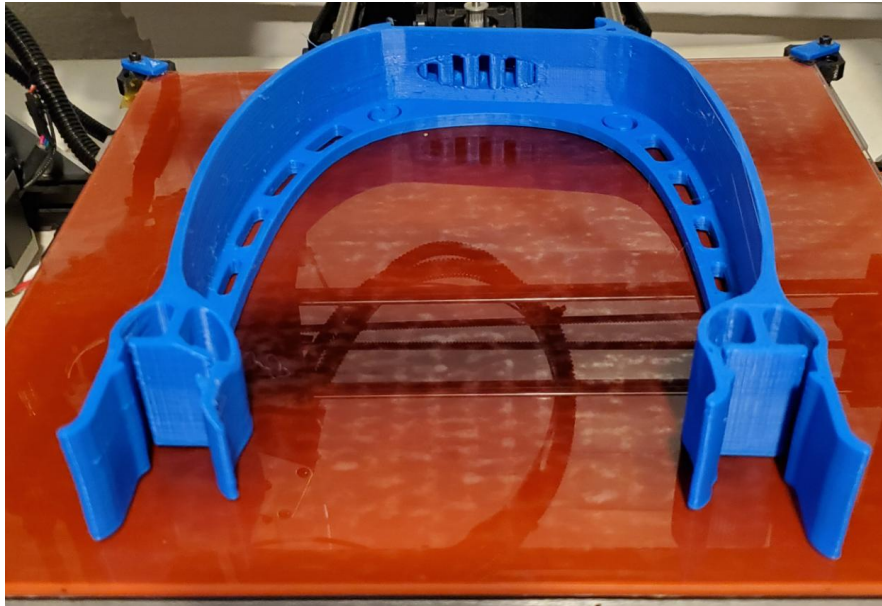


Figure 19. Printed Mounting Bracket for Enclosure



Figure 20. Installed Mounting Bracket for Enclosure

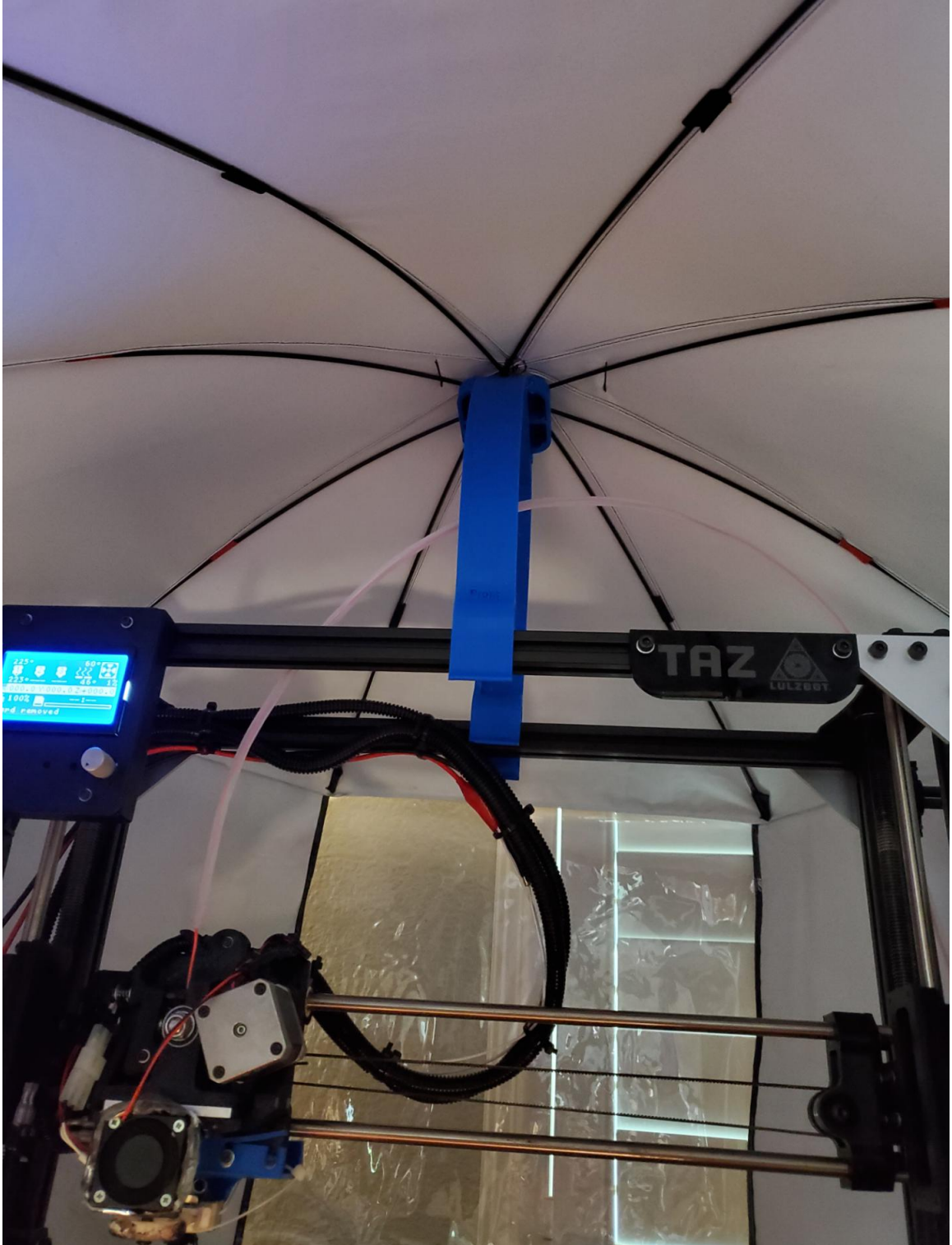


Figure 21. Inside View of Enclosure

There are concerns that the heat that does come off of the quartz heater could melt the ABS printer hardware. These parts were insulated to protect them from getting too

hot. An insulation that also acts as a reflector could work better to deflect the heat produced from the quartz heat lamp. A bubble foil film insulation could act as a shield for the heat that is radiating from the light. Figure 22 shows the fan that is above the heat lamp was insulated. If the area around the stepper motors was to get too hot there would need to be active cooling added with a heat sink and fan. If the control board were to get too hot it could be removed from the TAZ 5 frame and located outside of it. It was chosen to not create an enclosure and print with only the heat from the quartz heater directed at the previously deposited layer.

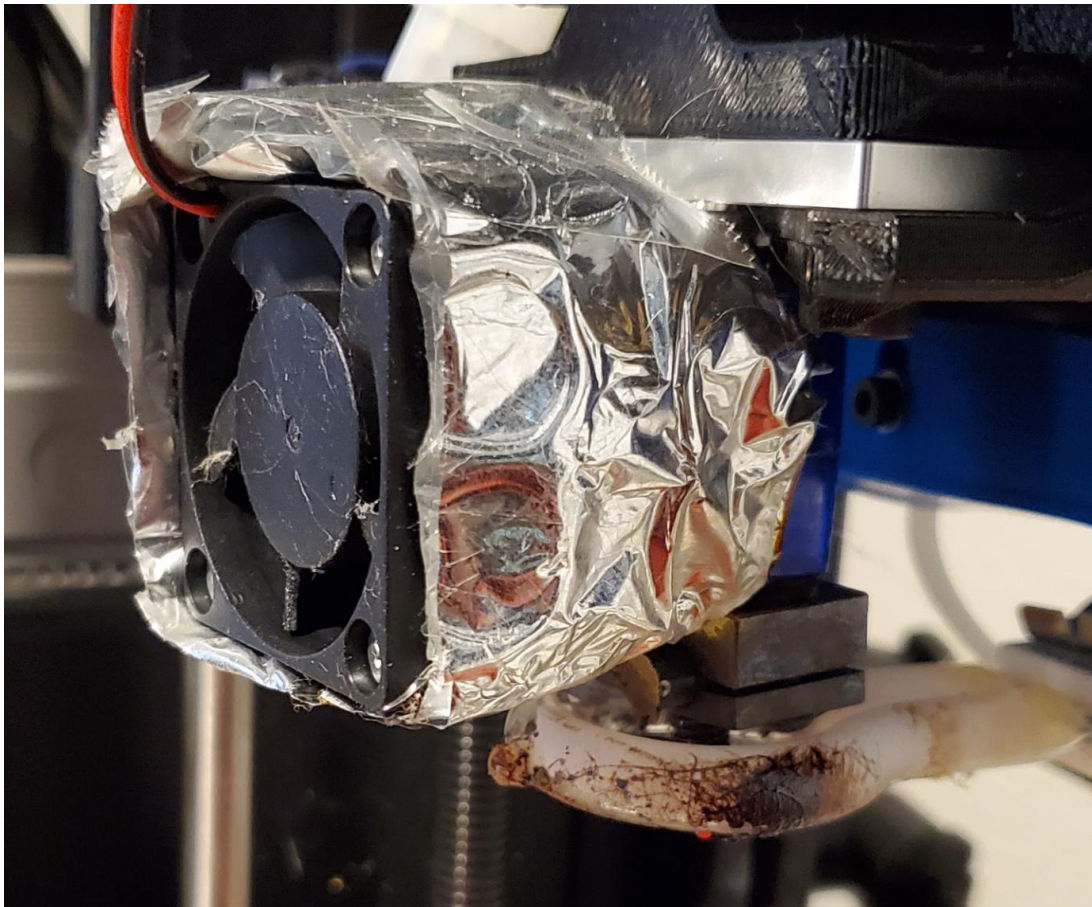


Figure 22. Insulated Fan to block the heat from the Infrared Heat Lamp

The high temperature polymer filaments were prone to taking up moisture from the humidity in the environment. If enough moisture was absorbed into the filament

bubbles would form while printing that resulted in voids in the parts. The filaments were dried in an oven at 120°C for four hours or longer to dry the filaments. A desiccant dryer filament box from PolyBox was used to keep the filaments dry while printing as shown in Figure 23.

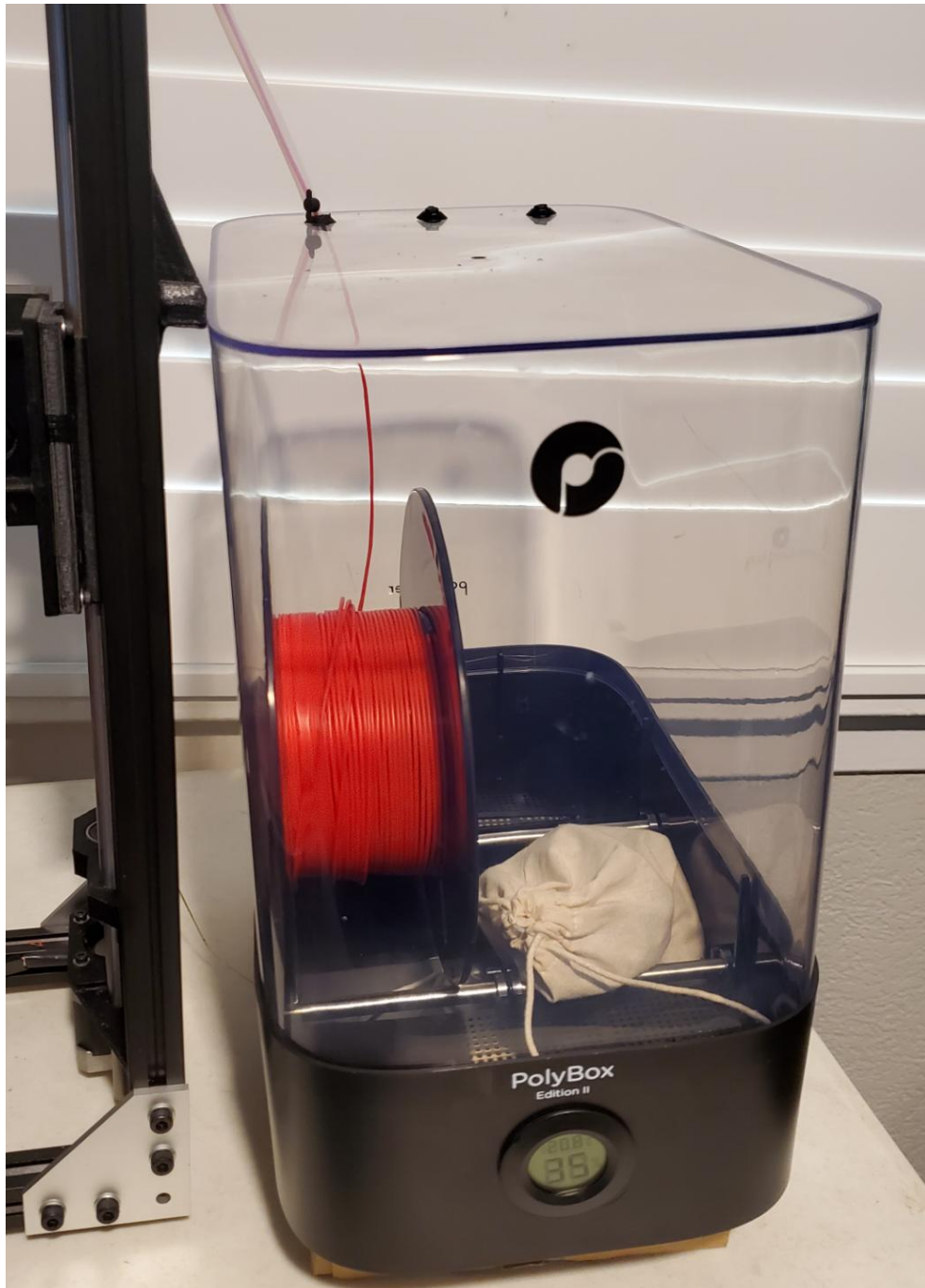


Figure 23. Desiccant Dryer for Filament while Printing

Different adhesion aids were used to get the high temperature filaments to stick to the print bed. Hair spray (Figure 24) and a glue stick (Figure 25) were used. The hair spray worked well for the PLA samples to stick directly to the glass print bed. For the high temperature materials a layer of PEI (Figure 26 to 27) and a layer of Kapton polyamide (Figure 28 to 29) were used to aid the materials to stick to the print bed. However, the PEI wasn't useable at temperatures above 100°C. When the temperature exceeded 100°C the adhesive between the PEI sheet and the print bed would bubble up which would make the surface unlevel for printing. For high temperature materials the best solution was a thin sheet of Kapton polyamide with the glue stick smeared on top.



Figure 24. Hairspray used to Stick Parts to Print Bed

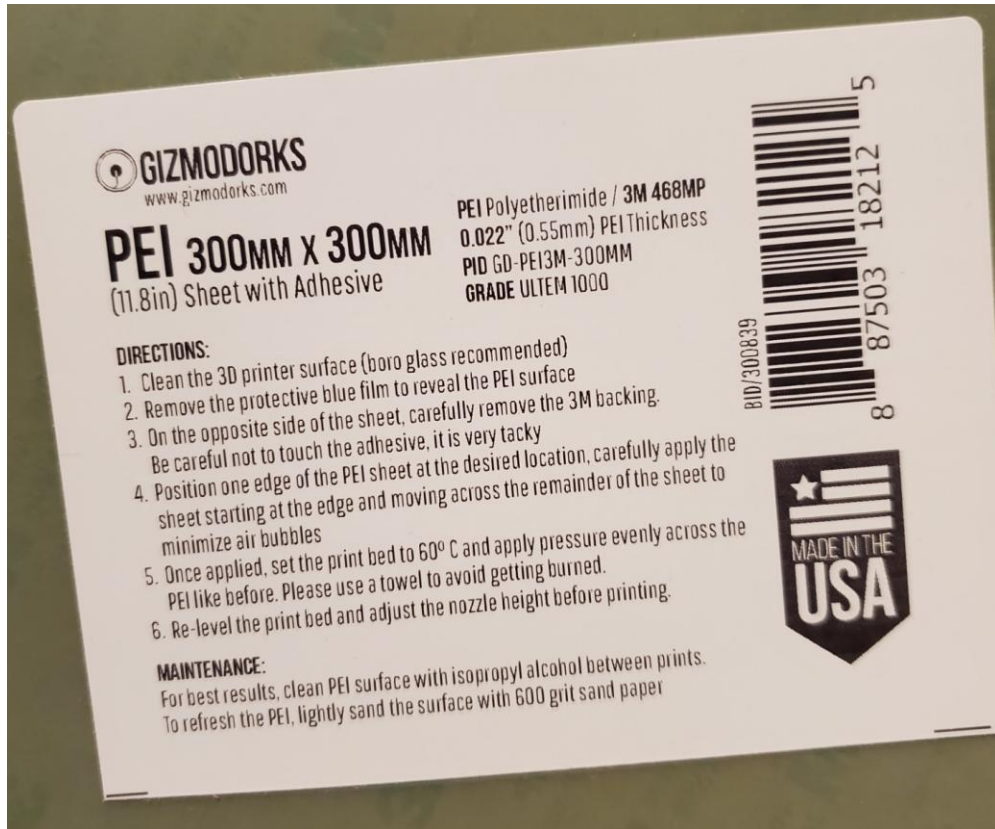


Figure 27. Label of PEI Sheet



Figure 28. Kapton Polyimide Tape to Stick Parts to Print Bed



Figure 29. Label of Kapton Polyimide Tape

Printing with the Omega Infrared Heat Lamp

The modified Lulzbot Taz 5 printer was used to print tensile and flexural specimens. To determine if the heat lamp would improve the mechanical properties of Polylactic Acid (PLA) printed with and without the heat lamp. The heat lamp was also used to determine if high temperature materials such as Poly-Ether-Ketone-Ketone (PEKK), Poly-Ether-Imide (PEI), and Polyether-Ether-Ketone (PEEK) could be printed on a low cost desktop printer such as the Lulzbot Taz 5. Previously these high temperature materials could only be printed with expensive printers that printed with a heated enclosure. The idea is that the material will bond together better when the layers are held close to the Tg.

For PLA the heat lamp was set to 60°C measured with a thermocouple placed near the tip of the nozzle. For the high temperature materials the heat lamp temperature was set to 120°C. There was a trade off to make sure that the parts maintained their dimensional accuracy and was at a temperature close to the Tg but not at it. It was decided that the temperatures would be set near the temperature of the heated print bed.

Figure 30 shows the three print orientations that were used for printing the tensile and flexural specimens. The XY orientation is flat, XZ orientation is on the edge and the ZX orientation is upright. In all three cases the direction of the filament is in the X direction.

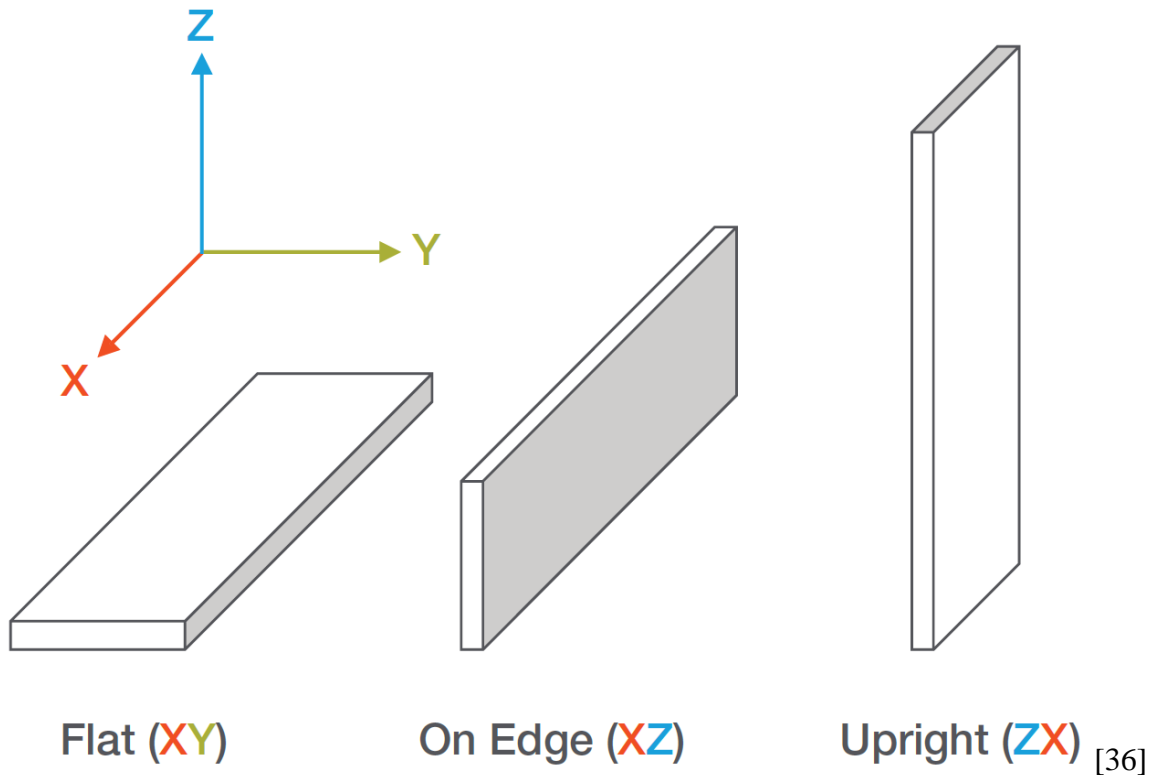


Figure 30. Print Orientation

For tensile testing ASTM D638-14 “Standard Test Method for Tensile Properties of Plastics” was used and for flexural testing ASTM D790-17 “Standard Test Methods for Flexural Properties of Unreinforced and Reinforced Plastics and Electrical Insulating Materials” was used. The tensile specimens used a Type I specimen with a thickness of 3.3 mm. The flexural test specimens were 12.70 mm x 3.175mm x 76.20 mm [37,38]. Table 2 shows the suggested material printing parameters for the materials that are used in this study.

Table 2. Material Printing Parameters

	Extrude Low (°C)	Extrude High (°C)	Bed Low (°C)	Bed High (°C)	Tg (°C)	Melt (°C)	Enclosure Low (°C)	Enclosure High (°C)
PEEK	375	410	130	145	143	343	70	140
PEKK	345	375	120	140	162	335	70	150
PEI	370	390	120	160	217	NA	warm	hot
PLA	190	220	25	60	62	180		

PLA is one of the most commonly used materials in FFF 3D printing because it prints at a low temperature of 190°C to 220°C and is relatively low cost. The material can be used in all desktop printers. A heated bed is not required. The bed temperature can be from 23°C to 60°C. A glue stick or hairspray is recommended to stick the first layer to the print bed. PLA is environmentally friendly because it is biodegradable. [39]

Unreinforced semicrystalline PLA has a tensile strength of 50 to 70 MPa, tensile modulus of 3 GPa, flexural strength of 100 MPa, a flexural modulus of 5 GPa, and an elongation at break of 4%. Most injection moldable PLA has some type of fiber reinforcement to increase the mechanical properties [40].

For the upright test specimens a base that held the specimens was used to make sure that it would stay on the print bed because of the large aspect ratio. Figure 31 shows the Upright (ZX) tensile specimens, Figure 32 shows the Flat (XY) tensile specimens, and Figure 33 shows the on Edge (XZ) tensile specimens being printed out of PLA.

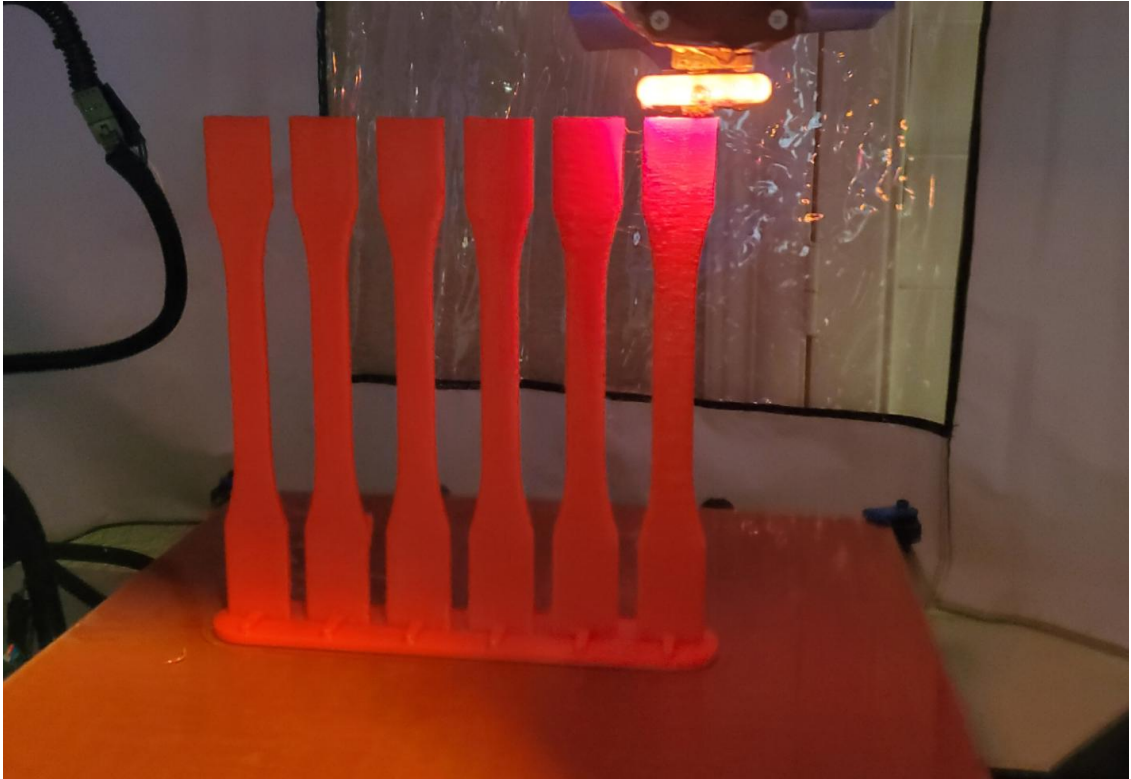


Figure 31. Printing Upright (ZX) PLA Tensile Specimens



Figure 32. Printed Flat (XY) PLA Tensile Specimens



Figure 33. Printed PLA Tensile Specimens on the Edge (XZ)

Figure 34 shows the on Edge (XZ) flexural test specimens and Figure 35 shows the Upright (ZX) flexural test specimens. Figure 35 is showing the Upright PLA flexural specimens that were printed without the heat lamp. Figure 36 shows the Upright PLA flexural specimen that had too much heat from the heat lamp and the part did not hold the required dimensional accuracy. For this part the heat lamp had to stay off until the base had been printed.

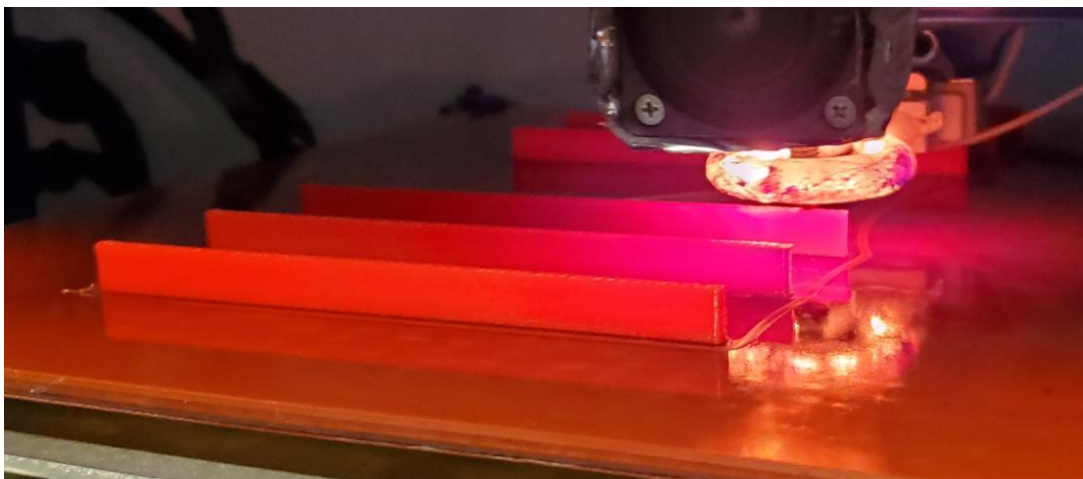


Figure 34. Printed PLA Flexural Specimens on the Edge (XZ)

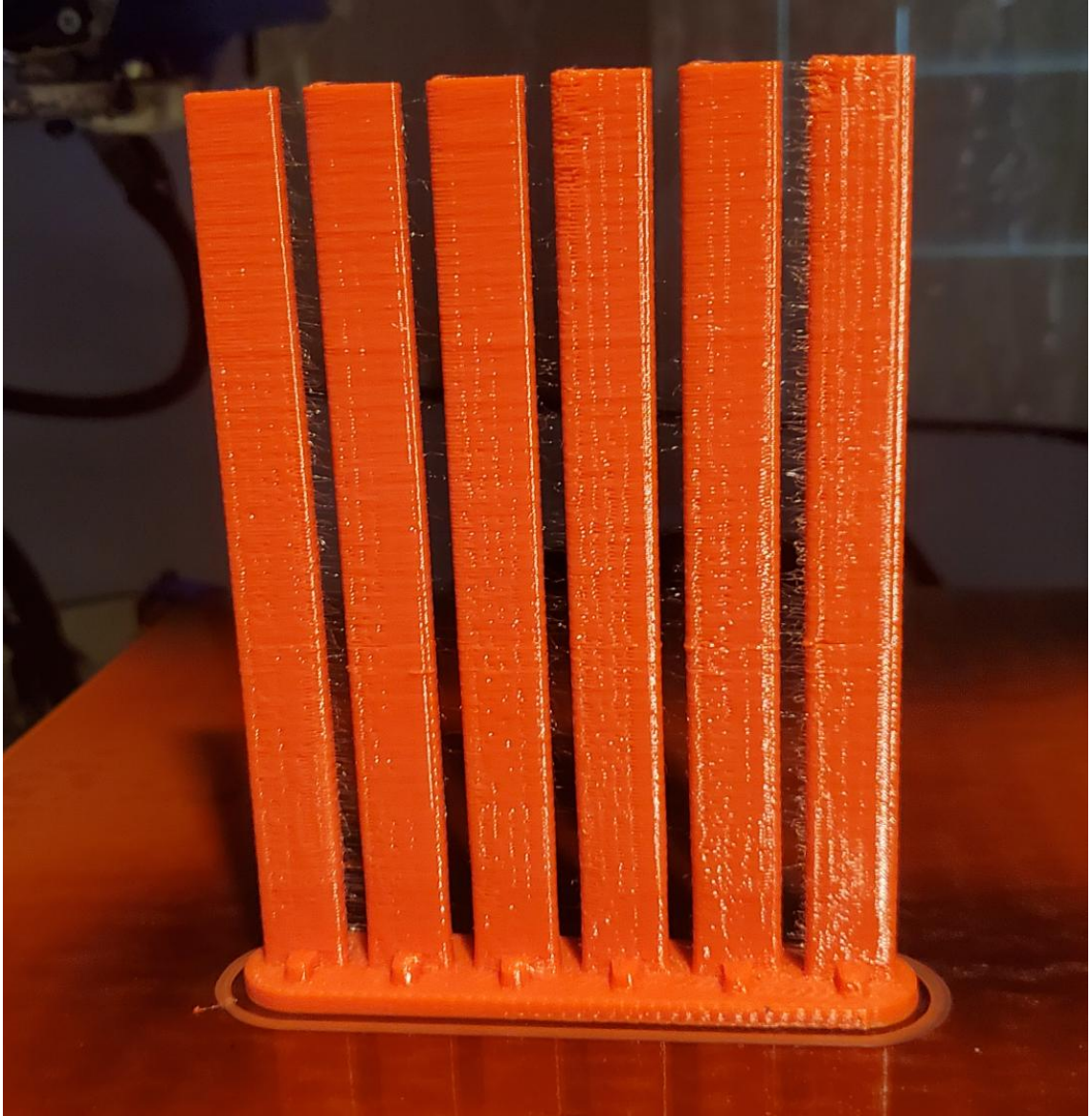


Figure 35. Printed PLA Flexural Specimens Vertical

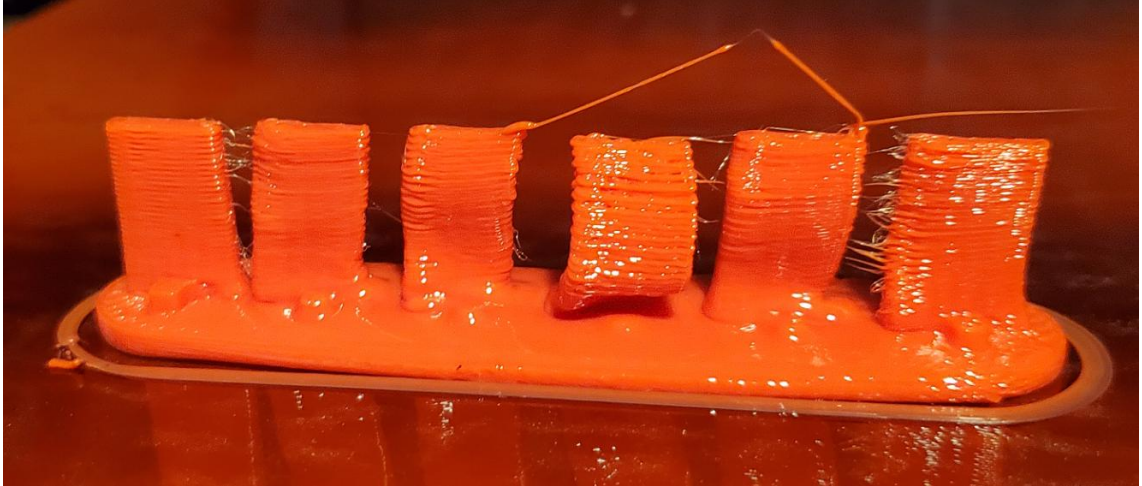


Figure 36. The first attempt at printing the Upright PLA Flexural Specimens

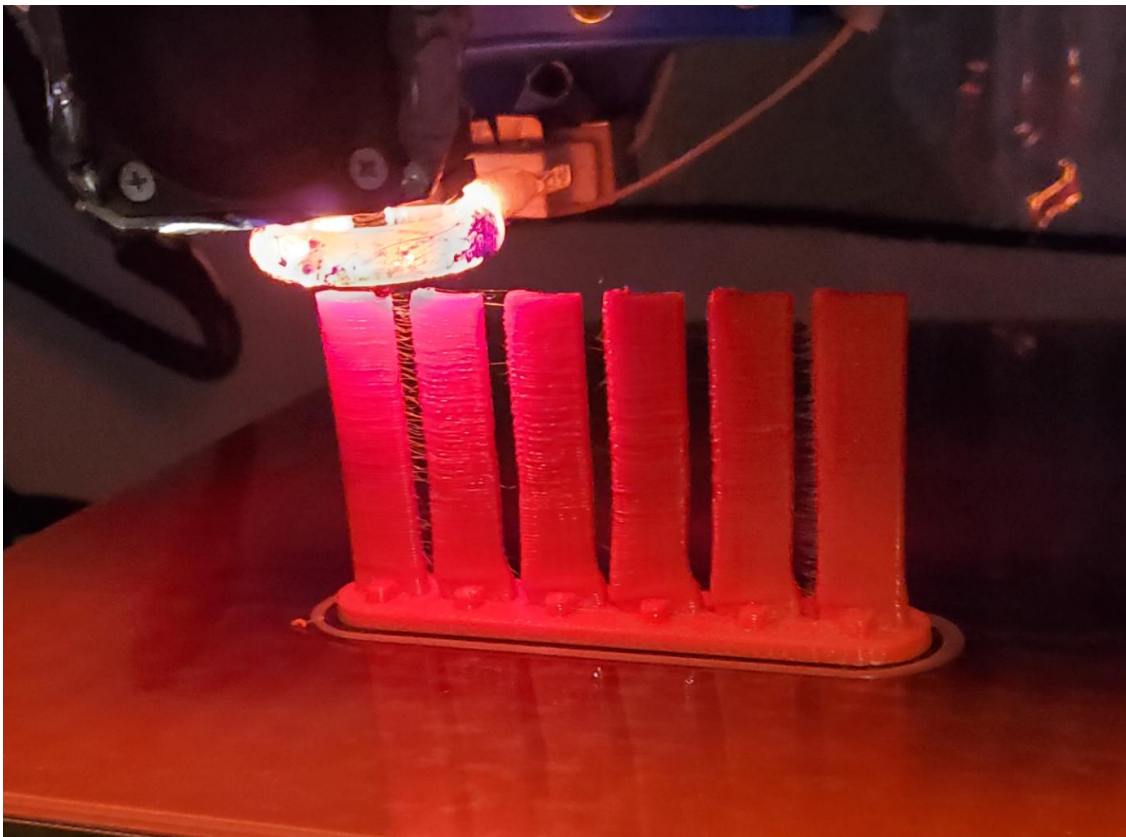


Figure 37. Printing the Upright PLA Flexural Test Specimens with the Heat Lamp

ThermaX™ PEKK 3D Filament (PEEK-C) from 3DXTECH was used for the 3D printing trials. PEKK has great mechanical, thermal, and chemical resistance performance. PEKK has proven to be easier to print with than PEEK because it has a lower rate and degree of crystallinity. The recommended extrusion temperature for

PEKK is 340°C to 360°C. The PEKK-C formulation is a 70/30 PEKK copolymer with a continuous use temperature of 260°C. The melt temperature is 335°C and the Tg is 162°C. PEKK has a low smoke generation and a UL94 V-0 flame resistance which makes it acceptable for aerospace applications. An extruder temperature of 345°C to 375° and a bed temperature of 120°C to 140°C are recommended. If a heated enclosure is used it is recommended at 70°C to 150°C. It is best to dry the filament out at 120°C for a minimum of four hours. If moisture is picked up from the atmosphere bubbles will form in the filament when extruded. The printed parts can be annealed to increase the crystallinity to increase the mechanical, thermal, and chemical resistance to increase the maximum use temperature from 150°C to 260°C. The annealing process calls for 30 minutes at 160°C, then 200° in an oven until the color turns to a uniform tan color [41].

KEPSTAN™ PEKK 6000 series is an unfilled injection moldable PEKK material. The mechanical properties are a tensile strength of 88 MPa, tensile modulus of 2.9 GPa, flexural strength of 128 MPa, and a flexural modulus of 3.0 GPa [42].

Stratasys Antero™ 800NA is a PEKK filament that is used in their F900 and Fortus 450mc printers. The technical data sheet reports the properties printed on edge in the XZ orientation and upright in the ZX orientation as shown in the following figure. It is assumed that the Flat (XY) orientation was not printed because the results would match the on Edge (XZ) orientation. The mechanical properties are a tensile strength of 90 MPa to 93 MPa in the XZ orientation and 45 MPa to 55 MPa in the ZX orientation, tensile modulus of 2.9 GPa to 3.1 GPa in the XZ orientation and 2.8 GPa to 3.5 GPa in the ZX orientation, flexural strength of 140 MPa in the XZ orientation and 65MPa to 90 MPa in

the ZX orientation, and a flexural modulus of 3.1 in the XZ orientation and 2.7 in the ZX orientation. [43]

Figure 38 to 40 shows the printing of PEKK on Edge (XZ) tensile specimens. Figure 41 shows printing PEKK flat (XY) with a $\pm 45^\circ$ infill tensile specimens. Figure 42 shows printing of PEKK flat (XY) tensile specimens with the extrusion in the X direction. Figure 43 shows the printing of the upright (ZX) tensile specimens. The accuracy of the specimens declined as the height grew. Figure 44 and 45 shows the upright (ZX) flexural specimens. The bottom portion has a darker color because of the heat interaction between the heat lamp and the heated print bed. Figure 46 shows the on Edge (XZ) flexural test specimens printing with PEEK.

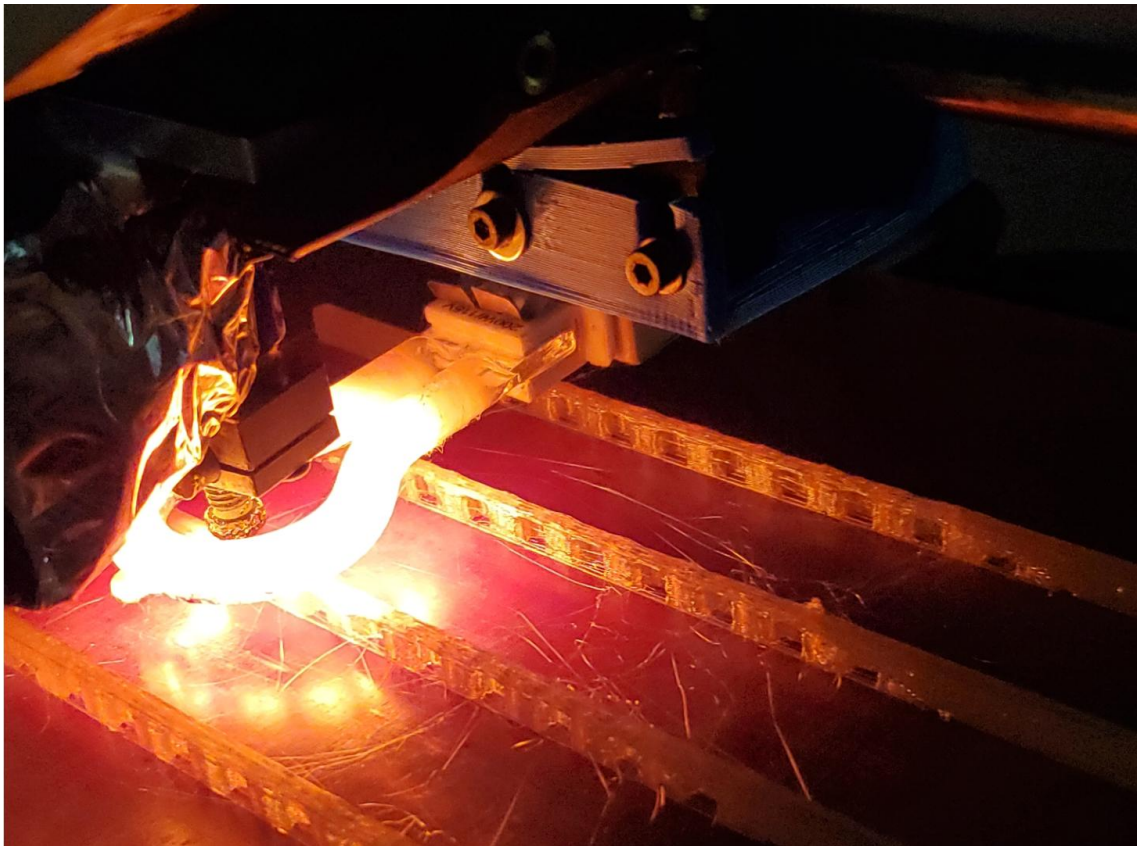


Figure 38. Printing PEKK Tensile Specimens on the Edge (XZ)



Figure 39. Printing PEKK Tensile Specimens on the Edge (XZ) Image 2

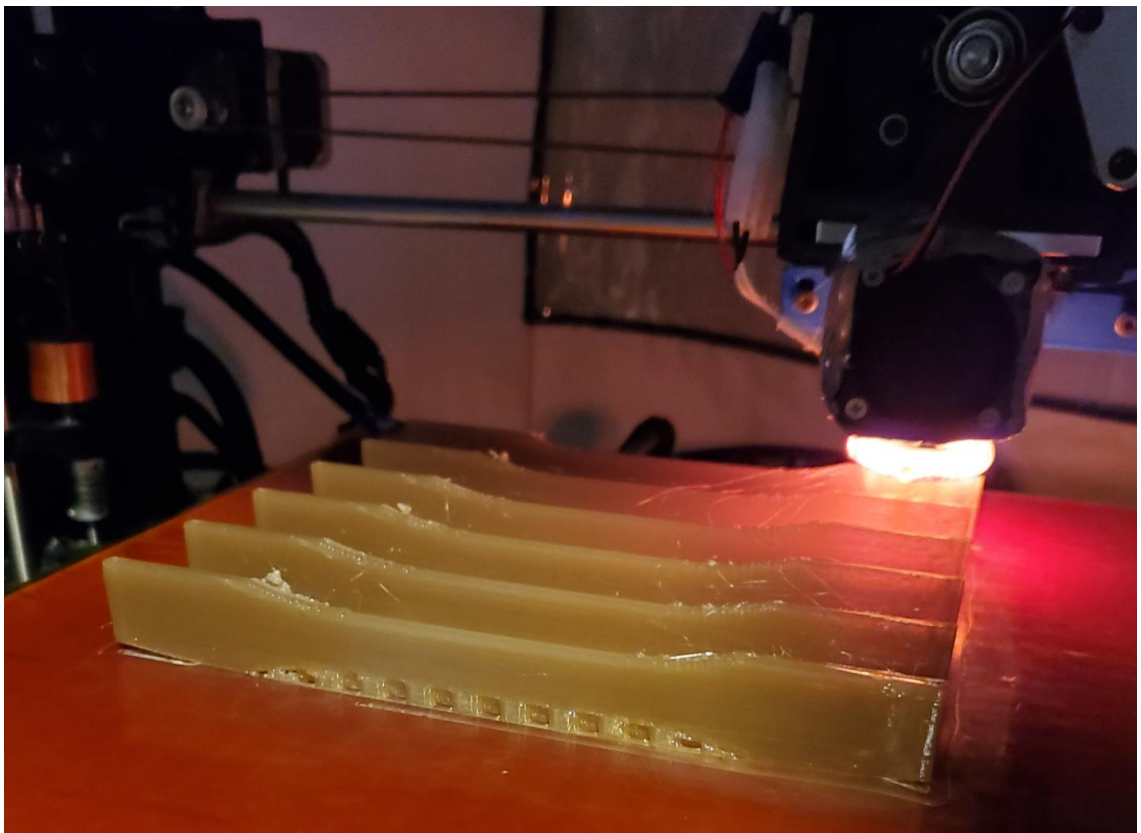


Figure 40. Printing PEKK Tensile Specimens on Edge (XZ) Image 3

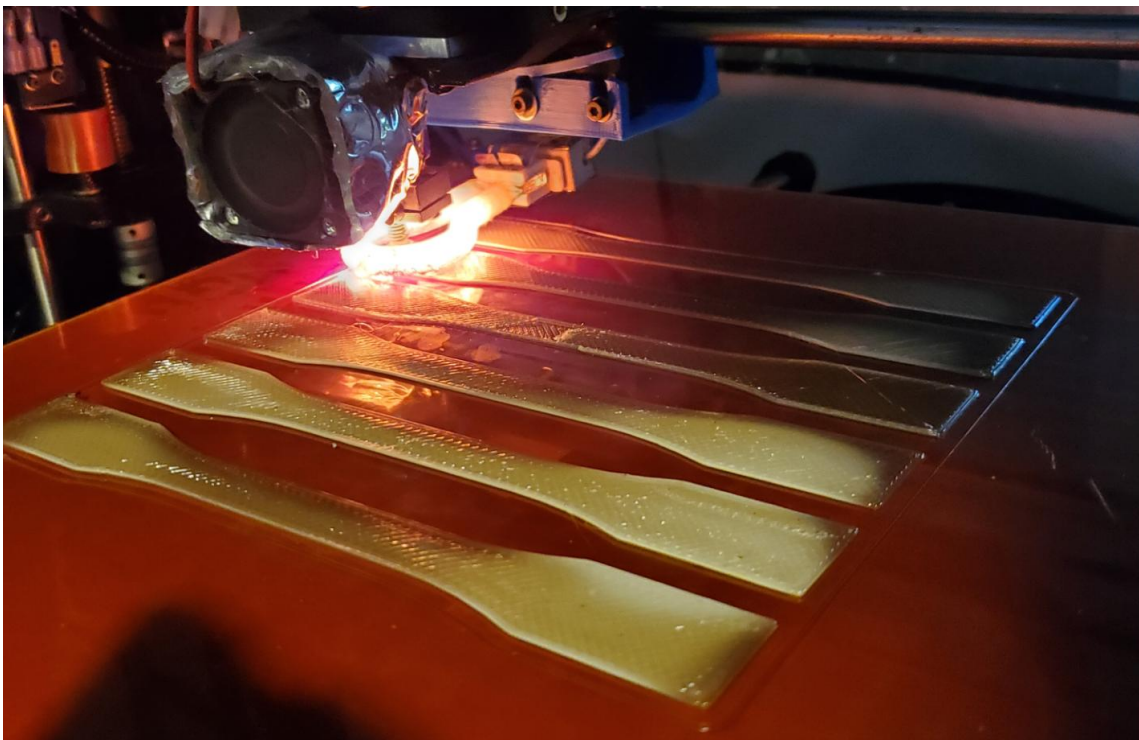


Figure 41. First Attempt at Printing PEEK Tensile Specimens Flat (XY)

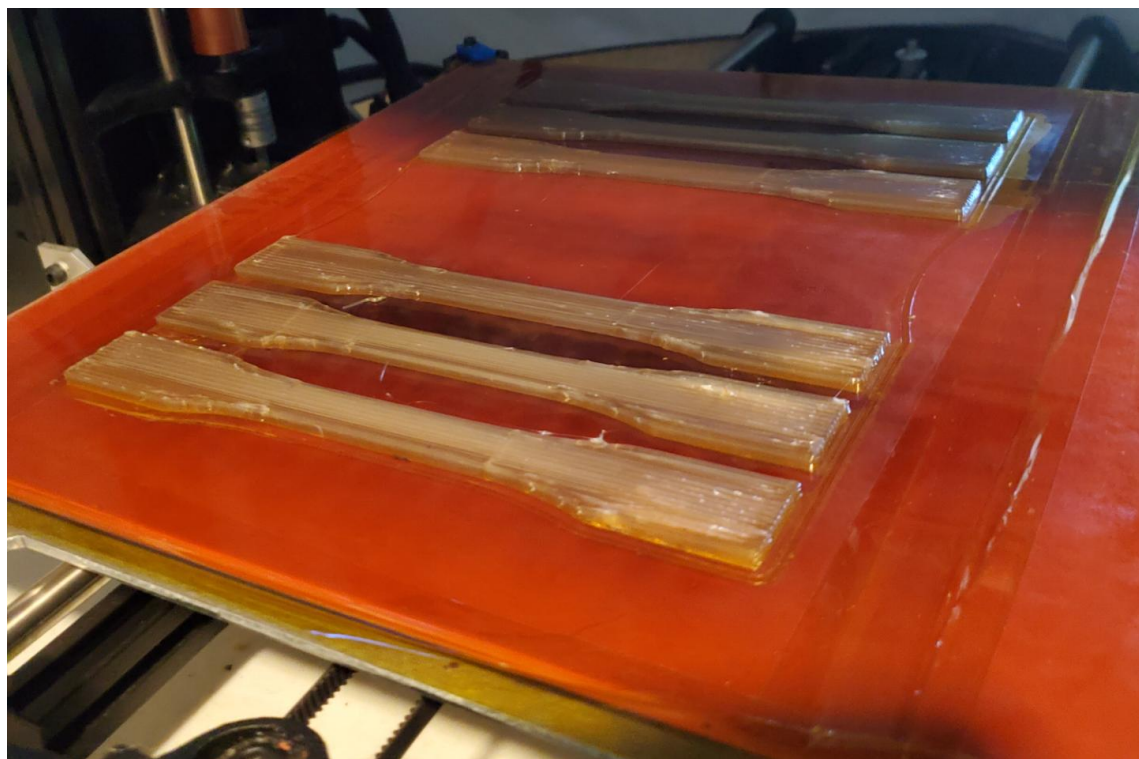


Figure 42. Printed Flat (XY) PEKK Tensile Specimens

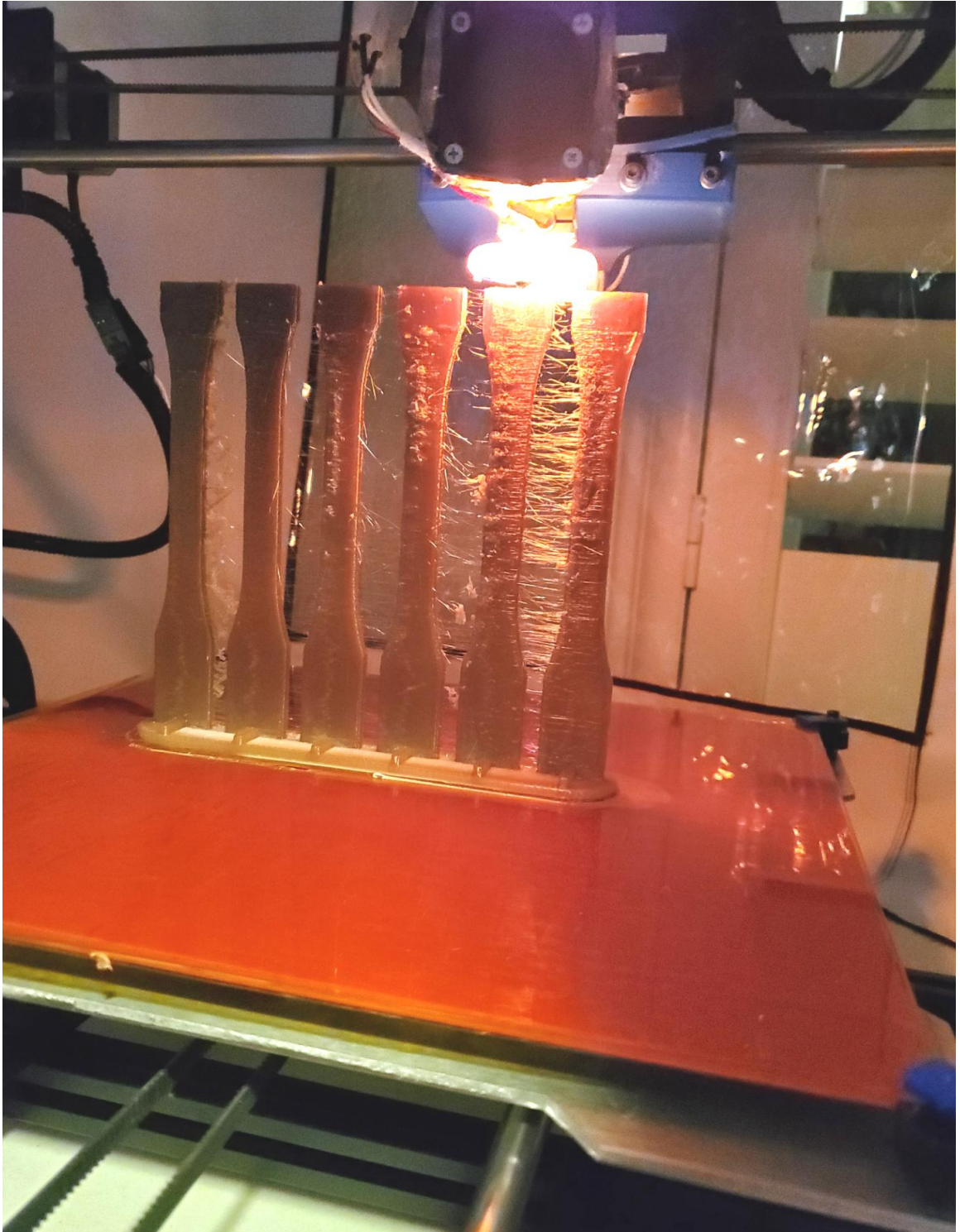


Figure 43. Printing PEKK Upright (ZX) Tensile Specimens

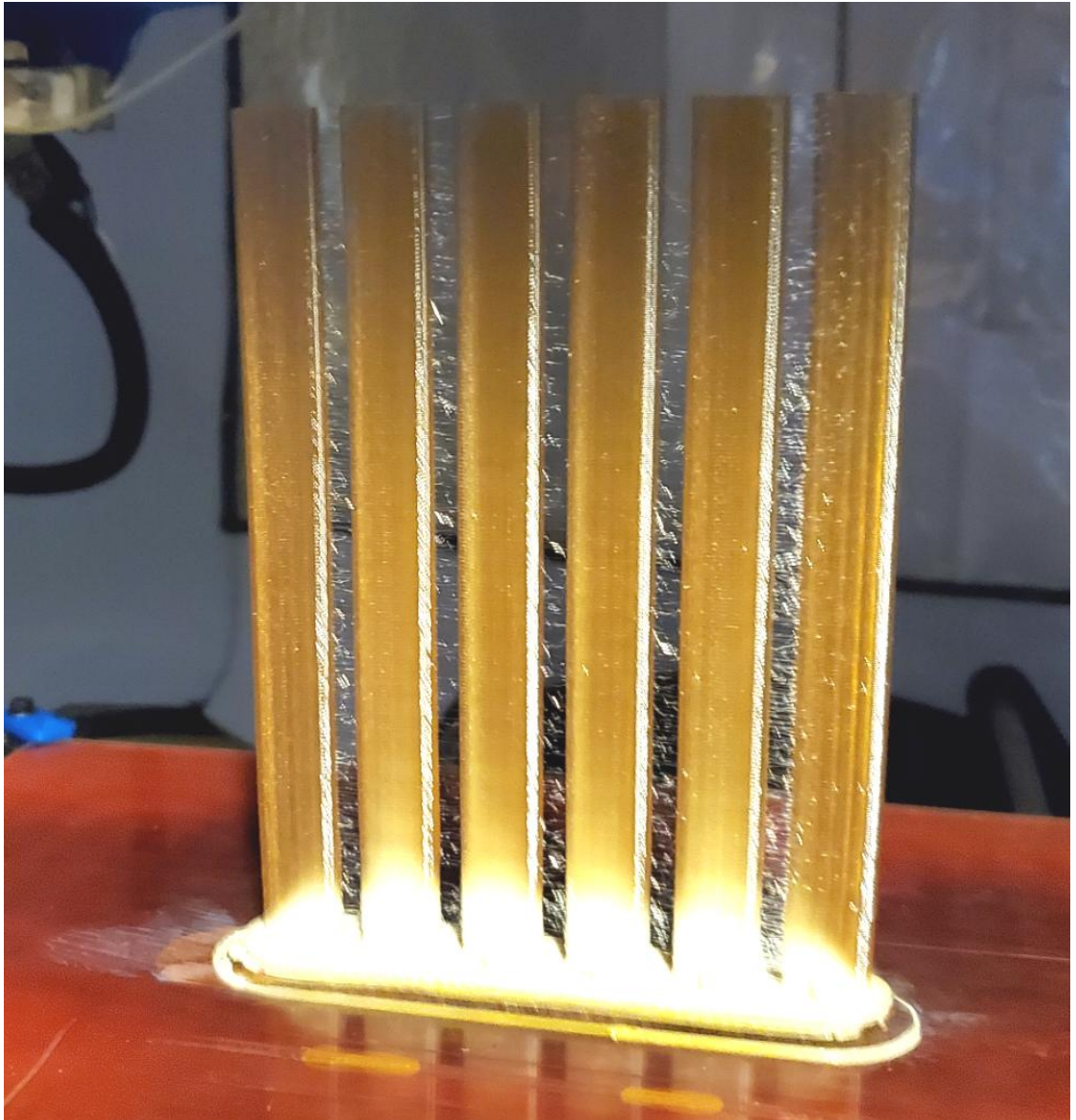


Figure 44. Printing PEKK Upright (ZX) Flexural Specimens Image 1



Figure 45. Printing PEKK Upright (ZX) Flexural Specimens Image 2

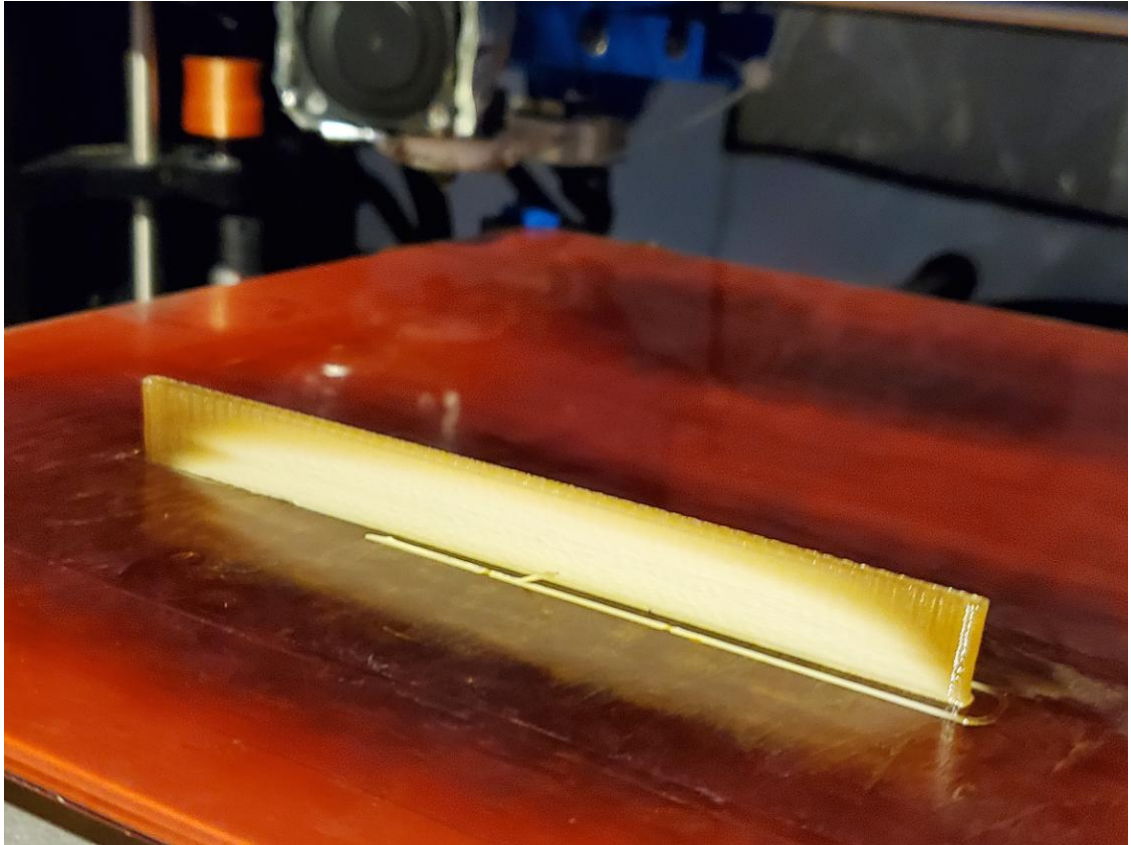


Figure 46. Printing PEKK on Edge (XZ) Flexural Specimen

ThermaX™ PEI Filament made using Ultem™ 1010 PEI from 3DXTECH was used in the experimentation. PEI is an amorphous polymer with great thermal properties, dimensional stability, low creep sensitivity, flame retardancy, and chemical resistance. The T_g is 217°C that contributed to the high strength and modulus at elevated temperatures. The recommended print conditions are an extruder temperature of 370°C to 390°C , bed temperature of 120°C to 160°C , and a hot build environment. The drying instructions are the same as PEEK and PEKK at 120°C for four hours or more. Printed in stresses can affect the mechanical properties. An annealing process of 150°C for one hour, 200°C for one hour, reducing the heat to 150°C for thirty minutes and then slowly cooling in the oven can relieve the built in stresses to increase the mechanical properties [44].

RTP 2100 is an unreinforced Ultem 1010 PEI material that is injection molded. The material properties are tensile strength of 109 MPa, tensile modulus of 3.31 GPa, flexural strength of 145 MPa, and flexural modulus of 3.31 MPa [45].

Stratasys Ultem 1010 is a PEI filament that is used in their Fortus 900mc printer. The technical data sheet reports the properties printed on edge in the XZ orientation and upright in the ZX orientation as shown in the following figure. The mechanical properties are a tensile strength of 80 MPa in the XZ orientation and 30 MPa in the ZX orientation, tensile modulus of 3.0 GPa in the XZ and the ZX orientation, flexural strength of 130 MPa in the XZ orientation and 80MPa in the ZX orientation, and a flexural modulus of 2.91 in the XZ orientation and 2.6 in the ZX orientation. [46]

Figure 47 shows the printing of the Upright (ZX) specimens using PEI and Figure 48 shows after the printing was finished. Figure 49 shows printing PEI on Edge (XZ). These specimens were difficult to print in PEI as they would tend to warp at the sides and pull away from the print bed. Figure 50 shows printing the flat (XY) flexural specimens. For all these specimens the printing worked best on Kapton polyimide sheets with a glue stick on top of the polyamide. The polyamide would stick to the specimen so well that it tends to be bonded to the parts after printing.

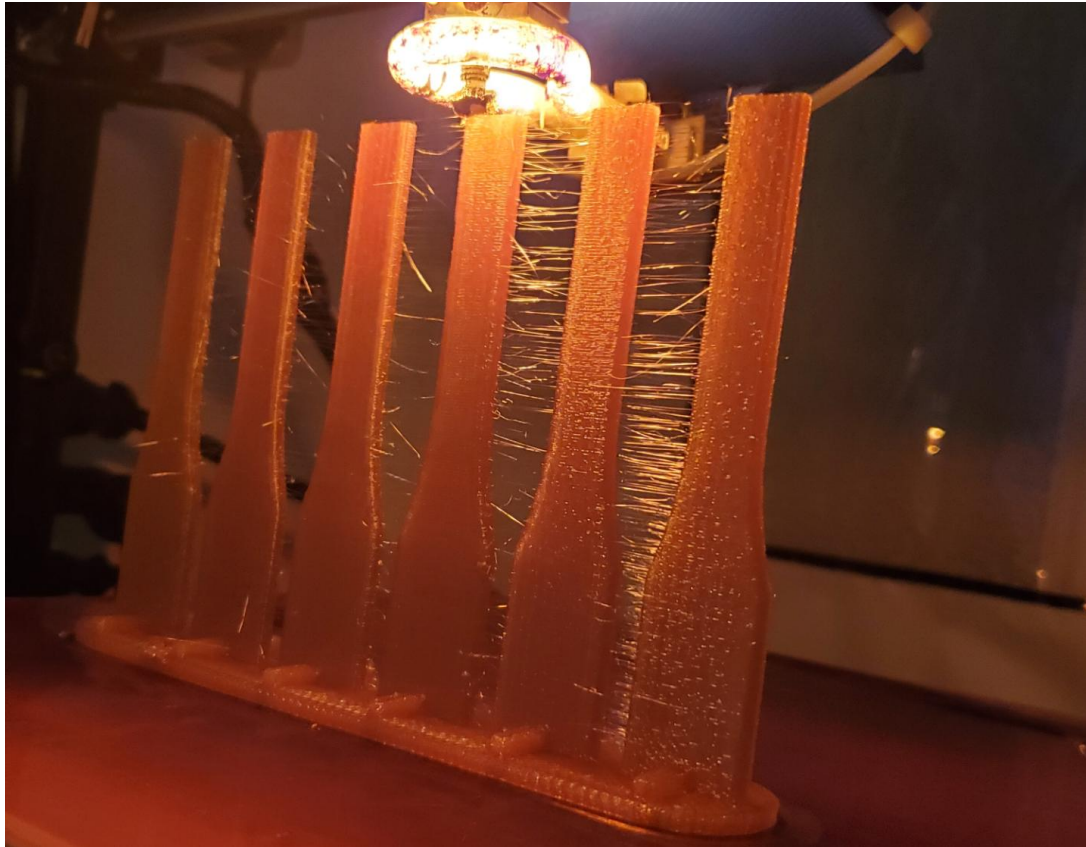


Figure 47. Printing PEI Upright (ZX) Tensile Specimens

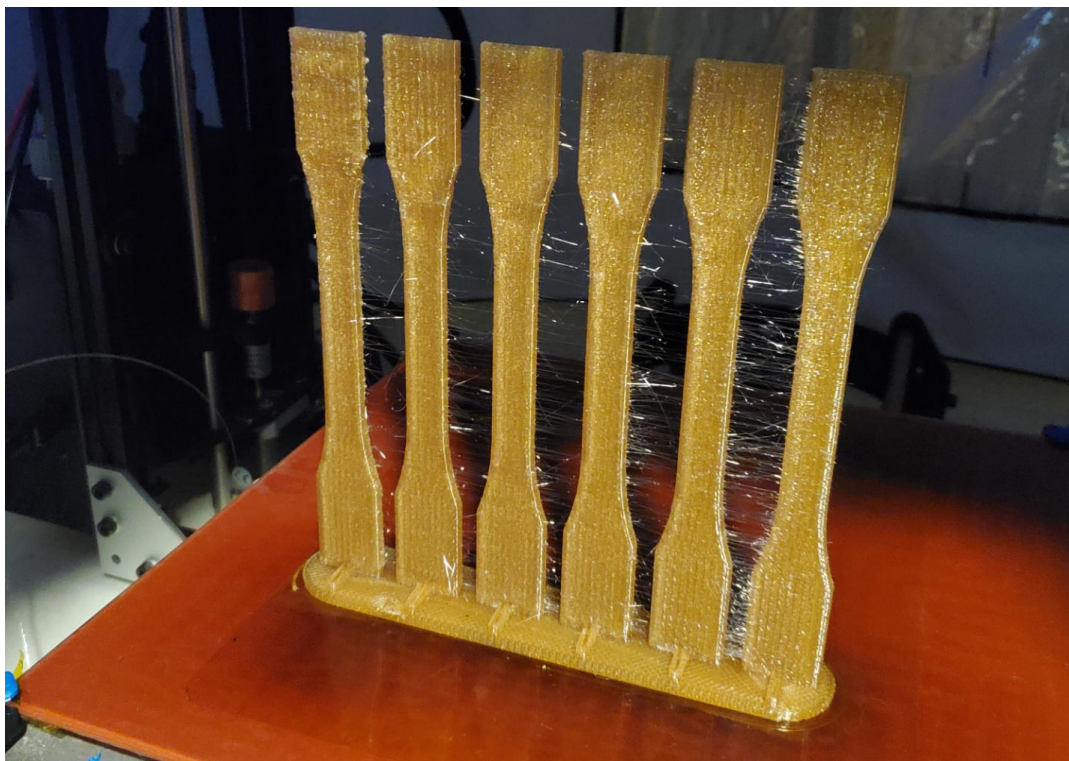


Figure 48. Finished PEI Upright (ZX) Tensile Specimens

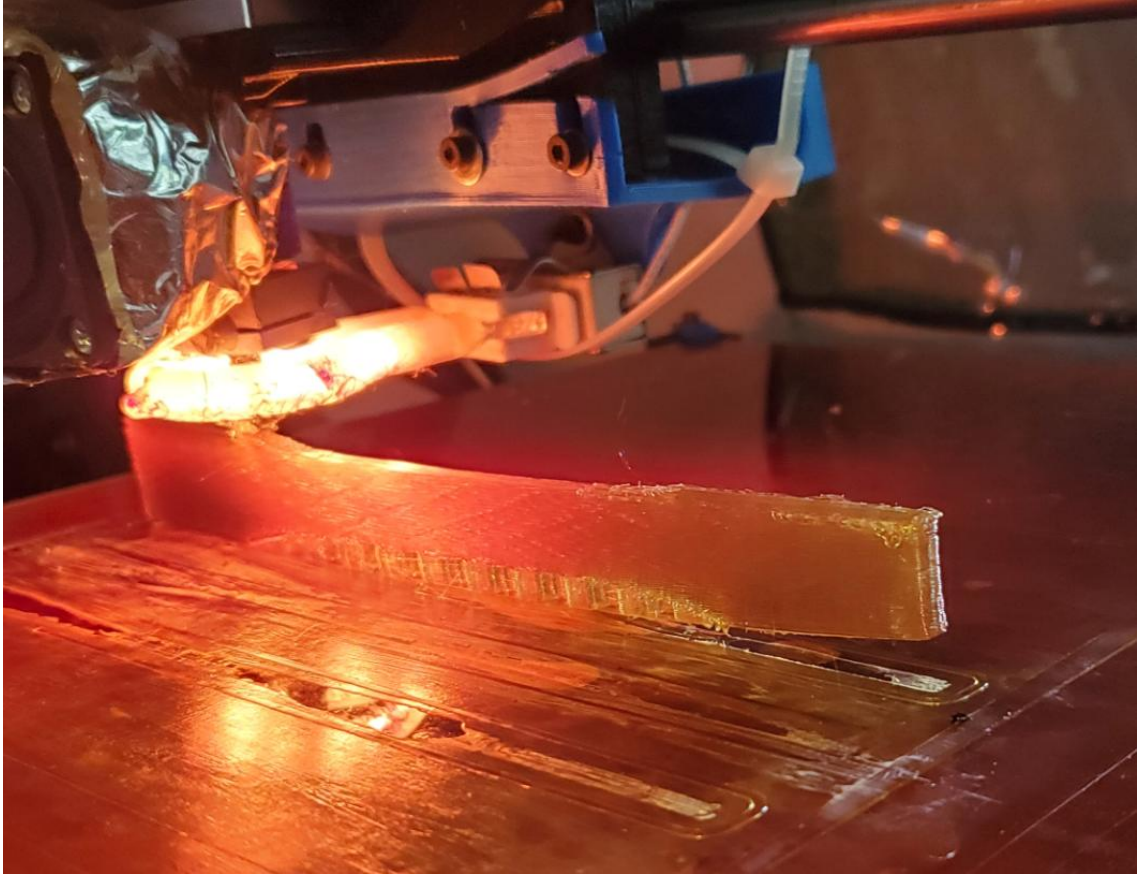


Figure 49. Printing PEI on Edge (XZ) Tensile Specimens



Figure 50. Printing PEI Flat (XY) Flexural Specimens

PEEK is a high performance material. It is a semi-crystalline polymer that has mechanical qualities of high strength, stiffness and toughness. The degree of crystallinity changes with the rate of cooling from the liquid state. Slower cooling rates produce more crystallinity. AM of PEEK using open source FFF printers currently does not easily or inexpensively allow for the printing due to the difficulties of producing FFF machines that operate at the temperatures capable of printing PEEK with a melting point of 343°C and a flow point of 400°C. The optimal parameters for printing PEEK without warping and delamination of the part and avoiding polymer degradation are a hot end temperature of 410°C, heated bed of 130°C to 145°C and an ambient temperature of 70°C to 140°C. The importance of heat management during the printing process is to get adhesion to the build plate, layer to layer bonding, and an environmental heat distribution around the part to increase the crystallinity produced in the printed PEEK [3]. For the experiments ThermaX™ PEEK Natural from 3DXTECH was used [47]. The annealing process calls for a ramp up at 10°C steps per hour, then soak at 200°C for 1 hour per mm of part thickness, then ramp down at 10°C per hour to 140°C [48].

The FFF printing process inherently has a reduction in the tensile strength of the polymer compared to an injection molded part. Wu et al has reported injection molded PEEK has a tensile strength of 100 MPa whereas FFF printed peak with a 100% infill has a tensile strength of 57 MPa. This can be attributed to the porosity that is created by the air gaps in the infill pattern and air bubbles that can be inside the filament. The recommended printing temperature for PEEK to extrude for FFF is 410°C which is 67°C above the melting temperature. The recommended temperature for the build plate is 130°C and 80°C for the ambient environment. However typical off the shelf desktop FFF

printers have a maximum hot end temperature of 260°C, build plate temperature of 100°C, and ambient environment temperature at room temperature. [3]

RTP 2200 LF PEEK is an unreinforced injection molded PEEK. This material has a tensile strength of 93 MPa, tensile modulus of 3.79 GPa, flexural strength of 145 MPa, and a flexural modulus of 3.79 GPa [49].

3DXTECH has published material properties for ThermaX PEEK using FFF. Rahman et. al. at South Dakota State University has also published PEEK properties using FFF on a Arevo Labs 3D printer. They report the properties in the flat XY orientation only. The ThermaX PEEK mechanical properties are a tensile strength of 100 MPa, tensile modulus of 3.72 GPa, flexural strength of 130 MPa, and a flexural modulus of 2.7 GPa [50]. The Arevo Labs 3D printer PEEK by South Dakota State University mechanical properties are a tensile strength of 73.013 MPa, tensile modulus of 2.78 GPa, flexural strength of 111.67 MPa, and a flexural modulus of 1.919 GPa [51].

PEEK is by far the most difficult of these materials to print. Without the heat lamp there wouldn't be any bonding between the layers. Figure 51 shows the printing of the on Edge (XZ) specimens. The first attempt had too much warpage on the sides to get a good print. It was determined that the best way to print the material was to print one specimen at a time. Figure 52 to 55 shows the printing attempts of the upright (ZX) specimens out of PEEK. None of the attempts at printing the upright tensile or flexural specimens out of PEEK were successful. The parts would easily break apart in your hands. Figure 56 shows the printing of the flat (XY) flexural specimens and Figure 57 shows the printing of the on Edge (XZ) flexural specimens.

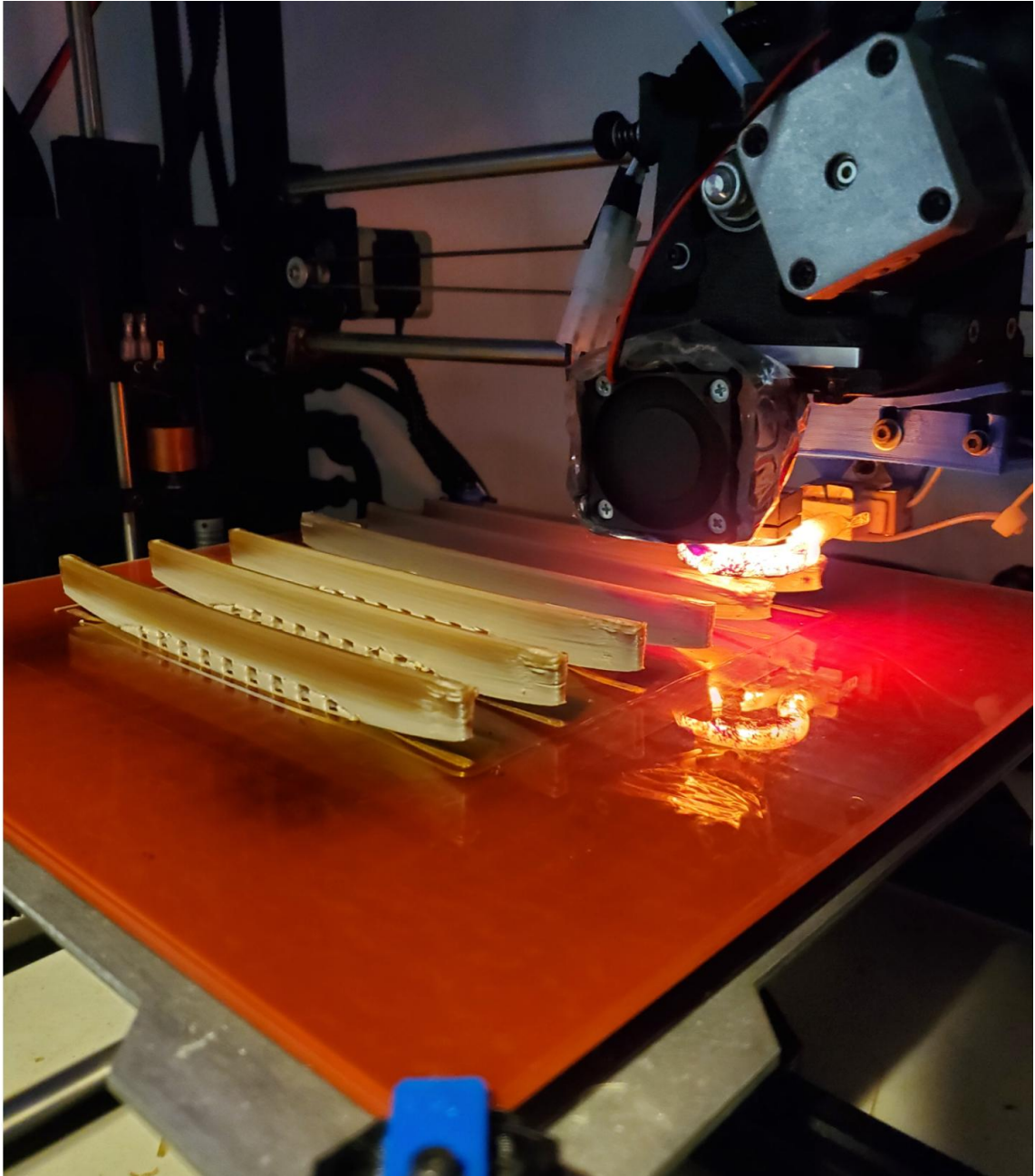


Figure 51. First Attempt at Printing PEEK Tensile Specimens on the Edge (XZ)

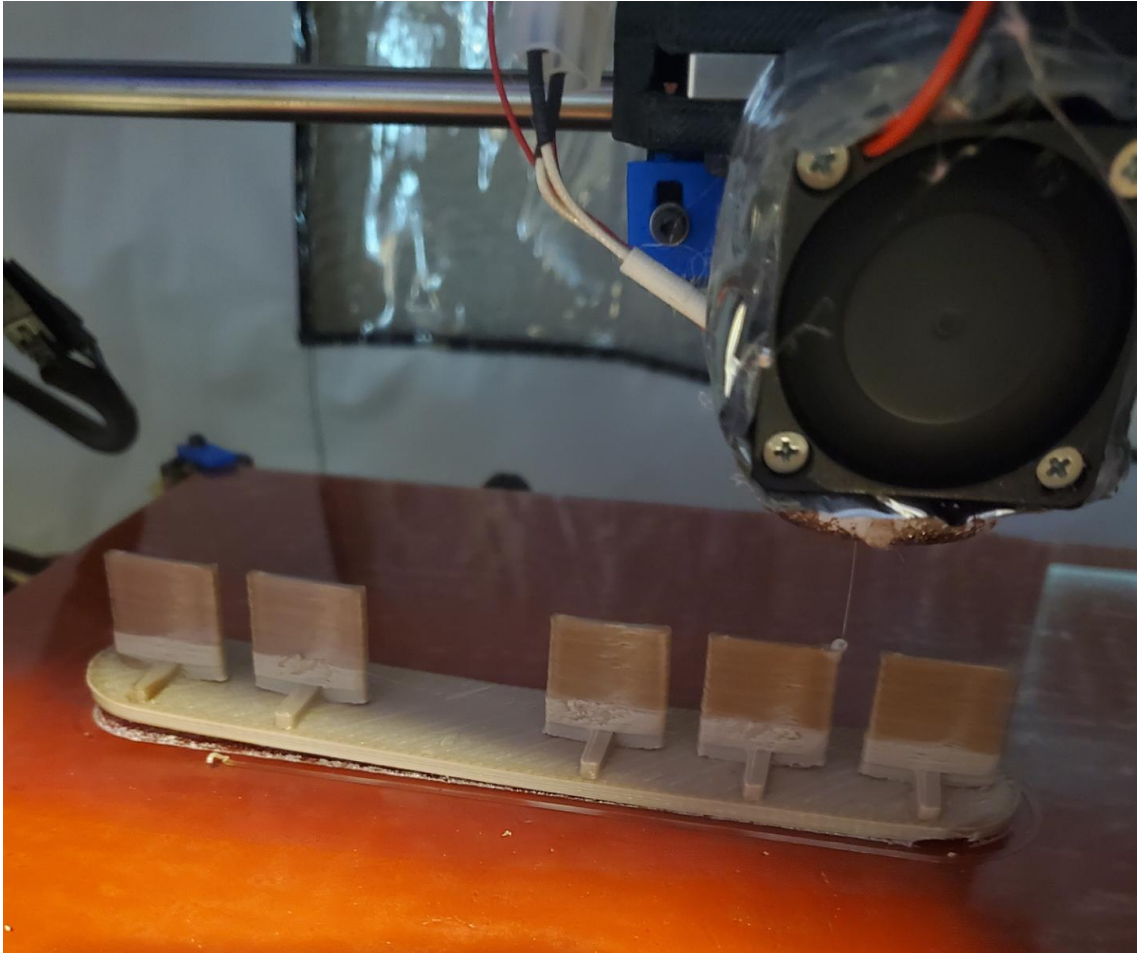


Figure 52. First Attempt at Printing PEEK Upright (ZX) Tensile Specimens

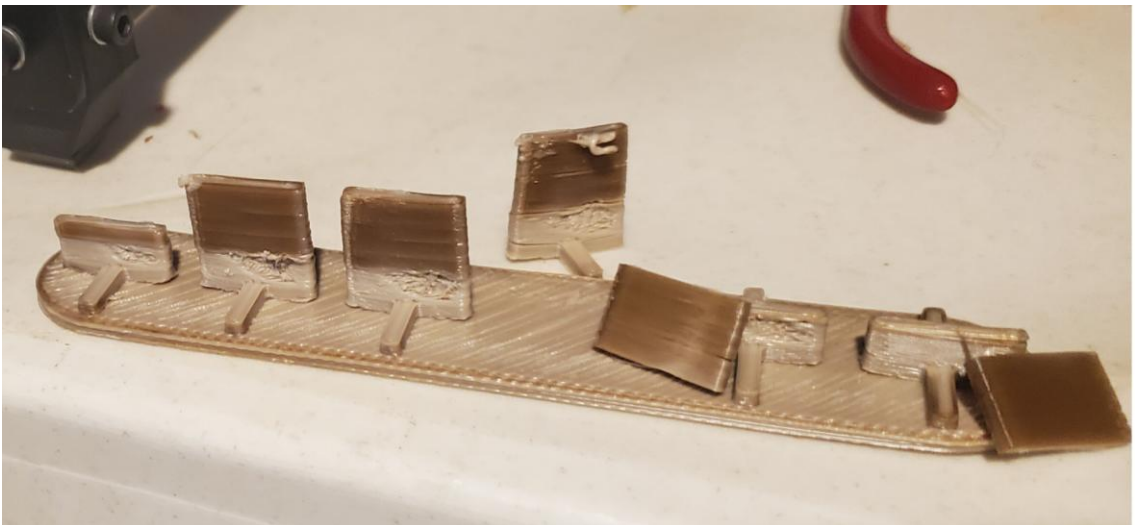


Figure 53. First Attempt at Printing PEEK Upright (ZX) Tensile Specimens that Broke off and had no Bonding between Layers

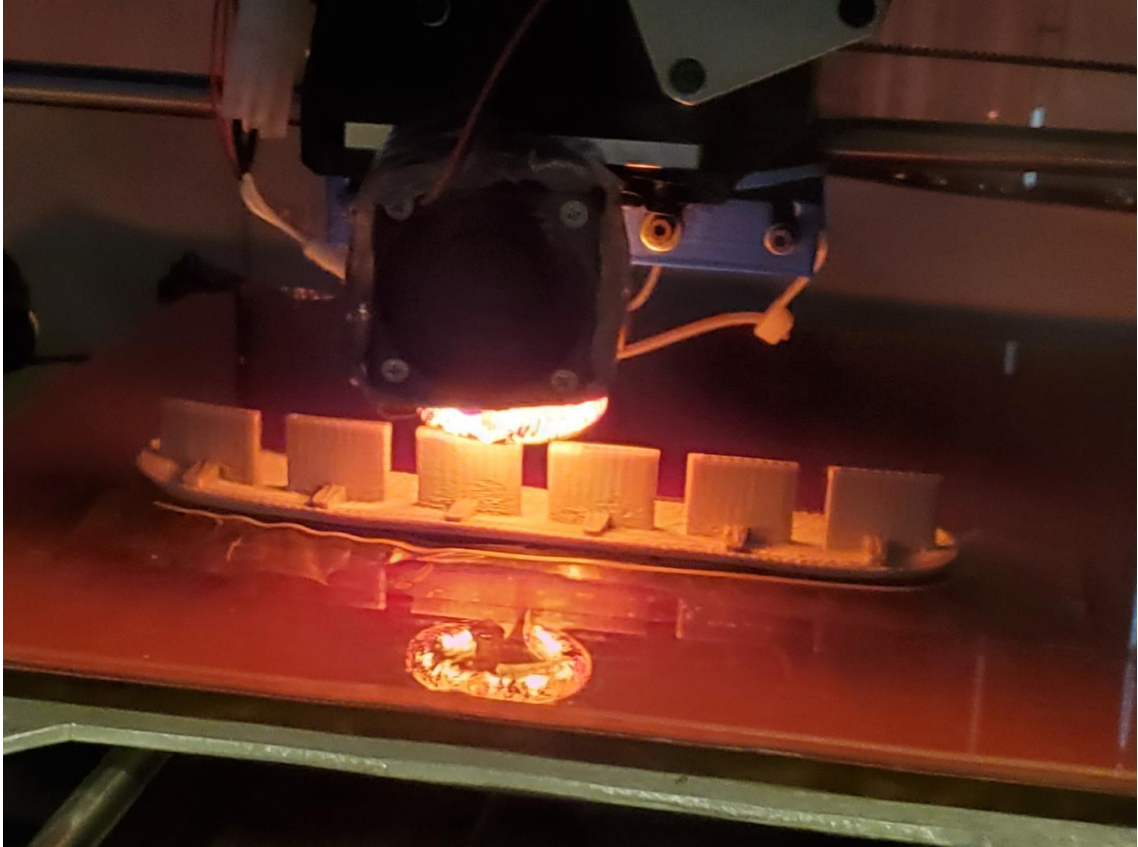


Figure 54. Second Attempt at Printing PEEK Upright (ZX) Tensile Specimens with Warpage at the Print Bed

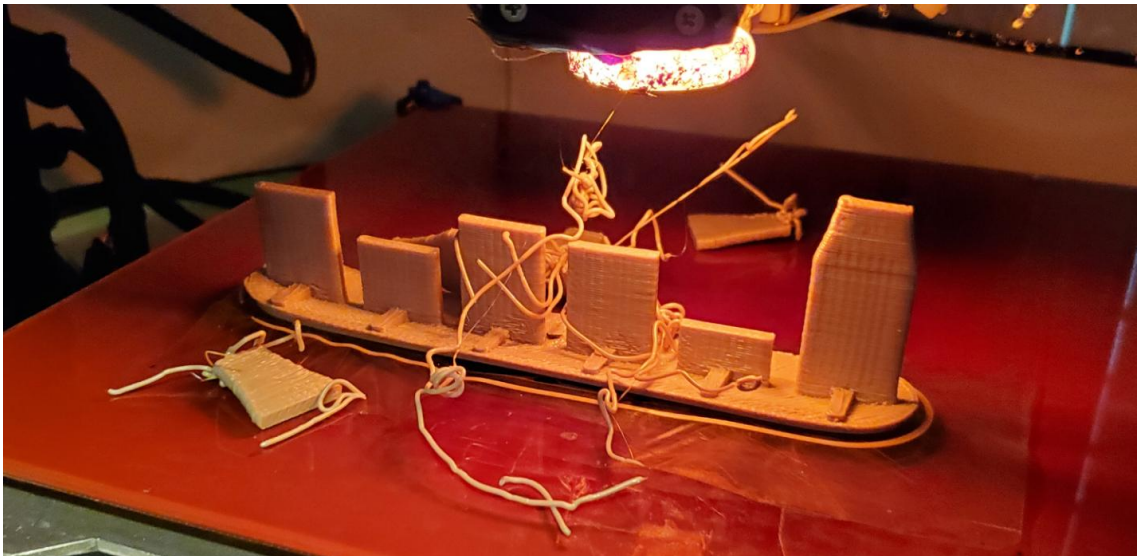


Figure 55. Second Attempt at Printing PEEK Upright (ZX) Tensile Specimens that Broke off because of Poor Bonding between Layers

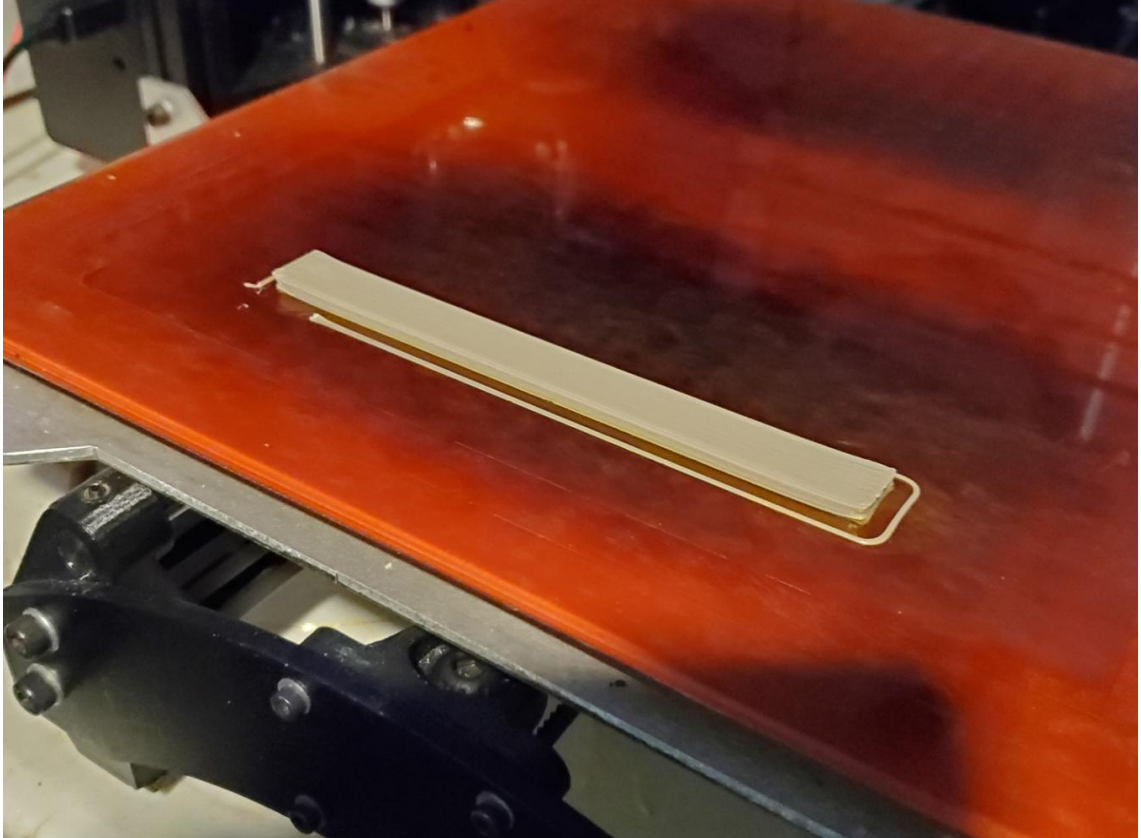


Figure 56. Printing of PEEK Flat (XY) Flexural Specimen

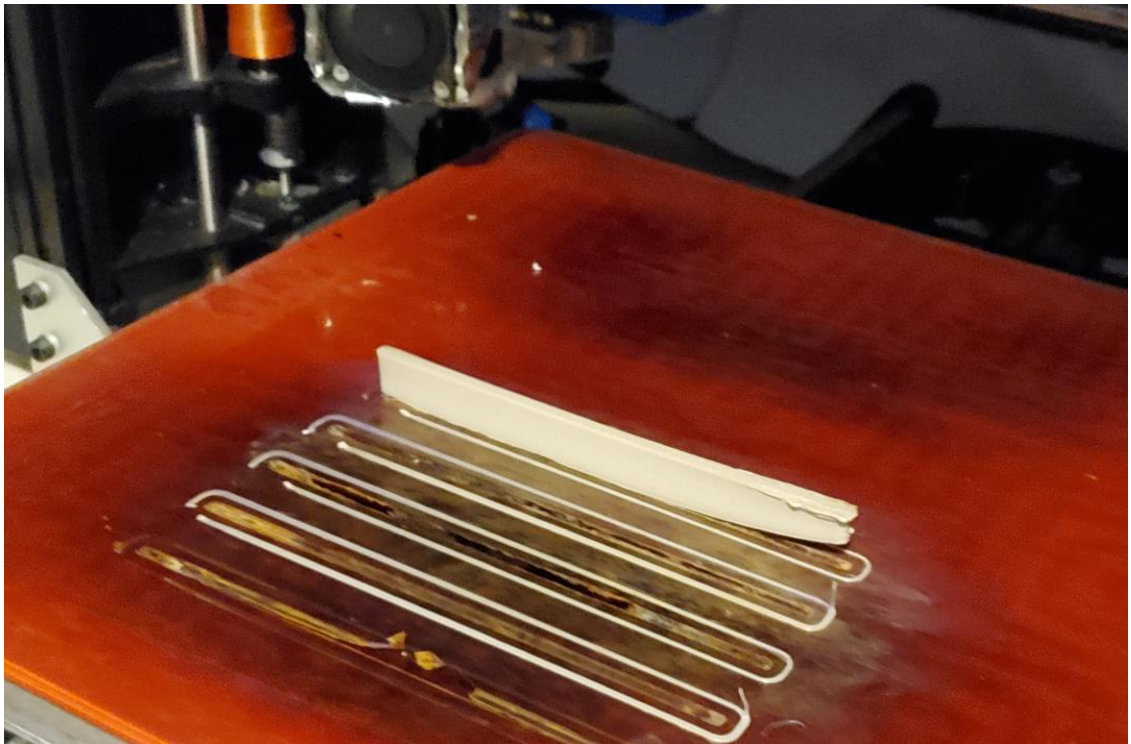


Figure 57. Printing of PEEK on Edge (XZ) Flexural Specimen

IV. RESULTS

An investigation was conducted to characterize the tensile and flexural properties using the newly implemented FFF high temperature material printing solution. A series of tests were performed to evaluate the properties printed in three orientations with the printing in one direction; flat on the print bed, on the edge on the print bed, and in the vertical Z direction. The PLA specimens were printed with and without the infrared heat lamp. The PEEK, PEKK, and PEI specimens were only printed with the infrared heat lamp as the material would not print properly without the heat lamp. All specimens were printed with 100% infill. The heat lamp was set at a power to equal the temperature of the heated print bed. The PLA specimens were printed directly onto the glass surface with hair spray on the glass to act as an adhesive. The high temperature material used a layer of Kapton tape to provide grip between the print and build plate. A new layer of Kapton tape was used for each print. Six specimens were printed for each set of specimens to make sure that at least five would be of good quality.

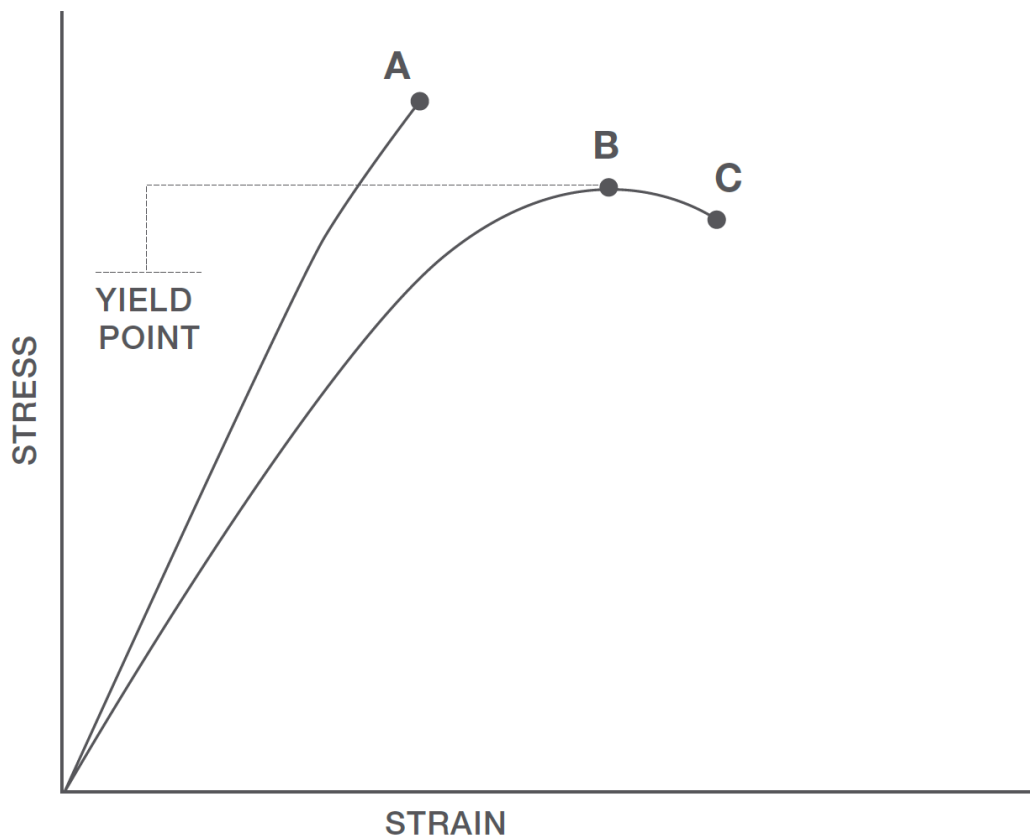
The gold standard is if the material properties can be close to the isotropic properties of injection molded materials. Table 3 shows a summary of the injection molded properties. The properties were also compared against the high end printers that Stratasys has developed for their FDM materials. If the properties are close to the Stratasys properties that use a heated enclosure with a desktop printer using a heat lamp the design will be considered a success.

Table 3. Injection Molding Material Properties

	Tensile Strength (MPa)	Tensile Modulus (GPa)	Flexural Strength (MPa)	Flexural Modulus (GPa)	Density (g/cm³)	Coefficient of Linear Thermal Expansion (1/°C)
PEEK	93	3.79	145	3.79	1.30	4.68E-05
PEKK	88	2.90	128	3.00	1.27	2.65E-05
PEI	109	3.31	145	3.31	1.27	5.60E-05
PLA	60	3.00	100	5.00	1.24	6.80E-05

[40,42,45,49,53,54,55,56]

Figure 58 shows an explanation of how the tensile properties are shown.



A = Tensile at break, elongation at break (no yield point)

B = Tensile at yield, elongation at yield

C = Tensile at break, elongation at break

[36]

Figure 58. Tensile Curves Explanation

A 4505 Series Instron test frame shown in Figure 59 was used to testing the tensile and flexural properties. The Instron is set up with a 10 kN load cell for both the tensile and flexural testing. An axial extensometer model 3542 from Epsilon is a strain gage extensometer that was used for measuring the tensile strain on a 2 inch gage length as shown in Figure 60. Tensile testing was performed to ASTM D638 Type 1 samples with a thickness of 3.3 mm. Figure 61 shows the full tensile testing set up with the grips and load cell. Tensile testing was performed at a speed of 12.7 mm/min with a sampling rate of 10 points per second. Figure 62 shows the flexural testing setup. All the flexural tests were performed to ASTM D790 using procedure A with dimensions of 12.70 mm x 3.18 mm x 76.20 mm. The span was set to 50.80 mm with 6.35 mm pins. The failure of the flexural specimens was taken at maximum stress before 5% strain or at 5% strain if there was not a break. All of the specimens were conditioned for a minimum of 40 hours at $23 \pm 2^{\circ}\text{C}$ and $50 \pm 10\%$ relative humidity prior to testing.



Figure 59. 4505 Series Instron Test Frame used for Tensile and Flexural Testing.



Figure 60. Axial extensometer model 3542 from Epsilon that was used to Measure the Tensile Strain

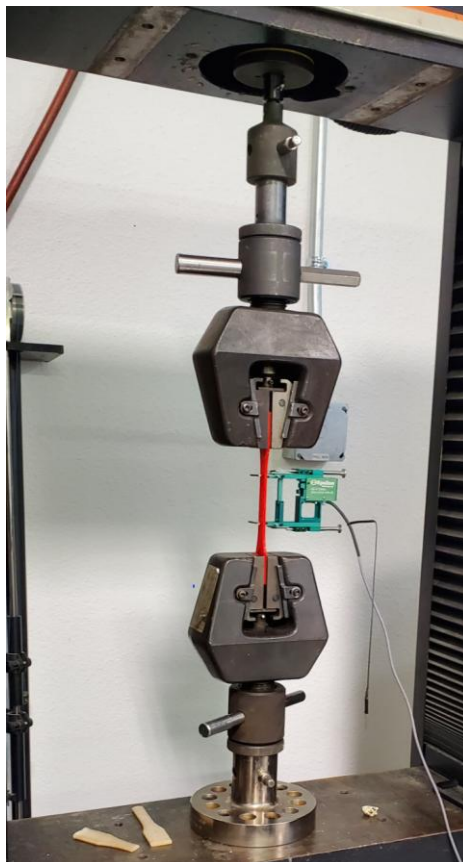


Figure 61. Tensile Testing Setup

PLA Testing

PLA was tested by printing at room temperature (22°C) and with the infrared heat lamp set at the temperature of the bed (60°C). Figure 62 shows the flexural testing setup and Figure 63 shows the tensile test specimens. All specimens were printed with a 0.3 mm layer height, 0.8 mm layer width, 220°C printing temperature, 60°C build plate temperature, 60 mm/s print speed, and 100% infill.



Figure 62. Flexural Testing Setup



Figure 63. PLA Tensile Test Specimens, Flat (XY), Upright (ZX), on Edge (XZ), and Flat $\pm 45^\circ$ Infill (XY)

PLA Flat (XY) Tensile Specimens at Room Temperature (22°C)

Figure 64 shows the PLA Flat (XY) tensile specimens. Table 4 shows the dimension of these specimens. Table 5 shows the tensile properties for tensile strength, percent elongation and modulus of elasticity. Figure 65 shows the stress vs. strain plots.



Figure 64. PLA Flat (XY) Tensile Specimens

Table 4. PLA 22°C Tensile Flat (XY) Specimen Dimensions

Specimen	Width (mm)	Thickness (mm)
1	12.725	2.946
2	12.751	2.946
3	12.700	2.972
4	12.852	2.972
5	12.751	2.946
6	12.751	2.997
Average	12.755	2.963
SD	0.052	0.021

Table 5. PLA Flat (XY) Tensile Properties at Room Temperature (22°C)

Specimen ID	Tensile Strength (MPa)	% Elongation at Break	Modulus of Elasticity (GPa)
1	40.880	1.684%	2.619
2	35.813	1.432%	2.645
3	38.853	1.529%	2.695
4	38.855	1.594%	2.576
5	35.792	1.422%	2.684
6	37.358	1.495%	2.642
Average	37.925	1.526%	2.644
SD	1.989	0.100%	0.043

**PLA Flat (XY) Tensile Test
Room Temperature (22°C) Extrusion**

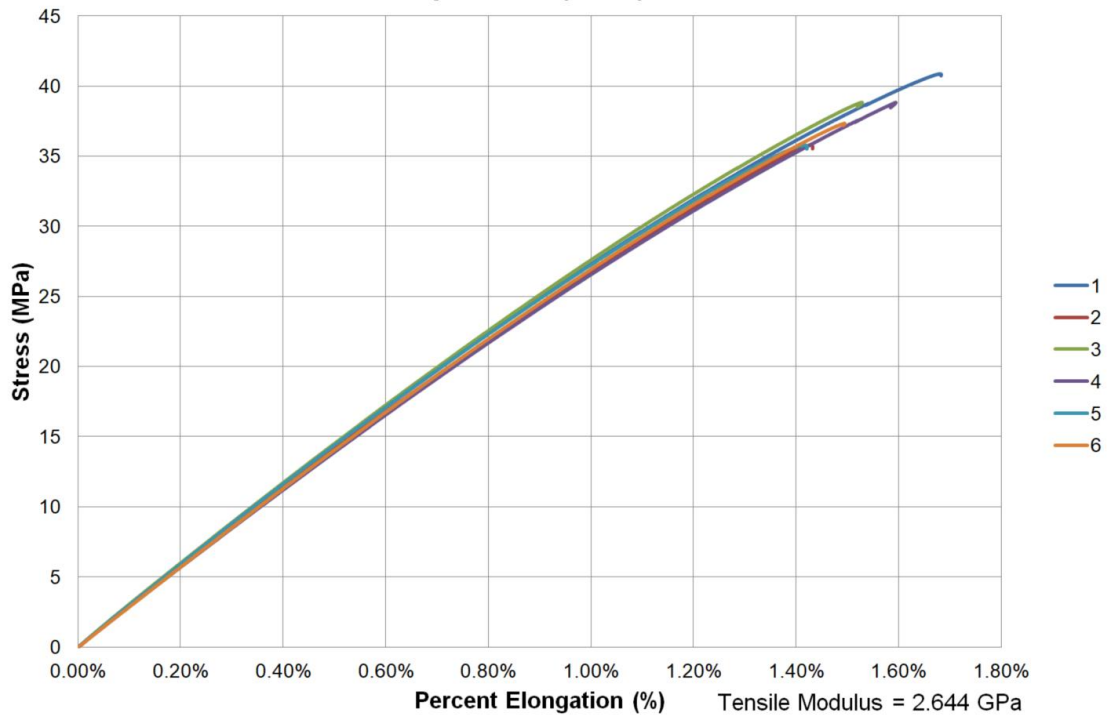


Figure 65. PLA Flat (XY) Tensile Properties at Room Temperature 22°C Stress vs. Strain Plot

PLA Flat (XY) Tensile Specimens with 60°C Heat Lamp

Figure 66 shows the PLA Flat (XY) tensile specimens after testing. Table 6 shows the dimension of these specimens. Table 7 shows the tensile properties for tensile strength, percent elongation and modulus of elasticity. Figure 67 shows the stress vs. strain plots.

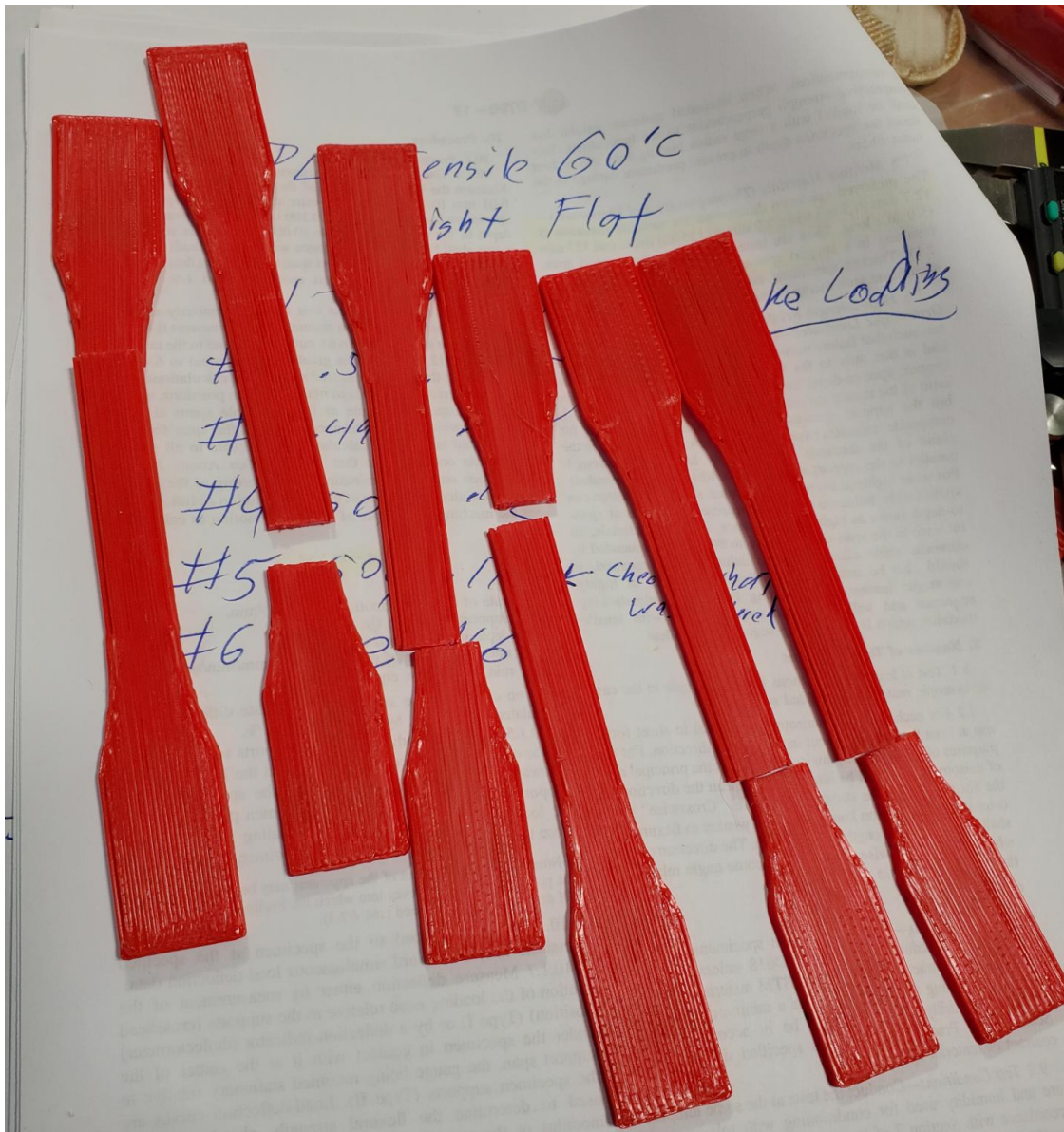


Figure 66. PLA Flat (XY) Tensile Specimens after testing

Table 6. PLA 60°C Tensile Flat (XY) Specimen Dimensions

Specimen	Width (mm)	Thickness (mm)
1	12.700	2.845
2	12.751	2.921
3	12.675	2.997
4	12.700	2.845
5	12.725	2.794
6	12.700	2.946
Average	12.708	2.891
SD	0.026	0.076

Table 7. PLA Flat (XY) Tensile Properties with Heat Lamp at 60°C

Specimen ID	Tensile Strength (MPa)	% Elongation at Break	Modulus of Elasticity (GPa)
1	Broken During Loading	Broken During Loading	Broken During Loading
2	52.429	2.019%	2.841
3	45.885	1.643%	2.965
4	53.410	1.777%	3.233
5	52.694	1.986%	2.920
6	49.241	1.722%	3.046
Average	50.732	1.829%	3.001
SD	3.147	0.166%	0.149

**PLA Flat (XY) Tensile Test
60°C Heat Lamp**

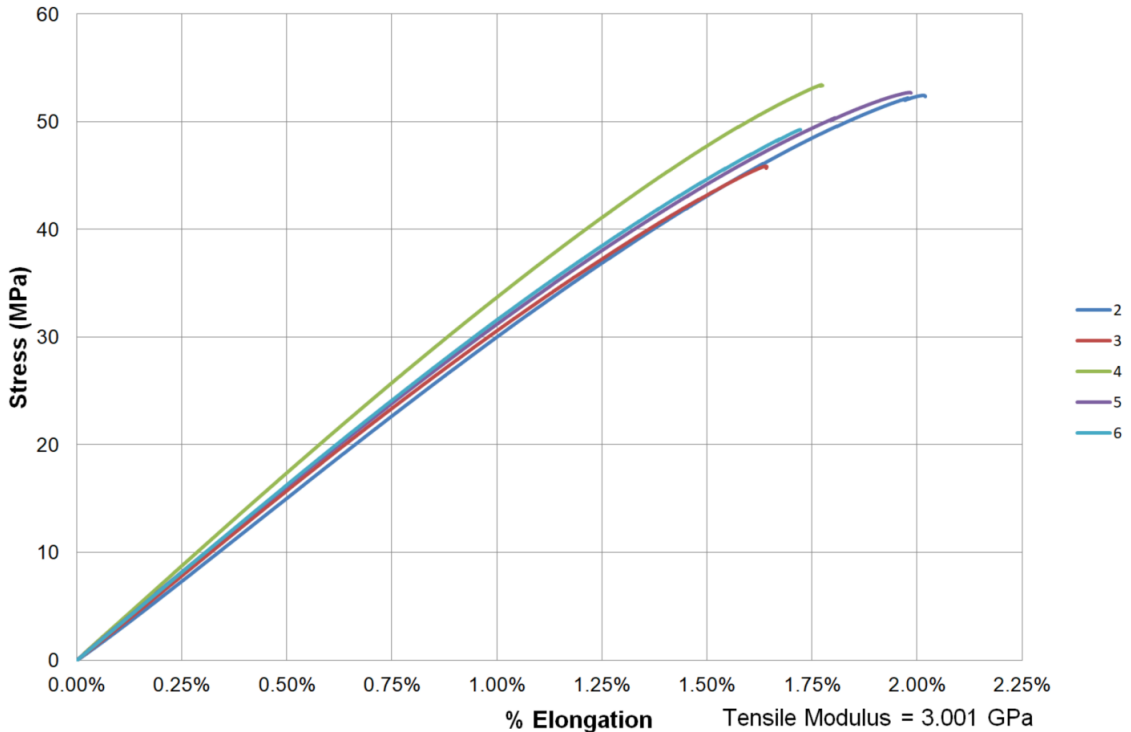


Figure 67. PLA Flat (XY) Tensile Properties with Heat Lamp at 60°C Stress vs. Strain Plot

PLA Flat (XY± 45° Infill) Tensile Specimens at Room Temperature (22°C)

Figure 68 shows the PLA Flat (XY) with ± 45° infill tensile specimens after testing. Table 8 shows the dimension of these specimens. Table 9 shows the tensile properties for tensile strength, percent elongation and modulus of elasticity. Figure 69 shows the stress vs. strain plots.

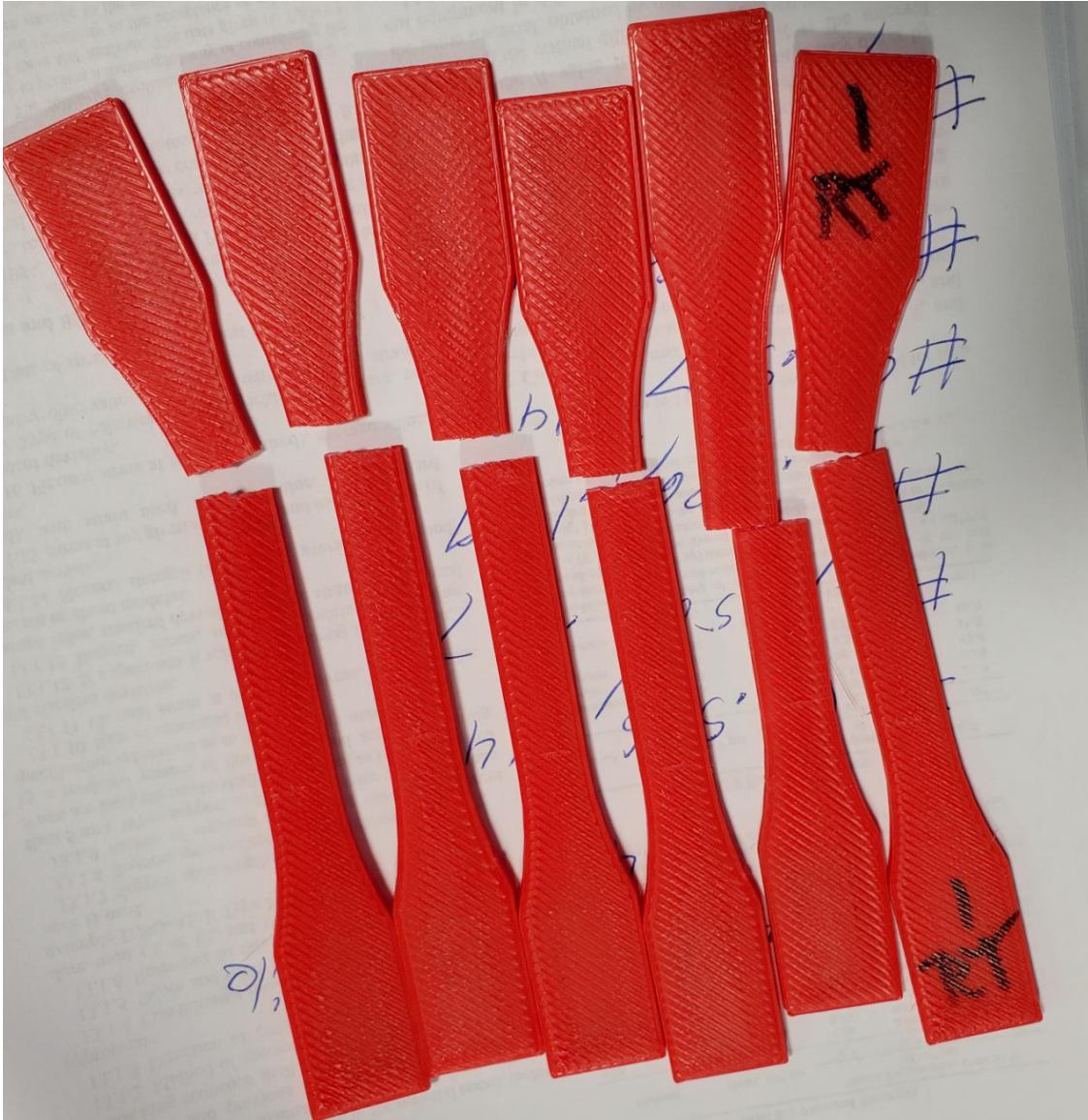


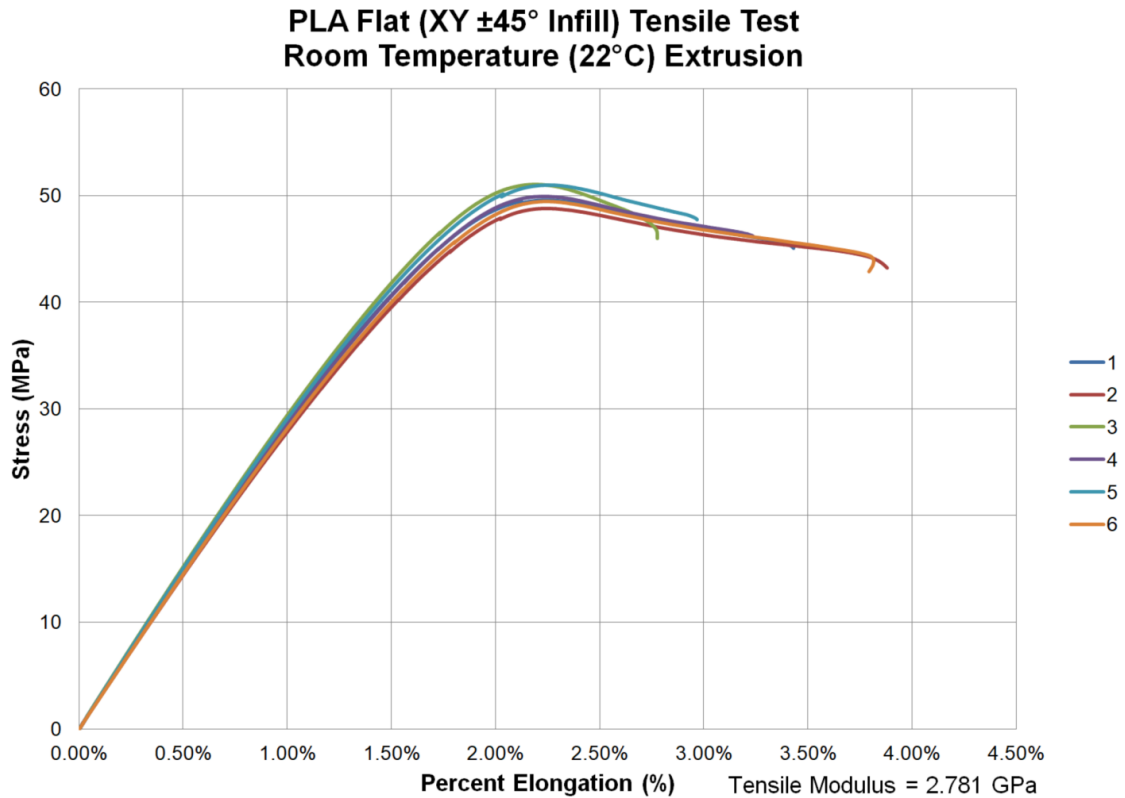
Figure 68. PLA Flat (XY± 45° Infill) Tensile Specimens after Testing

Table 8. PLA 22°C Tensile Flat (XZ) ±45° Infill Specimen Dimensions

Specimen	Width (mm)	Thickness (mm)
1	12.852	3.607
2	12.827	3.734
3	12.852	3.531
4	12.878	3.632
5	12.903	3.607
6	12.878	3.683
Average	12.865	3.632
SD	0.027	0.070

Table 9. PLA Flat (XY ± 45° Infill) Tensile Properties at Room Temperature 22°C.

Specimen ID	Tensile Strength (MPa)	% Elongation at Break	Modulus of Elasticity (GPa)	% Elongation at Yield
1	49.584	3.433%	2.825	2.232%
2	48.814	3.882%	2.745	2.232%
3	51.059	2.778%	2.864	2.201%
4	49.902	3.239%	2.804	2.244%
5	51.010	2.967%	2.684	2.253%
6	49.467	3.818%	2.763	2.242%
Average	49.973	3.353%	2.781	2.234%
SD	0.896	0.446%	0.064	0.018%



**Figure 69. PLA Flat (XY ± 45° Infill) Tensile Properties at Room Temperature 22°C
Stress vs. Strain Plot**

PLA 60°C Tensile Flat (XZ) ±45° Infill Specimen with Heat Lamp at 60°C

Table 10 shows the dimension of these specimens. Table 11 shows the tensile properties for tensile strength, percent elongation and modulus of elasticity. Figure 70 shows the stress vs. strain plots.

Table 10. PLA 60°C Tensile Flat (XZ) ±45° Infill Specimen Dimensions

Specimen	Width (mm)	Thickness (mm)
1	12.802	3.810
2	12.878	4.013
3	12.954	3.835
4	12.827	3.835
5	12.878	3.835
6	12.954	3.861
Average	12.882	3.865
SD	0.063	0.074

Table 11. PLA Flat (XY ± 45° Infill) Tensile Properties with Heat Lamp at 60°C.

Specimen ID	Tensile Strength (MPa)	% Elongation at Break	Modulus of Elasticity (GPa)	% Elongation at Yield
1	49.925	2.280%	2.892	2.104%
2	51.998	3.241%	3.069	2.046%
3	49.967	3.638%	2.839	2.162%
4	50.531	2.594%	2.794	2.163%
5	51.426	2.557%	2.961	2.075%
6	50.179	2.244%	3.284	1.942%
Average	50.671	2.759%	2.973	2.082%
SD	0.854	0.560%	0.180	0.083%

**PLA Flat (XY ± 45° Infill) Tensile Test
60°C Heat Lamp**

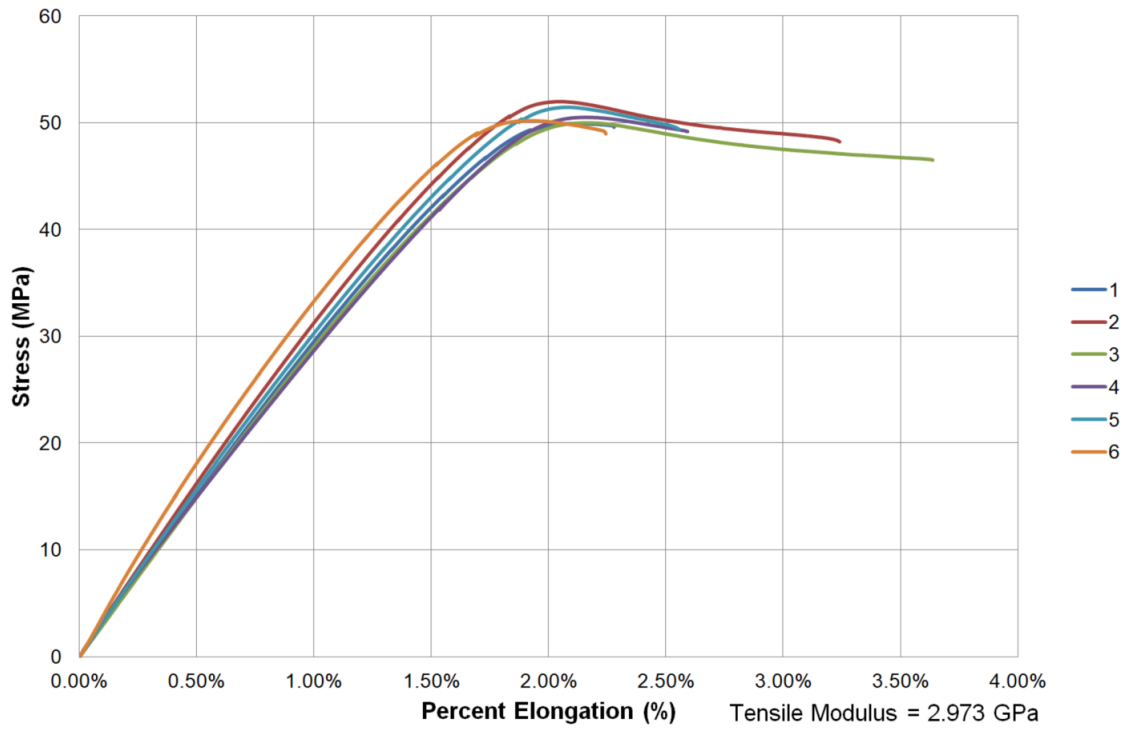


**Figure 70. PLA Flat (XY ± 45° Infill) Tensile Properties with Heat Lamp at 60°C
Stress vs. Strain Plot**

PLA on Edge (XZ) Tensile Specimens at Room Temperature (22°C)

Figure 71 shows the PLA on Edge (XZ) at room temperature (22°C) printing tensile specimens before removing the printing supports. Figure 72 shows the specimens after testing. Table 12 shows the dimension of these specimens. Table 13 shows the tensile properties for tensile strength, percent elongation and modulus of elasticity. Figure 73 shows the stress vs. strain plots.



Figure 71. PLA on Edge (XZ) Tensile Specimens before Testing and Removing the Printing Supports

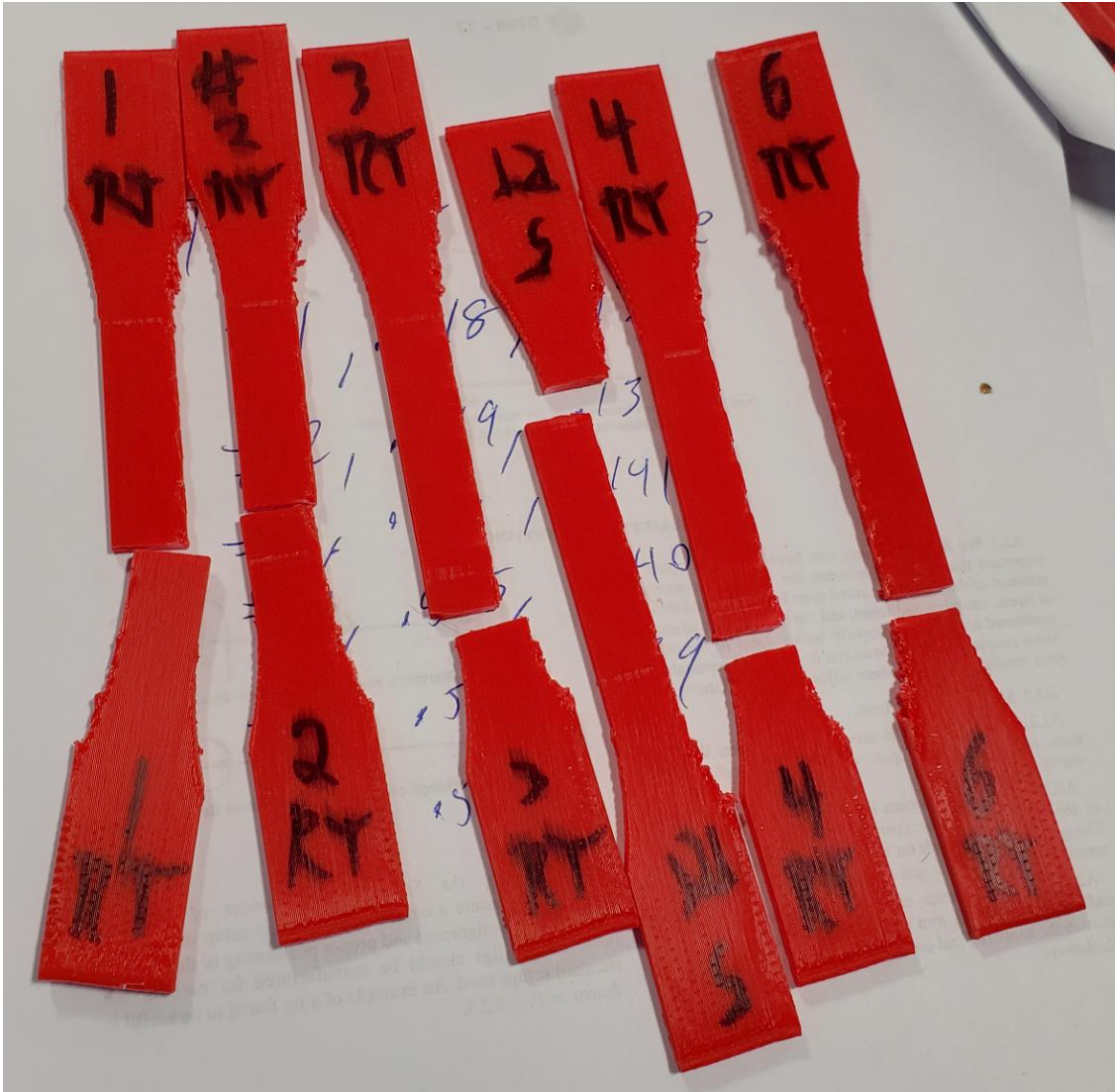


Figure 72. PLA on Edge (XZ) Tensile Specimens after Testing

Table 12. PLA 22°C Tensile on Edge (XZ) Specimen Dimensions

Specimen	Width (mm)	Thickness (mm)
1	13.157	3.531
2	13.183	3.531
3	13.106	3.581
4	13.081	3.556
5	13.106	3.531
6	13.005	3.556
Average	13.106	3.548
SD	0.062	0.021

Table 13. PLA on Edge (XZ) Tensile Properties at Room Temperature (22°C)

Specimen ID	Tensile Strength (MPa)	% Elongation at Break	Modulus of Elasticity (GPa)	% Elongation at Yield
1	53.508	2.451%	3.064	2.174%
2	51.498	2.156%	3.095	2.058%
3	54.060	3.224%	3.063	2.177%
4	52.589	3.995%	3.052	2.083%
5	53.890	2.406%	3.021	2.145%
6	53.909	4.321%	3.097	2.101%
Average	53.242	3.092%	3.065	2.123%
SD	1.007	0.906%	0.028	0.050%

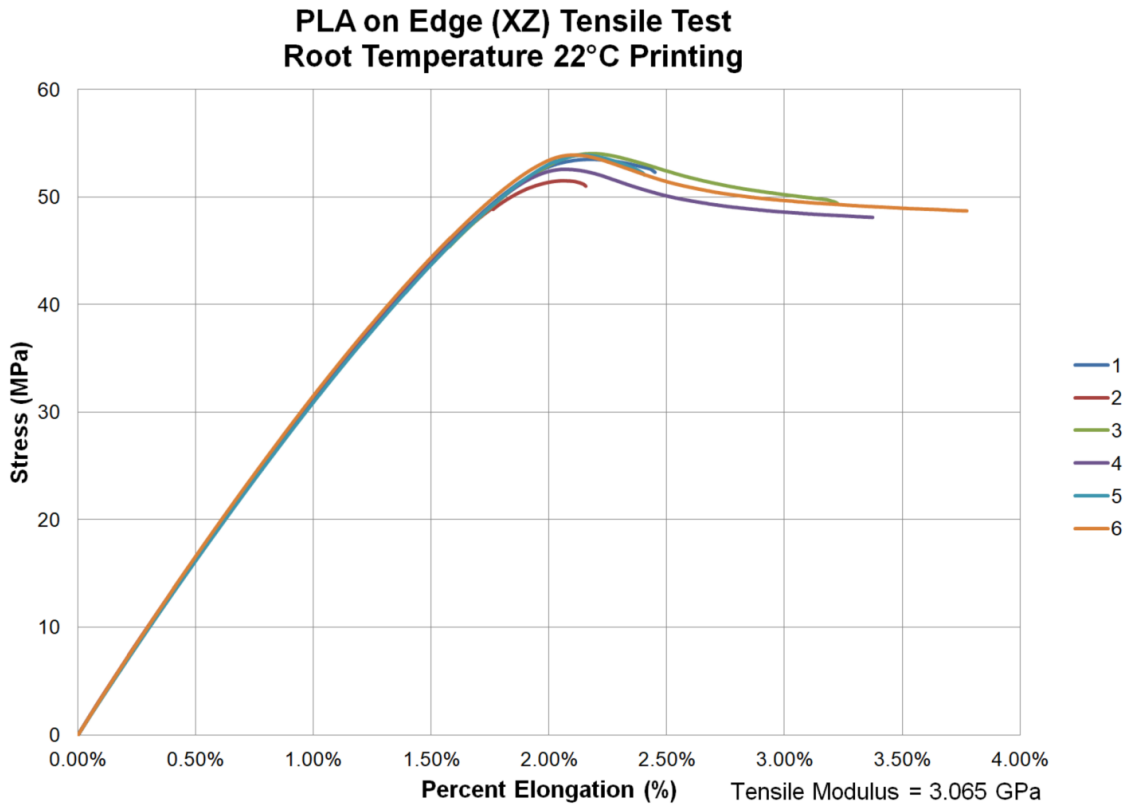


Figure 73. PLA on Edge (XZ) Tensile Properties at Room Temperature 22°C Stress vs. Strain Plot

PLA on Edge (XZ) Tensile Specimens with Heat Lamp at 60°C

Figure 74 shows the PLA on Edge (XZ) with the heat lamp set at 60°C printing tensile specimens after testing. Table 14 shows the dimension of these specimens. Table 15 shows the tensile properties for tensile strength, percent elongation and modulus of elasticity. Figure 75 shows the stress vs. strain plots.

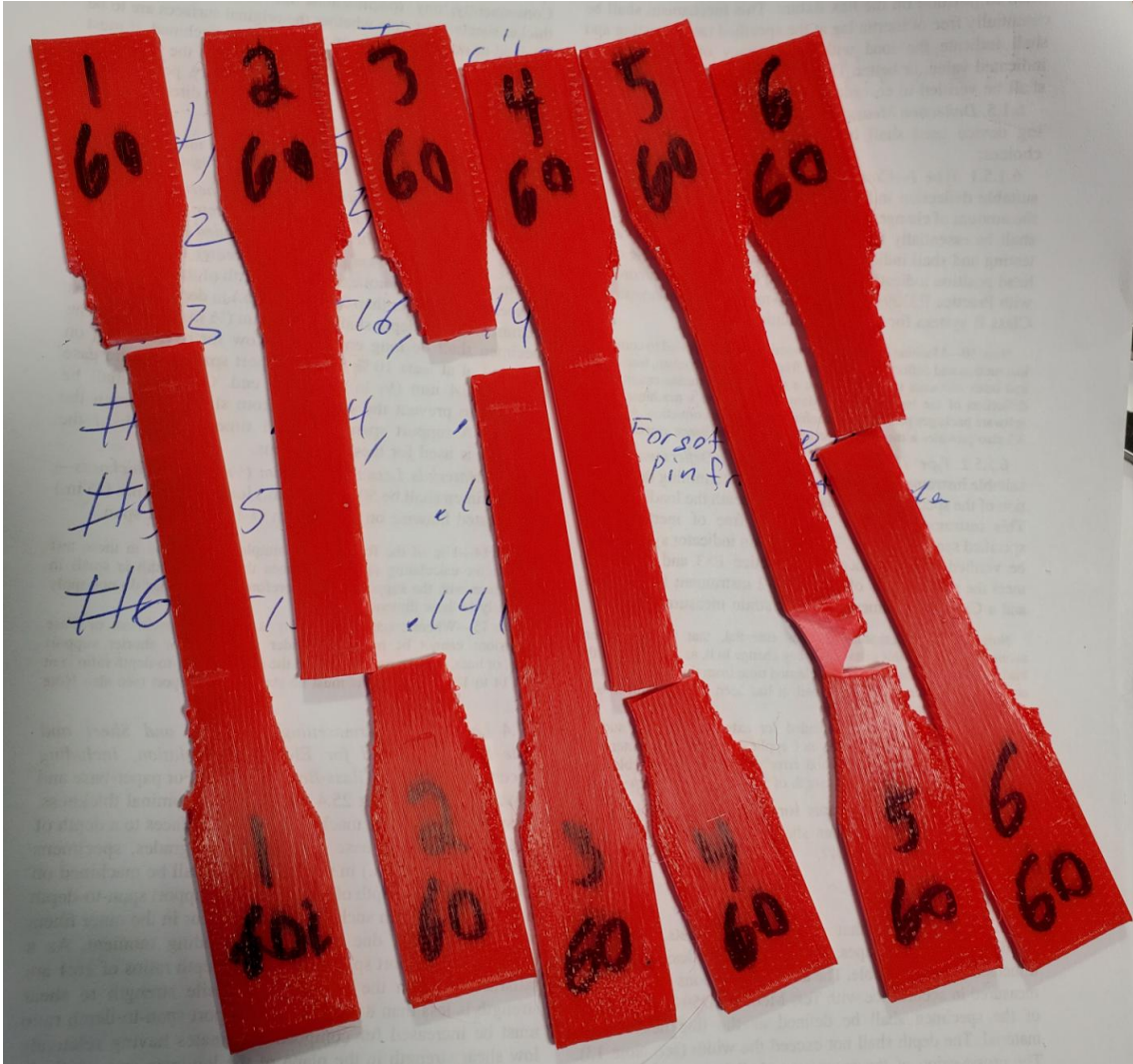


Figure 74. PLA on Edge (XZ) Tensile Specimens with Heat Lamp at 60°C after Testing

Table 14. PLA 60°C Tensile on Edge (XZ) Specimen Dimensions

Specimen	Width (mm)	Thickness (mm)
1	12.776	3.581
2	13.056	3.607
3	13.106	3.581
4	13.056	3.581
5	13.081	3.607
6	13.081	3.581
Average	13.026	3.590
SD	0.124	0.013

Table 15. PLA on Edge (XZ) Tensile Properties with Heat Lamp at 60°C

Specimen ID	Tensile Strength (MPa)	% Elongation at Break	Modulus of Elasticity (GPa)	% Elongation at Yield
1	55.230	3.158%	3.110	2.237%
2	53.068	2.242%	3.002	2.212%
3	52.791	2.216%	2.945	2.207%
4	53.522	Extensometer Malfunction (Forgot to remove pin)		
5	53.726	2.746%	2.946	2.347%
6	54.124	2.825%	3.066	2.206%
Average	53.743	2.637%	3.014	2.242%
SD	0.868	0.404%	0.073	0.060%

**PLA on Edge (XZ) Tensile Test
60°C Heat Lamp Printing**

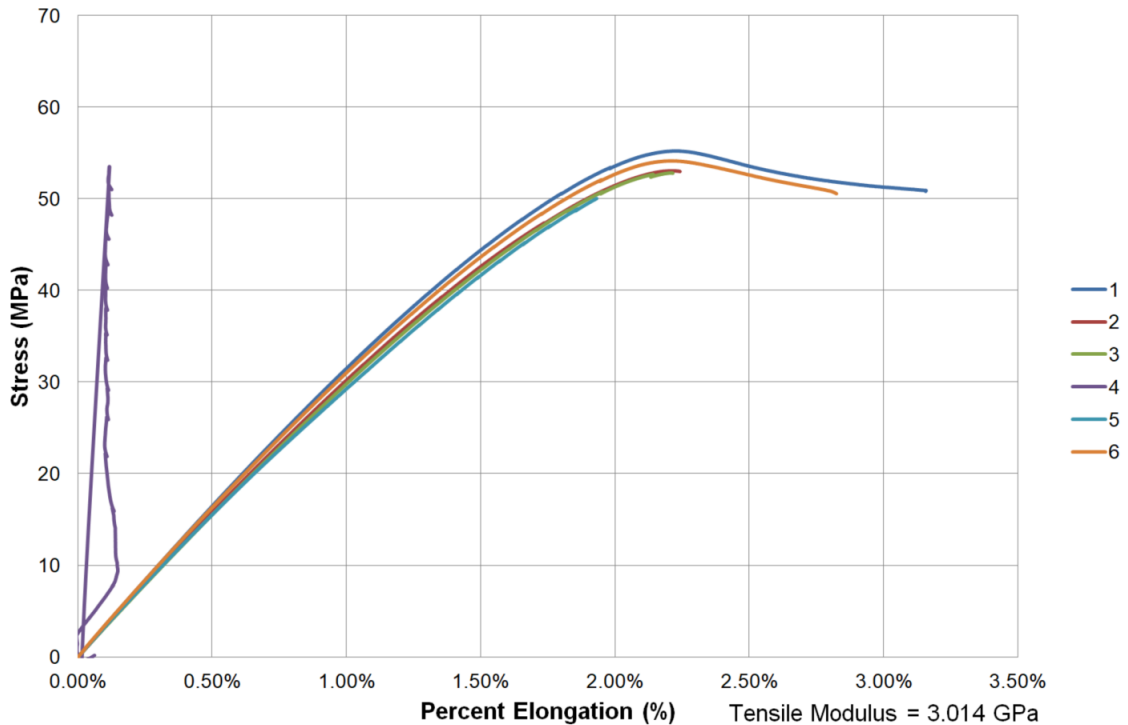


Figure 75. PLA on Edge (XZ) Tensile Properties with Heat Lamp at 60°C Stress vs. Strain Plot

PLA Upright (ZX) Tensile Properties at Room Temperature (22°C).

Figure 76 shows the PLA Upright (ZX) at room temperature (22°C) printing tensile specimens before testing. Figure 77 shows the specimens after testing. Table 16 shows the dimension of these specimens. Table 17 shows the tensile properties for tensile strength, percent elongation and modulus of elasticity. Figure 78 shows the stress vs. strain plots.



Figure 76. PLA Upright (ZX) Tensile Specimens Printed at Room Temperature before Testing

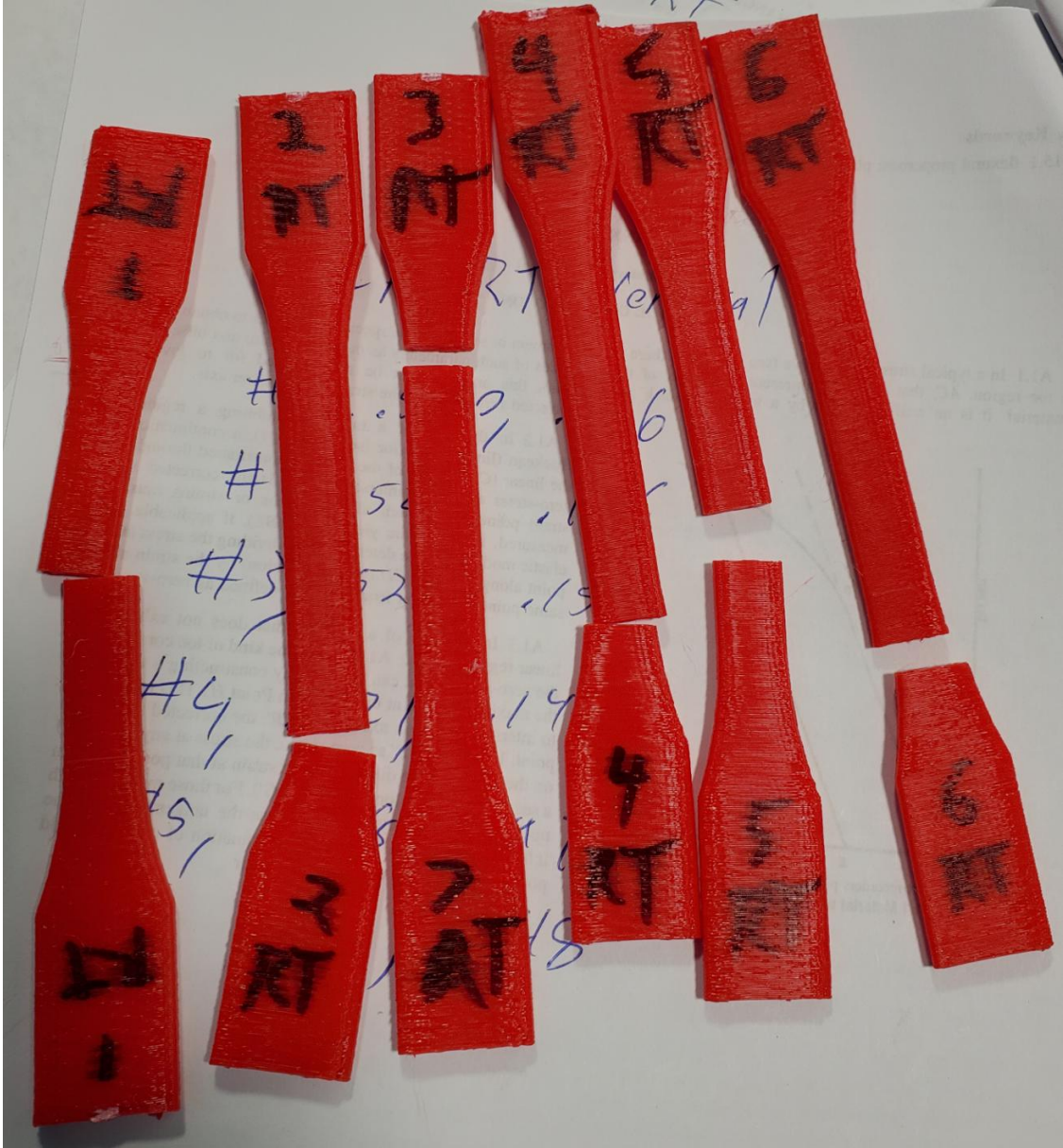


Figure 77. PLA Upright (ZX) Tensile Specimens Printed at Room Temperature after Testing

Table 16. PLA 22°C Tensile Upright (ZX) Specimen Dimensions

Specimen	Width (mm)	Thickness (mm)
1	13.208	3.708
2	13.233	3.708
3	13.208	3.810
4	13.233	3.759
5	13.157	3.734
6	13.157	3.759
Average	13.200	3.747
SD	0.035	0.039

Table 17. PLA Upright (ZX) Tensile Properties at Room Temperature (22°C)

Specimen ID	Tensile Strength (MPa)	% Elongation at Break	Modulus of Elasticity (GPa)
1	34.159	1.361%	2.735
2	27.078	0.929%	2.979
3	39.351	1.507%	2.881
4	30.998	1.507%	2.926
5	37.144	1.341%	2.971
6	34.446	1.233%	2.926
Average	33.863	1.313%	2.903
SD	4.372	0.215%	0.090

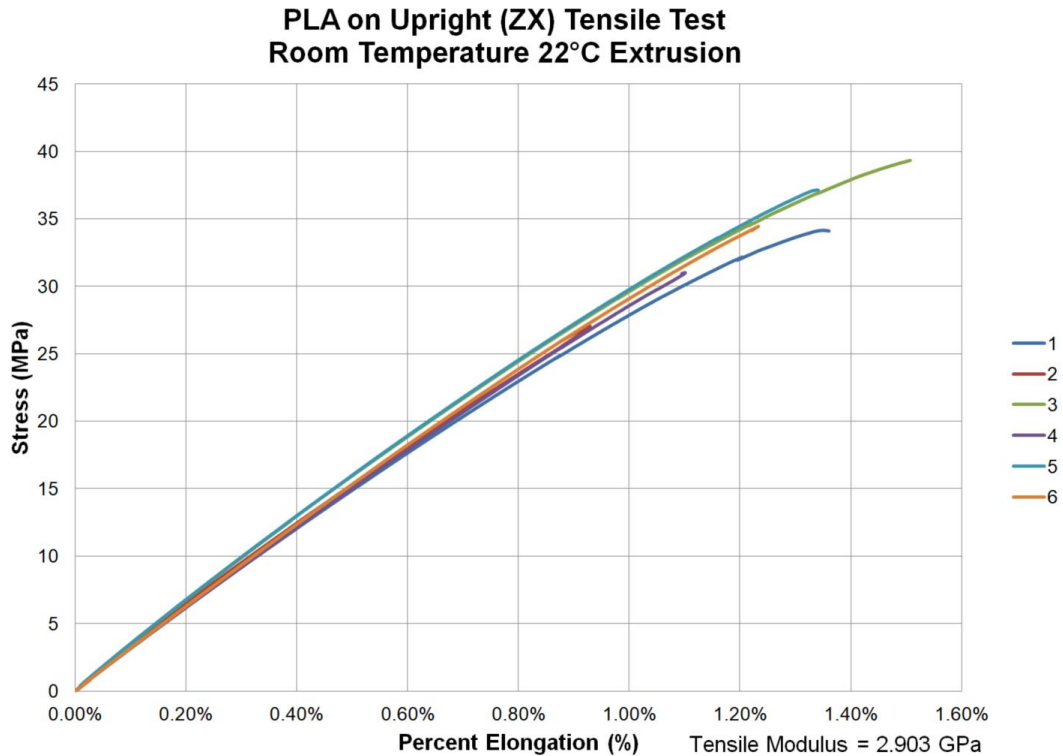


Figure 78. PLA Upright (ZX) Tensile Properties at Room Temperature 22°C Stress vs. Strain Plot

PLA Upright (ZX) Tensile Specimens Printed with Heat Lamp at 60°C

Figure 79 shows the PLA Upright (ZX) with the heat lamp set at 60°C printing tensile specimens before testing. Figure 80 shows the specimens after testing. Table 18 shows the dimension of these specimens. Table 19 shows the tensile properties for tensile strength, percent elongation and modulus of elasticity. Figure 81 shows the stress vs. strain plots.



Figure 79. PLA Upright (ZX) Tensile Specimens Printed with Heat Lamp at 60°C before Testing

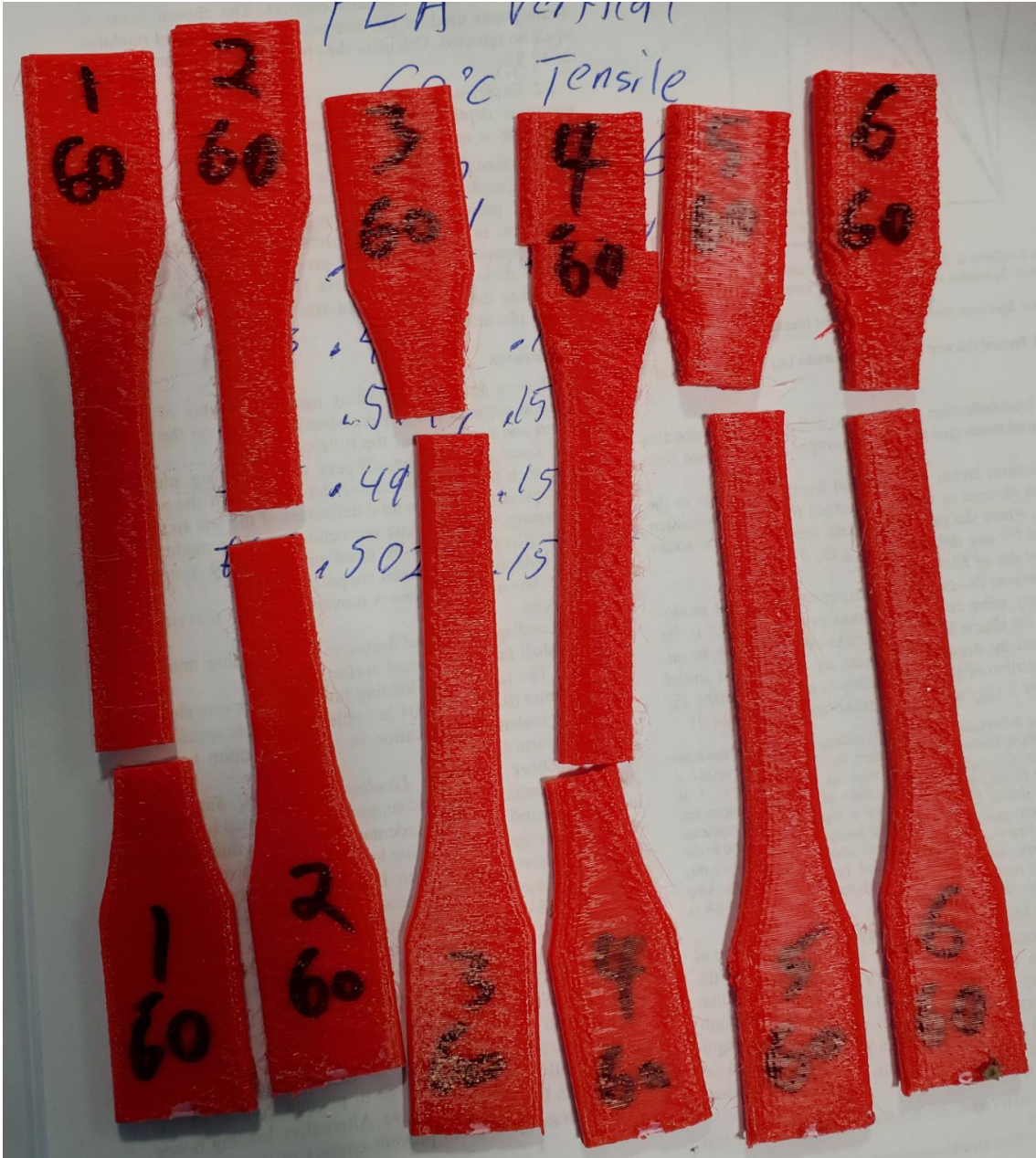


Figure 80. PLA Upright (ZX) Tensile Specimens Printed with Heat Lamp at 60°C after Testing

Table 18. PLA 60°C Tensile Upright (ZX) Specimen Dimensions

Specimen	Width (mm)	Thickness (mm)
1	12.497	3.962
2	12.573	3.912
3	12.675	3.835
4	13.132	3.988
5	12.649	3.886
6	12.751	4.013
Average	12.713	3.933
SD	0.223	0.067

Table 19. PLA Upright (ZX) Tensile Properties with Heat Lamp at 60°C.

Specimen ID	Tensile Strength (MPa)	% Elongation at Break	Modulus of Elasticity (GPa)
1	31.932	1.100%	3.016
2	24.564	0.880%	2.896
3	36.870	1.372%	2.821
4	24.317	1.372%	2.952
5	35.887	1.285%	2.929
6	28.062	0.985%	2.952
Average	30.272	1.166%	2.928
SD	5.491	0.209%	0.065

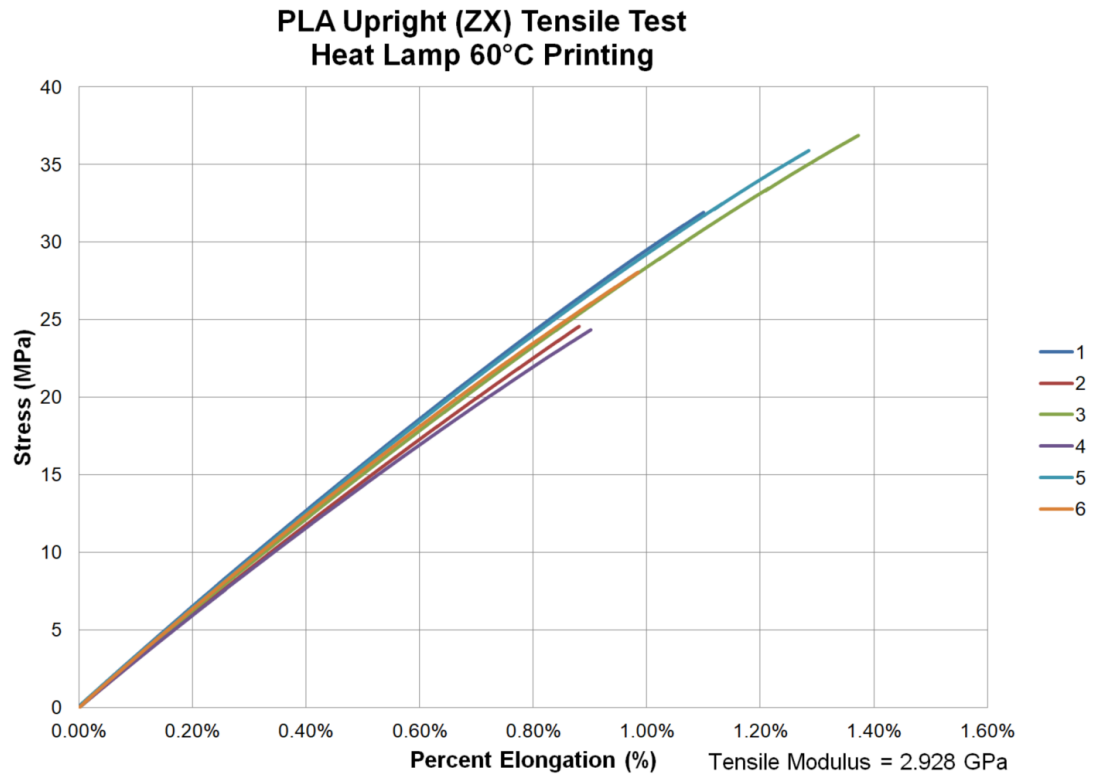


Figure 81. PLA Upright (ZX) Tensile Properties with Heat Lamp at 60°C Stress vs. Strain Plot

PLA Tensile Properties Summary with and without Heat Lamp

Table 20 shows the summary of the PLA tensile specimens with and without the heat lamp. Figure 82 shows the summary of the tensile strength. The heat lamp showed an improvement in the tensile strength of the flat (XY) orientation by 33% and an increase in modulus by 13%. Figure 83 shows a summary of the tensile modulus. Figure 84 shows a summary of the percent elongation.

Table 20. Summary of PLA Tensile Properties with and without the Heat Lamp

	Tensile Strength (MPa)	SD (Mpa)	% Elongation at Break	SD (%)	Modulus of Elasticity (GPa)	SD (Gpa)	% Elongation @ yield	SD (%)
PLA Flat (XY) RT	37.925	1.989	1.526%	0.100%	2.644	0.043		
PLA Flat (XY) 60°C	50.732	3.147	1.829%	0.166%	3.001	0.149		
PLA Flat (XY) @ ±45° RT	49.973	0.896	3.353%	0.446%	2.781	0.064	2.234%	0.018%
PLA Flat (XY) @ ±45° 60°C	50.671	0.854	2.759%	0.560%	2.973	0.180	2.082%	0.083%
PLA on Edge (XZ) RT	53.242	1.007	3.092%	0.906%	3.065	0.028	2.123%	0.050%
PLA on Edge (XZ) 60°C	53.743	0.868	2.637%	0.404%	3.014	0.073	2.242%	0.060%
PLA Upright (ZX) RT	33.863	4.372	1.313%	0.215%	2.903	0.090		
PLAUpright (ZX) 60°C	30.272	5.491	1.166%	0.209%	2.928	0.065		

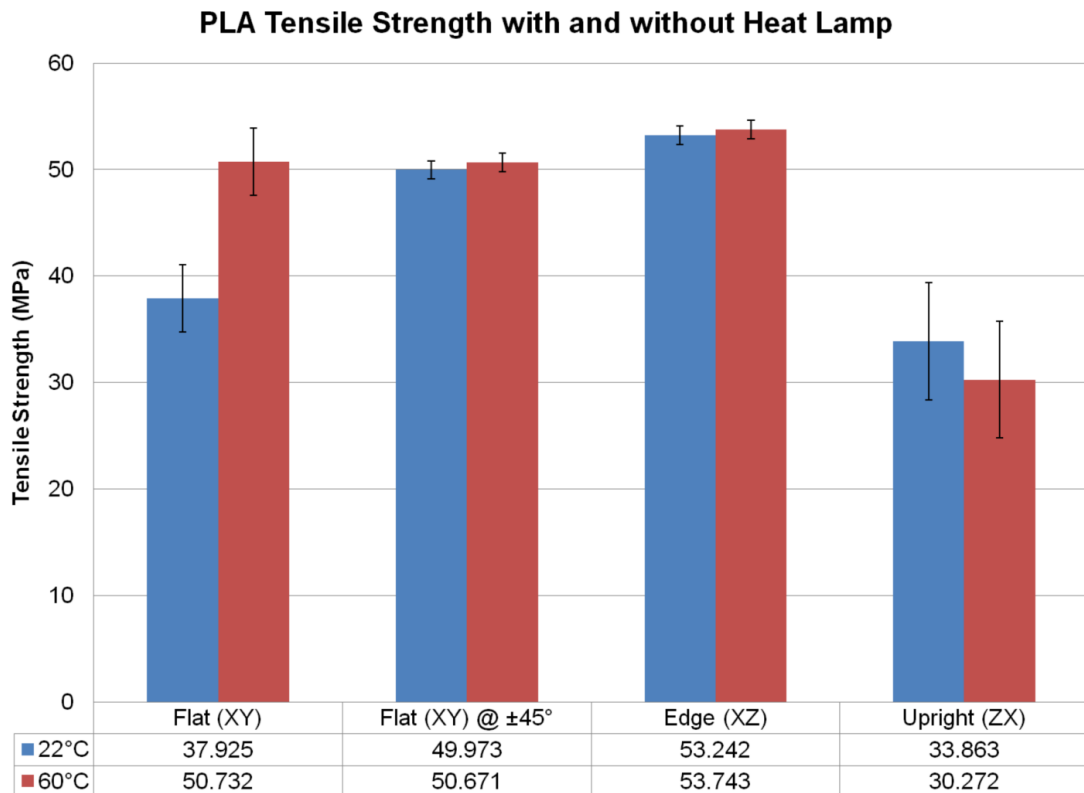


Figure 82. PLA Tensile Strength Summary

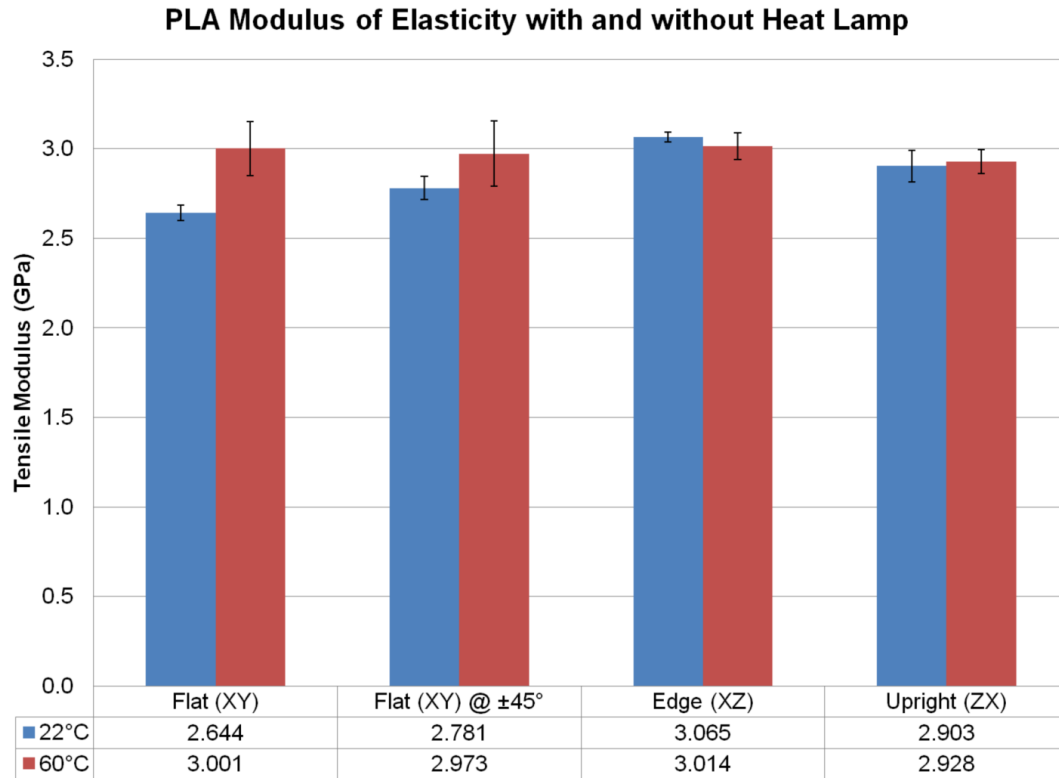


Figure 83. PLA Tensile Modulus Summary

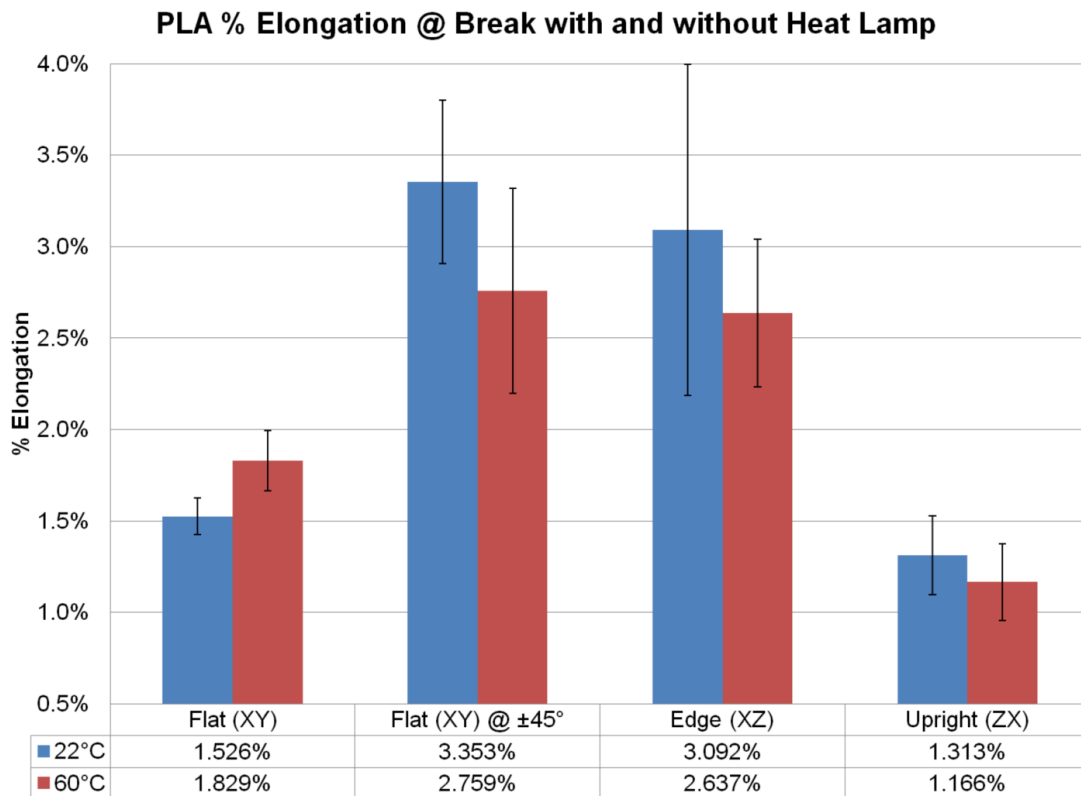


Figure 84. PLA % Elongation at Break Summary

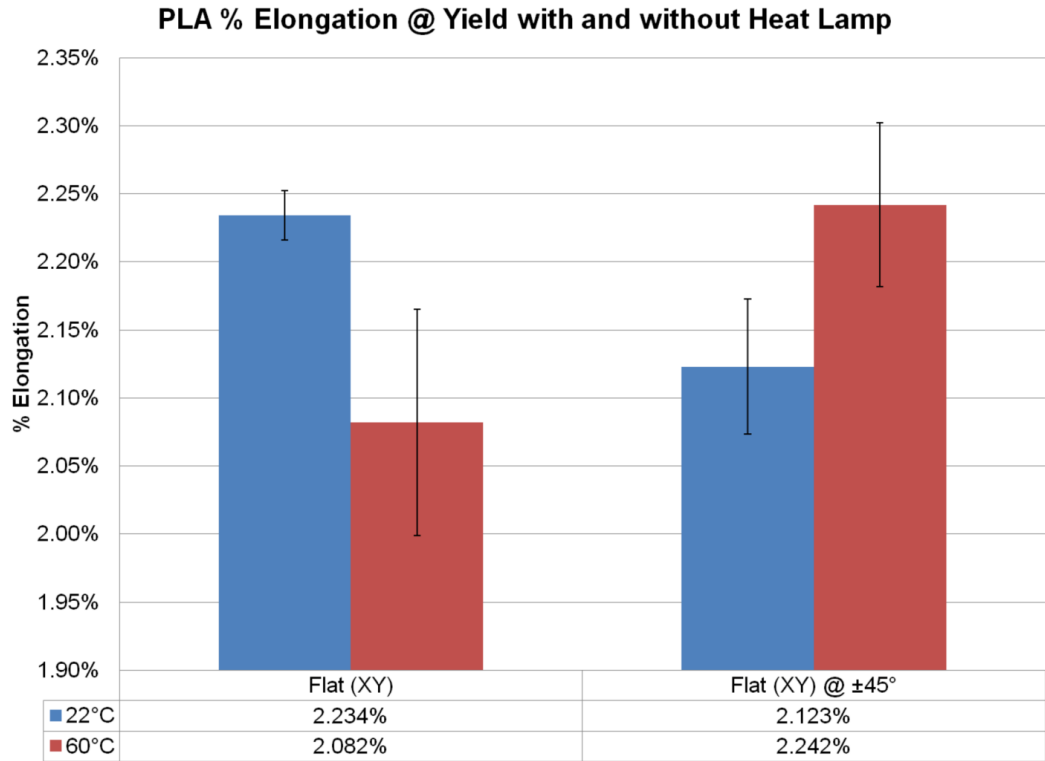


Figure 85. PLA % Elongation at Yield Summary

PLA Flexural Flat (XY) Specimen at Room Temperature (22°C)

Figure 86 shows the PLA Flat (XY) at room temperature (22°C) printing flexural specimens before testing. Table 21 shows the dimension of these specimens. Table 22 shows the flexural properties for flexural strength, flexural strain and flexural modulus. Figure 87 shows the stress vs. strain plots.



Figure 86. PLA Flat (XY) Flexural Specimens

Table 21. PLA 22°C Flexural Flat (XY) Specimen Dimensions

Specimen	Width (mm)	Thickness (mm)
1	12.649	2.946
2	12.979	2.946
3	12.700	2.896
4	12.649	2.946
5	12.776	2.896
6	12.675	2.921
Average	12.738	2.925
SD	0.127	0.025

Table 22. PLA Flat (XY) Flexural Properties at Room Temperature (22°C)

Specimen ID	Flexural Strength (MPa)	Flexural Strain @ Max Stress	Flexural Modulus (GPa)
1	84.571	3.647%	2.940
2	79.692	3.606%	2.749
3	83.420	3.520%	2.883
4	84.348	3.628%	2.914
5	83.673	3.522%	2.922
6	81.568	3.604%	2.790
Average	82.879	3.588%	2.867
SD	1.888	0.054%	0.078

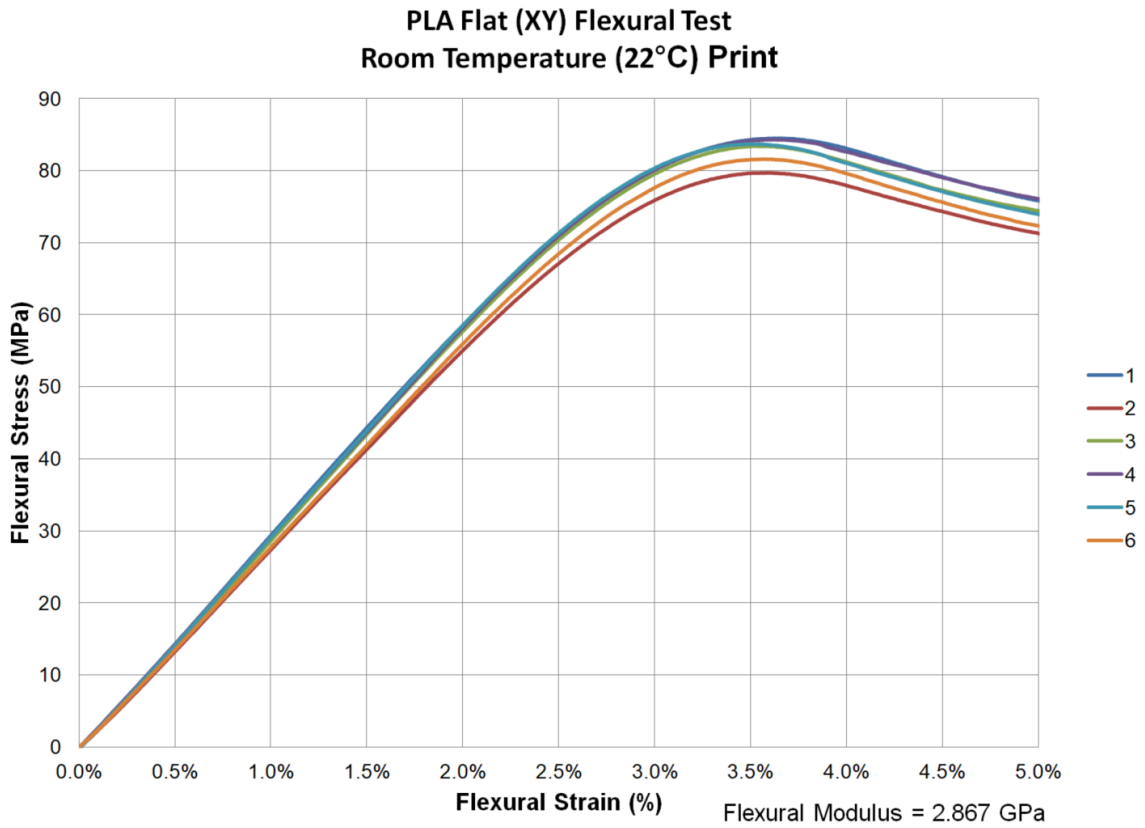


Figure 87. PLA Flat (XY) Flexural Properties at Room Temperature 22°C Stress vs. Strain Plot

PLA Flexural Flat (XY) Specimen Printed with Heat Lamp at 60°C

Table 23 shows the dimension of the PLA Flat (XY) with the heat lamp at 69°C.

Table 24 shows the flexural properties for flexural strength, flexural strain and flexural modulus. Figure 88 shows the stress vs. strain plots.

Table 23. PLA 60°C Flexural Flat (XY) Specimen Dimensions

Specimen	Width (mm)	Thickness (mm)
1	12.725	2.794
2	12.675	2.896
3	12.751	2.921
4	12.802	2.921
5	12.649	2.870
6	12.700	2.845
Average	12.717	2.874
SD	0.055	0.049

Table 24. PLA Flat (XY) Flexural Properties with Heat Lamp at 60°C

Specimen ID	Flexural Strength (MPa)	Flexural Strain @ Max Stress	Flexural Modulus (GPa)
1	94.815	3.682%	3.404
2	87.393	3.602%	3.088
3	90.521	3.799%	3.080
4	98.158	3.665%	3.471
5	95.006	3.801%	3.253
6	96.797	3.765%	3.378
Average	93.782	3.719%	3.279
SD	4.056	0.082%	0.167

PLA Flat (XY) Flexural Test
60°C Heat Lamp Print

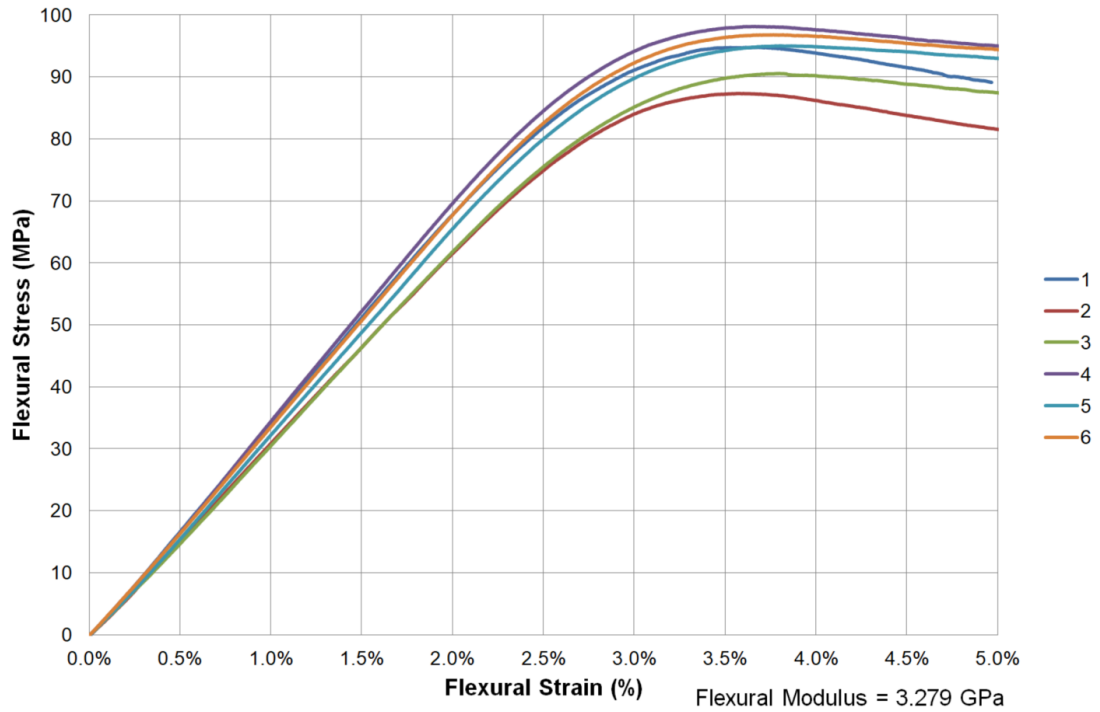


Figure 88. PLA Flat (XY) Flexural Properties with Heat Lamp at 60°C Stress vs. Strain Plot

PLA Flexural on Edge (XZ) Specimen at Room Temperature (22°C)

Table 25 shows the dimension of the PLA on Edge (XZ) at room temperature (22°C). Table 26 shows the flexural properties for flexural strength, flexural strain and flexural modulus. Figure 89 shows the stress vs. strain plots.

Table 25. PLA 22 °C Flexural on Edge (XZ) Specimen Dimensions

Specimen	Width (mm)	Thickness (mm)
1	12.192	3.480
2	12.268	3.480
3	12.268	3.454
4	12.243	3.505
5	12.344	3.505
6	12.294	3.505
Average	12.268	3.488
SD	0.051	0.021

Table 26. PLA on Edge (XZ) Flexural Properties at Room Temperature (22°C)

Specimen ID	Flexural Strength (MPa)	Flexural Strain @ Max Stress	Flexural Modulus (GPa)
1	85.594	4.197%	2.541
2	87.275	4.233%	2.621
3	86.852	4.266%	2.576
4	84.065	4.235%	2.504
5	83.439	4.166%	2.429
6	82.954	4.194%	2.445
Average	85.030	4.215%	2.519
SD	1.814	0.036%	0.075

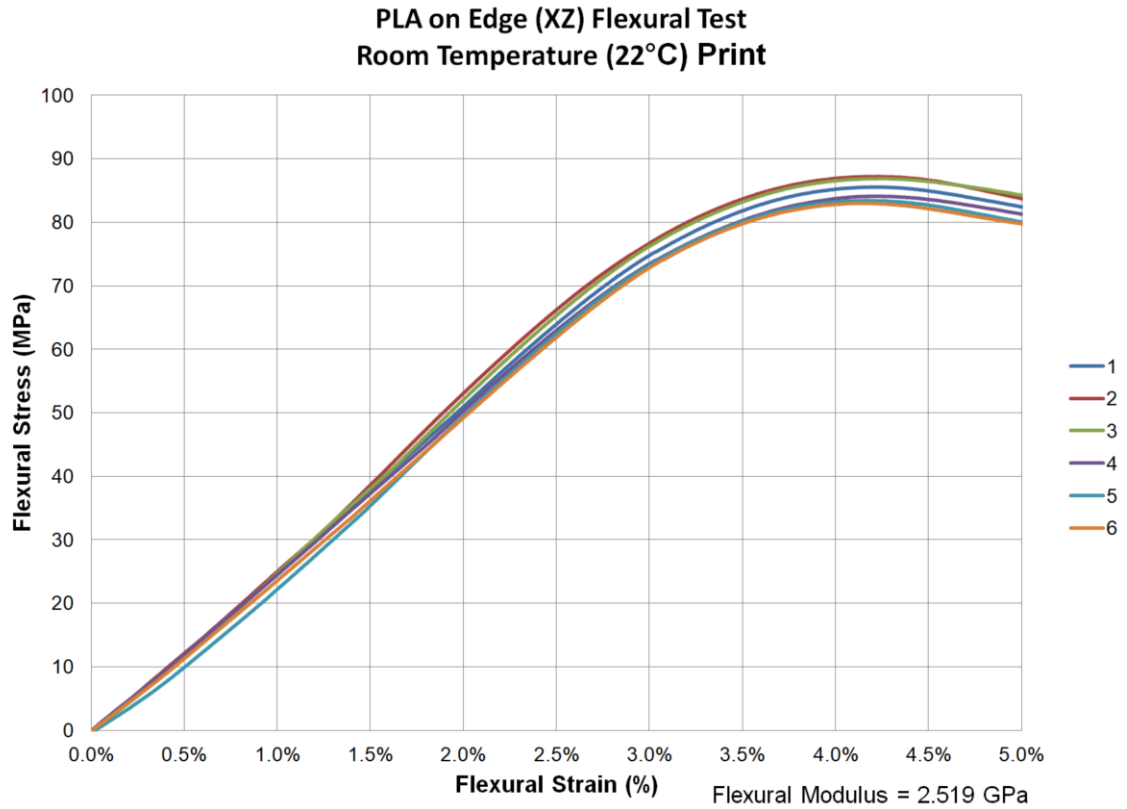


Figure 89. PLA on Edge (XZ) Flexural Properties at Room Temperature 22°C Stress vs. Strain Plot

PLA Flexural on Edge (XZ) Specimen with Heat Lamp at 60°C

Table 27 shows the dimension of the PLA on Edge (XZ) specimens with the heat lamp at 60°C. Table 28 shows the flexural properties for flexural strength, flexural strain and flexural modulus. Figure 90 shows the stress vs. strain plots.

Table 27. PLA 60°C Flexural on Edge (XZ) Specimen Dimensions

Specimen	Width (mm)	Thickness (mm)
1	12.319	3.531
2	12.319	3.581
3	12.268	3.683
4	12.294	3.531
5	12.294	3.556
6	12.268	3.581
Average	12.294	3.577
SD	0.023	0.057

Table 28. PLA on Edge (XZ) Flexural Properties with Heat Lamp at 60°C

Specimen ID	Flexural Strength (MPa)	Flexural Strain @ Max Stress	Flexural Modulus (GPa)
1	92.183	4.307%	2.550
2	91.032	4.449%	2.552
3	84.458	3.924%	2.503
4	86.404	3.254%	2.742
5	89.126	4.296%	2.604
6	89.798	3.972%	2.566
Average	88.833	4.034%	2.586
SD	2.902	0.433%	0.083

PLA on Edge (XZ) Flexural Test
60°C Heat Lamp Print

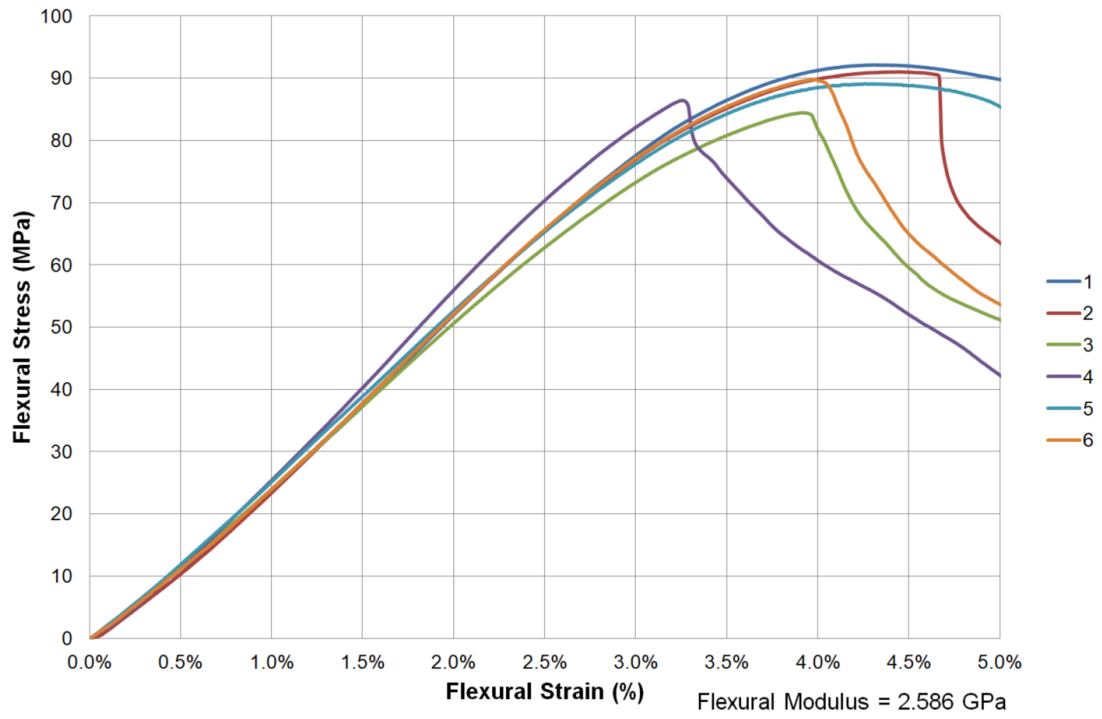


*Figure 90. PLA on Edge (XZ) Flexural Properties with Heat Lamp at 60°C
Stress vs. Strain Plot*

PLA Flexural Upright (ZX) Specimen at Room Temperature (22°C)

Table 29 shows the dimension of the PLA Upright (ZX) specimens at room temperature (22°C) printing. Table 30 shows the flexural properties for flexural strength, flexural strain and flexural modulus. Figure 91 shows the stress vs. strain plots.

Table 29. PLA 22°C Flexural Upright (ZX) Specimen Dimensions

Specimen	Width (mm)	Thickness (mm)
1	13.221	3.759
2	13.183	3.912
3	13.132	3.861
4	13.183	3.759
5	13.284	3.785
6	13.157	3.810
Average	13.193	3.814
SD	0.054	0.061

Table 30. PLA Upright (ZX) Flexural Properties at Room Temperature (22°C)

Specimen ID	Flexural Strength (MPa)	Flexural Strain @ Max Stress	Flexural Modulus (GPa)
1	50.574	3.159%	1.873
2	50.130	3.579%	1.673
3	48.045	3.237%	1.651
4	53.146	3.126%	1.920
5	54.794	3.422%	1.980
6	52.521	3.272%	1.882
Average	51.535	3.299%	1.830
SD	2.419	0.172%	0.136

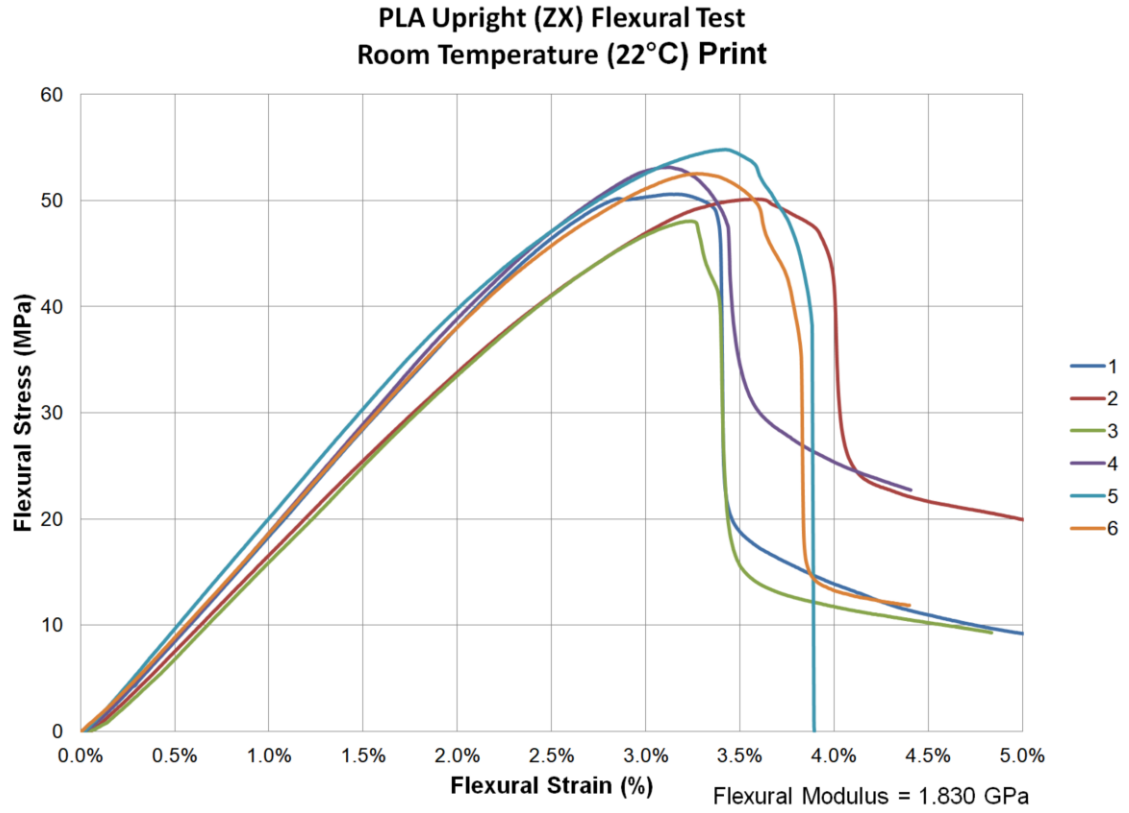


Figure 91. PLA Upright (ZX) Flexural Properties at Room Temperature 22°C Stress vs. Strain Plot

PLA Flexural Upright (ZX) Specimen with Heat Lamp at 60°C

Figure 92 shows the PLA Upright (ZX) printed with the heat lamp at 60°C flexural specimens before testing. Figure 93 shows the specimens after testing. Table 31 shows the dimension of these specimens. Table 32 shows the flexural properties for flexural strength, flexural strain and flexural modulus. Figure 94 shows the stress vs. strain plots.

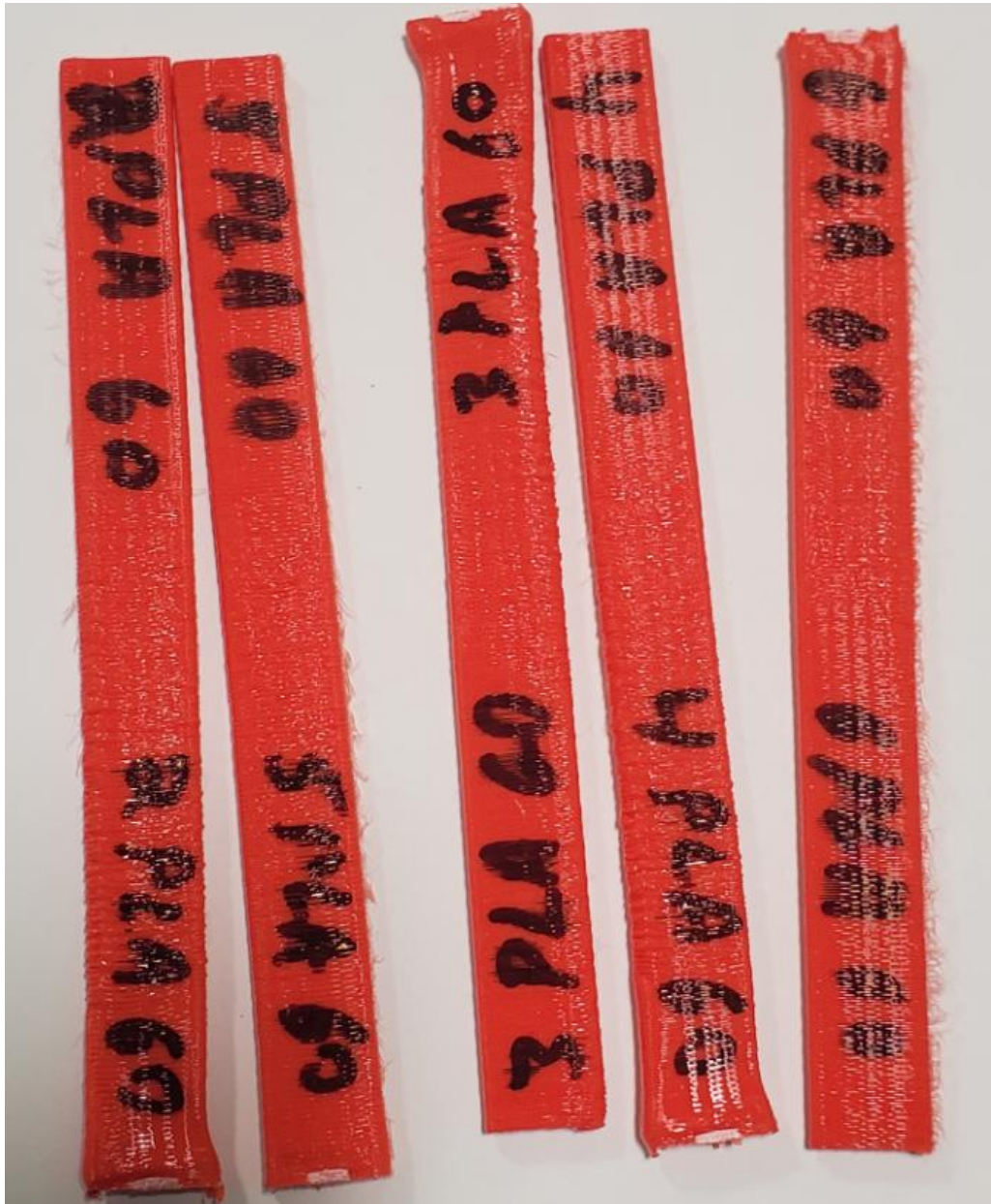


Figure 92. PLA Upright (ZX) Flexural Specimens before Testing

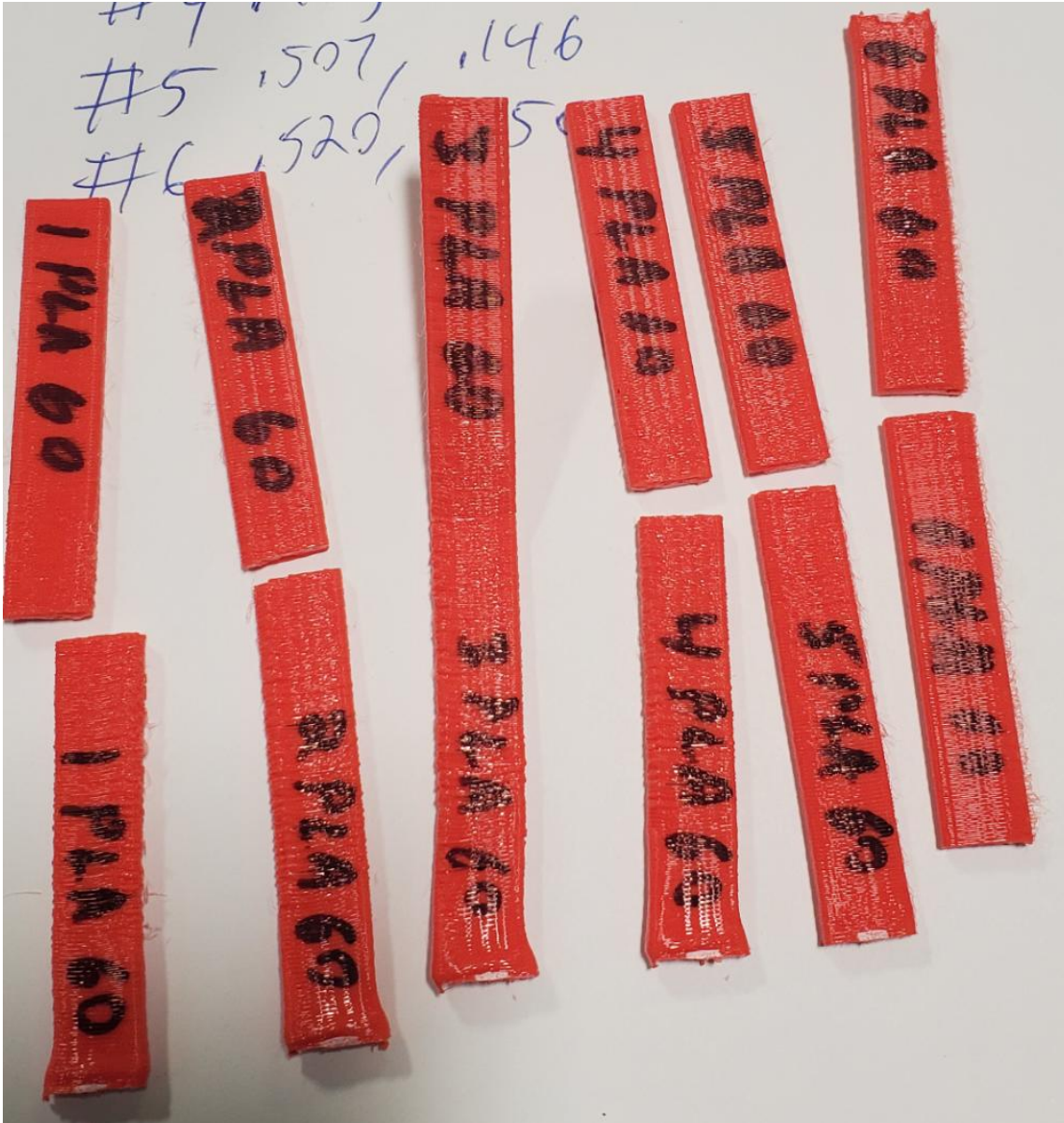


Figure 93. PLA Upright (ZX) Flexural Specimens after Testing

Table 31. PLA 60°C Flexural Upright (ZX) Specimen Dimensions

Specimen	Width (mm)	Thickness (mm)
1	12.624	3.861
2	12.649	3.810
3	12.573	3.810
4	12.675	3.886
5	12.878	3.708
6	13.208	3.810
Average	12.768	3.814
SD	0.240	0.061

Table 32. PLA Upright (ZX) Flexural Properties with Heat Lamp at 60°C

Specimen ID	Flexural Strength (MPa)	Flexural Strain @ Max Stress	Flexural Modulus (GPa)
1	65.722	3.768%	2.232
2	60.891	3.580%	2.093
3	66.274	3.809%	2.309
4	61.312	4.536%	1.884
5	63.755	3.800%	2.198
6	57.202	3.610%	1.991
Average	62.526	3.851%	2.118
SD	3.414	0.350%	0.160

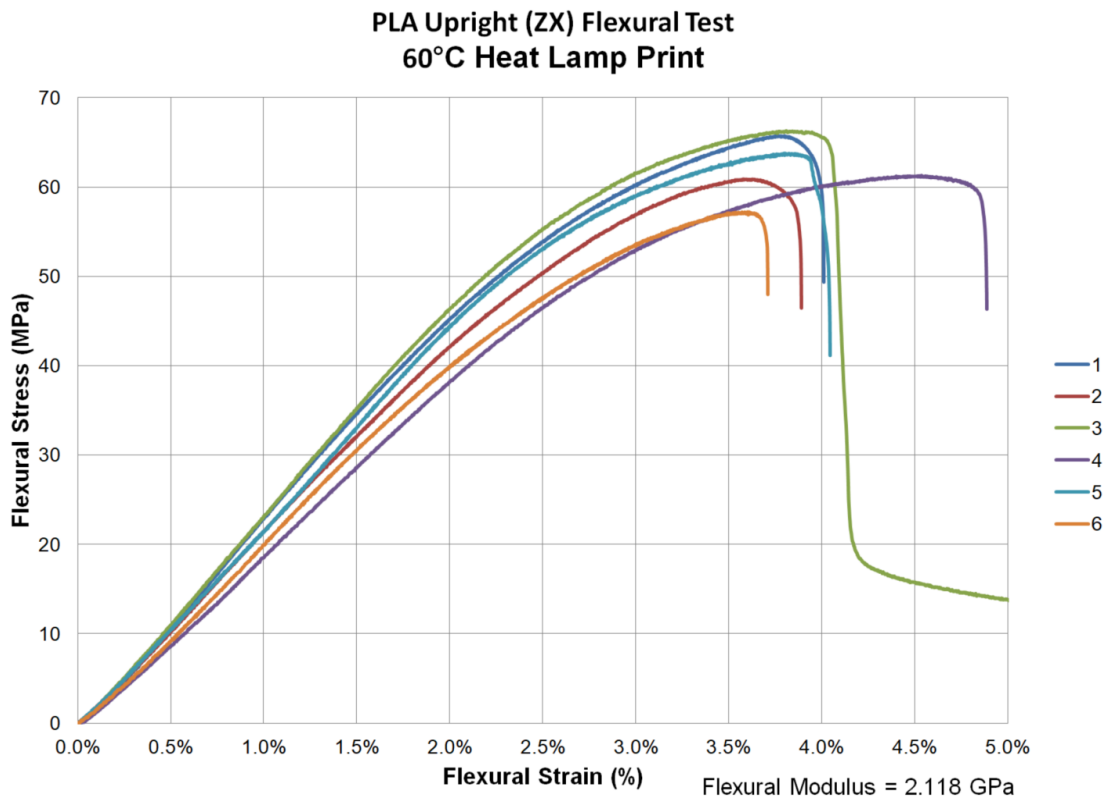


Figure 94. PLA Upright (ZX) Flexural Properties with Heat Lamp at 60°C Stress vs. Strain Plot

PLA Flexural Summary

Table 33 shows the summary of the PLA flexural specimens with and without the heat lamp. Figure 95 shows the summary of the flexural strength. The heat lamp showed an improvement in the flexural strength of the flat (XY) orientation by 13% and an increase in modulus by 14%. The Upright (ZX) flexural strength improved by 21% with using the heat lamp. Figure 96 shows a summary of the flexural modulus. Figure 97 shows a summary of the percent elongation.

Table 33. Summary of PLA Flexural Properties with and without the Heat Lamp

	Flexural Strength (MPa)	SD (Mpa)	Flexural Strain @ Break	SD (%)	Flexural Modulus (GPa)	SD (Gpa)
PLA Flat (XY) RT	82.879	1.888	3.588%	0.054%	2.867	0.078
PLA Flat (XY) 60°C	93.782	4.056	3.719%	0.082%	3.279	0.167
PLA on Edge (XZ) RT	85.030	1.814	4.215%	0.036%	2.519	0.075
PLA on Edge (XZ) 60°C	88.833	2.902	4.034%	0.433%	2.586	0.083
PLA Upright (ZX) RT	51.535	2.419	3.299%	0.172%	1.830	0.136
PLA Upright (ZX) 60°C	62.526	3.414	3.851%	0.350%	2.118	0.160

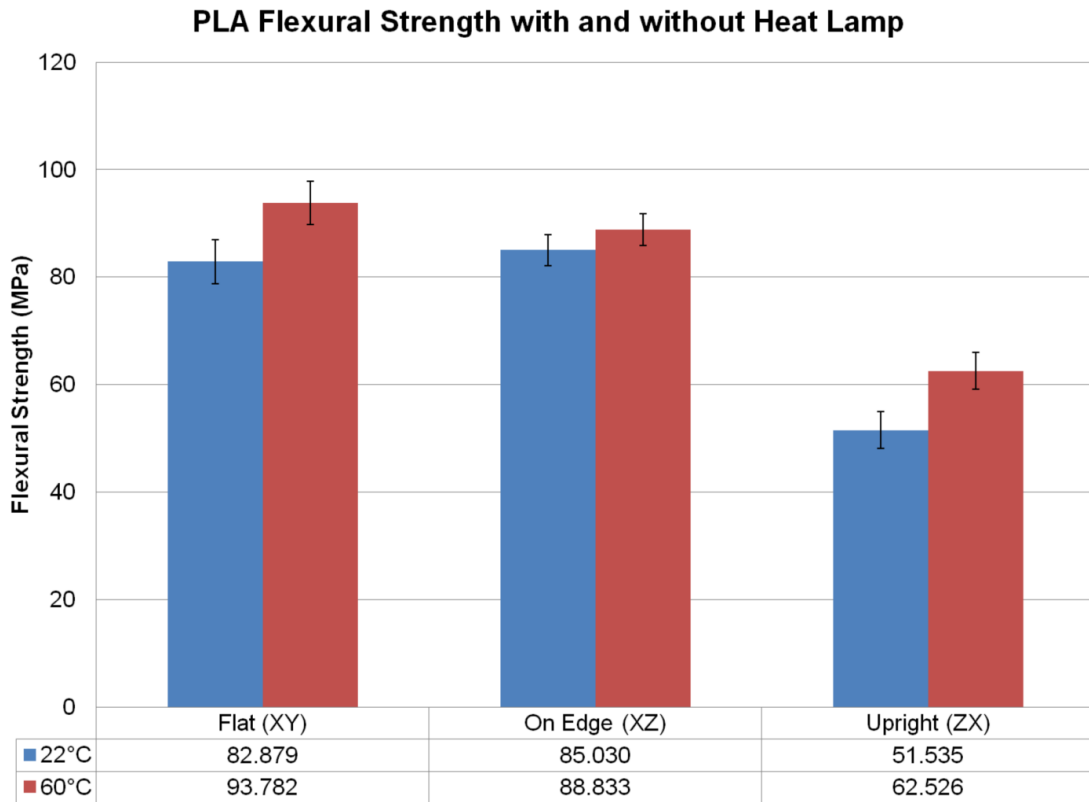


Figure 95. PLA Flexural Strength Summary

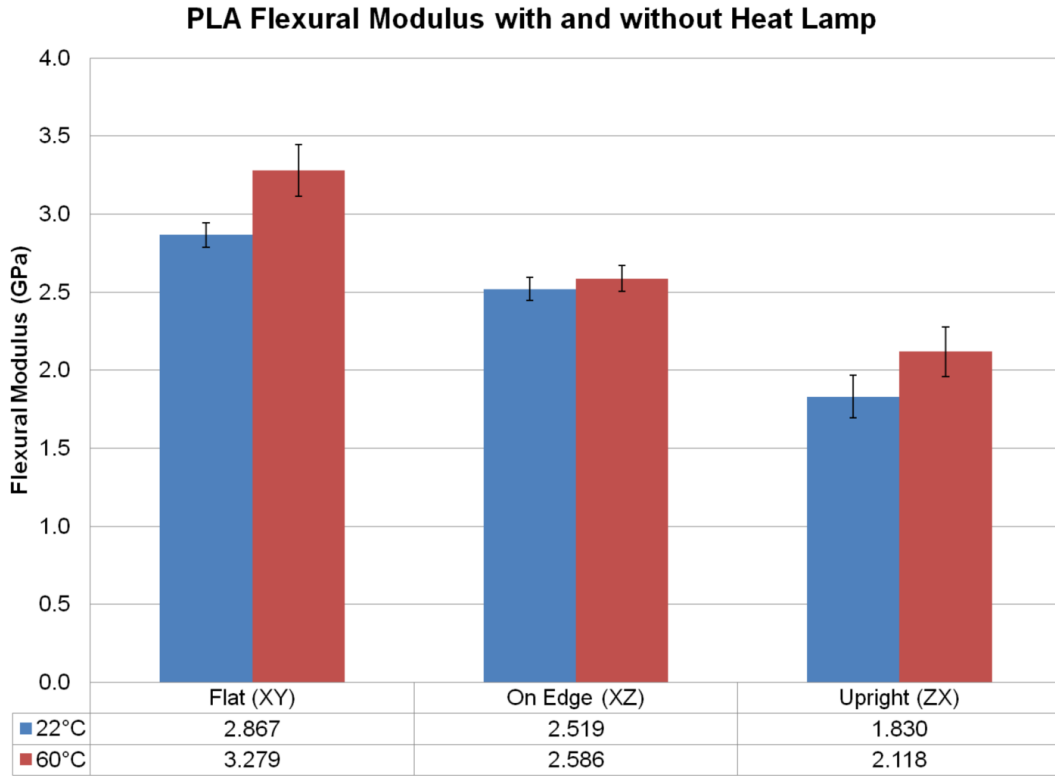


Figure 96. PLA Flexural Modulus Summary

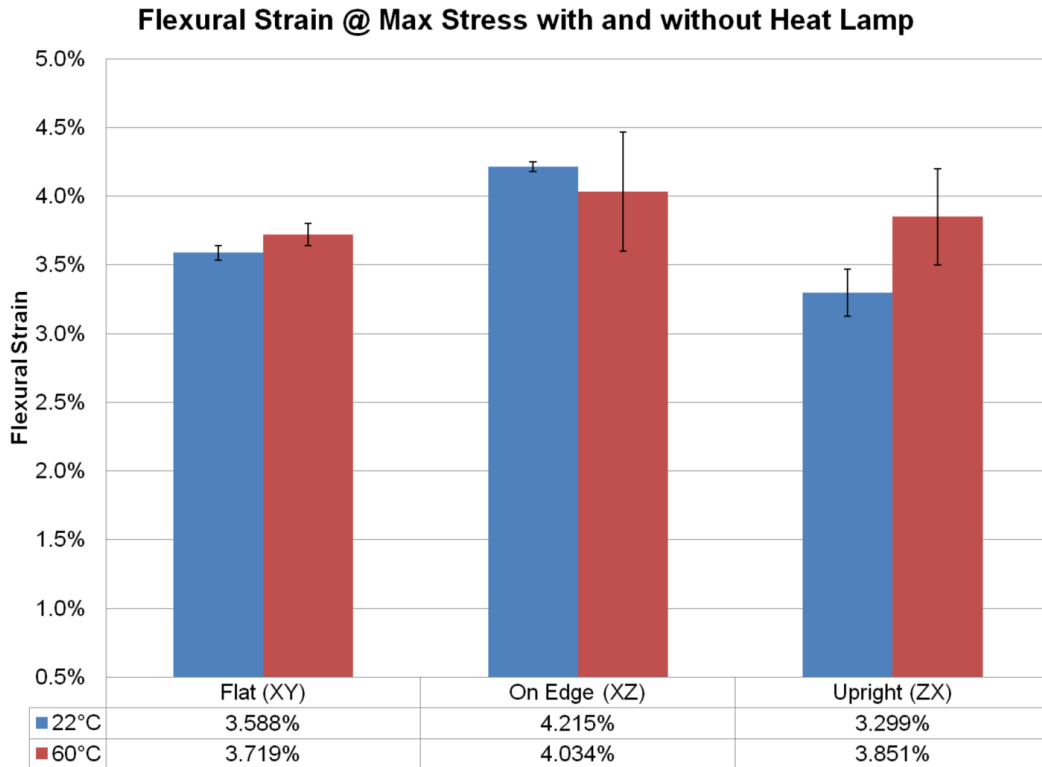


Figure 97. PLA Flexural Strain at Maximum Stress Summary

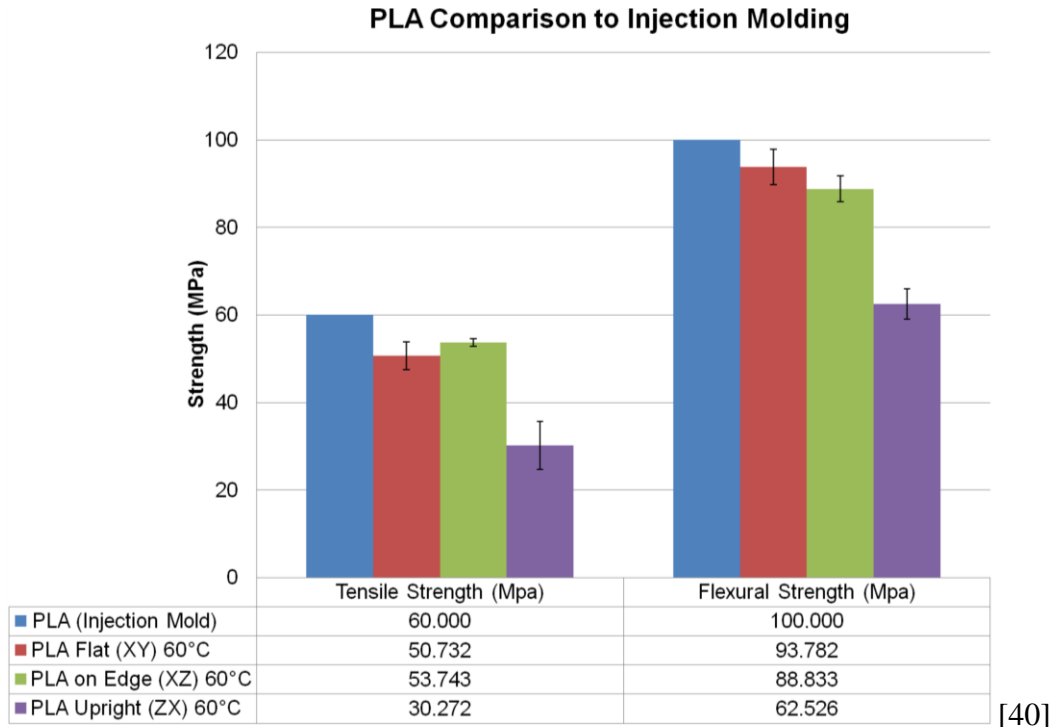
PLA Properties with the Heat Lamp at 60°C compared to Injection Molded PLA

Table 34 shows the comparison of the FFF PLA printing with the heat lamp at 60°C compared to an isotropic injection molded sample. Figure 98 shows the comparison of the tensile and flexural strength. Figure 99 shows a comparison with the tensile and flexural modulus. The tensile and flexural strength are close to the same in the Flat (XY) and on Edge (XZ) orientations but there is still a significant knockdown for the Upright (ZX) orientation. The tensile modulus for the FFF parts is the same as the injection molding. However there is a significant knockdown for the flexural modulus.

Table 34. Comparison of Injection Molded PLA to FFF with the Heat Lamp at 60°C.

	Tensile Strength (Mpa)	SD (Mpa)	Tensile Modulus (Gpa)	SD (Gpa)	Flexural Strength (Mpa)	SD (Mpa)	Flexural Modulus (Gpa)	SD (Gpa)
PLA (Injection Mold)	60.000	-	3.000	-	100.000	-	5.000	-
PLA Flat (XY) 60°C	50.732	3.147	3.001	0.149	93.782	4.056	3.279	0.167
PLA on Edge (XZ) 60°C	53.743	0.868	3.014	0.073	88.833	2.902	2.586	0.083
PLA Upright (ZX) 60°C	30.272	5.491	2.928	0.065	62.526	3.414	2.118	0.160

[40]



[40]

Figure 98. Comparison of Injection Molded PLA to FFF Strength with the Heat Lamp at 60°C

PLA Comparison to Injection Molding

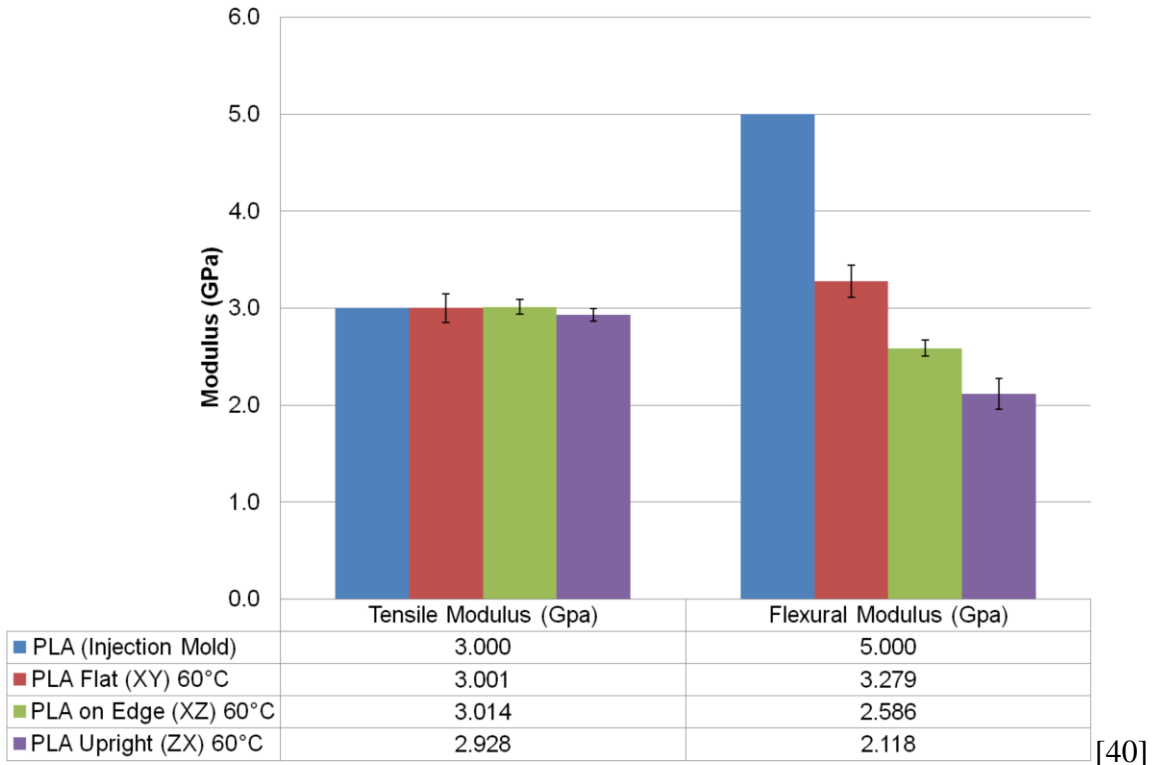


Figure 99. Comparison of Injection Molded PLA to FFF Modulus with the Heat Lamp at 60°C

PEKK Testing

PEKK was tested by printing with the infrared heat lamp set at the temperature of 120°C. This temperature is within the range of the recommended print bed temperature. Figure 100 shows the tensile and flexural specimens after being annealed in the oven. The annealing process was done in an oven for 30 minutes at 160°C then raised to 200°C and held until the color turned a uniform tan color. Figure 101 shows the tensile test specimens. Figure 102 shows the tensile testing setup with a PEKK specimen. All specimens were printed with a 0.3 mm layer height, 0.8 mm layer width, 415°C printing temperature, 120°C to 140°C build plate temperature, 60 mm/s print speed, and 100% infill. It was found that by increasing the build plate temperature to 140°C the parts would warp less. If the heat lamp came close to the location of the thermocouple it would sometimes raise the temperature to the 150°C limit and stop printing. To avoid this from happening, the specimens were printed far enough away from the thermocouple to avoid this temperature rise.



Figure 100. Annealing PEKK Specimens



Figure 101. PEKK Tensile Specimens



Figure 102. Testing PEKK Tensile Specimen

PEKK Flat (XY) Tensile Specimens

Figure 103 shows the PEKK Flat (XY) tensile specimens before testing and Figure 104 shows them after testing. Table 35 shows the dimension of these specimens. Table 36 shows the tensile properties for tensile strength, percent elongation and modulus of elasticity. Figure 105 shows the stress vs. strain plots.

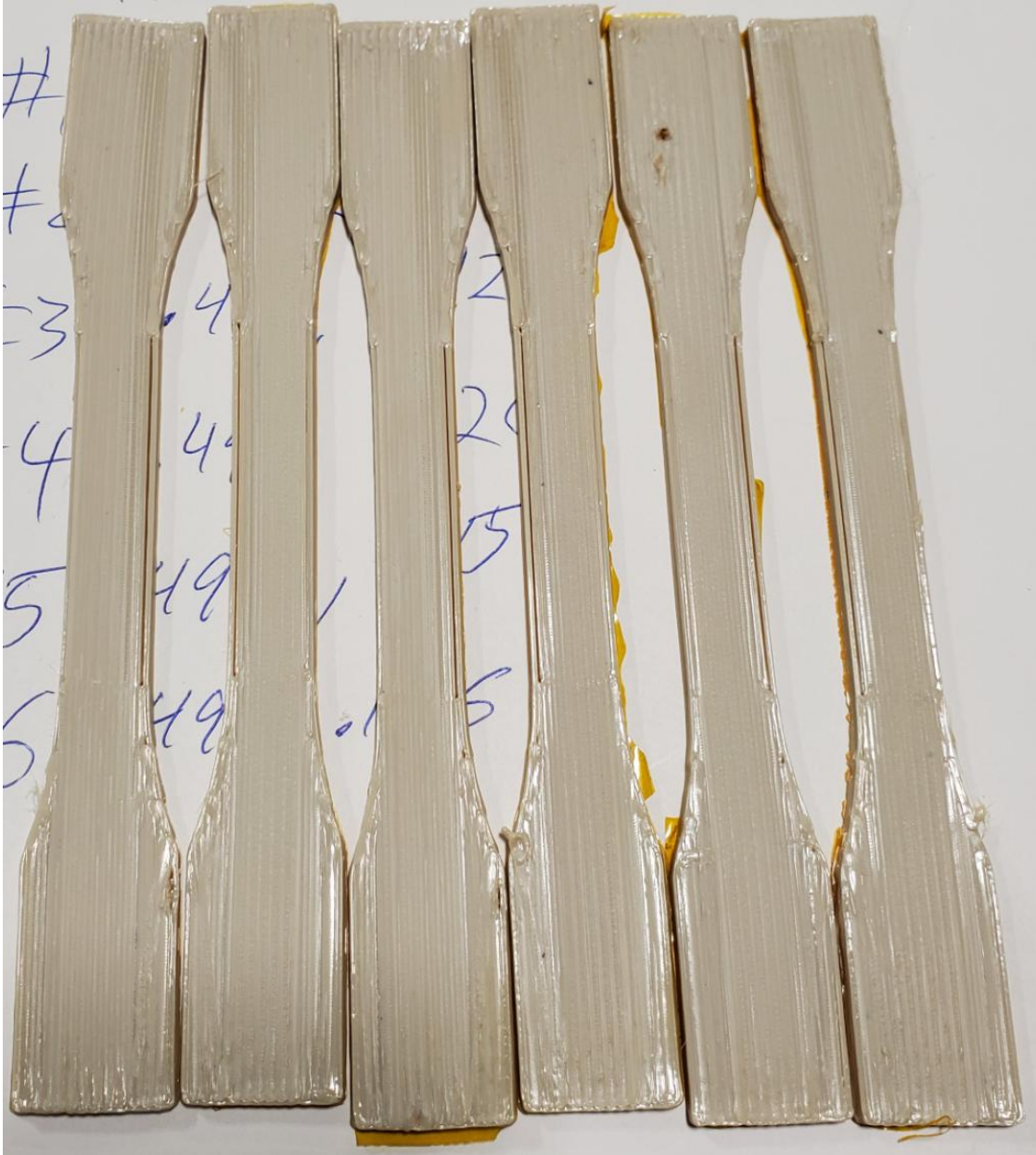


Figure 103. PEKK Flat (XY) Tensile Specimens before Testing



Figure 104. PEKK Flat (XY) Tensile Specimens after Testing

Table 35. PEKK Tensile Flat (XY) Specimen Dimensions

Specimen	Width (mm)	Thickness (mm)
1	12.497	3.124
2	12.497	3.124
3	12.548	3.048
4	12.497	3.048
5	12.522	2.921
6	12.649	2.946
Average	12.535	3.035
SD	0.060	0.086

Table 36. PEKK Flat (XY) Tensile Properties with 120°C Heat Lamp

Specimen ID	Tensile Strength (MPa)	% Elongation at Break	Modulus of Elasticity (GPa)
1	67.537	2.035%	3.438
2	51.527	1.480%	3.558
3	87.211	2.820%	3.273
4	59.938	2.820%	3.521
5	79.220	2.314%	3.595
6	74.723	2.202%	3.521
Average	70.026	2.279%	3.484
SD	13.054	0.508%	0.116

**PEKK Flat (XY) Tensile Test
120°C Heat Lamp Printing**

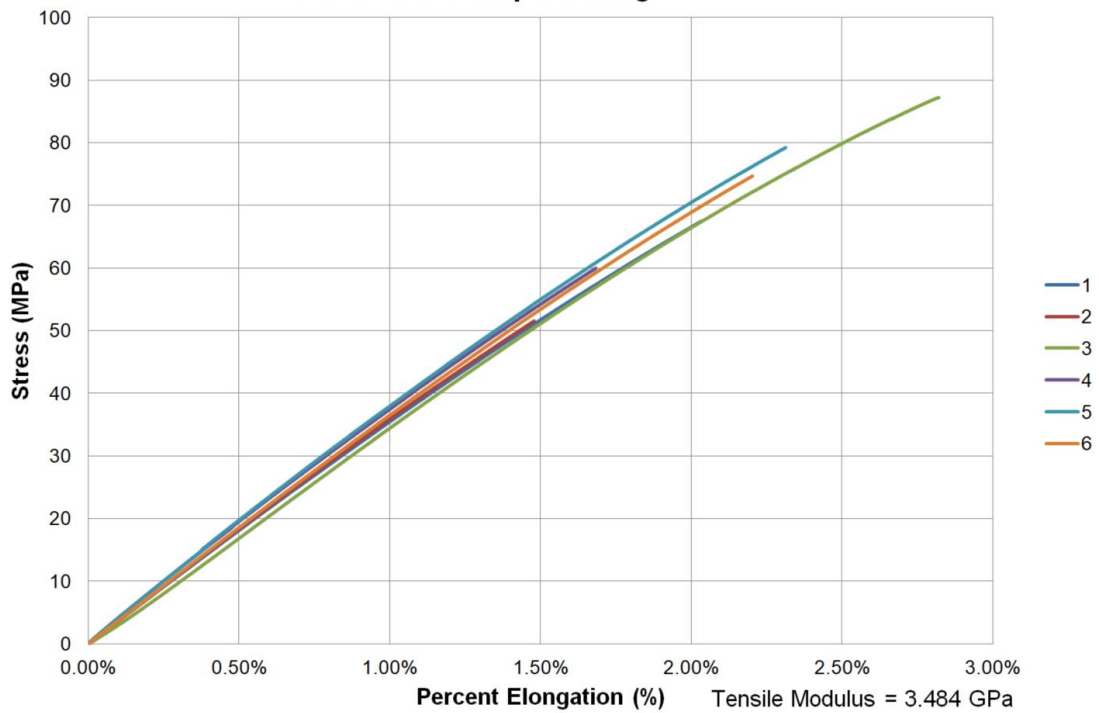


Figure 105. PEKK Flat (XY) Tensile Properties with 120°C Heat Lamp Stress vs. Strain Plot

PEKK Flat (XY) $\pm 45^\circ$ Infill Tensile Specimens

Figure 106 shows the PEKK Flat (XY) with a $\pm 45^\circ$ tensile specimens before testing and Figure 107 shows them after testing. Table 37 shows the dimension of these specimens. Table 38 shows the tensile properties for tensile strength, percent elongation and modulus of elasticity. Figure 108 shows the stress vs. strain plots.

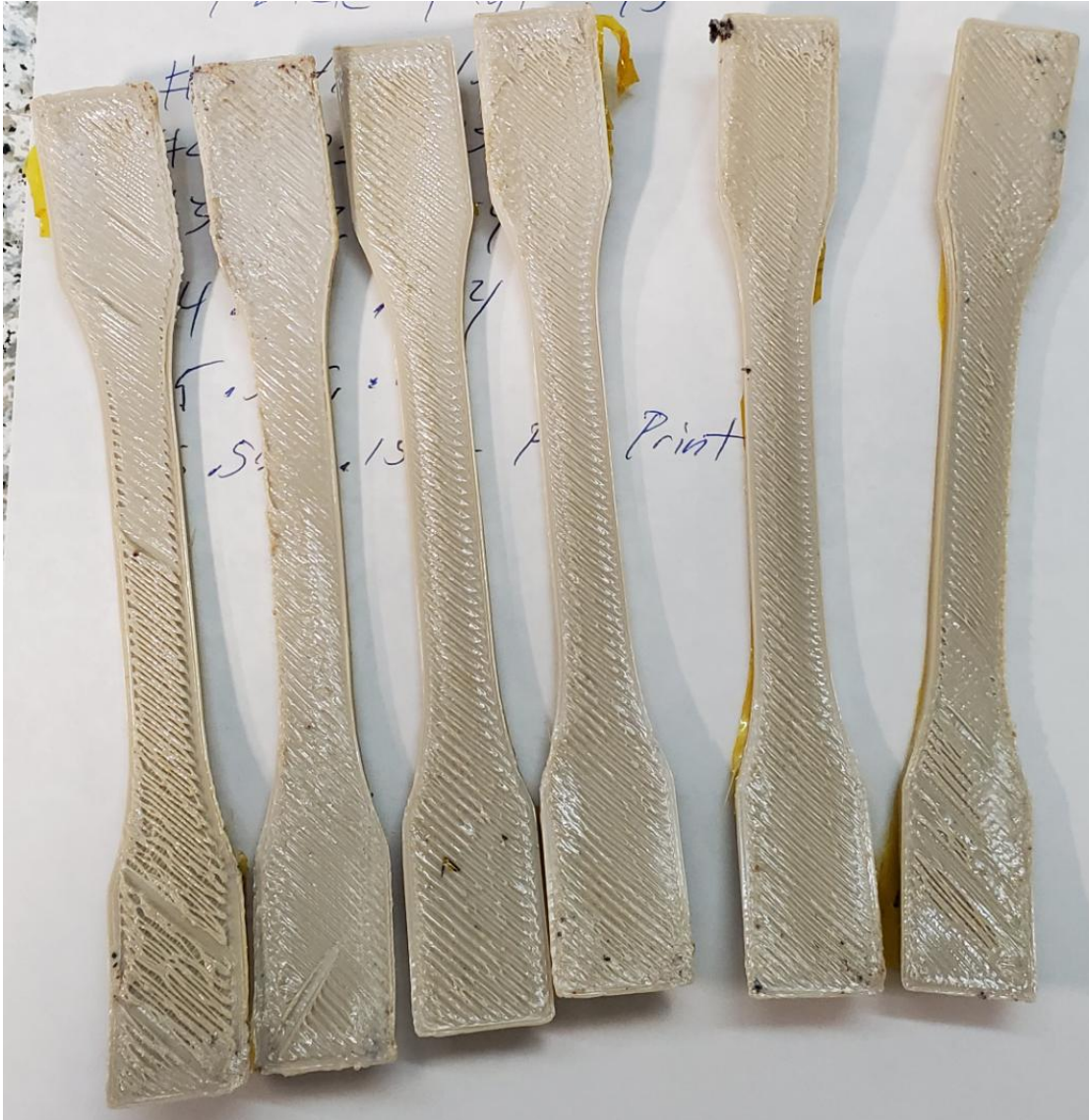


Figure 106. PEKK Flat (XY) $\pm 45^\circ$ Infill Tensile Specimens before Testing



Figure 107. PEKK Flat (XY) $\pm 45^\circ$ Infill Tensile Specimens after Testing

Table 37. PEKK Tensile Flat (XZ) $\pm 45^\circ$ Infill Specimen Dimensions

Specimen	Width (mm)	Thickness (mm)
1	12.649	3.937
2	12.751	3.861
3	12.878	3.912
4	12.954	3.912
5	12.903	3.708
6	12.878	3.835
Average	12.835	3.861
SD	0.113	0.083

Table 38. PEKK Flat (XY) ±45° Infill Tensile Properties with 120°C Heat Lamp

Specimen ID	Tensile Strength (MPa)	% Elongation at Break	Modulus of Elasticity (GPa)
1	80.409	2.338%	3.803
2	Grip Failure		
3	69.155	2.015%	3.693
4	71.314	2.015%	4.972
5	71.530	1.951%	3.939
6	Grip Failure		
Average	73.102	2.080%	4.102
SD	4.988	0.175%	0.589

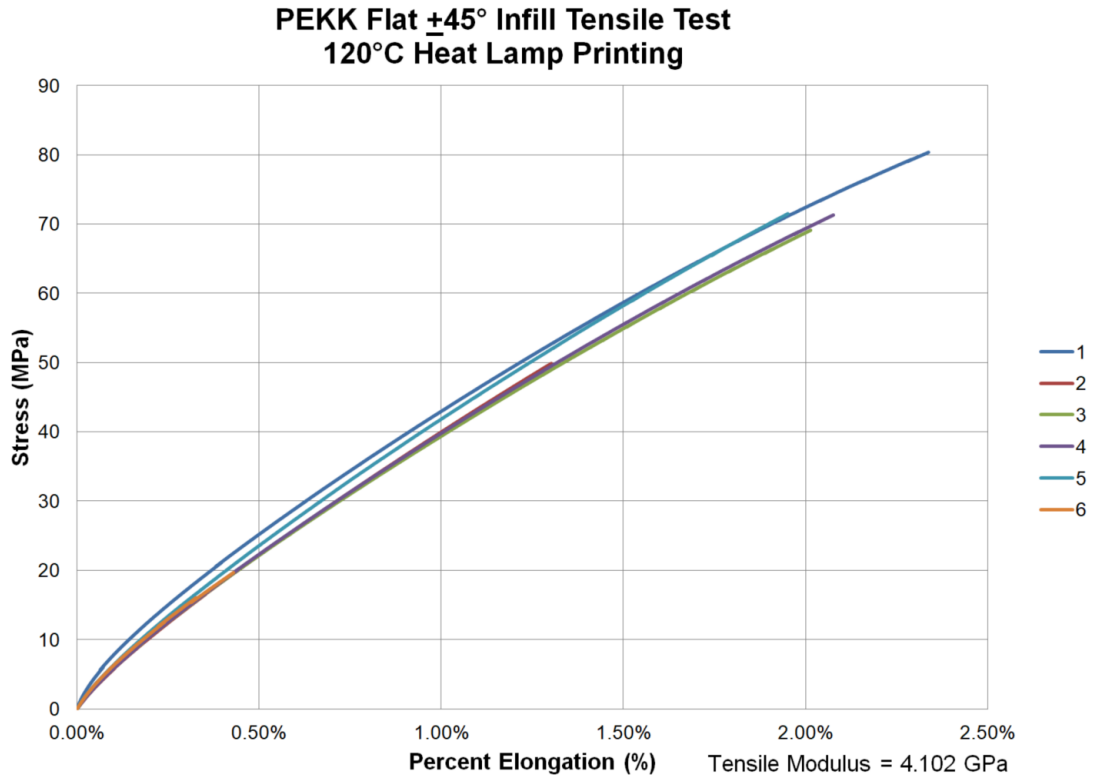


Figure 108. PEKK on Edge (XZ) ±45° Infill Tensile Properties with Heat Lamp at 120°C Stress vs. Strain Plot

PEKK on Edge (XZ) Tensile Specimens

Figure 109 shows the PEKK on Edge (XZ) tensile specimens before testing and Figure 110 shows them after testing. Table 39 shows the dimension of these specimens. Table 40 shows the tensile properties for tensile strength, percent elongation and modulus of elasticity. Figure 111 shows the stress vs. strain plots.

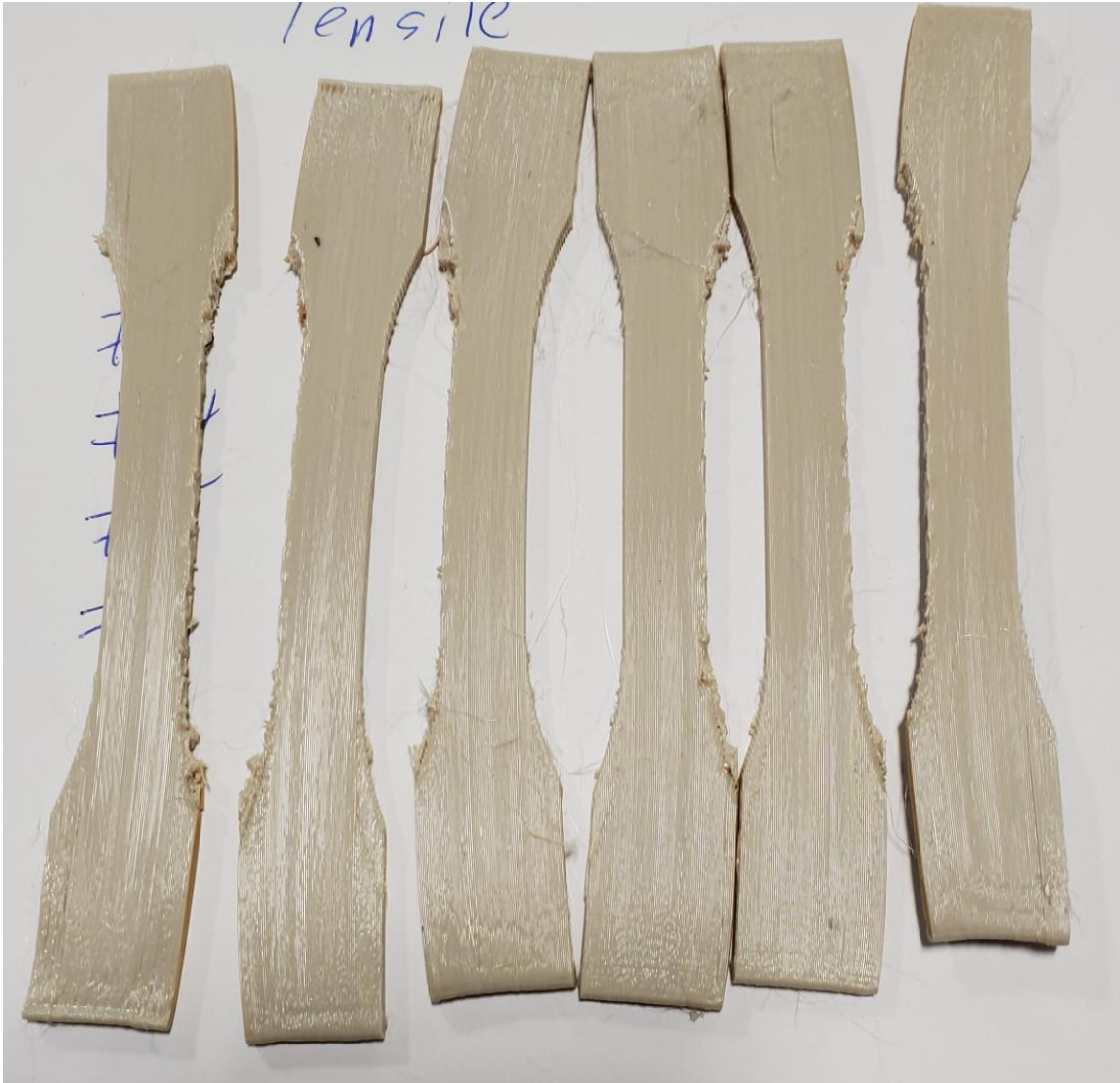


Figure 109. PEKK on Edge (XZ) Tensile Specimens before Testing



Figure 110. PEKK on Edge (XZ) Tensile Specimens before Testing

Table 39. PEKK Tensile on Edge (XZ) Specimen Dimensions

Specimen	Width (mm)	Thickness (mm)
1	13.792	3.556
2	13.995	3.556
3	13.970	3.607
4	13.945	3.556
5	13.792	3.556
6	14.046	3.607
Average	13.923	3.573
SD	0.107	0.026

Table 40. PEKK on Edge (XZ) Tensile Properties with Heat Lamp at 120°C

Specimen ID	Tensile Strength (MPa)	% Elongation at Break	Modulus of Elasticity (GPa)
1	93.970	3.365%	3.097
2	89.937	3.127%	3.161
3	86.307	2.889%	3.262
4	106.496	5.104%	2.959
5	105.251	4.474%	3.310
6	90.022	3.361%	2.959
Average	95.330	3.720%	3.125
SD	8.528	0.870%	0.148

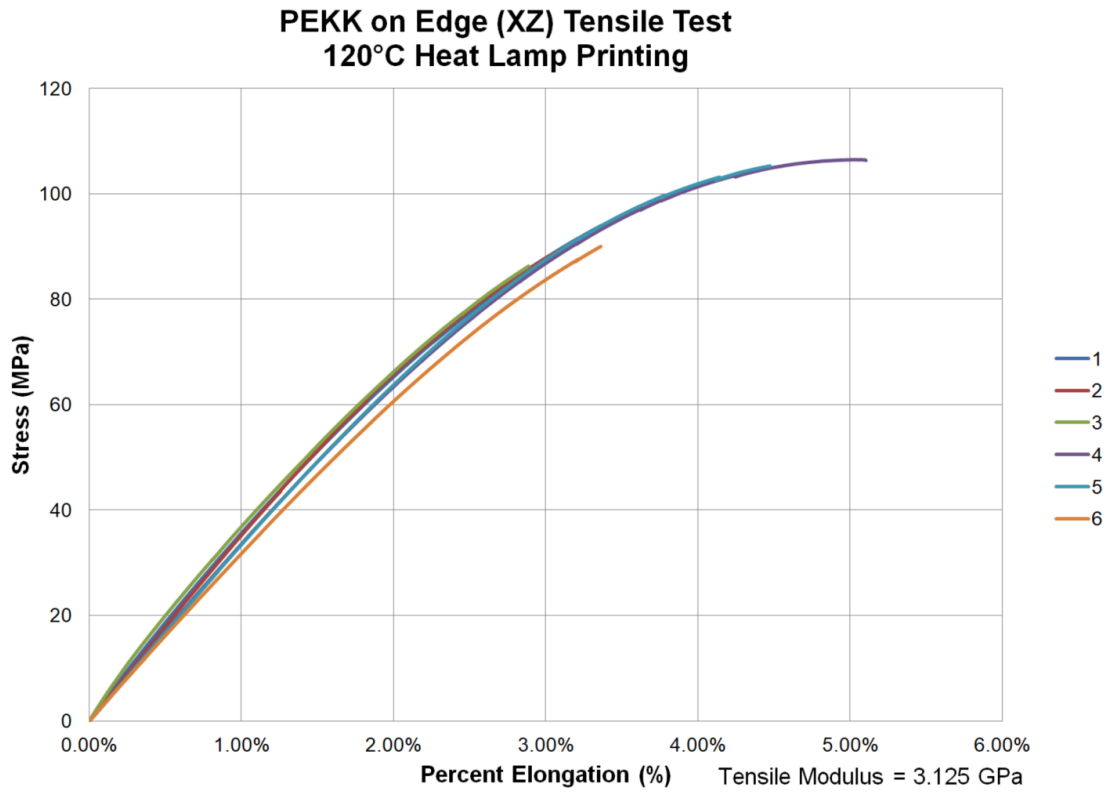


Figure 111. PEKK on Edge (XZ) Tensile Properties with Heat Lamp at 120°C Stress vs. Strain Plot

PEKK Upright (ZX) Tensile Specimens

Figure 112 shows the PEKK Upright (ZX) tensile specimens before testing and Figure 113 shows them after testing. Table 41 shows the dimension of these specimens. Table 42 shows the tensile properties for tensile strength, percent elongation and modulus of elasticity. Figure 114 shows the stress vs. strain plots.



Figure 112. PEKK Upright (ZX) Tensile Specimens before Testing

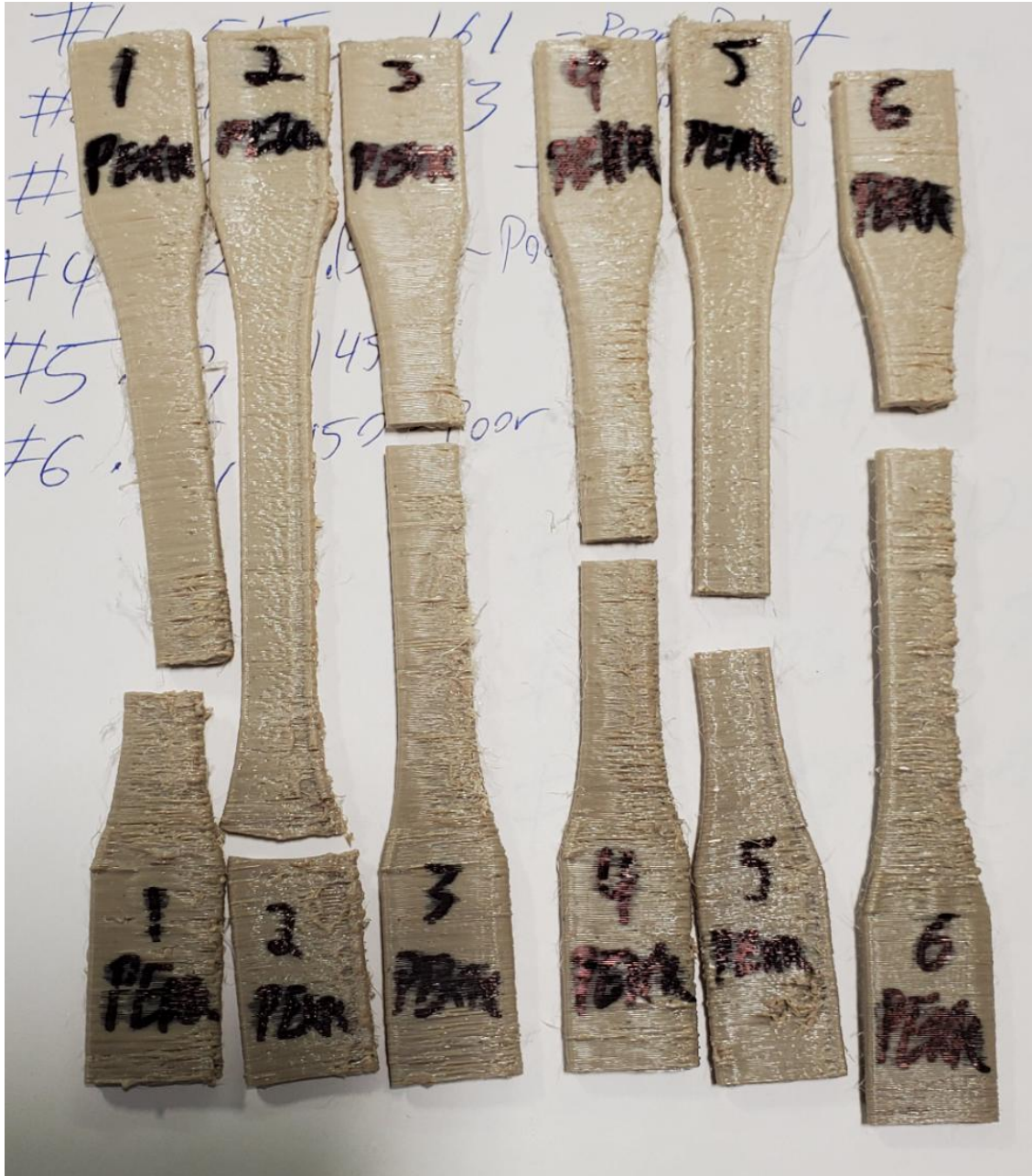


Figure 113. PEKK Upright (ZX) Tensile Specimens after Testing

Table 41. PEKK Tensile Upright (ZX) Specimen Dimensions

Specimen	Width (mm)	Thickness (mm)
1	13.081	4.089
2	12.675	3.886
3	12.751	3.683
4	13.005	3.988
5	12.954	3.683
6	13.081	3.810
Average	12.924	3.857
SD	0.173	0.164

Table 42. PEKK Upright (ZX) Tensile Properties with Heat Lamp at 120°C

Specimen ID	Tensile Strength (MPa)	% Elongation at Break	Modulus of Elasticity (GPa)
1	16.955	0.875%	1.853
2	15.623	0.560%	2.695
3	19.647	0.719%	2.823
4	15.281	0.719%	2.691
5	21.310	0.785%	2.748
6	15.187	0.592%	2.691
Average	17.334	0.708%	2.584
SD	2.571	0.118%	0.362

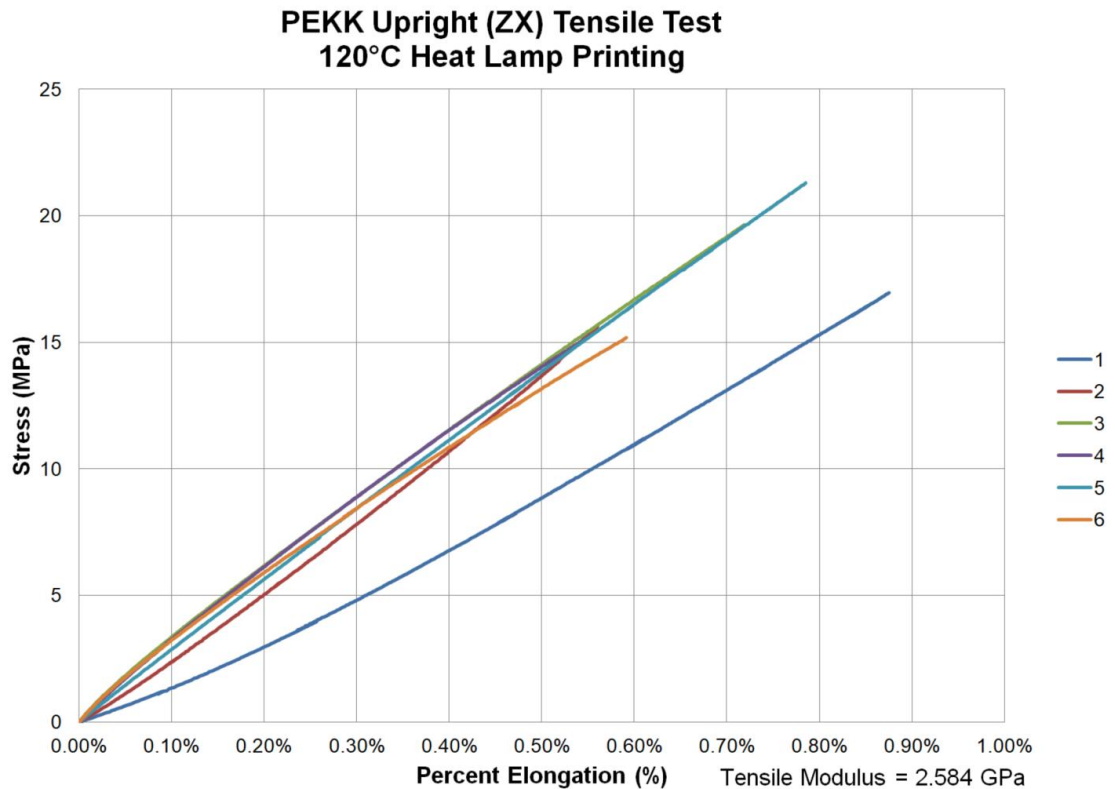


Figure 114. PEKK on Upright (ZX) Tensile Properties with Heat Lamp at 120°C Stress vs. Strain Plot

PEKK Tensile Testing Summary

Table 43 shows the summary of the PEKK tensile specimens with the heat lamp. Table 44 shows the published data for Stratasys Antero 800NA PEKK filament printed on the F900 FDM printer. Table 45 shows the published data for Stratasys Antero 800NA PEKK filament printed on the Fortus 450mc FDM printer. Figure 115 shows the summary of the tensile strength compared to Stratasys 899NA. The tensile strength of on Edge (XZ) is the same as the Stratasys 800 NA. However, the Upright (ZX) tensile strength is greatly reduced. Figure 116 shows a summary of the tensile modulus. The tensile modulus of on Edge (XZ) and Flat (XY) are similar to the Stratasys 800 NA. However, the Upright (ZX) tensile modulus is reduced. Figure 117 shows the summary of the percent elongation. The on Edge (XZ) percent elongation is comparable but the other two orientations are reduced.

Table 43. Tensile Testing Summary PEKK on Lulzbot Taz 5 with 120°C Heat Lamp

Thermax PEKK Lulzbot Taz 5	Tensile Strength (MPa)	SD (Mpa)	% Elongation at Break	SD (%)	Modulus of Elasticity (GPa)	SD (Gpa)
Flat (XY)	70.026	13.054	2.279%	0.508%	3.484	0.116
On Edge (XZ)	95.330	8.528	3.720%	0.870%	3.125	0.148
Upright (ZX)	17.334	2.571	0.708%	0.118%	2.584	0.362

Table 44. Published Tensile Testing Data for FDM PEKK from Stratasys Antero 800 NA – F900 with T20D Tip

PEKK Stratasys 800 NA F900	Tensile Strength (MPa)	SD (Mpa)	% Elongation at Break	SD (%)	Modulus of Elasticity (GPa)	SD (Gpa)
Flat (XY)						
On Edge (XZ)	90.000	3.000	4.300%	0.300%	2.900	0.100
Upright (ZX)	55.000	5.000	1.900%	0.300%	2.900	0.100

[43]

Table 45. Published Tensile Testing Data for FDM PEKK from Stratasys Antero 800 NA –Fortus 450mc with T20D Tip

PEKK Stratasys 800 NA Fortu	Tensile Strength (MPa)	SD (Mpa)	% Elongation at Break	SD (%)	Modulus of Elasticity (GPa)	SD (Gpa)
Flat (XY)						
On Edge (XZ)	93.000	1.000	4.300%	0.600%	3.100	0.300
Upright (ZX)	45.000	5.000	1.200%	0.300%	3.500	0.700

[43]

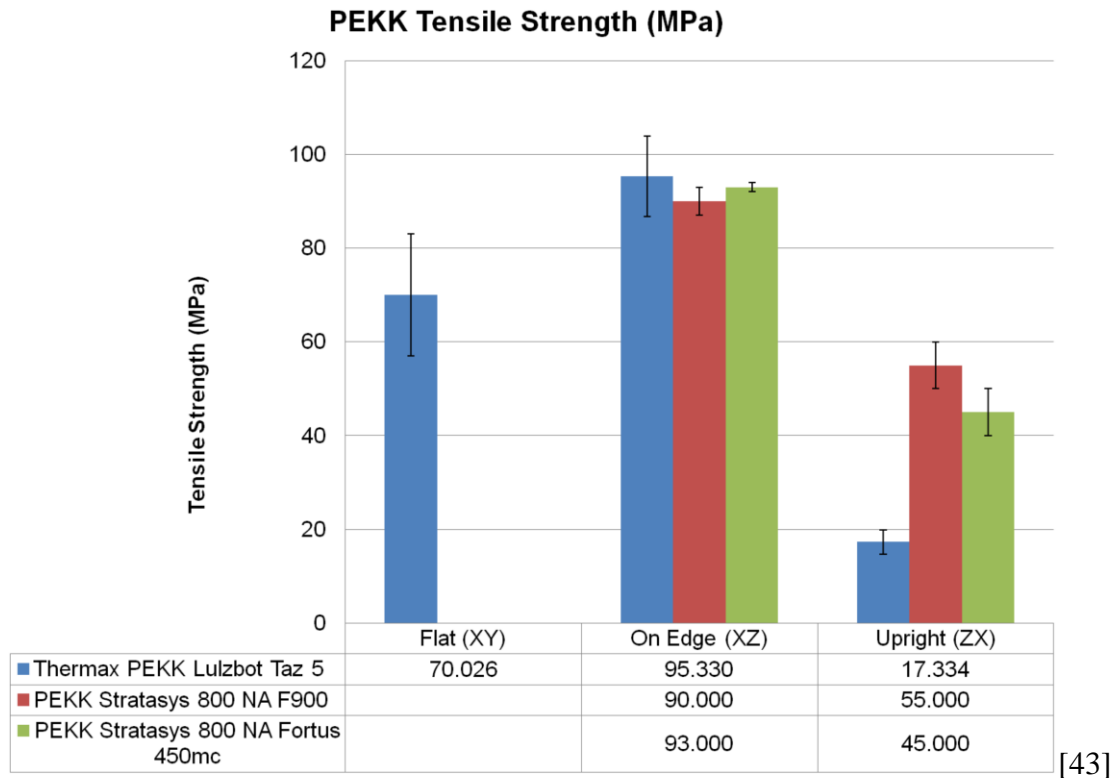


Figure 115. PEKK FFF Tensile Strength Printing with Lulzbot 5 with Heat Lamp at 120°C compared to Stratasys FDM Printers

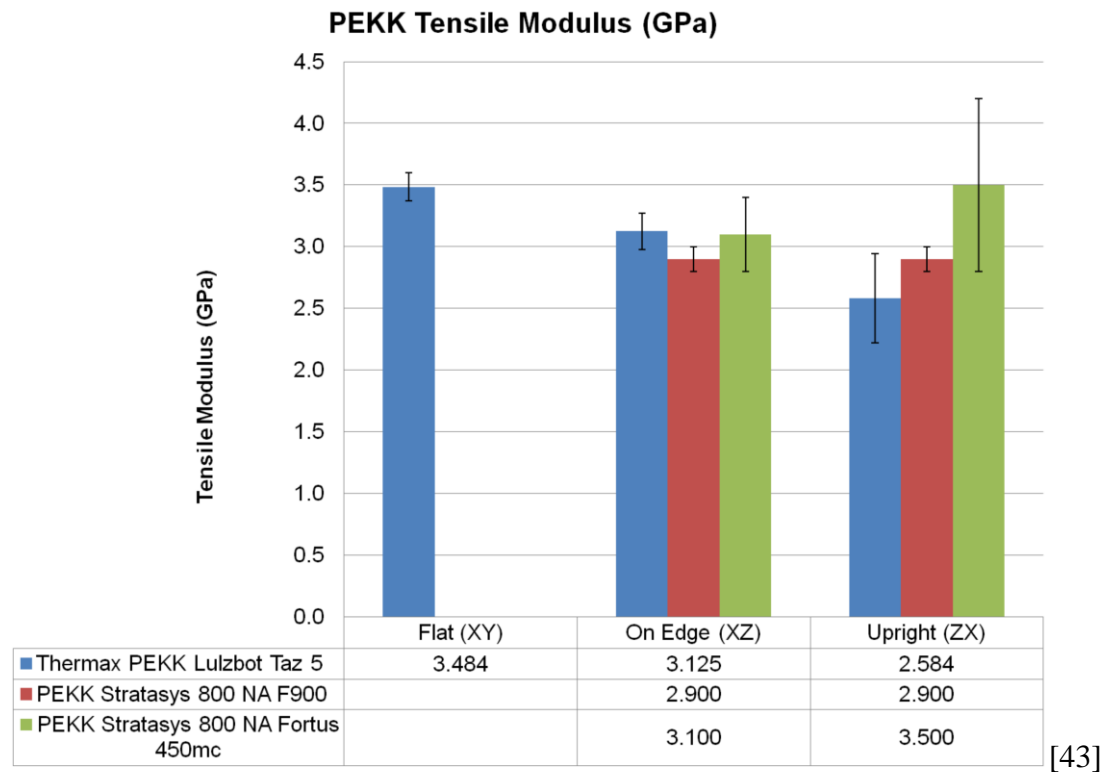


Figure 116. PEKK FFF Tensile Modulus Printing with Lulzbot 5 with Heat Lamp at 120°C compared to Stratasys FDM Printers

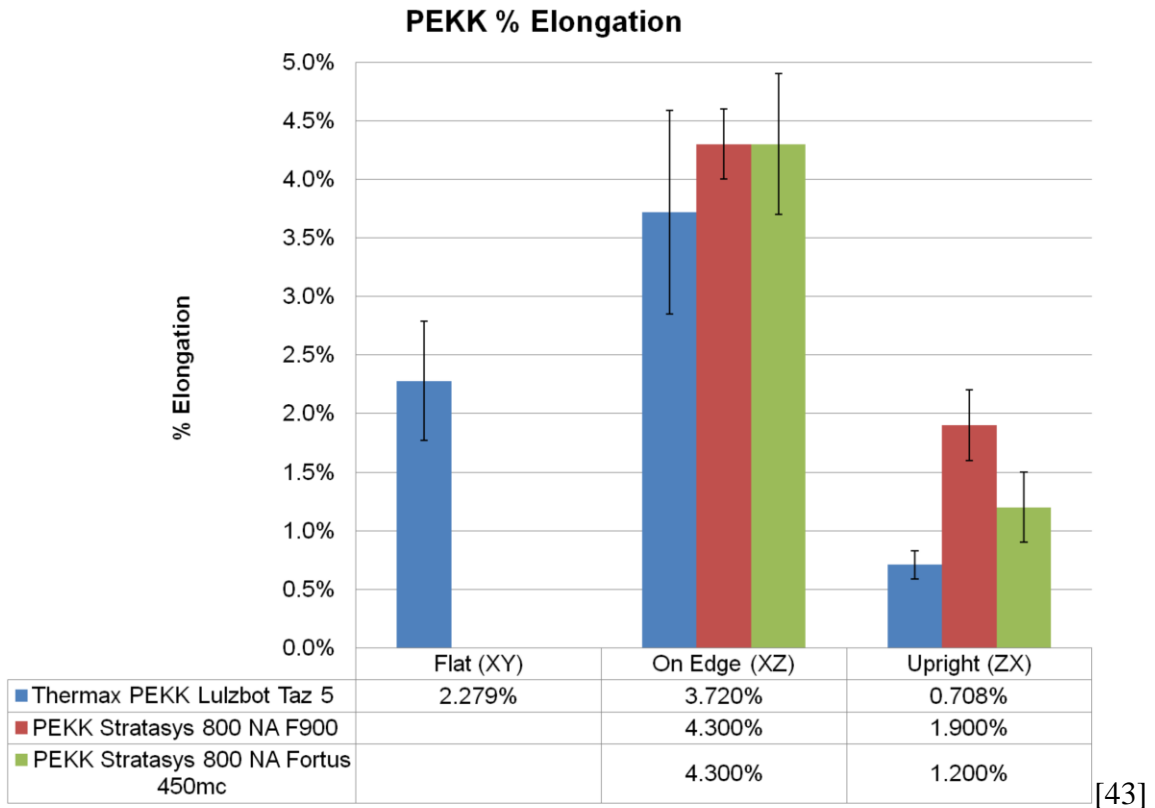


Figure 117. PEKK FFF % Elongation Printing with Lulzbot 5 with Heat Lamp at 120°C compared to Stratasys FDM Printers

PEKK Flat (XY) Flexural Specimens

Figure 118 shows the flexural testing setup with a PEKK specimen. Figure 119 shows the PEKK Flat (XY) flexural specimens before testing and Figure 120 shows them after testing. Table 46 shows the dimension of these specimens. Table 47 shows the flexural properties for flexural strength, flexural strain at maximum stress or 5%, and flexural modulus. Figure 121 shows the stress vs. strain plots.

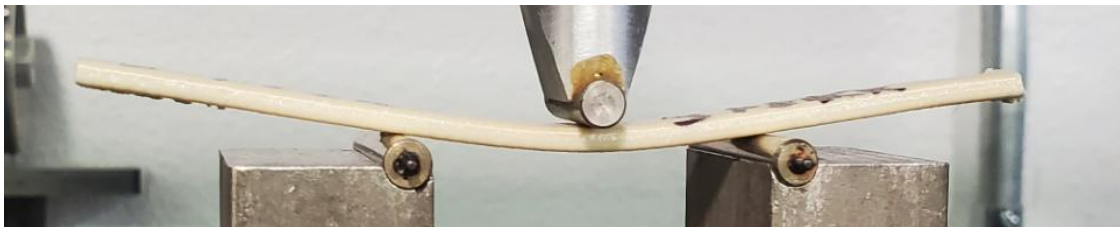


Figure 118. Flexural Testing of PEKK Specimen



Figure 119. PEKK Flat (XY) Flexural Specimens before Testing



Figure 120. PEKK Flat (XY) Flexural Specimens after Testing

Table 46. PEKK Flexural Flat (XY) Specimen Dimensions

Specimen	Width (mm)	Thickness (mm)
1	12.725	3.073
2	12.649	3.124
3	12.649	3.124
4	12.649	3.124
5	12.802	2.997
6	12.725	3.099
Average	12.700	3.090
SD	0.062	0.050

Table 47. PEKK Flat (XY) Flexural Properties with 120°C Heat Lamp

Specimen ID	Flexural Strength (MPa)	Flexural Strain @ Max Stress or 5%	Flexural Modulus (GPa)
1	164.963	5.000%	3.499
2	164.103	5.001%	3.585
3	170.732	5.001%	3.812
4	164.892	5.001%	3.695
5	156.462	4.275%	3.888
6	163.968	5.001%	3.541
Average	165.732	4.880%	3.626
SD	2.831	0.297%	0.127

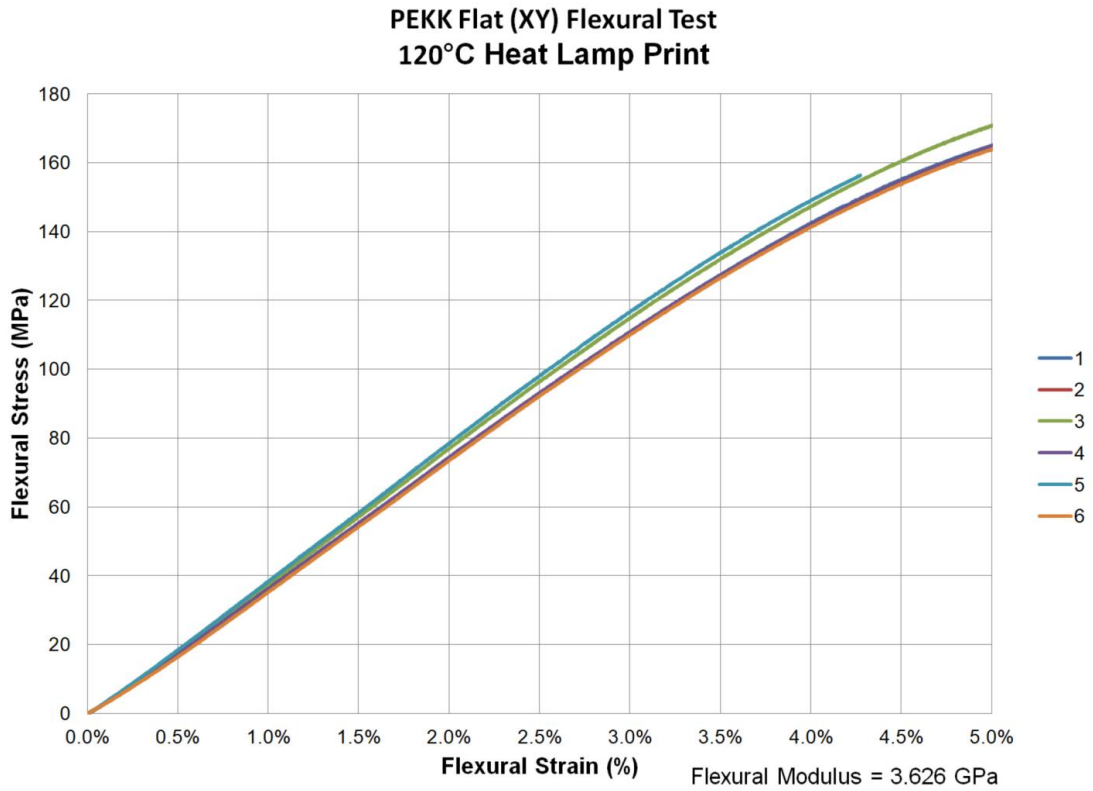


Figure 121. PEKK Flat (XY) Flexural Properties with 120°C Heat Lamp Stress vs. Strain Plot

PEKK Flexural on Edge (XZ) Specimen

Figure 122 shows the PEKK on Edge (XZ) flexural specimens before testing and Figure 123 shows them after testing. Table 48 shows the dimension of these specimens. Table 49 shows the flexural properties for flexural strength, flexural strain at maximum stress or 5%, and flexural modulus. Figure 124 shows the stress vs. strain plots.



Figure 122. PEKK on Edge (XZ) Flexural Specimens before Testing

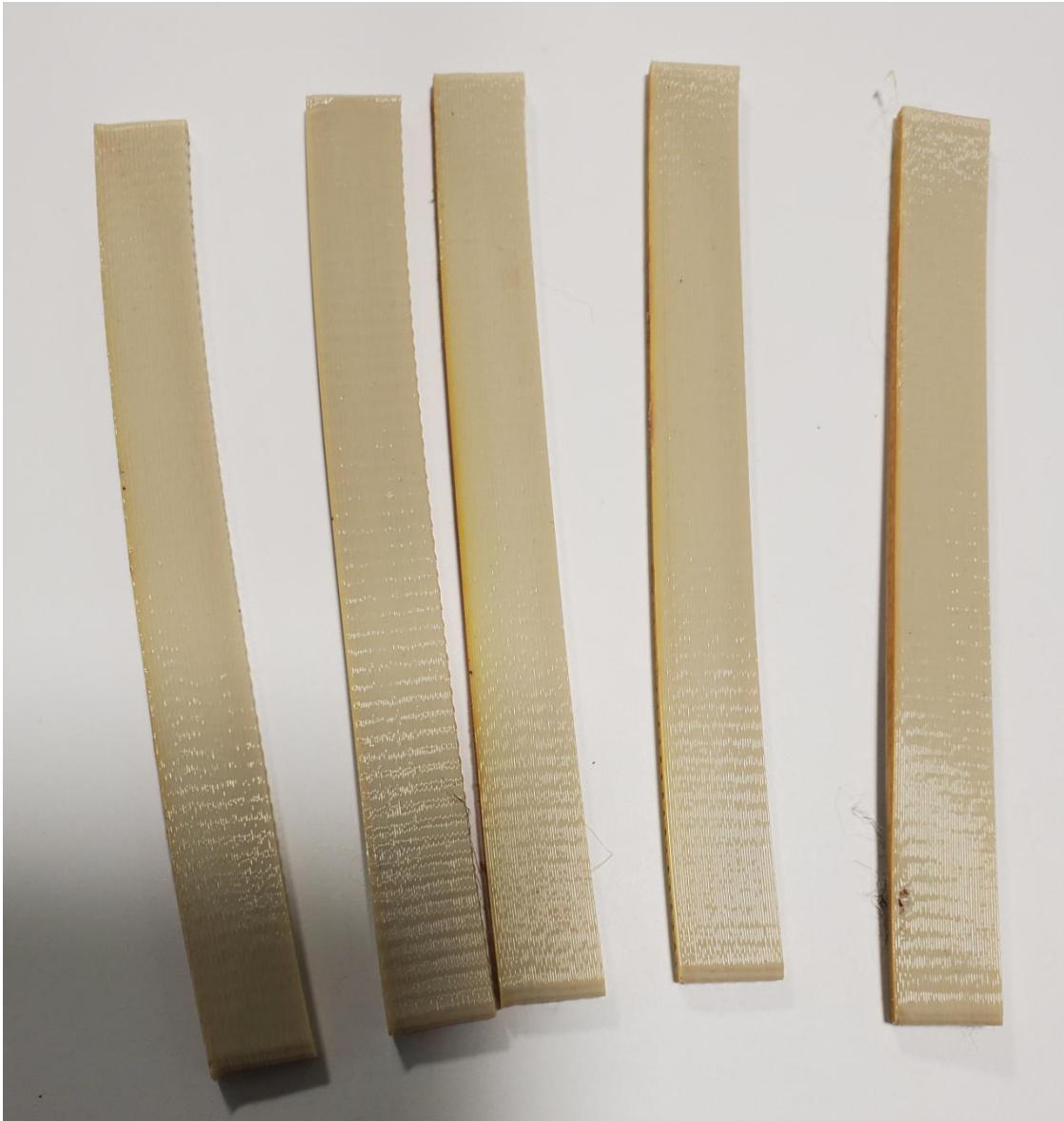


Figure 123. PEKK on Edge (XZ) Flexural Specimens after Testing

Table 48. PEKK Flexural on Edge (XZ) Specimen Dimensions

Specimen	Width (mm)	Thickness (mm)
1	12.192	3.480
2	12.446	3.404
3	12.598	3.531
4	12.573	3.429
5	12.421	3.404
Average	12.446	3.449
SD	0.162	0.055

Table 49. PEKK on Edge (XZ) Flexural Properties with Heat Lamp at 120°C

Specimen ID	Flexural Strength (MPa)	Flexural Strain @ 5%	Flexural Modulus (GPa)
1	151.847	5.001%	2.554
2	160.119	5.001%	3.303
3	153.189	5.000%	3.295
4	154.830	5.001%	3.322
5	164.224	5.001%	3.497
Average	156.842	5.001%	3.194
SD	5.186	0.001%	0.367

**PEKK on Edge (XZ) Flexural Test
120°C Heat Lamp Print**

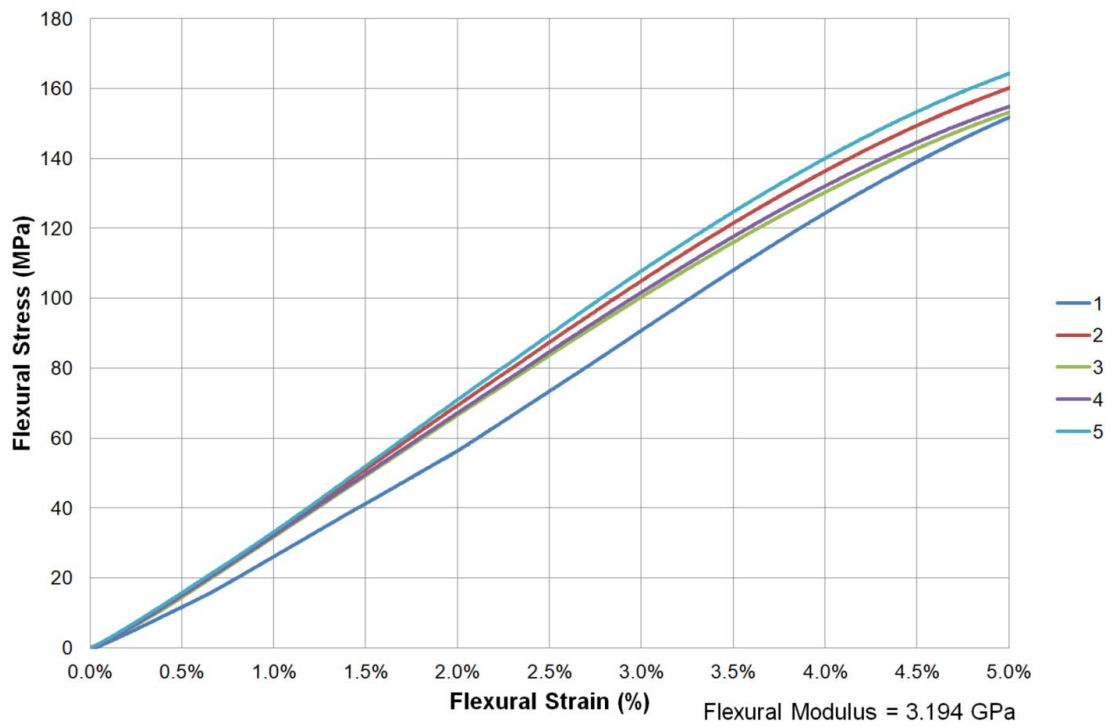


Figure 124. PEKK on Edge (XZ) Flexural Properties with Heat Lamp at 120°C Stress vs. Strain Plot

PEKK Upright (ZX) Flexural Specimens

Figure 125 shows the PEKK Upright (ZX) flexural specimens before testing and Figure 126 shows them after testing. Table 50 shows the dimension of these specimens. Table 51 shows the flexural properties for flexural strength, flexural strain at maximum stress or 5%, and flexural modulus. Figure 127 shows the stress vs. strain plots.



Figure 125. PEKK Upright (ZX) Flexural Specimens

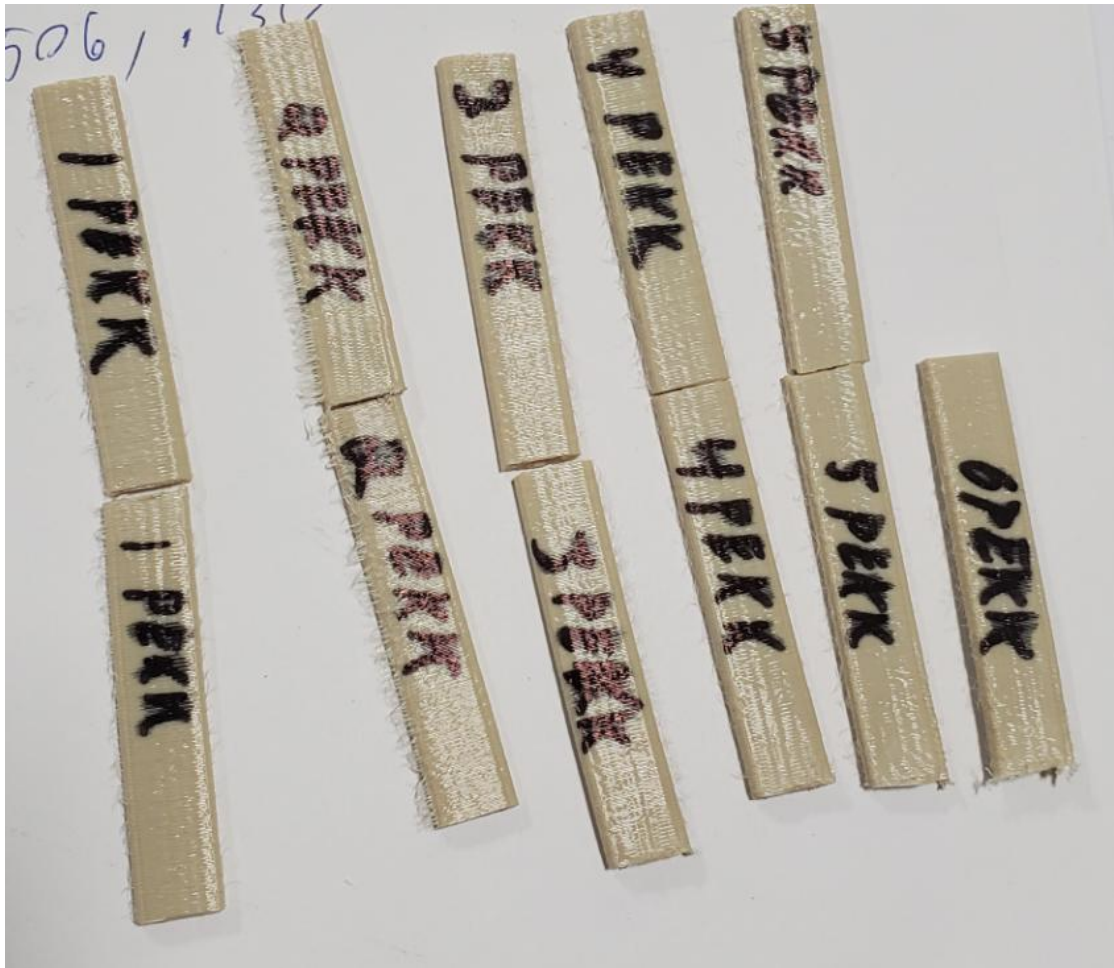


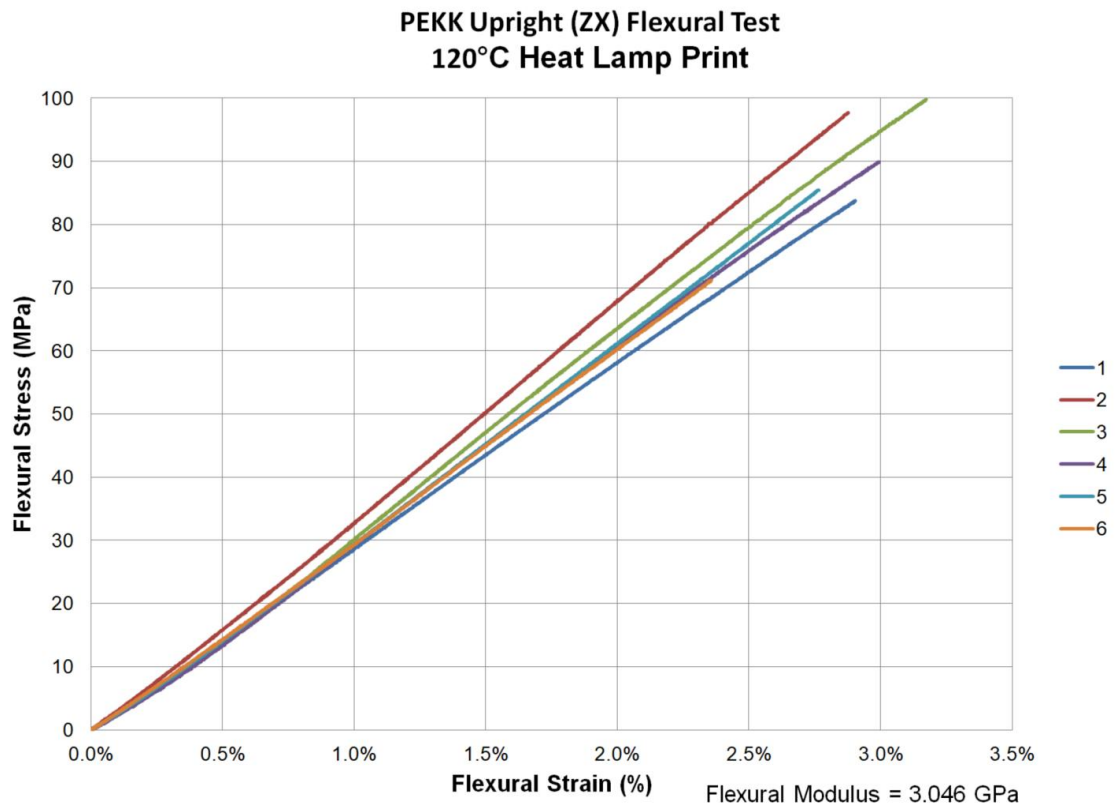
Figure 126. PEKK Upright (ZX) Flexural Specimens after Testing.

Table 50. PEKK Flexural Upright (ZX) Specimen Dimensions

Specimen	Width (mm)	Thickness (mm)
1	12.878	3.632
2	12.827	3.353
3	12.827	3.505
4	12.852	3.556
5	12.827	3.505
6	12.852	3.505
Average	12.844	3.509
SD	0.021	0.091

Table 51. PEKK Upright (ZX) Flexural Properties with Heat Lamp at 120°C

Specimen ID	Flexural Strength (MPa)	Flexural Strain @ Max Stress	Flexural Modulus (GPa)
1	83.769	2.904%	2.835
2	97.684	2.877%	3.272
3	99.774	3.174%	3.132
4	89.888	2.994%	3.012
5	85.392	2.764%	3.033
6	71.126	2.359%	2.991
Average	87.939	2.845%	3.046
SD	10.444	0.275%	0.147



**Figure 127. PEKK on Upright (ZX) Flexural Properties with Heat Lamp at 120°C
Stress vs. Strain Plot**

PEKK Flexural Testing Summary

Table 52 shows the summary of the PEKK flexural specimens with the heat lamp. Table 53 shows the published data for Stratasys Antero 800NA PEKK filament printed on the F900 FDM printer. Table 54 shows the published data for Stratasys Antero 800NA PEKK filament printed on the Fortus 450mc FDM printer. Figure 128 shows the summary of the flexural strength compared to Stratasys 899NA. The flexural strength of on Edge (XZ) and Flat (XY) show an improvement of 12 to 18% compared to the Stratasys 800 NA. The Upright (ZX) flexural strength is the same as Stratasys. Figure 129 shows a summary of the flexural modulus. The flexural modulus of on Edge (XZ) is similar to the Stratasys 800 NA. However, the Upright (ZX) flexural modulus shows a slight improvement. Figure 130 shows the summary of the flexural strain at break for Upright (ZX). The flexural strain is comparable to Stratasys.

Table 52. Flexural Testing Summary PEKK on Lulzbot Taz 5 with 120°C Heat Lamp

Thermax PEKK Lulzbot Taz 5	Flexural Strength (MPa)	SD (Mpa)	Flexural Modulus (GPa)	SD (GPa)	Flexural Strain	SD (%)
Flat (XY)	165.732	2.831	3.626	0.127	No Break	-
On Edge (XZ)	156.842	5.186	3.194	0.367	No Break	-
Upright (ZX)	87.939	10.444	3.046	0.147	2.845%	0.275%

Table 53. Published Flexural Testing Data for FFF PEKK from Stratasys Antero 800 NA – F900 with T20D Tip

PEKK Stratasys 800NA F900	Flexural Strength (MPa)	SD (Mpa)	Flexural Modulus (GPa)	SD (GPa)	Flexural Strain	SD (%)
On Edge (XZ)	140.000	4.000	3.100	0.100	No Break	-
Upright (ZX)	90.000	13.000	2.700	0.100	3.300%	0.500%

[43]

Table 54. Published Flexural Testing Data for FFF PEKK from Stratasys Antero 800 NA –Fortus 450mc with T20D Tip

PEKK Stratasys 800NA Fortus	Flexural Strength (MPa)	SD (Mpa)	Flexural Modulus (GPa)	SD (GPa)	Flexural Strain	SD (%)
On Edge (XZ)	140.000	3.000	3.100	0.100	No Break	-
Upright (ZX)	65.000	10.000	2.700	0.100	2.400%	0.400%

[43]

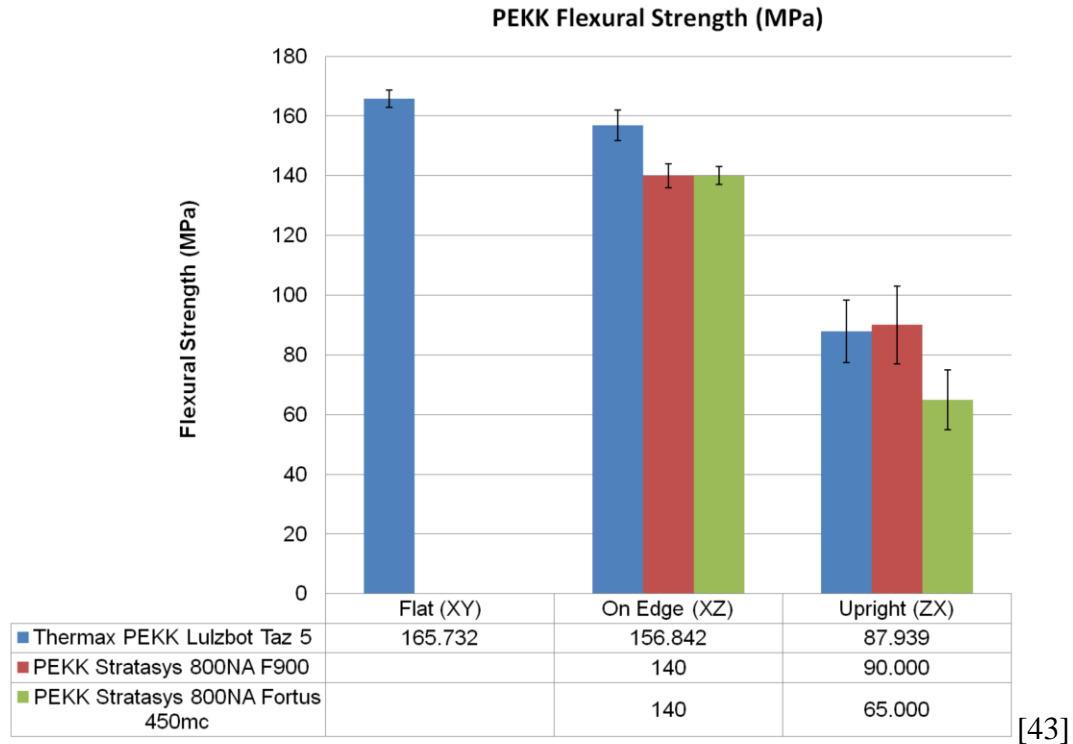


Figure 128. PEKK FFF Flexural Strength Printing with Lulzbot 5 with Heat Lamp at 120°C compared to Stratasys FDM Printers

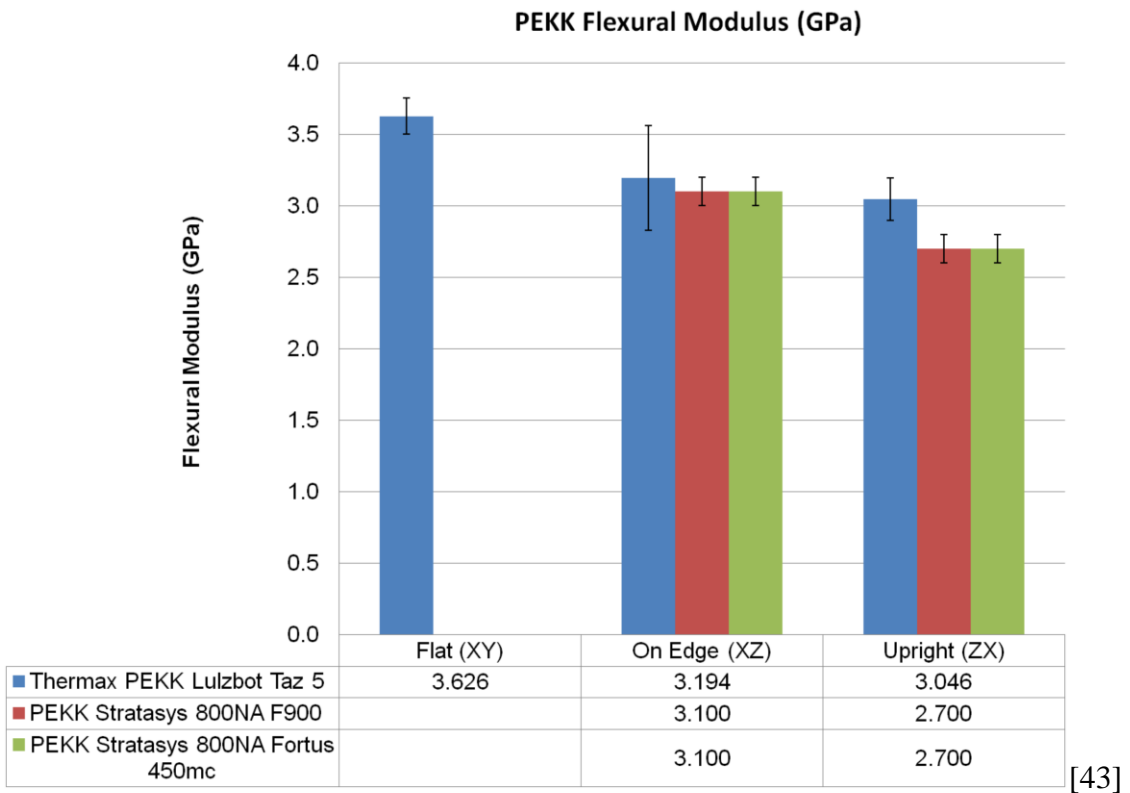


Figure 129. PEKK FFF Flexural Modulus Printing with Lulzbot 5 with Heat Lamp at 120°C compared to Stratasys FDM Printers

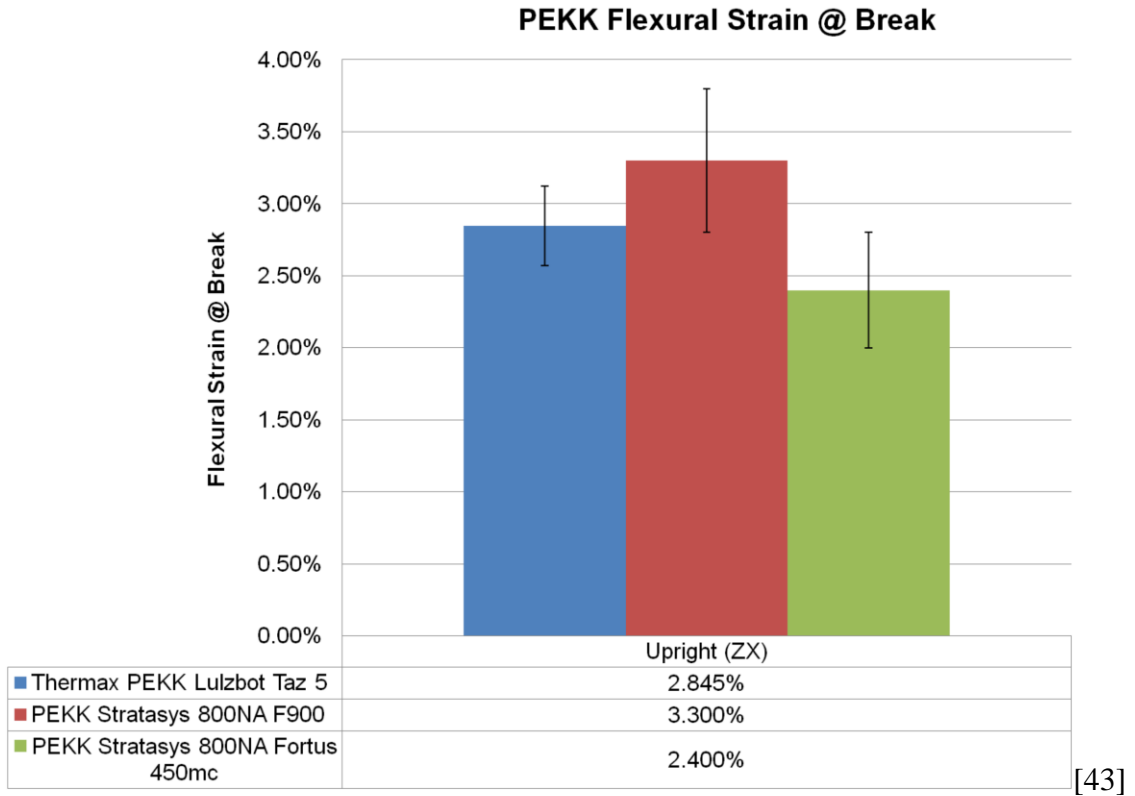


Figure 130. PEKK FFF Flexural Strain at Break Printing with Lulzbot 5 with Heat Lamp at 120°C compared to Stratasys FDM Printers

FFF PEKK with the Heat Lamp at 120°C compared to Injection Molded PEKK

Table 55 shows the comparison of the FFF PEKK printing with the heat lamp at 120°C compared to an isotropic injection molded sample. Figure 131 shows the comparison of the tensile and flexural strength. Figure 132 shows a comparison with the tensile and flexural modulus. The tensile strength is close to the same in the Flat (XY) and on Edge (XZ) orientations but there is still a significant knockdown for the Upright (ZX) orientation. The flexural strength shows an improvement in the Flat (XY) and on Edge (XZ) orientations but there is still a significant knockdown for the Upright (ZX) orientation. The tensile and flexural modulus for the FFF parts is the same as the injection molding with a slight improvement in the Flat (XY) orientation.

Table 55. Comparison of Injection Molded PEKK to FFF with the Heat Lamp at 120°C

	Tensile Strength (Mpa)	SD (Mpa)	Tensile Modulus (Gpa)	SD (Gpa)	Flexural Strength (Mpa)	SD (Mpa)	Flexural Modulus (Gpa)	SD (Gpa)
PEKK (Injection Mold)	88.000	-	2.900	-	128.000	-	3.000	-
PEKK Flat (XY) 120°C	70.026	13.054	3.484	0.116	165.732	2.831	3.626	0.127
PEKK on Edge (XZ) 120°C	95.330	8.528	3.125	0.148	156.842	5.186	3.194	0.367
PEKK Upright (ZX) 120°C	17.334	2.571	2.584	0.362	87.939	10.444	3.046	0.147

[42]

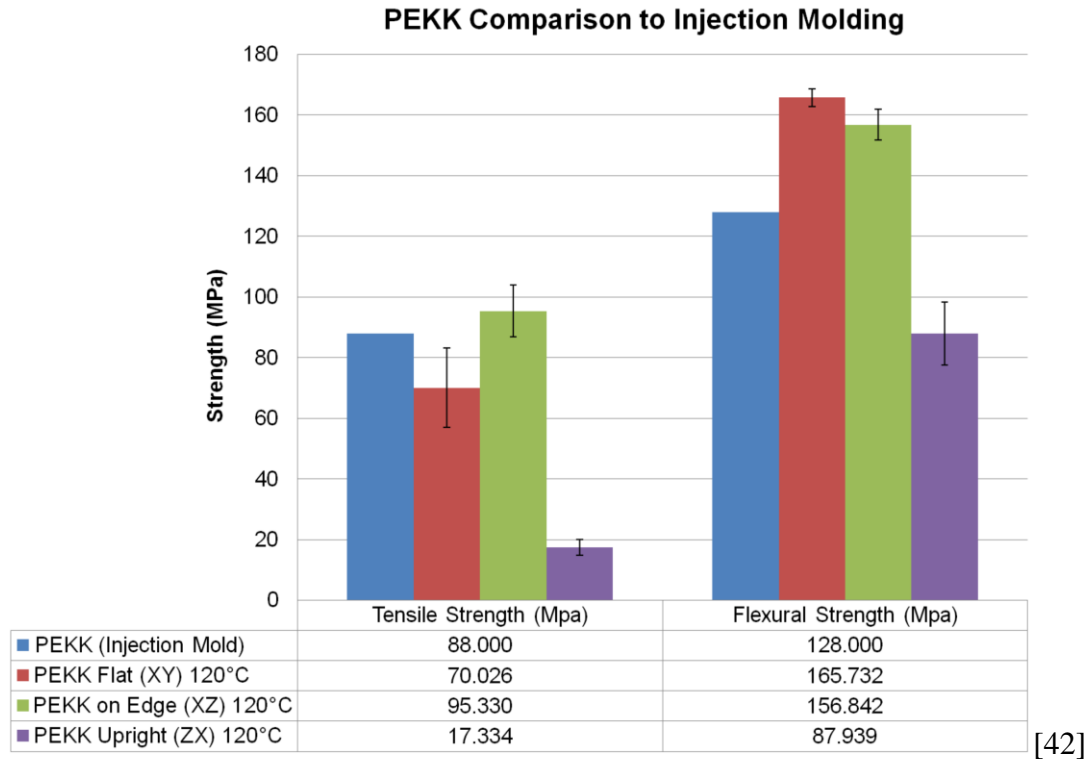


Figure 131. Comparison of Injection Molded PEKK Strength to FFF with the Heat Lamp at 120°C

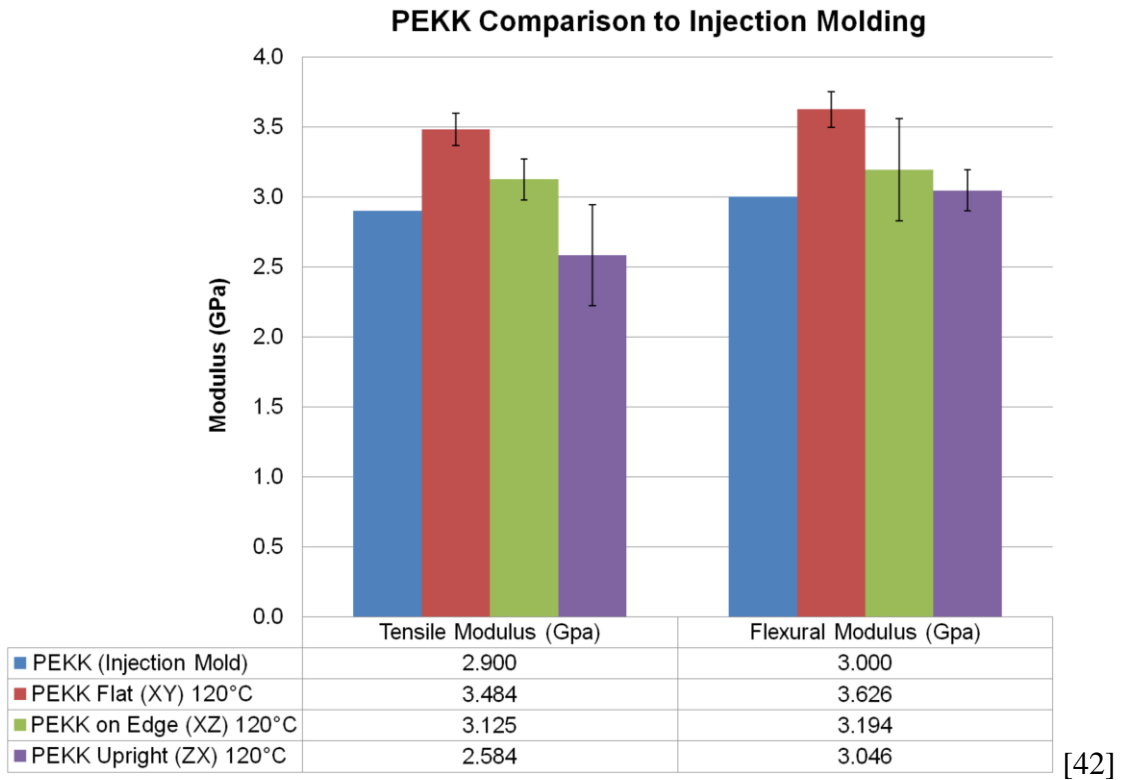


Figure 132. Comparison of Injection Molded PEKK Modulus to FFF with the Heat Lamp at 120°C

PEI Ultem 1010 Testing

PEI was tested by printing with the infrared heat lamp set at the temperature of 120°C. This temperature is within the range of the recommended print bed temperature. The annealing process was done in an oven for one hour at 150°C for one hour, then one hour at 200°C, then reducing the heat to 150°C for thirty minutes, and then slowly cooling in the oven. Figure 133 shows the tensile and flexural PEI test specimens. Figure 134 shows the tensile testing setup with a PEI specimen. All specimens were printed with a 0.3 mm layer height, 0.8 mm layer width, 415°C printing temperature, 140°C build plate temperature, 60 mm/s print speed, and 100% infill.



Figure 133. PEI Tensile and Flexural Test Specimens



Figure 134. PEI Tensile Testing

PEI Ultem 1010 Flat (XY) Tensile Specimens

Figure 135 shows the PEI Flat (XY) tensile specimens before testing and Figure 136 shows them after testing. Twelve specimens were tested because the first attempt was thinner than expected. Table 56 shows the dimension of these specimens. Table 57 shows the tensile properties for tensile strength, percent elongation and modulus of elasticity. Figure 137 shows the stress vs. strain plots.



Figure 135. PEI Ultem 1010 Flat (XY) Tensile Specimens before Testing



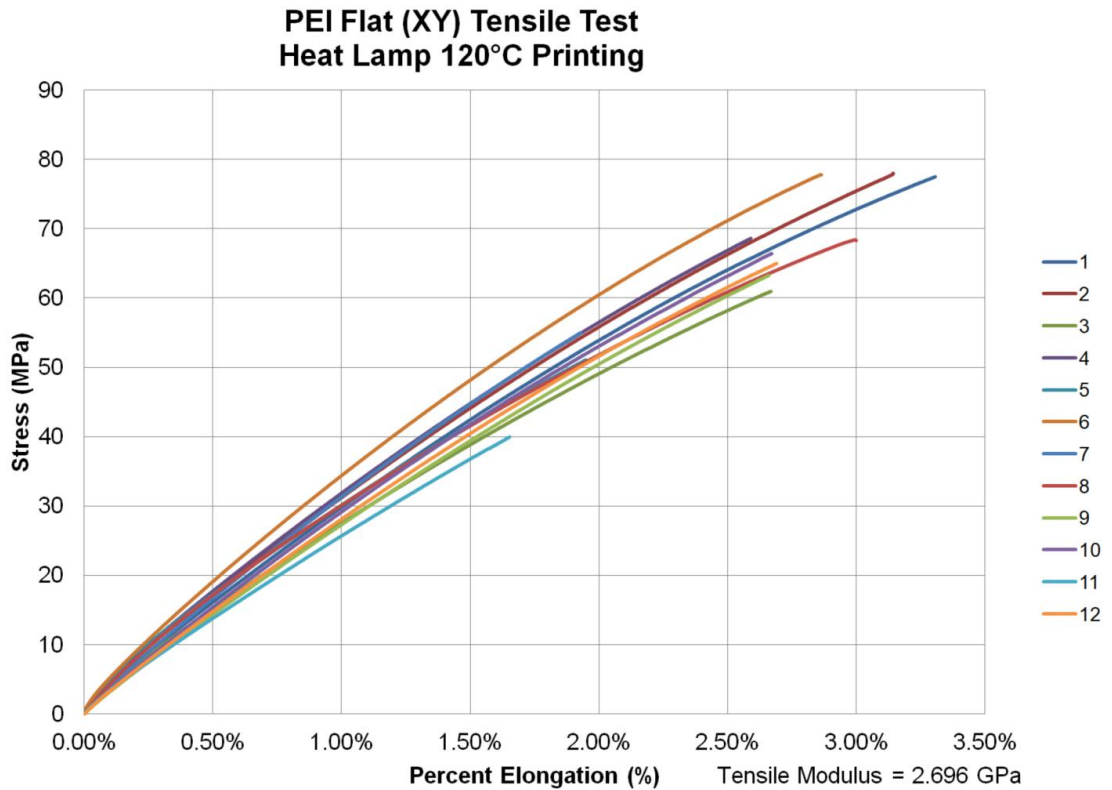
Figure 136. PEI Ultem 1010 Flat (XY) Tensile Specimens after Testing

Table 56. PEI Tensile Flat (XY) Specimen Dimensions

Specimen	Width (mm)	Thickness (mm)
1	13.310	1.930
2	13.538	1.854
3	13.411	2.489
4	13.462	2.184
5	13.233	2.438
6	12.065	2.007
7	10.897	2.337
8	11.786	2.565
9	12.395	2.286
10	11.735	2.311
11	11.811	2.286
12	12.573	2.184
Average	12.518	2.239
SD	0.872	0.220

Table 57. PEI Ultem 1010 Flat (XY) Tensile Properties with 120°C Heat Lamp

Specimen ID	Tensile Strength (MPa)	% Elongation at Break	Modulus of Elasticity (GPa)
1	77.501	3.307%	2.572
2	78.012	3.144%	2.696
3	60.987	2.669%	2.467
4	76.295	3.049%	2.986
5	51.044	1.948%	2.825
6	77.759	2.865%	2.986
7	54.989	1.929%	3.003
8	68.433	3.000%	2.537
9	63.278	2.661%	2.525
10	66.447	2.672%	2.657
11	39.987	1.655%	2.516
12	65.040	2.690%	2.582
Average	64.981	2.632%	2.696
SD	11.945	0.523%	0.202



**Figure 137. PEI Ultem 1010 Flat (XY) Tensile Properties with 120°C Heat Lamp
Stress vs. Strain Plot**

PEI Ultem 1010 on Edge (XZ) Tensile Specimens

Figure 138 shows the PEI on Edge (XZ) tensile specimens before testing and Figure 139 shows them after testing. Table 58 shows the dimension of these specimens. Table 59 shows the tensile properties for tensile strength, percent elongation and modulus of elasticity. Figure 140 shows the stress vs. strain plots.



Figure 138. PEI Ultem 1010 on Edge (XZ) Tensile Specimens before Testing



Figure 139. PEI Ultem 1010 on Edge (XZ) Tensile Specimens after Testing

Table 58. PEI Tensile on Edge (XZ) Specimen Dimensions

Specimen	Width (mm)	Thickness (mm)
1	12.903	4.369
2	13.208	4.166
3	13.183	4.318
4	12.979	4.242
5	13.056	4.115
6	13.233	4.293
Average	13.094	4.250
SD	0.135	0.096

Table 59. PEI Ultem 1010 on Edge (XZ) Tensile Properties with Heat Lamp at 120°C

Specimen ID	Tensile Strength (MPa)	% Elongation at Break	Modulus of Elasticity (GPa)
1	61.290	2.309%	2.765
2	78.619	3.029%	2.781
3	76.999	2.927%	2.811
4	73.853	2.927%	2.784
5	76.952	2.914%	2.840
6	71.309	2.730%	2.784
Average	73.170	2.806%	2.794
SD	6.383	0.262%	0.027

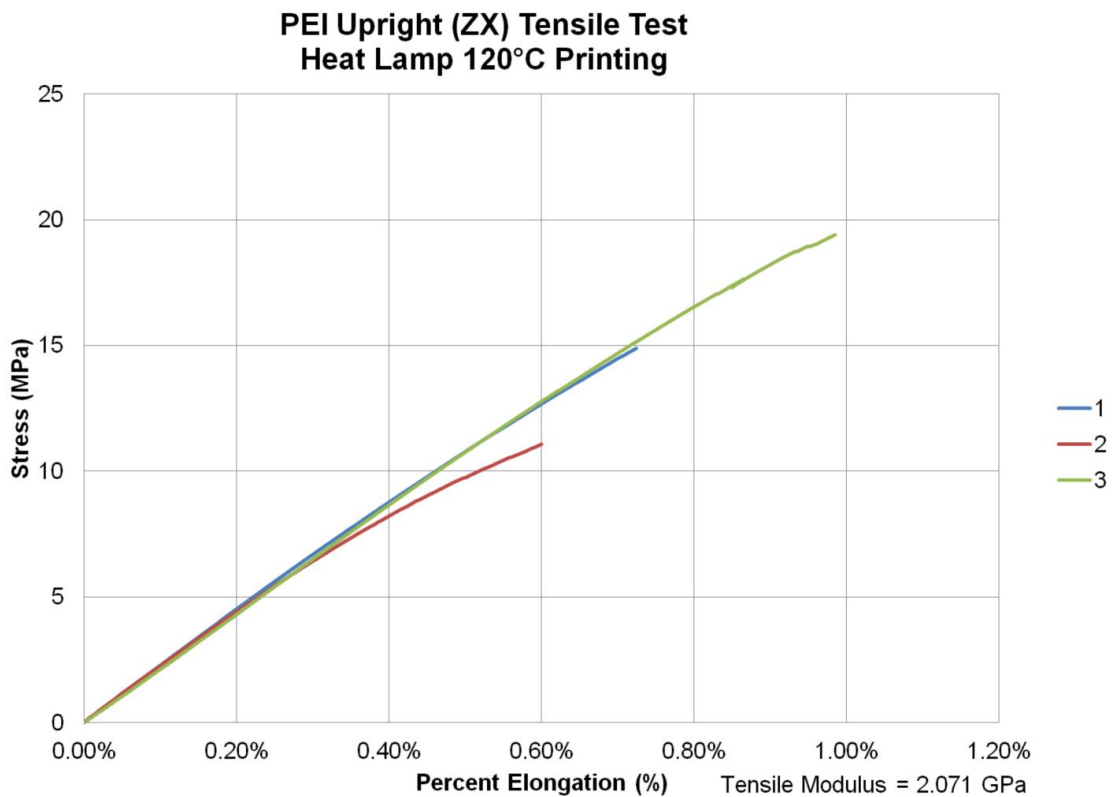


Figure 140. PEI Ultem 1010 on Edge (XZ) Tensile Properties with Heat Lamp at 120°C Stress vs. Strain Plot

PEI Ultem 1010 Upright (ZX) Tensile Specimens

Figure 141 shows the PEI Upright (ZX) tensile specimens before testing and Figure 142 shows them after testing. Table 60 shows the dimension of these specimens. Table 61 shows the tensile properties for tensile strength, percent elongation and modulus of elasticity. Figure 143 shows the stress vs. strain plots.



Figure 141. PEI Ultem 1010 Upright (ZX) Tensile Specimens before Testing



Figure 142. PEI Ultem 1010 Upright (ZX) Tensile Specimens after Testing

Table 60. PEI Tensile Upright (ZX) Specimen Dimensions

Specimen	Width (mm)	Thickness (mm)
1	13.462	4.140
2	13.310	4.166
3	13.259	3.988
4	13.208	4.064
5	13.183	4.039
6	1.308	4.064
Average	11.288	4.077
SD	4.890	0.066

Table 61. PEI Ultem 1010 Upright (ZX) Tensile Properties with Heat Lamp at 120°C, Specimens 4 to 6 had Grip Failures.

Specimen ID	Tensile Strength (MPa)	% Elongation at Break	Modulus of Elasticity (GPa)
1	14.897	0.724%	2.135
2	11.081	0.600%	2.005
3	19.408	0.985%	2.074
Average	15.129	0.770%	2.071
STD	4.169	0.197%	0.065

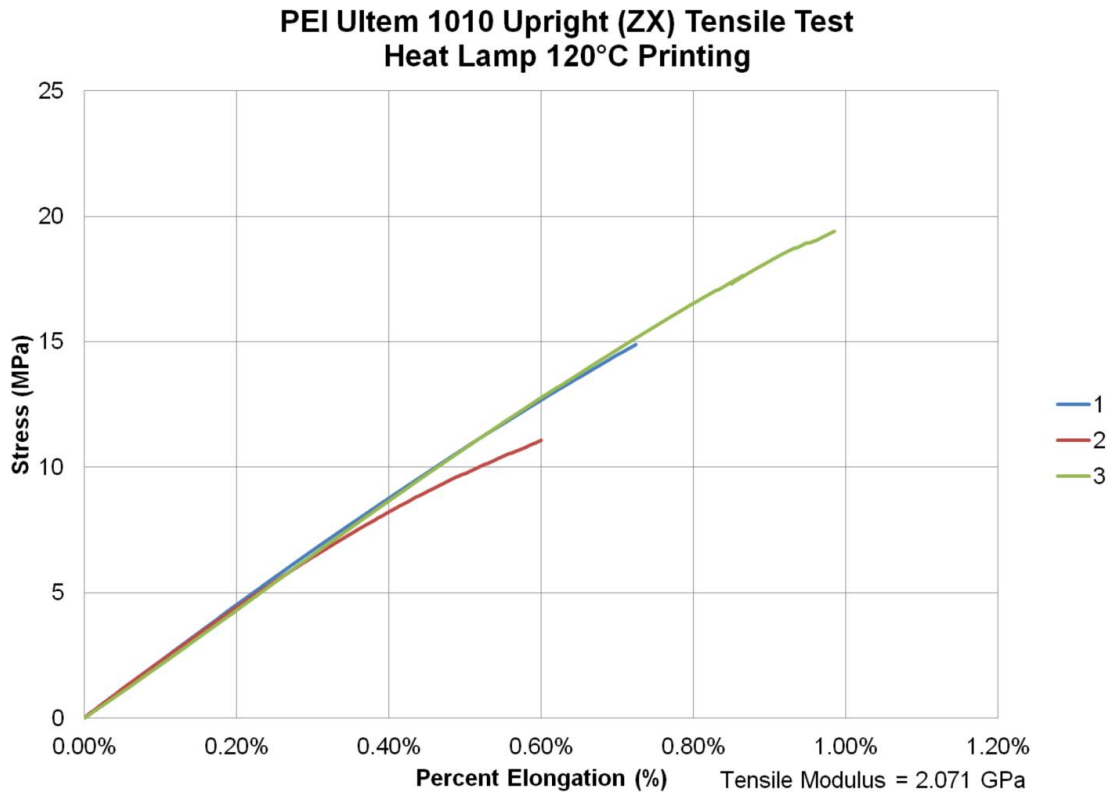


Figure 143. PEI Ultem 1010 Upright (ZX) Tensile Properties with Heat Lamp at 120°C Stress vs. Strain Plot

PEI Ultem 1010 Tensile Testing Summary

Table 62 shows the summary of the PEI tensile specimens with the heat lamp.

Table 63 shows the published data for Stratasys Ultem 1010 PEI filament printed on the Fortus 900mc FDM printer. Figure 144 shows the summary of the tensile strength compared to Stratasys. The tensile strength of on Edge (XZ) is about the same as Stratasys. However, the Upright (ZX) tensile strength is greatly reduced. Figure 145 shows a summary of the tensile modulus. The tensile modulus of on Edge (XZ) and Flat (XY) are similar to Stratasys. However, the Upright (ZX) tensile modulus is reduced. Figure 146 shows the summary of the percent elongation. In all orientations the percent elongation is reduced compared to Stratasys.

Table 62. Tensile Testing Summary PEI on Lulzbot Taz 5 with 120°C Heat Lamp

PEI Lulzbot Taz 5	Tensile Strength (MPa)	SD (Mpa)	% Elongation at Break	SD (%)	Modulus of Elasticity (GPa)	SD (Gpa)
Flat (XY)	64.981	11.945	2.632%	0.523%	2.696	0.202
On Edge (XZ)	73.170	6.383	2.806%	0.262%	2.794	0.027
Upright (ZX)	15.129	4.169	0.770%	0.197%	2.071	0.065

Table 63. Published Tensile Testing Data for FFF Ultem 1010 Stratasys Fortus 900mc with T14 Tip

PEI Stratasys Fortus	Tensile Strength (MPa)	SD (Mpa)	% Elongation at Break	SD (%)	Modulus of Elasticity (GPa)	SD (Gpa)
On Edge (XZ)	80.000	5.000	4.000%	0.400%	3.000	0.100
Upright (ZX)	30.000	10.000	1.100%	0.400%	3.000	0.400

[46]

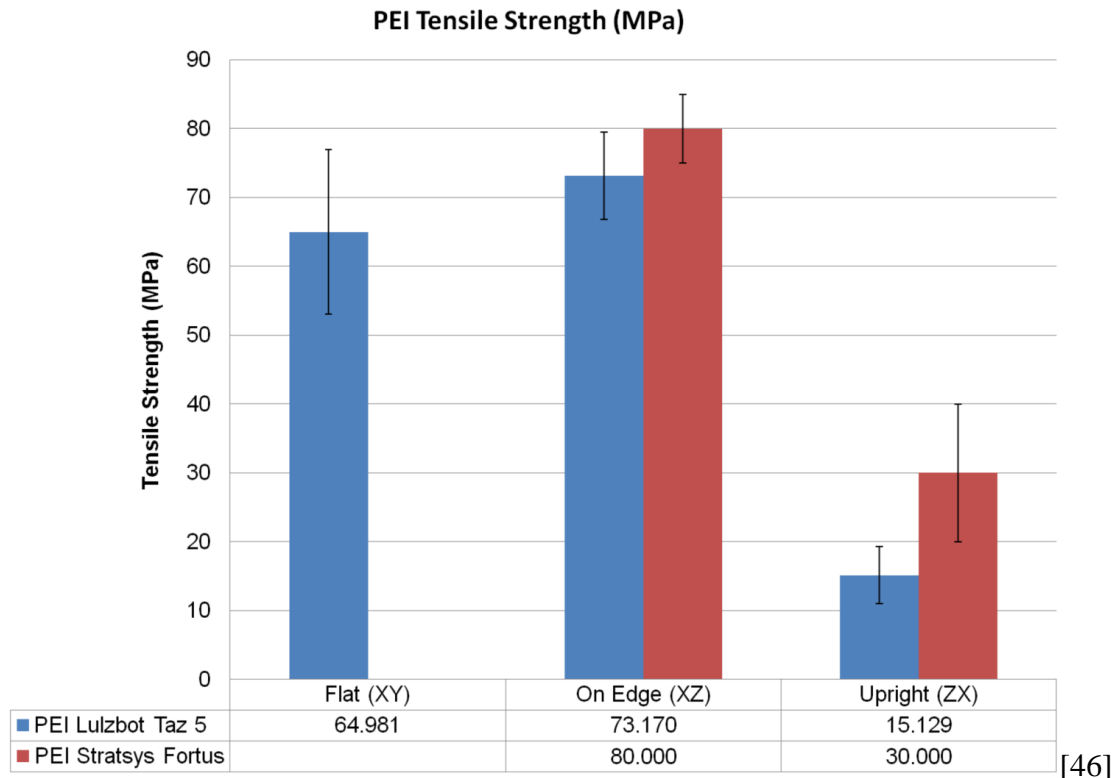


Figure 144. PEI FFF Tensile Strength Printing with Lulzbot 5 with Heat Lamp at 120°C compared to Stratasys FDM Printers

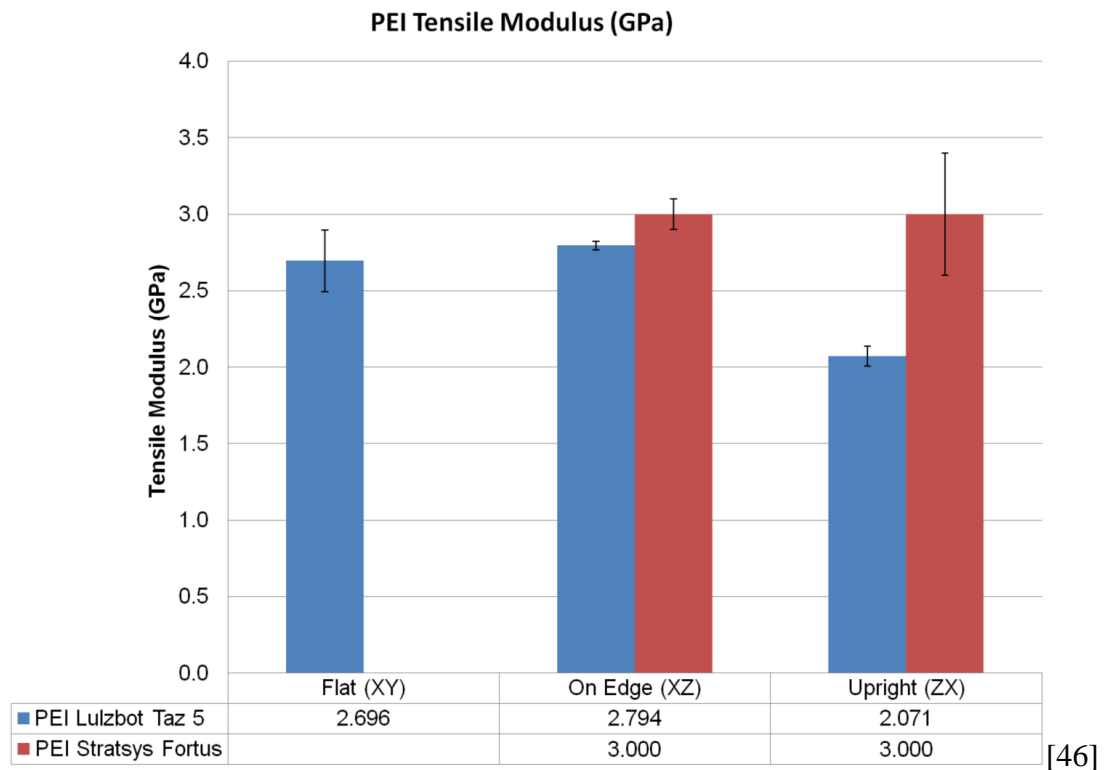


Figure 145. PEI FFF Tensile Modulus Printing with Lulzbot 5 with Heat Lamp at 120°C compared to Stratasys FDM Printers

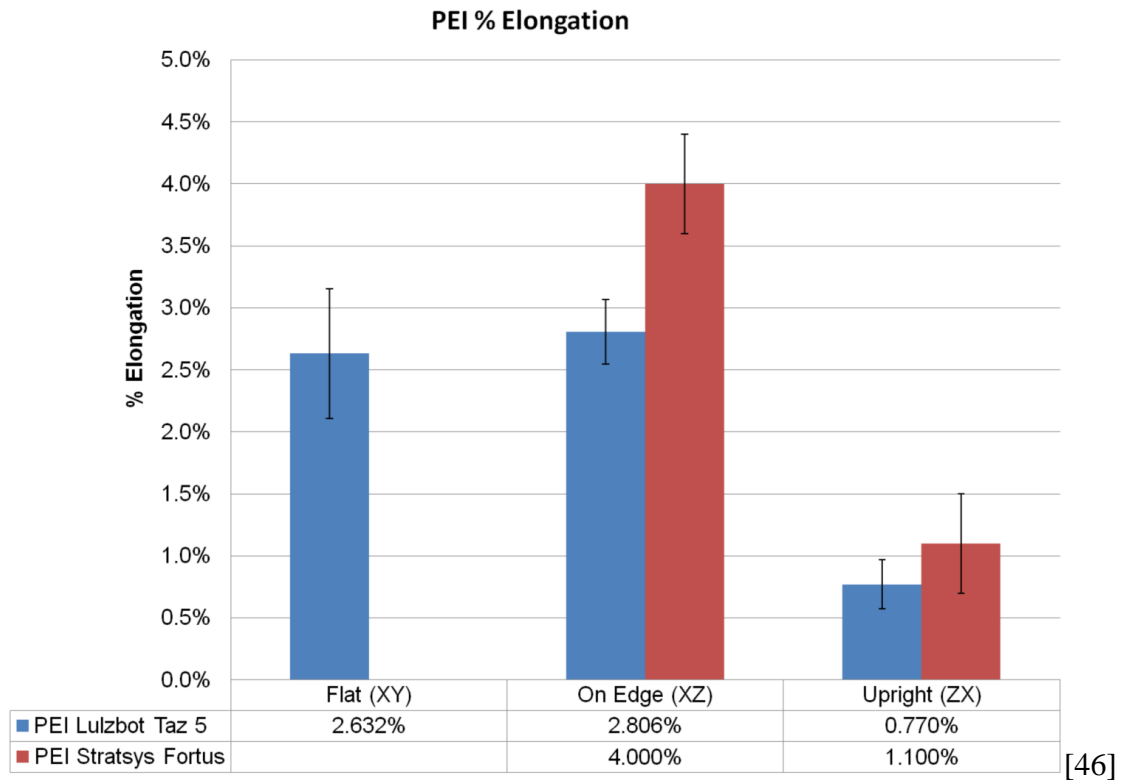


Figure 146. PEI FFF % Elongation Printing with Lulzbot 5 with Heat Lamp at 120°C compared to Stratsys FDM Printers

PEI Ultem 1010 Flat (XY) Flexural Specimens

Figure 147 shows the flexural testing setup with a PEI specimen. Figure 148 shows the PEI Flat (XY) flexural specimens before testing and Figure 149 shows them after testing. Table 64 shows the dimension of these specimens. Table 65 shows the flexural properties for flexural strength, flexural strain at maximum stress or 5%, and flexural modulus. Figure 150 shows the stress vs. strain plots.

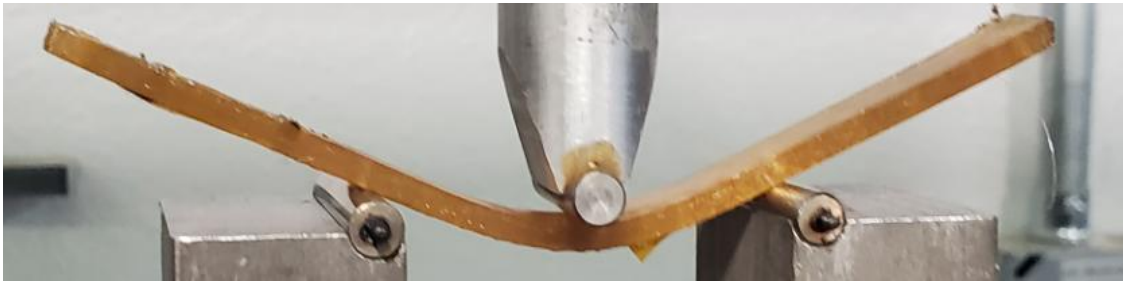


Figure 147. PEI Flexural Testing



Figure 148. PEI Ultem 1010 Flat (XY) Flexural Specimens before Testing



Figure 149. PEI Ultem 1010 Flat (XY) Flexural Specimens after Testing

Table 64. PEI Flexural Flat (XY) Specimen Dimensions

Specimen	Width (mm)	Thickness (mm)
1	13.183	3.454
2	13.081	3.505
3	13.183	3.353
4	13.056	3.454
5	13.030	3.531
6	13.081	3.480
Average	13.102	3.463
SD	0.065	0.062

Table 65. PEI Ultem 1010 Flat (XY) Flexural Properties with 120°C Heat Lamp

Specimen ID	Flexural Strength (MPa)	Flexural Strain @ Max Stress	Flexural Modulus (GPa)
1	130.130	5.001%	2.909
2	123.788	5.000%	2.633
3	133.864	5.001%	2.987
4	136.424	5.000%	2.936
5	131.894	5.000%	2.897
6	128.068	5.002%	2.840
Average	130.695	5.001%	2.867
SD	4.455	0.001%	0.124

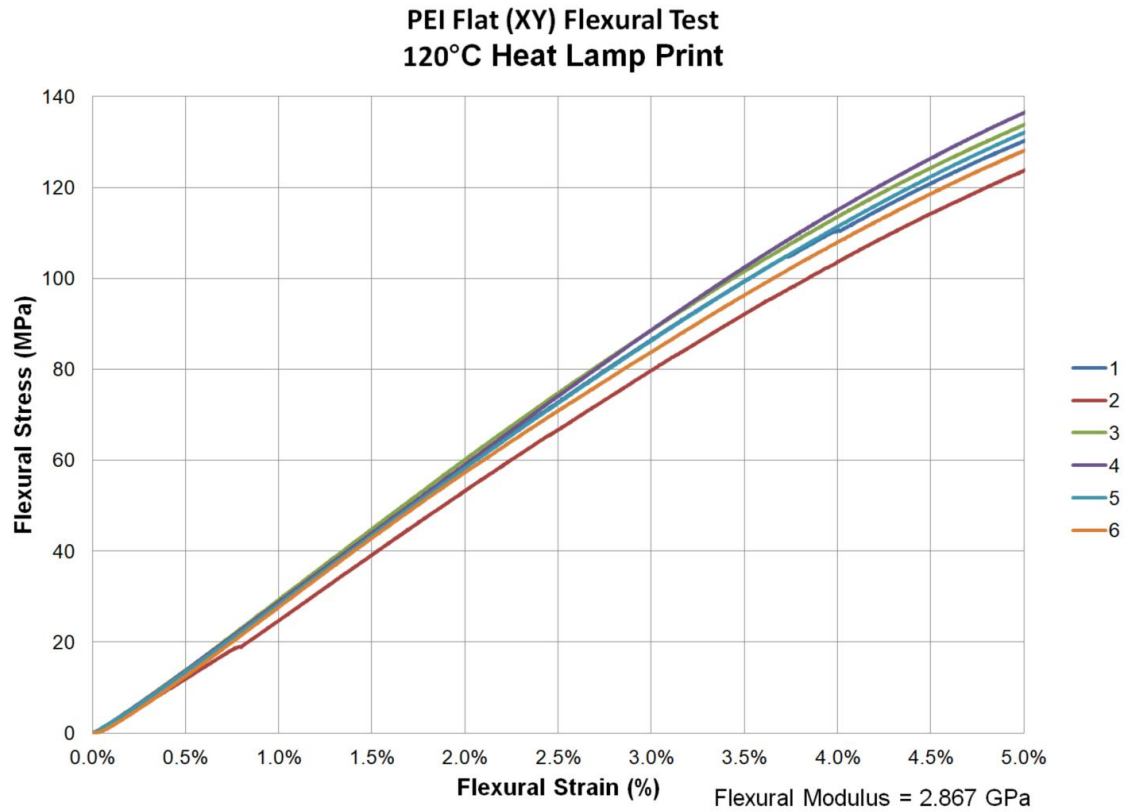


Figure 150. PEI Ultem 1010 Flat (XY) Flexural Properties with 120°C Heat Lamp Stress vs. Strain Plot

PEI Ultem 1010 on Edge (XZ) Flexural Specimens

Figure 151 shows the PEI on Edge (XZ) flexural specimens after testing. Table 66 shows the dimension of these specimens. Table 67 shows the flexural properties for flexural strength, flexural strain at maximum stress or 5%, and flexural modulus. Figure 152 shows the stress vs. strain plots.



Figure 151. PEI Ultem 1010 on Edge (XZ) Flexural Specimens

Table 66. PEI Flexural on Edge (XZ) Specimen Dimensions

Specimen	Width (mm)	Thickness (mm)
1	12.446	3.810
2	12.344	3.861
3	12.471	3.810
4	10.287	3.759
5	9.957	3.912
6	11.608	3.861
Average	11.519	3.835
SD	1.133	0.053

Table 67. PEI Ultem 1010 on Edge (XZ) Flexural Properties with Heat Lamp at 120°C

Specimen ID	Flexural Strength (MPa)	Flexural Strain @ Max Stress	Flexural Modulus (GPa)
1	122.945	5.002%	2.517
2	122.600	5.001%	2.625
3	128.303	5.001%	2.740
4	126.477	5.001%	2.568
5	120.787	5.002%	1.597
6	120.126	5.002%	2.503
Average	123.540	5.001%	2.425
SD	3.218	0.001%	0.415

**PEI on Wdge (XZ) Flexural Test
120°C Heat Lamp Print**

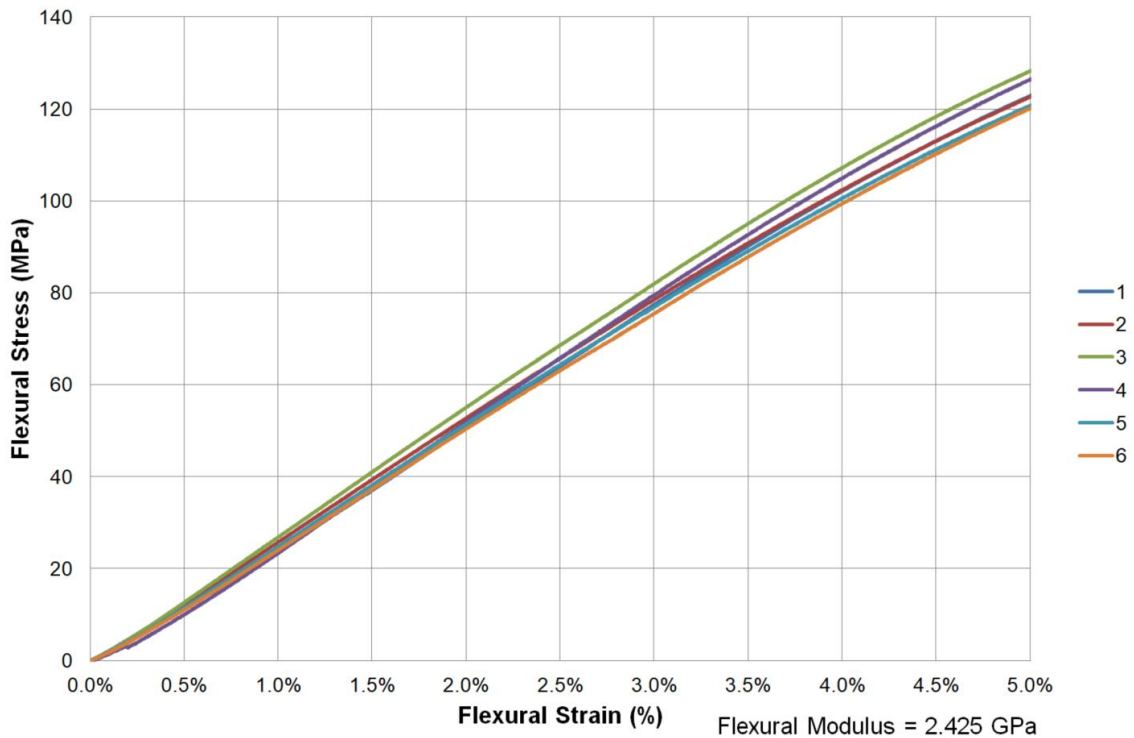


Figure 152. PEI Ultem 1010 on Edge (XZ) Flexural Properties with Heat Lamp at 120°C Stress vs. Strain Plot

PEI Ultem 1010 Upright (ZX) Flexural Specimens

Figure 153 shows the PEI Flat (XY) flexural specimens before testing and Figure 154 shows them after testing. Table 68 shows the dimension of these specimens. Table 69 shows the flexural properties for flexural strength, flexural strain at maximum stress or 5%, and flexural modulus. Figure 155 shows the stress vs. strain plots.



Figure 153. PEI Ultem 1010 Upright (ZX) Flexural Specimens before Testing

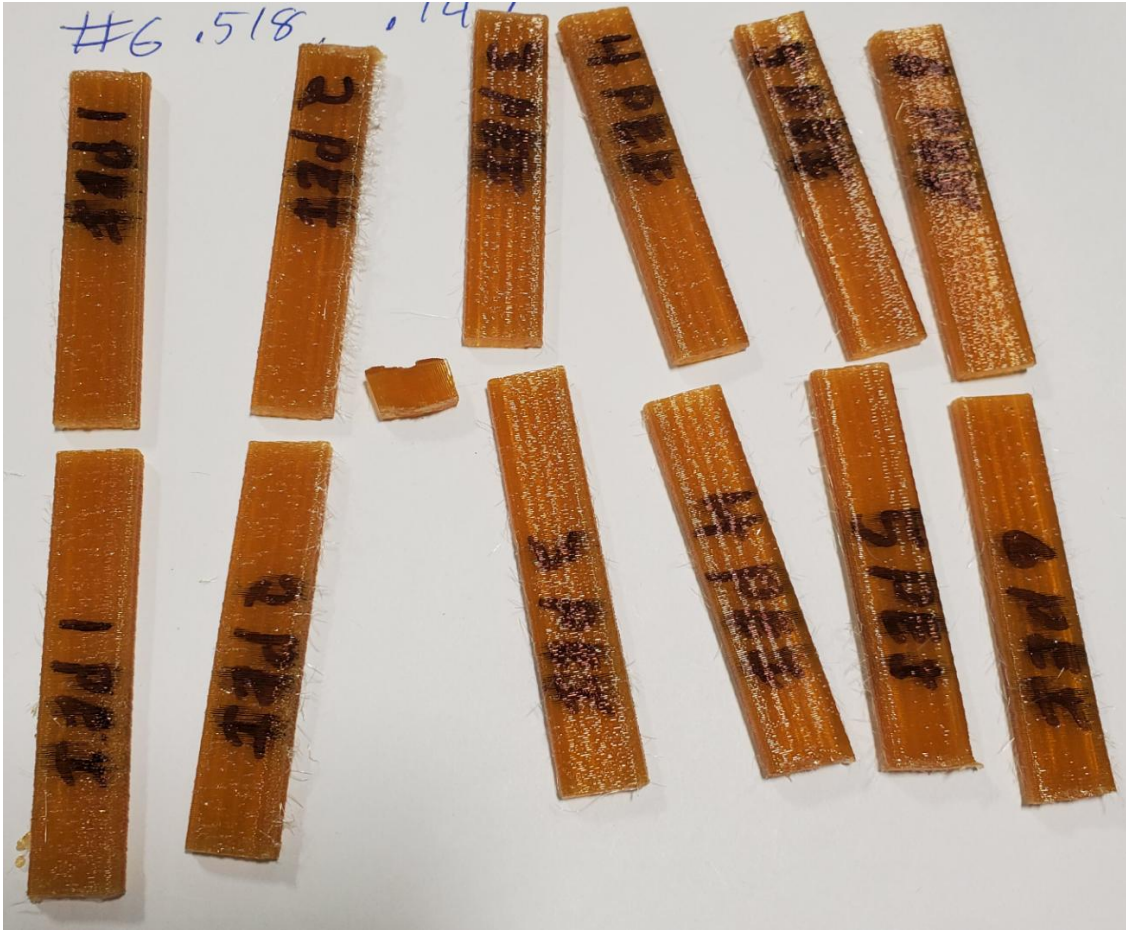


Figure 154. PEI Ultem 1010 Upright (ZX) Flexural Specimens after Testing

Table 68. PEI Flexural Upright (ZX) Specimen Dimensions

Specimen	Width (mm)	Thickness (mm)
1	13.208	3.658
2	13.183	3.683
3	13.208	3.708
4	13.208	3.759
5	13.157	3.759
6	13.157	3.734
Average	13.187	3.717
SD	0.025	0.041

Table 69. PEI Ultem 1010 Upright (ZX) Flexural Properties with Heat Lamp at 120°C

Specimen ID	Flexural Strength (MPa)	Flexural Strain @ Max Stress	Flexural Modulus (GPa)
1	41.959	2.063%	2.806
2	29.211	2.104%	1.652
3	36.100	2.000%	1.813
4	31.541	1.806%	1.780
5	37.855	2.128%	1.777
6	37.592	1.934%	1.958
Average	35.710	2.006%	1.964
SD	4.625	0.121%	0.424

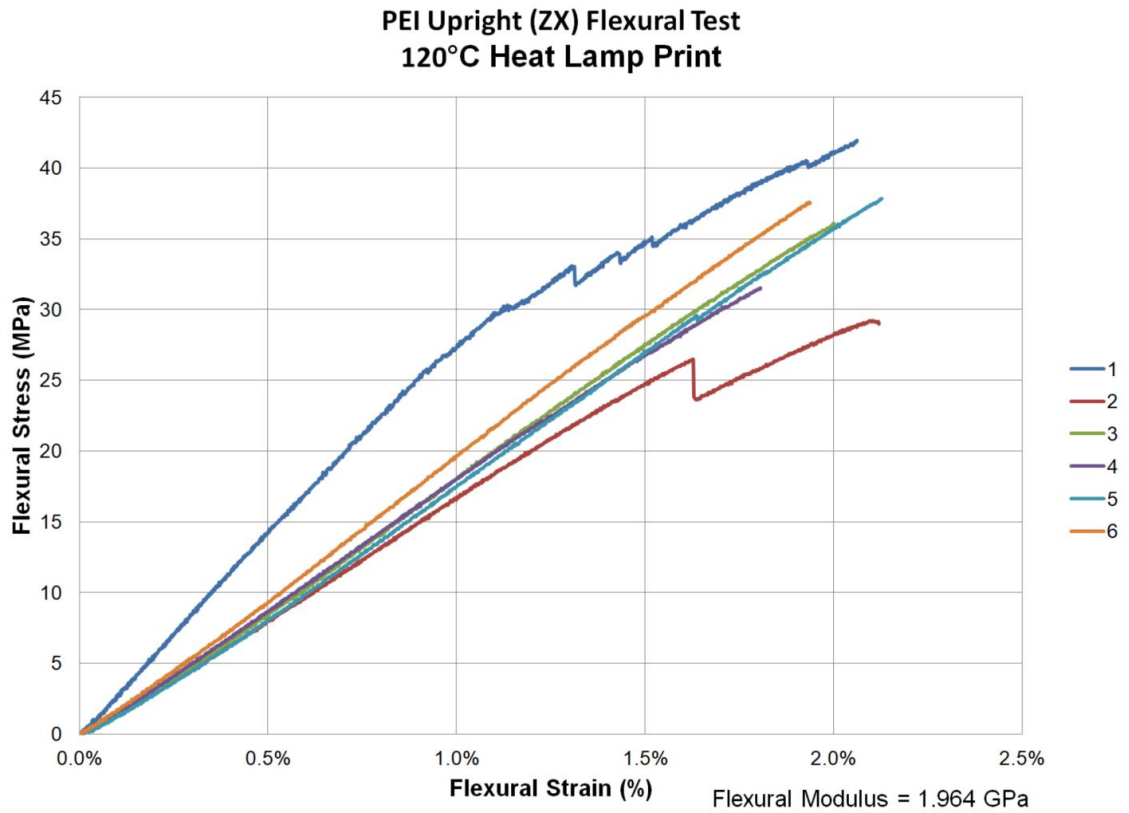


Figure 155. PEI Ultem 1010 Upright (ZX) Flexural Properties with Heat Lamp at 120°C Stress vs. Strain Plot

PEI Ultem 1010 Flexural Summary

Table 70 shows the summary of the PEI flexural specimens with the heat lamp.

Table 71 shows the published data for Stratasys FDM Ultem 1010 filament printed on the Fortus 900mc printer. Figure 156 shows the summary of the flexural strength compared to Stratasys. The flexural strength of on Edge (XZ) and Flat (XY) are similar to the Stratasys. The Upright (ZX) flexural strength significantly reduced compared to Stratasys. Figure 157 shows a summary of the flexural modulus. The flexural modulus of Flat (XY) and on Edge (XZ) is similar to the Stratasys 800 NA. However, the Upright (ZX) flexural modulus shows a reduced flexural modulus. Figure 158 shows the summary of the flexural strain at break for Upright (ZX). The flexural strain is reduced compared to Stratasys.

Table 70. Flexural Testing Summary PEI on Lulzbot Taz 5 with 120°C Heat Lamp

Lulzbot Taz 5	Flexural Strength (MPa)	SD (Mpa)	Flexural Strain (%)	SD (%)	Flexural Modulus (GPa)	SD (Gpa)
Flat (XY)	130.695	4.455	No Break	-	2.867	0.124
On Edge (XZ)	123.540	3.218	No Break	-	2.425	0.415
Upright (ZX)	35.710	4.625	2.006%	0.121%	1.964	0.424

Table 71. Published Flexural Testing Data for Stratasys FDM Ultem 1010 printed with a Fortus 900mc with T14 Tip.

Stratasys Fortus 900 mc	Flexural Strength (MPa)	SD (Mpa)	Flexural Strain (%)	SD (%)	Flexural Modulus (GPa)	STD (Gpa)
On Edge (XZ)	130.000	4.000	No Break	-	2.910	0.050
Upright (ZX)	80.000	13.000	3.200%	0.500%	2.600	0.100

[46]

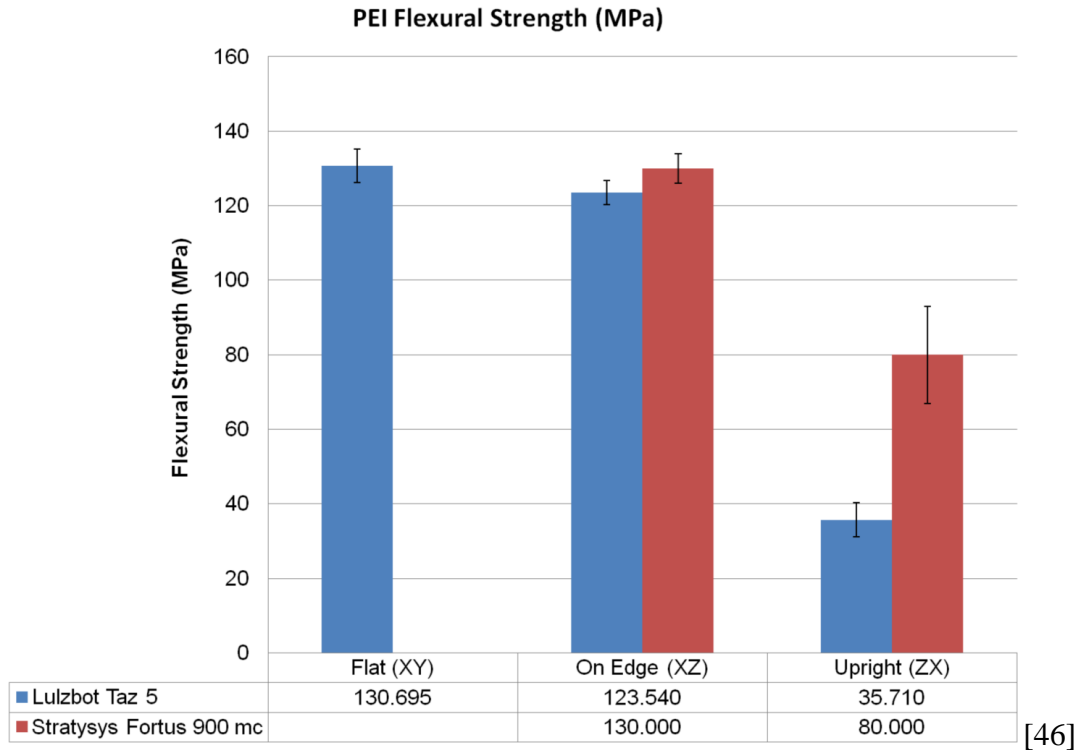


Figure 156. PEI FFF Flexural Strength Printing with Lulzbot 5 with Heat Lamp at 120°C compared to Stratsys FDM Printers

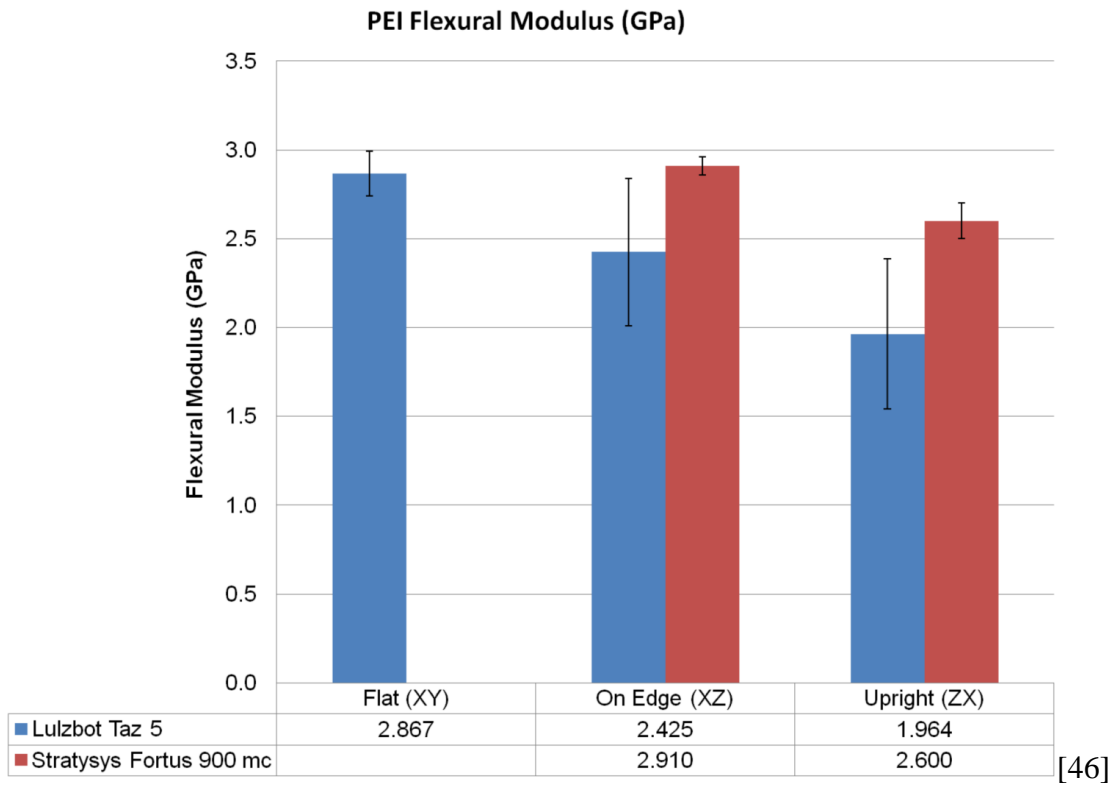


Figure 157. PEI FFF Flexural Modulus Printing with Lulzbot 5 with Heat Lamp at 120°C compared to Stratsys FDM Printers

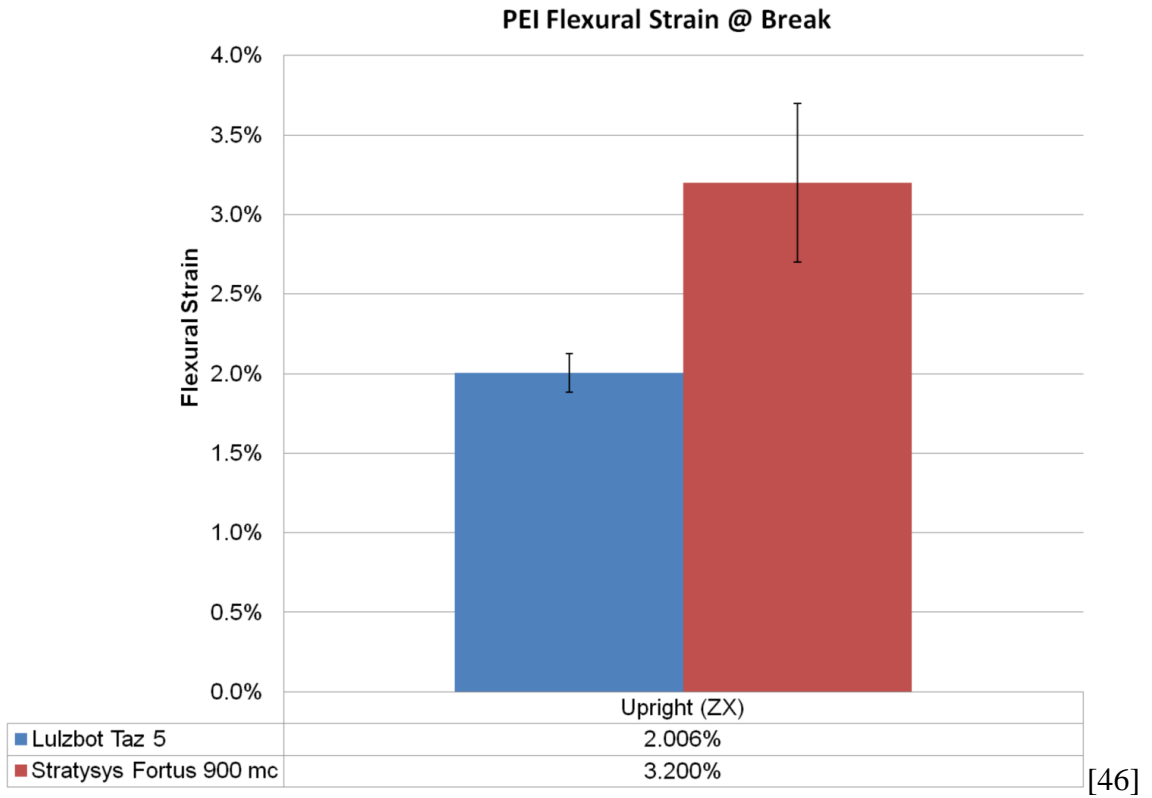


Figure 158. PEI FFF Flexural Strain Printing with Lulzbot 5 with Heat Lamp at 120°C compared to Stratasys FDM Printers

FFF PEI with the Heat Lamp at 120°C compared to Injection Molded PEI

Table 72 shows the comparison of the FFF PEI printing with the heat lamp at 120°C compared to an isotropic injection molded sample. Figure 159 shows the comparison of the tensile and flexural strength. Figure 160 shows a comparison with the tensile and flexural modulus. The tensile and flexural strength are all reduced compared to injection molding and there is a significant knockdown for the Upright (ZX) orientation. The tensile and flexural modulus for the FFF parts are also reduced compared to injection molding and there is a greater knock down for the Upright (ZX) orientation.

Table 72. Comparison of Injection Molded PEI to FFF with the Heat Lamp at 120 °C

	Tensile Strength (Mpa)	SD (Mpa)	Tensile Modulus (Gpa)	SD (Gpa)	Flexural Strength (Mpa)	SD (Mpa)	Flexural Modulus (Gpa)	SD (Gpa)
PEI (Injection Mold)	109.000	-	3.310	-	145.000	-	3.310	-
PEI Flat (XY) 120°C	64.981	11.945	2.696	0.202	130.695	4.455	2.867	0.124
PEI on Edge (XZ) 120°C	73.170	6.383	2.794	0.027	123.540	3.218	2.425	0.415
PEI Upright (ZX) 120°C	15.129	4.169	2.071	0.065	35.710	4.625	1.964	0.424

[45]

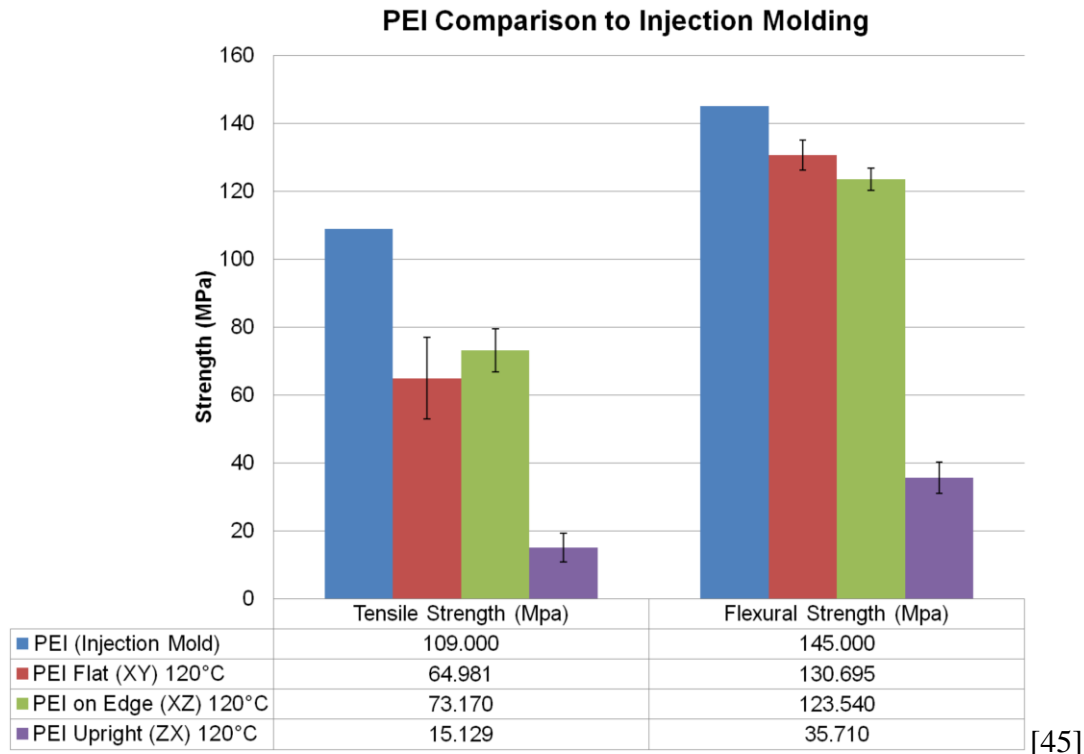


Figure 159. Comparison of Injection Molded PEI Strength to FFF with the Heat Lamp at 120 °C

PEI Comparison to Injection Molding

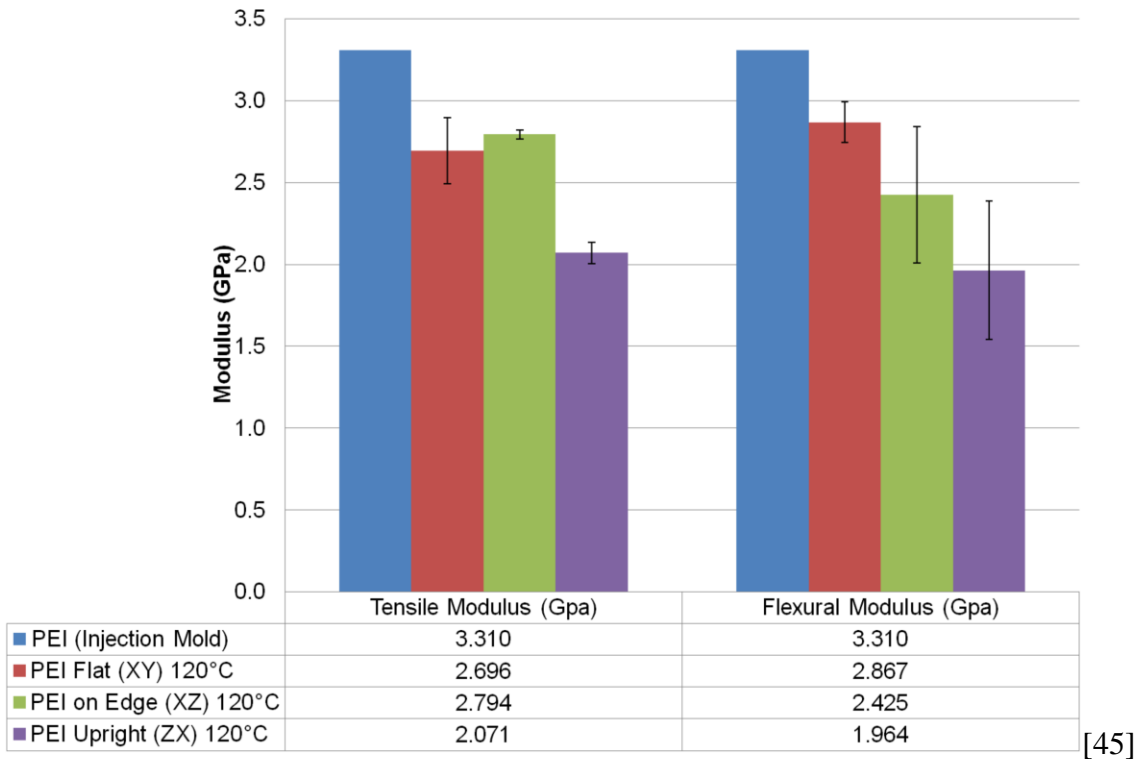


Figure 160. Comparison of Injection Molded PEI Modulus to FFF with the Heat Lamp at 120°C

PEEK Testing

PEEK was tested by printing with the infrared heat lamp set at the temperature of 120°C. This temperature is within the range of the recommended print bed temperature. The annealing process was done in an oven by ramping up the temperature by 10°C per hour, then soak at 200°C for 3.5 hours, then ramp down at 10°C per hour to 140°C. Figure 161 shows the tensile and flexural PEI test specimens after annealing. All specimens were printed with a 0.3 mm layer height, 0.8 mm layer width, 415°C printing temperature, 140°C build plate temperature, 60 mm/s print speed, and 100% infill. Only the Flat (XY) and on Edge (XZ) specimens could be printed. The Upright (ZX) specimens did not have enough strength in the Z direction bonding to complete the printing.



Figure 161. PEEK Test Specimen Annealing

PEEK Flat (XY) Tensile Specimens

Figure 162 shows the PEKK Flat (XY) tensile specimens before testing. Figure 163 shows a test specimen after testing and still in the grips. These test specimens had a failure mode of splitting individual filaments that came apart in the Z direction. Figure 164 shows the test specimens after testing. Table 73 shows the dimension of these specimens. Table 74 shows the tensile properties for tensile strength, percent elongation and modulus of elasticity. Figure 165 shows the stress vs. strain plots.



Figure 162. PEEK Flat (XY) Tensile Specimens before Testing



Figure 163. PEEK Flat (XY) Tensile Specimen after Testing



Figure 164. PEEK Flat (XY) Tensile Specimens after Testing

Table 73. PEEK Tensile Flat (XY) Specimen Dimensions

Specimen	Width (mm)	Thickness (mm)
1	12.344	3.353
2	12.776	3.404
3	12.344	3.200
4	12.827	3.353
5	12.522	3.200
6	12.802	3.124
Average	12.603	3.272
SD	0.228	0.112

Table 74. PEEK Flat (XY) Tensile Properties with 120°C Heat Lamp

Specimen ID	Tensile Strength (MPa)	% Elongation at Break	Modulus of Elasticity (GPa)
1	70.688	1.943%	4.177
2	76.684	2.706%	3.721
3	73.277	2.324%	3.825
4	68.944	2.324%	4.037
5	75.508	2.286%	4.132
6	60.045	1.490%	4.037
Average	70.858	2.178%	3.988
SD	6.034	0.415%	0.179

**PEEK Flat (XY) Tensile Test
120°C Heat Lamp Printing**

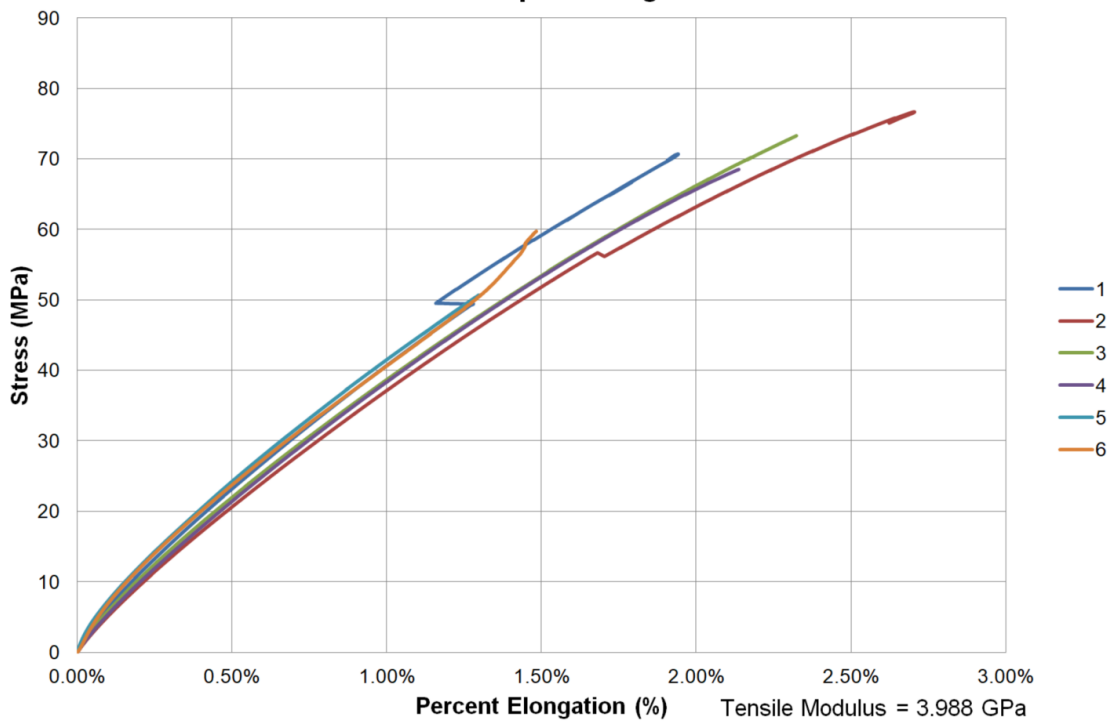


Figure 165. PEEK Flat (XY) Tensile Properties with 120°C Heat Lamp Stress vs. Strain Plot

PEEK on Edge (XZ) Tensile Specimens

Figure 166 shows the PEKK Flat (XY) tensile specimens before testing and Figure 167 shows the test specimens after testing. These test specimens had a failure mode of splitting down the XZ that came apart in the Z direction. Table 75 shows the dimension of these specimens. Table 76 shows the tensile properties for tensile strength, percent elongation and modulus of elasticity. Figure 168 shows the stress vs. strain plots. The zigzag shape of the stress strain plot is due to the splitting in the XZ plane that would result in slipping but not a full tensile failure.



Figure 166. PEEK on Edge (XZ) Tensile Specimens before Testing



Figure 167. PEEK on Edge (XZ) Tensile Specimens after Testing

Table 75. PEEK Tensile on Edge (XZ) Specimen Dimensions

Specimen	Width (mm)	Thickness (mm)
1	13.081	3.759
2	12.852	3.759
3	13.005	3.708
4	12.573	3.988
5	12.827	3.810
Average	12.868	3.805
SD	0.196	0.108

Table 76. PEEK on Edge (XZ) Tensile Properties with Heat Lamp at 120°C

Specimen ID	Tensile Strength (MPa)	% Elongation at Break	Modulus of Elasticity (GPa)
1	43.976	1.915%	3.449
2	52.039	1.571%	3.798
3	40.740	1.425%	3.739
4	42.935	Extensometer Malfunction (Forgot to remove Pin)	
5	37.696	1.048%	3.530
Average	43.477	1.490%	3.629
SD	5.356	0.359%	0.166

**PEKK on Edge (XZ) Tensile Test
120°C Heat Lamp Printing**

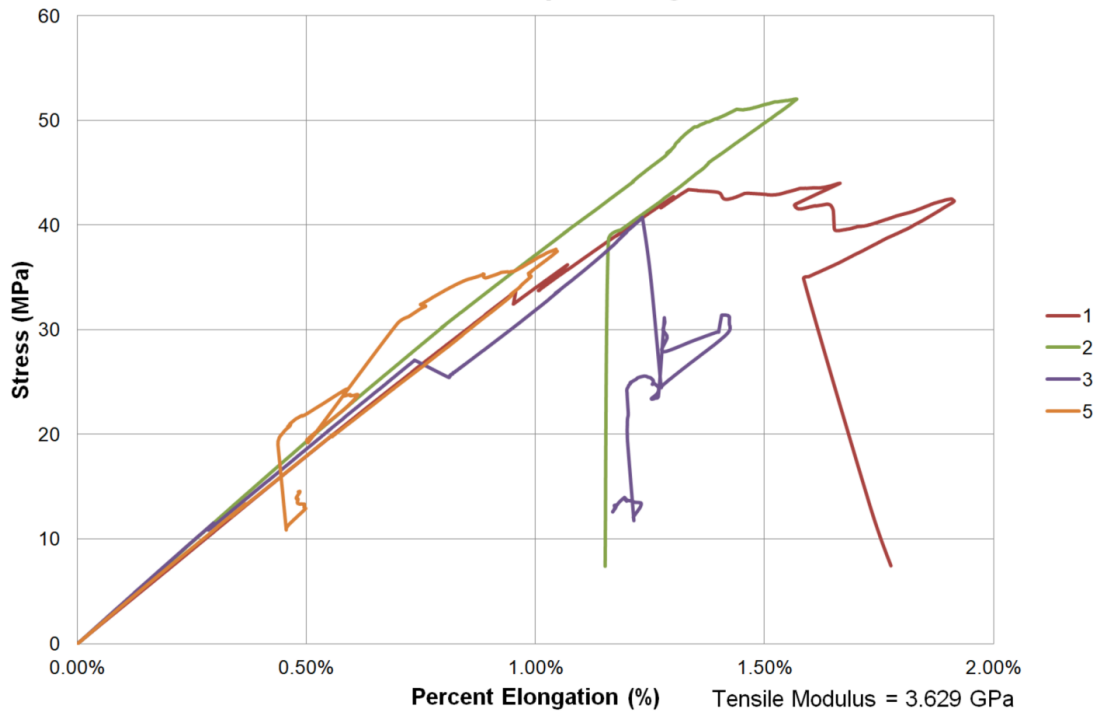


Figure 168. PEEK on Edge (XZ) Tensile Properties with Heat Lamp at 120°C Stress vs. Strain Plot

PEEK Tensile Testing Summary

Table 77 shows the summary of the PEI tensile specimens with the heat lamp. Table 78 shows the published data for 3DXTech for their ThermaX PEEK which was used in this study. Table 79 shows published data from South Dakota State University printing PEEK with FFF. Stratasys does not offer PEEK as a material that can be used in their FDM printers. Figure 169 shows the summary of the tensile strength compared to 3DXTech and South Dakota State University. The tensile strength of on Edge (XZ) is about the same as Flat (XY) data from 3DXTech. However, the Flat (XY) tensile strength is greatly reduced compared to 3DXTech and about the same as South Dakota State University. Figure 170 shows a summary of the tensile modulus. The tensile modulus of Flat (XY) is similar to 3DXTech. However, the on Edge (XZ) tensile modulus is reduced compared to the Flat (XY) 3DXTech data and greater than South Dakota State University Flat (XY). Figure 171 shows the summary of the percent elongation. The percent elongation is a little lower than 3DXTech and significantly lower than South Dakota State University in the Flat (XY) orientation.

Table 77. Tensile Testing Summary PEEK on Lulzbot Taz 5 with 120°C Heat Lamp

PEEK Lulzbot Taz 5	Tensile Strength (MPa)	STD (Mpa)	% Elongation at Break	STD (%)	Modulus of Elasticity (GPa)	STD (Gpa)
Flat (XY)	70.858	6.034	2.178%	0.415%	3.988	0.179
On Edge (XZ)	43.477	5.356	1.490%	0.359%	3.629	0.166

Table 78. Published Tensile Testing Data for PEEK 3DXTech ThermaX

PEEK 3DXTech Thermax	Tensile Strength (MPa)	STD (Mpa)	% Elongation at Break	STD (%)	Modulus of Elasticity (GPa)	STD (Gpa)
Flat (XY)	100.000		2.800%		3.720	

[50]

Table 79. Published Tensile Testing Data for PEEK FFF Printing from South Dakota State University

South Dakota State	Tensile Strength (MPa)	STD (Mpa)	% Elongation at Break	STD (%)	Modulus of Elasticity (GPa)	STD (Gpa)
Flat (XY)	73.013	1.572	4.483%	0.511%	2.780	0.121

[51]

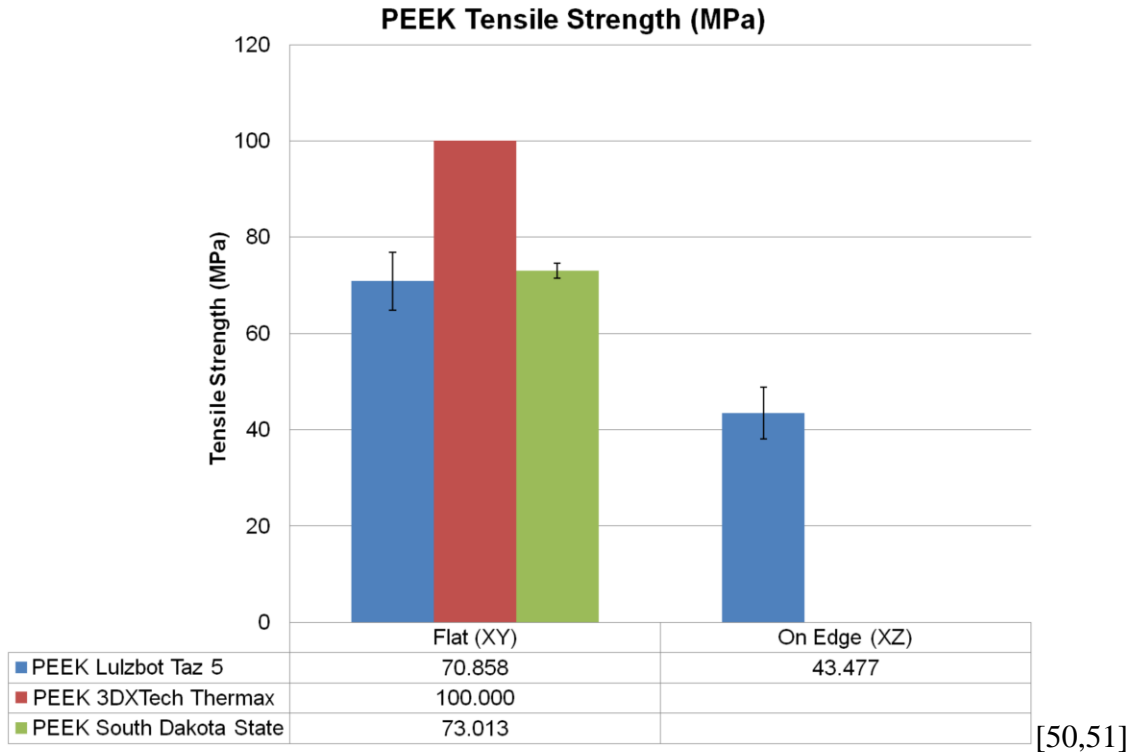


Figure 169. PEEK FFF Tensile Strength Printing with Lulzbot 5 with Heat Lamp at 120°C compared to Published Data

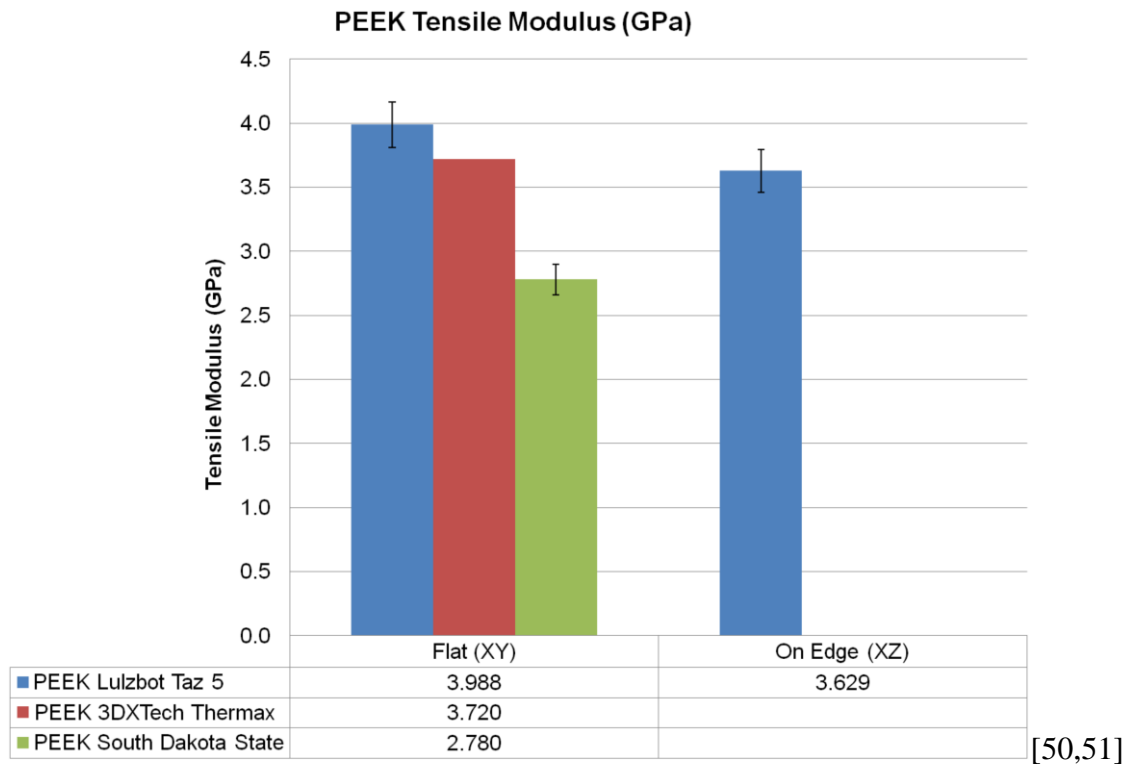


Figure 170. PEEK FFF Tensile Modulus Printing with Lulzbot 5 with Heat Lamp at 120°C compared to Published Data [50,51].

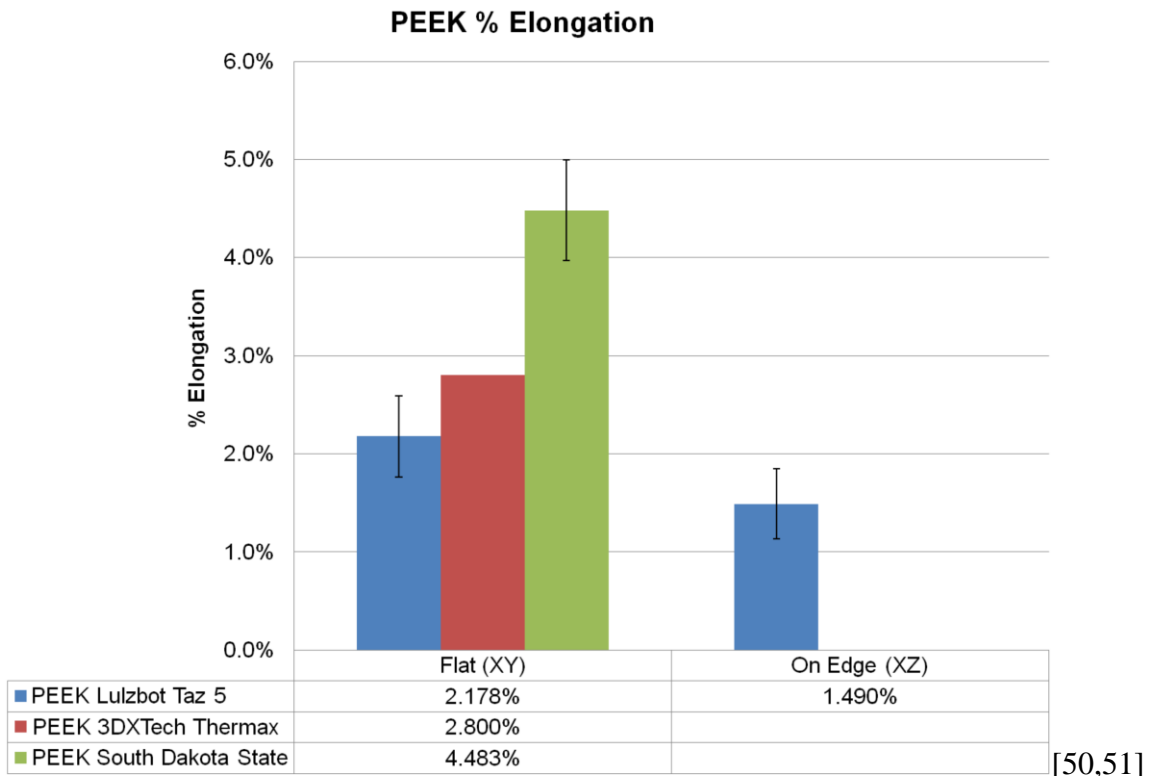


Figure 171. PEEK FFF % Elongation Printing with Lulzbot 5 with Heat Lamp at 120°C compared to Published Data

PEEK Flat (XY) Flexural Test Specimens

Figure 172 shows the flexural testing setup with a PEEK specimen. Figure 173 shows the PEEK Flat (XY) flexural specimens before testing and Figure 174 shows them after testing. The reason for the discoloration is the Kapton Polyamide tape is stuck to the back side. Table 80 shows the dimension of these specimens. Table 81 shows the flexural properties for flexural strength, flexural strain at maximum stress or 5%, and flexural modulus. Figure 175 shows the stress vs. strain plots.

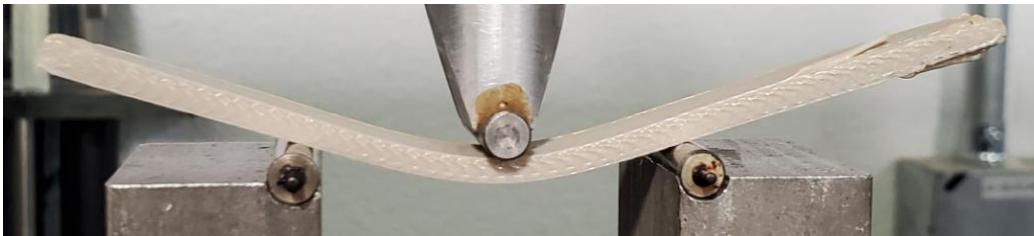


Figure 172. Flexural Testing of PEEK



Figure 173. PEEK Flat (XY) Flexural Test Specimens before Testing



Figure 174. PEEK Flat (XY) Flexural Test Specimens after Testing

Table 80. PEEK Flexural Flat (XY) Specimen Dimensions

Specimen	Width (mm)	Thickness (mm)
1	12.700	3.378
2	12.471	3.353
3	12.700	3.302
4	12.624	2.997
5	12.802	3.124
Average	12.659	3.231
SD	0.123	0.164

Table 81. PEEK Flat (XY) Flexural Properties with 120°C Heat Lamp

Specimen ID	Flexural Strength (MPa)	Flexural Strain @ Max Stress	Flexural Modulus (GPa)
1	140.839	5.000%	3.182
2	138.667	5.002%	3.256
3	154.810	5.001%	3.589
4	141.896	5.001%	3.310
5	149.898	5.000%	3.452
Average	145.222	5.001%	3.358
SD	6.838	0.001%	0.162

PEEK Flat (XY) Flexural Test
120°C Heat Lamp Print

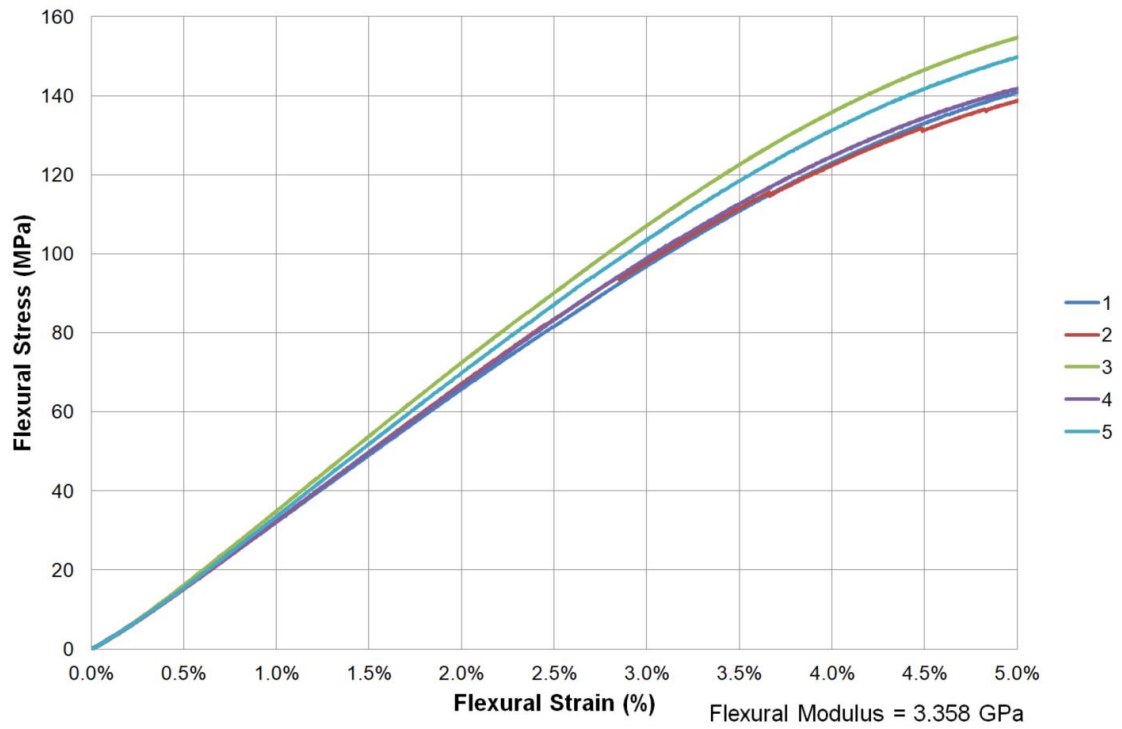


Figure 175. PEEK Flat (XY) Flexural Properties with 120°C Heat Lamp Stress vs. Strain Plot

PEEK on Edge (XZ) Flexural Specimens

Figure 176 shows the PEEK on Edge (XZ) flexural specimens before testing. Table 82 shows the dimension of these specimens. Table 83 shows the flexural properties for flexural strength, flexural strain at maximum stress or 5%, and flexural modulus. Figure 177 shows the stress vs. strain plots.



Figure 176. PEEK on Edge (XZ) Flexural Specimens

Table 82. PEEK Flexural on Edge (XZ) Specimen Dimensions

Specimen	Width (mm)	Thickness (mm)
1	12.471	3.302
2	12.471	3.454
3	12.497	3.429
4	12.471	3.378
5	12.268	3.404
Average	12.436	3.393
SD	0.094	0.058

Table 83. PEEK on Edge (XZ) Flexural Properties with Heat Lamp at 120°C

Specimen ID	Flexural Strength (MPa)	Flexural Strain @ Max Stress	Flexural Modulus (GPa)
1	136.427	5.000%	3.113
2	138.188	5.001%	3.199
3	146.603	5.001%	3.507
4	141.555	5.000%	3.215
5	144.515	5.001%	3.436
Average	141.458	5.001%	3.294
SD	4.238	0.001%	0.169

**PEEK on Edge (XZ) Flexural Test
120°C Heat Lamp Print**

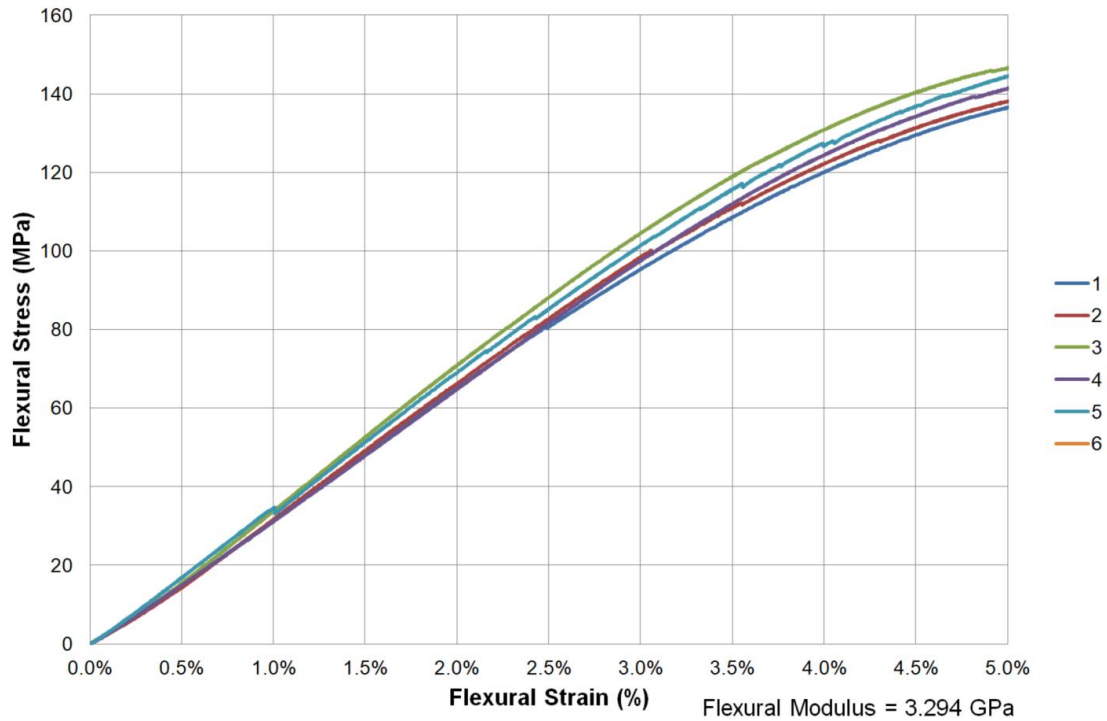


Figure 177. PEEK on Edge (XZ) Flexural Properties with Heat Lamp at 120°C Stress vs. Strain Plot

PEEK Flexural Testing Summary

Table 84 shows the summary of the PEEK flexural specimens with the heat lamp. Table 85 shows the published data for 3DXTech ThermaX PEEK filament. Table 86 shows the published data for South Dakota State University printing PEEK with FFF. Figure 178 shows the summary of the flexural strength compared to 3DXTech and South Dakota State University. The flexural strength is 11% greater and the flexural modulus is 24% greater than South Dakota State University.

Table 84. Flexural Testing Summary PEEK on Lulzbot Taz 5 with 120°C Heat Lamp

Lulzbot Taz 5	Flexural Strength (MPa)	SD (Mpa)	Flexural Strain	Flexural Modulus (GPa)	SD (Gpa)
Flat (XY)	145.222	6.838	No Break	3.358	0.162
On Edge (XZ)	141.458	4.238	No Break	3.294	0.169

Table 85. Published Flexural Testing Data for PEEK 3DXTech Thermax

PEEK 3DXTech Thermax	Flexural Strength (MPa)	SD (Mpa)	Flexural Strain	Flexural Modulus (GPa)	SD (Gpa)
Flat (XY)	130.000	-	No Break	2.700	-

[50]

Table 86. Published Flexural Testing Data for PEEK FFF Printing from South Dakota State University

South Dakota State	Flexural Strength (MPa)	SD (Mpa)	Flexural Strain	Flexural Modulus (GPa)	SD (Gpa)
Flat (XY)	111.670	3.521	No Break	1.919	0.075

[51]

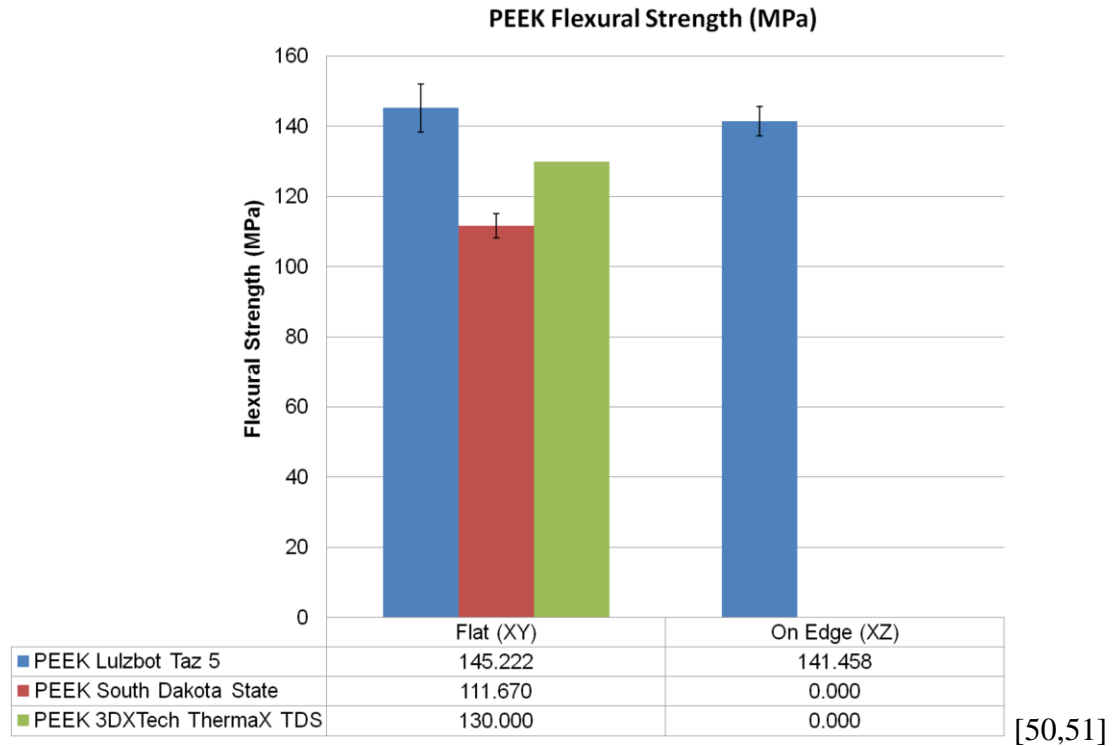


Figure 178. PEEK FFF Flexural Strength Printing with Lulzbot 5 with Heat Lamp at 120°C compared to Published Data

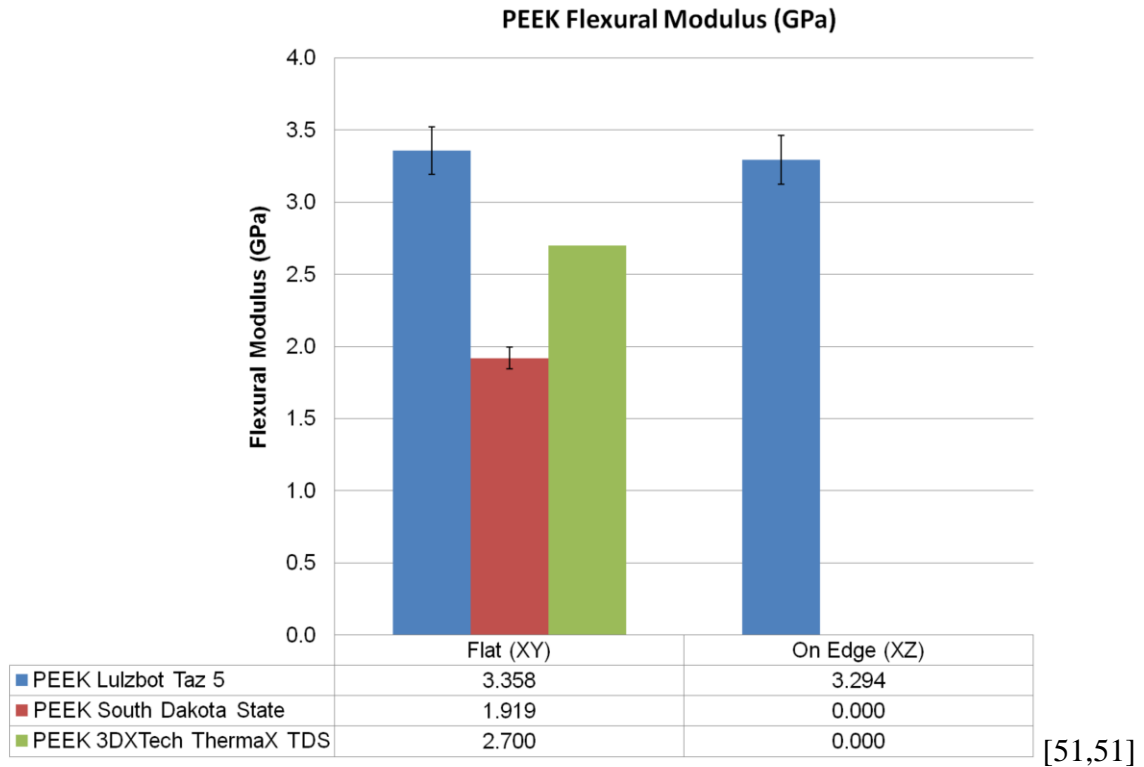


Figure 179. PEEK FFF Flexural Modulus Printing with Lulzbot 5 with Heat Lamp at 120°C compared to Published Data

FFF PEEK with the Heat Lamp at 120°C compared to Injection Molded PEEK

Table 87 shows the comparison of the FFF PEEK printing with the heat lamp at 120°C compared to an isotropic injection molded sample. Figure 180 shows the comparison of the tensile and flexural strength. Figure 181 shows a comparison with the tensile and flexural modulus. The tensile strength of the on Edge (XZ) is similar to injection molding but the Flat (XY) is reduced. The flexural strength are all the same compared to injection molding. The tensile and flexural modulus for the FFF parts are reduced compared to injection molding.

Table 87. Comparison of Injection Molded PEEK to FFF with the Heat Lamp at 120°C

	Tensile Strength (Mpa)	SD (Mpa)	Tensile Modulus (Gpa)	SD (Gpa)	Flexural Strength (Mpa)	SD (Mpa)	Flexural Modulus (Gpa)	SD (Gpa)
PEEK (Injection Mold)	93.000	-	3.790	-	145.000	-	3.790	-
PEEK Flat (XY) 120°C	70.026	13.054	3.484	0.116	145.222	6.838	3.358	0.162
PEEK on Edge (XZ) 120°	95.330	8.528	3.125	0.148	141.458	4.238	3.294	0.169

[49]

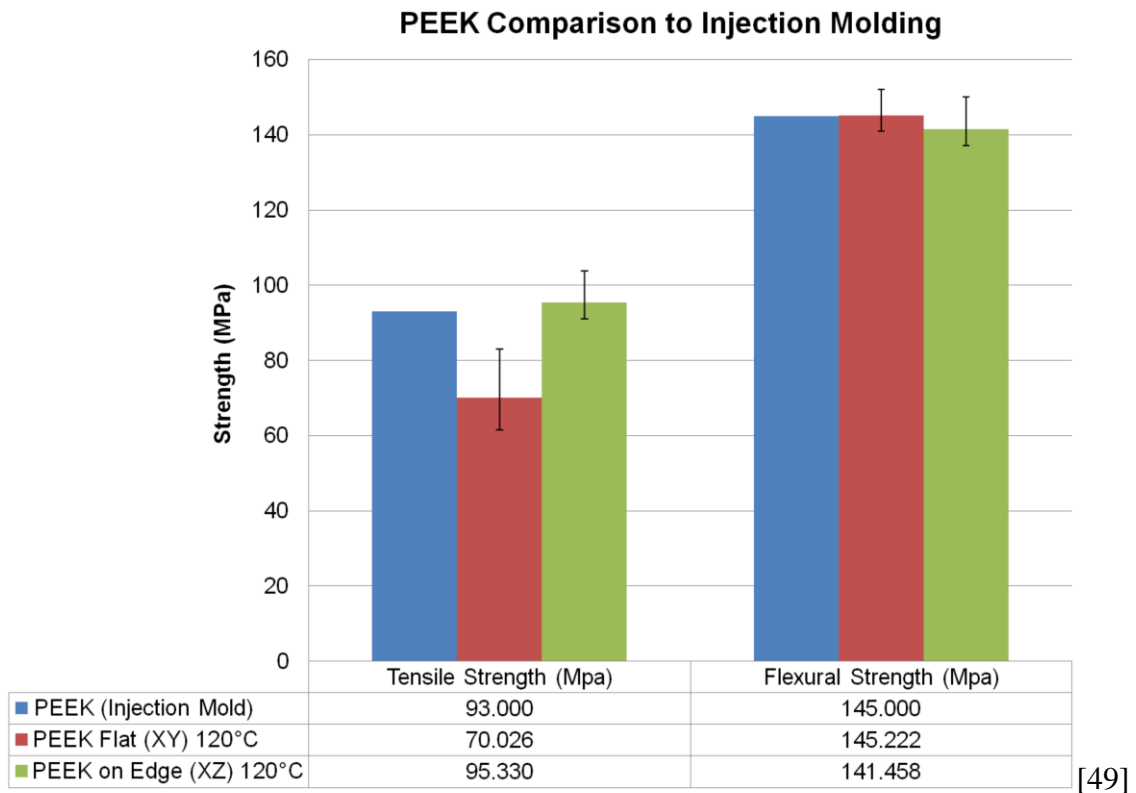


Figure 180. Comparison of Injection Molded PEEK Strength to FFF with the Heat Lamp at 120 °C

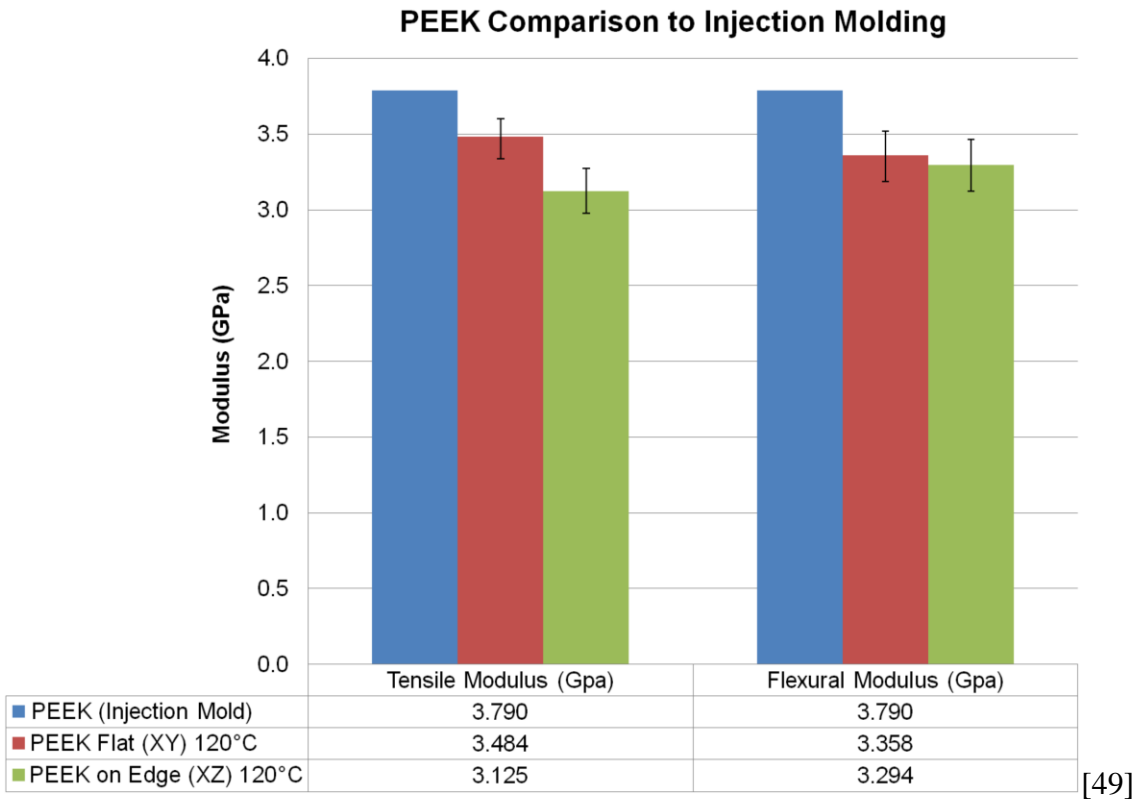


Figure 181. Comparison of Injection Molded PEEK Modulus to FFF with the Heat Lamp at 120 °C

Density and Porosity

ASTM D792-13 “Standard Test Methods for Density and Specific Gravity (Relative Density) of Plastics by Displacement” was used to measure the density and porosity of each of the tensile and flexural specimens [52]. The porosity was calculated by comparing it to the density in the filament form. Figure 182 shows the scale that was used to measure the specimens in air and in water. The density and porosity summary is shown in Table 88 to Table 91.



Figure 182. Measuring the Weight in Water to Calculate Density

Table 88. PLA Density and Porosity

	PLA Density (Filament Density = 1.24 g/cm ³)													
	Upright				On Edge				Flat					
	Flexural		Tensile		Flexural		Tensile		Flexural		Tensile 0°		Tensile ±45°	
	22°C	60°C	22°C	60°C	22°C	60°C	22°C	60°C	22°C	60°C	22°C	60°C	22°C	60°C
Density (g/cm ³)	1.2967	1.2373	1.2437	1.2417	1.2433	1.2437	1.2439	1.2457	1.2188	1.2436	1.1891	1.2388	1.2571	1.2651
SD (g/cm ³)	0.0195	0.0028	0.0022	0.0046	0.0008	0.0003	0.0004	0.0047	0.0030	0.0010	0.0116	0.0029	0.0071	0.0074
Porosity (%)	0.000%	0.219%	0.000%	0.000%	0.000%	0.000%	0.000%	0.000%	1.736%	0.000%	4.276%	0.094%	0.000%	0.000%

[53].

Table 89. PEKK Density and Porosity

	PEKK (Filament Density = 1.27 g/cm ³)						
	Upright		On Edge		Flat		
	Flexural	Tensile	Flexural	Tensile	Flexural	Tensile 0°	Tensile ±45°
Density (g/cm ³)	1.2872	1.2103	1.2845	1.2842	1.2960	1.2881	1.2884
SD (g/cm ³)	0.0048	0.0235	0.0125	0.0041	0.0004	0.0092	0.0124
Porosity (%)	0.000%	4.929%	0.000%	0.000%	0.000%	0.000%	0.000%

[54]

Table 90. PEI Density and Porosity

	PEI (Filament Density = 1.27 g/cm ³)					
	Upright		On Edge		Flat	
	Flexural	Tensile	Flexural	Tensile	Flexural	Tensile 0°
Density (g/cm ³)	1.2474	1.2473	1.2622	1.2807	1.2705	1.2155
SD (g/cm ³)	0.0073	0.0110	0.0036	0.0047	0.0050	0.0265
Porosity (%)	1.809%	1.821%	0.621%	0.000%	0.000%	4.486%

[55]

Table 91. PEEK Density and Porosity

	PEEK (Filament Density = 1.30 g/cm ³)			
	On Edge		Flat	
	Flexural	Tensile	Flexural	Tensile 0°
Density (g/cm ³)	1.3087	1.2925	1.2962	1.2923
SD (g/cm ³)	0.0105	0.0039	0.0095	0.0370
Porosity (%)	0.000%	0.578%	0.294%	0.596%

[56]

Material Property Comparison

A comparison was made of all the materials that were tested for the tensile strength (Figure 183), percent elongation (Figure 184), tensile modulus (Figure 185), flexural strength (Figure 186), and flexural modulus (Figure 187).

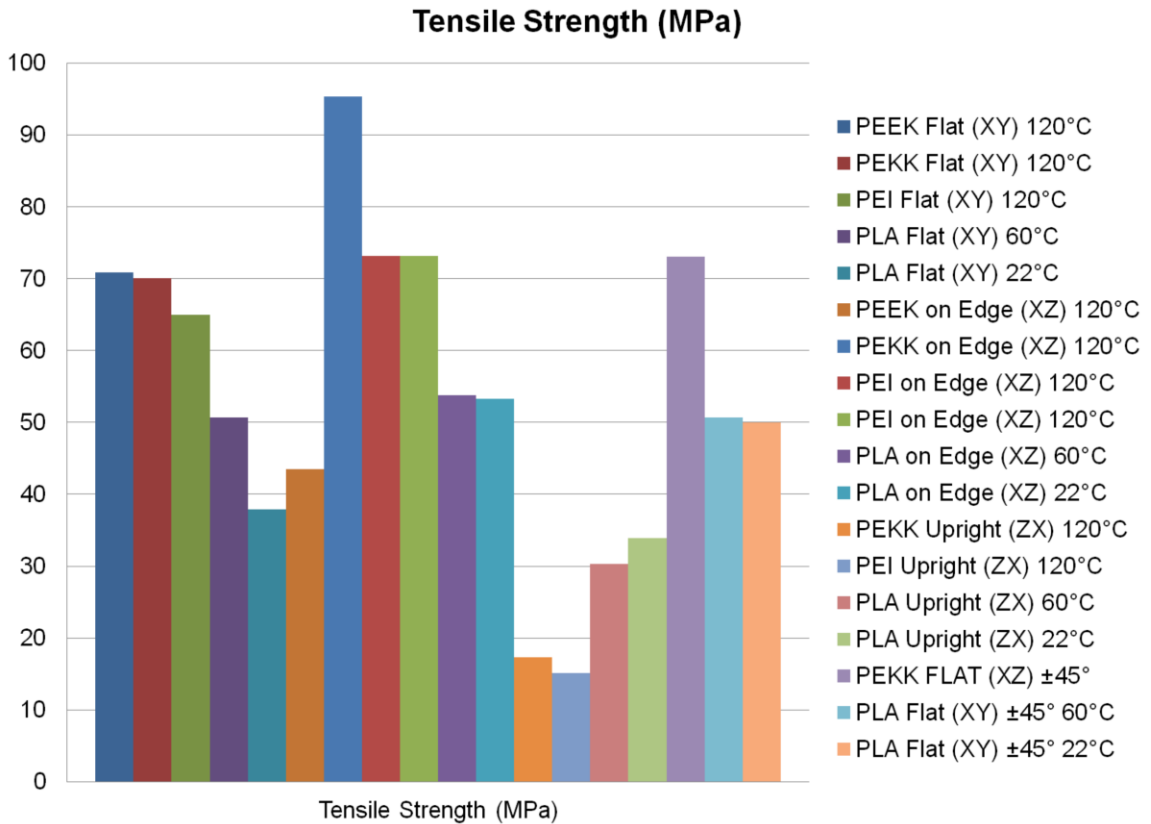


Figure 183. Tensile Testing Comparison

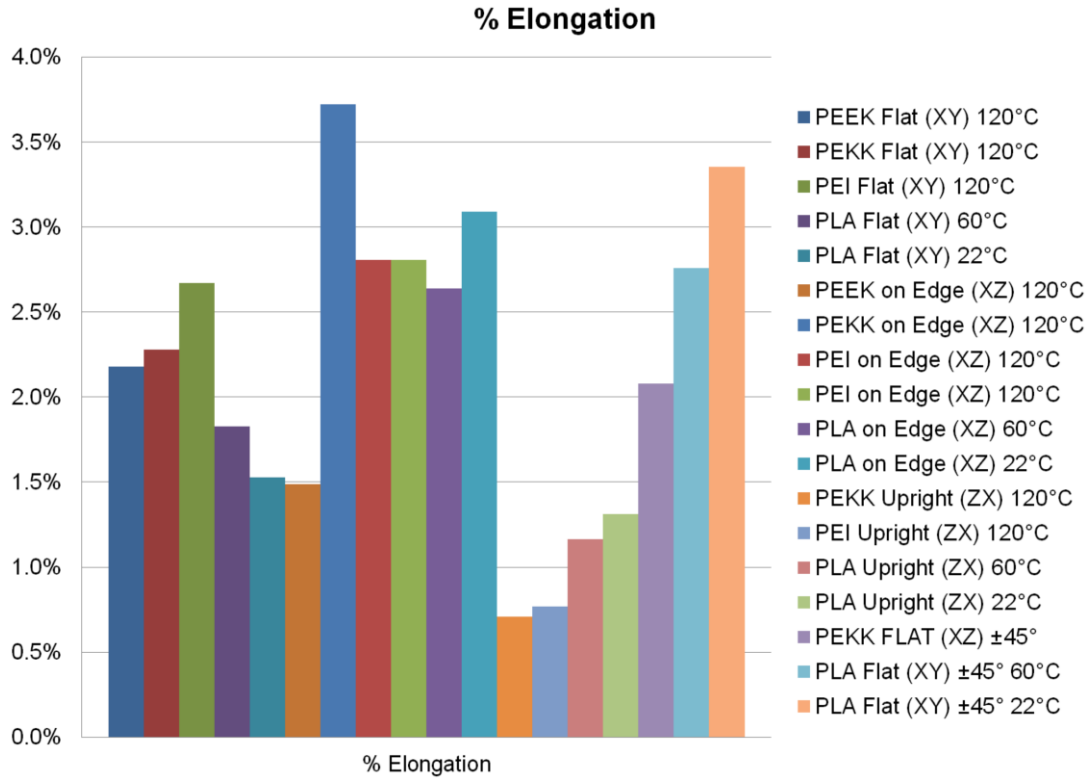


Figure 184. Percent Elongation Comparison

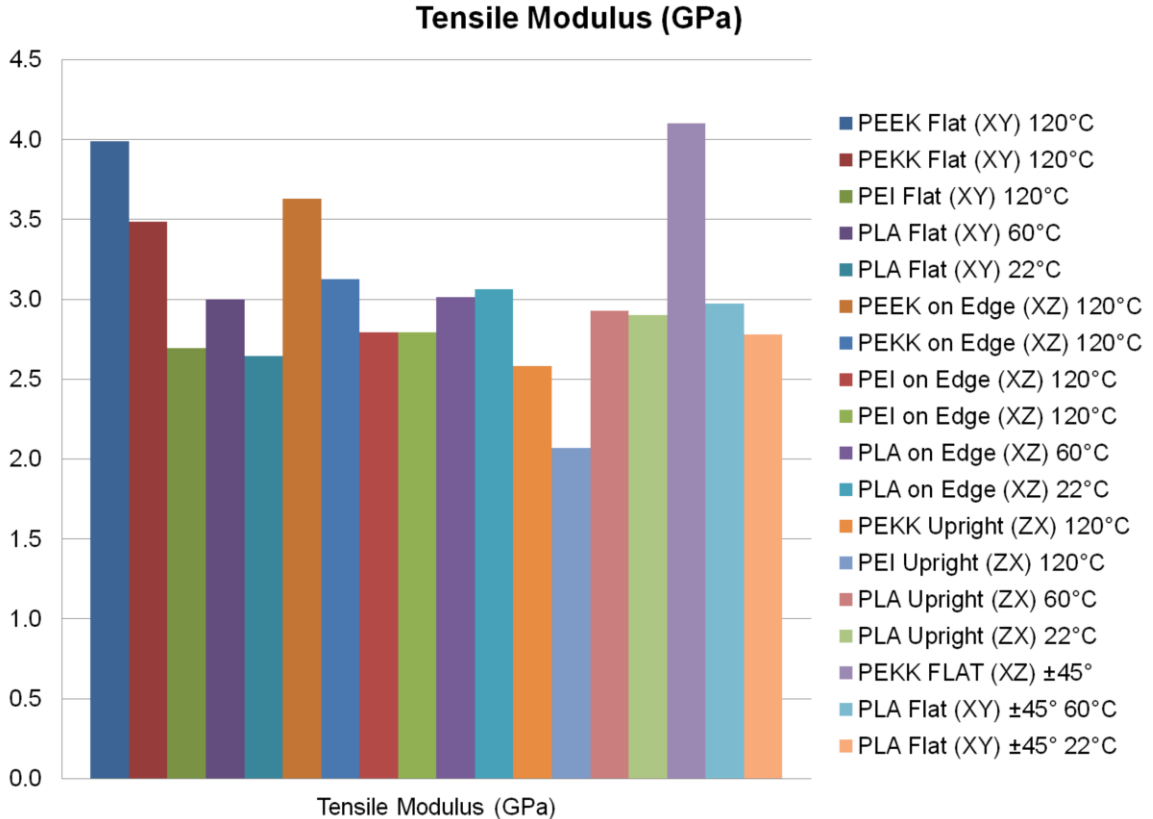


Figure 185. Tensile Modulus Comparison

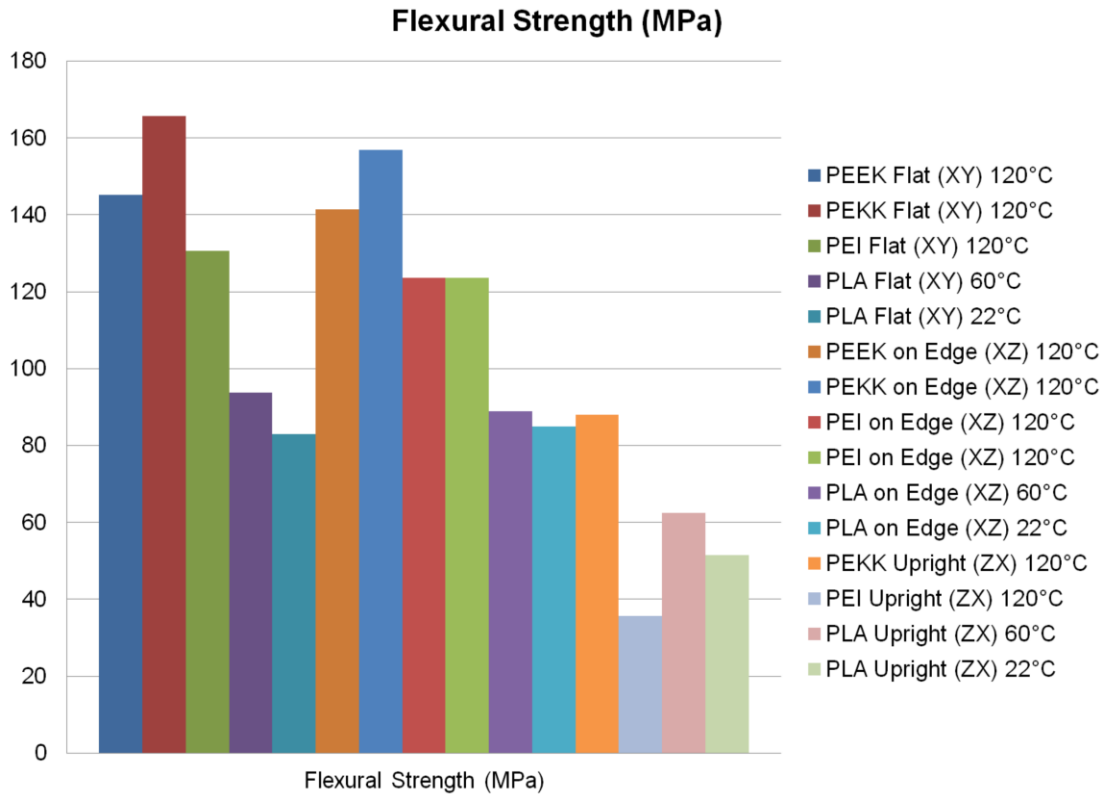


Figure 186. Flexural Strength Comparison

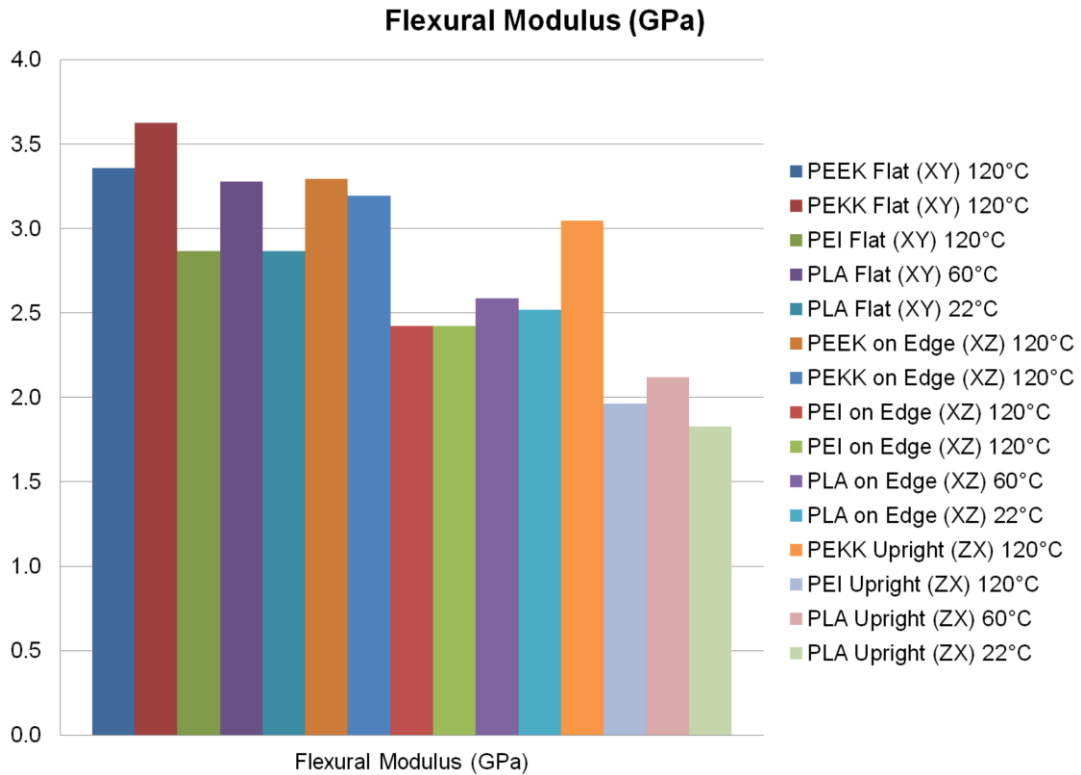


Figure 187. Flexural Modulus Comparison

V. CONCLUSIONS

The goal of this research was to develop and conduct proof-of-principle studies and demonstrations showing how a desktop modified 3D printer can print high temperature polymer material. The investigation used filament materials for (Fused Filament Fabrication) FFF high temperature 3D printing. Testing was performed on 3D printed materials demonstrate the material durability. The goal of developing the desktop 3D printer to print materials equivalent to high end printers was achieved. A second goal was to investigate a pre-deposition heating system (PDHS) using an infrared heat lamp to increasing the part strength in the transverse direction.

A LulzBot Taz 5 3D Printer, which is an open source and customizable 3D printer, was modified to include an enclosure and IR heating lamp to keep the part being printed at a temperature close to the glass transition temperature (T_g) of the polymer filament to eliminate warpage and delaminations between print layers. An E3D-v6 Universal all metal new hot end, 0.8mm nozzle, heat sink, thermal break, and fan shroud was installed that allowed for temperatures above 400°C. The firmware files were modified so the printer could operate successfully at higher temperatures, including adjustments to the maximum hot end and print bed temperatures. Commercial off the shelf high temperature filament materials were investigated. To optimize the new design, test specimens were 3D printed and evaluated against the requirements to test both the printer material and the printer parameters used to fabricate the materials.

The objectives were to characterize the Lulzbot Taz 5 FFF printer and identify the modifications needed to print high temperature materials. Hardware and software changes were required to enable the printing of high temperature materials. 3D printing investigations were conducted to develop the system and analyze the results of the tensile

and flexural properties in the Flat (XY), on Edge (XZ), and Upright (ZX) printing orientations. The material properties were then compared to existing literature of these materials printed with high end printers and with injection molding properties.

A second objective was to characterize the predeposition heating with infrared heat lamp on a lower temperature material to determine if the heating system would improve the mechanical properties. By performing the test with and without the heat lamp on PLA it showed the changes in dimensional accuracy, materials properties, and transverse “Z” direction part strength.

A literature review was conducted to understand the background of the “Z” strength problem and the PDHS that had been used before to try to improve the “Z” strength. The literature review outlined the background of the FFF additive manufacturing process and how the nonisothermal nature results in a reduced “Z” strength. A review of how the thermoplastic welding process relates to the FFF extrusion process was laid out the background for understanding how the parameters in FFF additive manufacturing affect the weld strength. The research into the literature established the requirements for printing high temperature materials using FFF on a desktop Lulzbot Taz 5 printer.

The Lulzbot Taz 5 printer was evaluated in detail on how to modify the system and process to print high temperature materials by using an omega shaped quartz infrared heater as the PDHS that would heat the previous layer before and after the next filament layer was deposited. The research concluded that with the modification detailed in this research a Lulzbot Taz 5 printer can produce parts with high temperature materials by modifying the hot end, print bed, and the addition of a infrared heat lamp. An iterative

process is outline on how to modify the hardware and software to achieve the goal of printing high temperature materials with a desk top Lulzbot Taz 5 printer.

Experiments were conducted to test the effects of this system on tensile and flexural properties in the Flat (XY), on Edge (XZ), and Upright (ZX) orientations as well as maintaining dimensional accuracy. A set of specimens was fabricated for each of these variables and tested using the modified FFF printer. The base thermoplastic resin materials that were investigated were polylactic acid (PLA), polyetheretherketone (PEEK), polyetherketoneketone (PEKK) and polyetherimide (PEI). The modified printer was used to print material property testing specimens to validate the printer design.

PLA properties were compared with and without the infrared heat lamp. The heat lamp showed an improvement in the tensile strength of the Flat (XY) orientation by 33% and an increase in modulus by 13%. The heat lamp showed an improvement in the flexural strength of the Flat (XY) orientation by 13% and an increase in modulus by 14%. The Upright (ZX) flexural strength improved by 21% when using the heat lamp.

When comparing the PLA properties with the heat lamp at 60°C to injection molded PLA the tensile and flexural strength are close to the same in the Flat (XY) and on Edge (XZ) orientations but there is still a significant knockdown for the Upright (ZX) orientation. The tensile modulus for the FFF parts is the same as the injection molding. However there is a significant knockdown for the flexural modulus.

PEKK material property testing was compared to high end Stratasys printers. The tensile strength of on Edge (XZ) is the same as the Stratasys 800 NA. However, the Upright (ZX) tensile strength is greatly reduced. The tensile modulus of on Edge (XZ) and Flat (XY) are similar to the Stratasys 800 NA. However, the Upright (ZX) tensile

modulus is reduced. The on Edge (XZ) percent elongation is comparable but the other two orientations are reduced. The flexural strength of on Edge (XZ) and Flat (XY) show an improvement of 12 to 18% compared to the Stratasys 800 NA. The Upright (ZX) flexural strength is the same as Stratasys. The flexural modulus of on Edge (XZ) is similar to the Stratasys 800 NA. However, the Upright (ZX) flexural modulus shows a slight improvement. The flexural strain is comparable to Stratasys.

When comparing FFF PEKK with the heat lamp at 120°C to injection molded PEKK the tensile strength is close to the same in the Flat (XY) and on Edge (XZ) orientations but there is still a significant knockdown for the Upright (ZX) orientation. The flexural strength shows an improvement in the Flat (XY) and on Edge (XZ) orientations but there is still a significant knockdown for the Upright (ZX) orientation. The tensile and flexural modulus for the FFF parts is the same as the injection molding with a slight improvement in the Flat (XY) orientation.

PEI Ultem 1010 material property testing was also compared to high end Stratasys printers. The tensile strength of on Edge (XZ) is about the same as Stratasys. However, the Upright (ZX) tensile strength is greatly reduced. The tensile modulus of on Edge (XZ) and Flat (XY) are similar to Stratasys. However, the Upright (ZX) tensile modulus is reduced. In all orientations the percent elongation is reduced compared to Stratasys. The flexural strength of on Edge (XZ) and Flat (XY) are similar to the Stratasys. The Upright (ZX) flexural strength significantly reduced compared to Stratasys. The flexural modulus of Flat (XY) and on Edge (XZ) are similar to the Stratasys 800 NA. However, the Upright (ZX) flexural modulus shows a reduced flexural modulus. The flexural strain is reduced compared to Stratasys.

When comparing FFF PEI Ultem 1010 with the heat lamp at 120°C to injection molded PEI the tensile and flexural strength are all reduced compared to injection molding and there is a significant knockdown for the Upright (ZX) orientation. The tensile and flexural modulus for the FFF parts are also reduced compared to injection molding and there is a greater knock down for the Upright (ZX) orientation.

The PEEK test data had to be compared to a technical data sheet from 3DXTech and a paper from South Dakota State University because Stratasys does not offer a PEEK material for printing. The Upright (ZX) orientation could not be printed because of the poor bonding between the layers. The poor bonding between the layers was prevalent in the tensile testing specimens. The tensile strength of on Edge (XZ) is about the same as Flat (XY) data from 3DXTech. However, the Flat (XY) tensile strength is greatly reduced compared to 3DXTech and about the same as South Dakota State University. The tensile modulus of Flat (XY) is similar to 3DXTech. However, the on Edge (XZ) tensile modulus is reduced compared to the Flat (XY) 3DXTech data and greater than South Dakota State University Flat (XY). The percent elongation is a little lower than 3DXTech and significantly lower than South Dakota State University in the Flat (XY) orientation. The flexural strength is 11% greater and the flexural modulus is 24% greater than South Dakota State University.

When comparing FFF PEEK with the heat lamp at 120°C to injection molded PEEK the tensile strength of the on Edge (XZ) is similar to injection molding but the Flat (XY) is reduced. The flexural strength are all the same compared to injection molding. The tensile and flexural modulus for the FFF parts are reduced compared to injection molding.

The testing concluded that the printer modifications were successful in improving the material properties of low temperature PLA and that it gives the functionality to print high temperature materials such as PEKK and PEI. However, the modifications did not improve the “Z” strength anisotropy problem. PEKK was the easiest high temperature material to print and had the better material properties than PEI or PEEK. PEEK was the most difficult material to print. Overall, the material properties were comparable to material printed with a Stratasys printer and to some of the injection molded properties.

Future research is needed to establish an algorithm that can be used to vary the heat coming from the infrared heat lamp at different times. The distance from the heated bed will affect the heat input into the part. The time that the predeposition heater is over the part will also affect the heat input into the part. The time is changed by the speed of the print and the amount of time for the printer to return to the previous location. Future work should explore this opportunity.

LITERATURE CITED

- [1] ISO/ASTM International. (2016). ISO/ASTM 52900:2015(E), Standard terminology for additive manufacturing – General principles – Terminology (ISO/ASTM 52900:2015(E)). Retrieved from <https://compass-astm-org.libproxy.txstate.edu/>
- [2] Hull, C. (1986). U.S. Patent No. 4,575,330. Washington, DC: U.S. Patent and Trademark Office.
- [3] McHugh, M. (2016). Developing capacity to 3D print polyether-ether-ketone using fused filament fabrication (Dissertation). Trinity College Dublin, The University of Dublin. Retrieved from https://pdfkul.com/fffpeekfinal-originalpdf_59d7f9881723ddf891b0fb9e.html
- [4] Ravi, A. K., Deshpande, A., & Hsu, K. H. (2016). An in-process laser localized predeposition heating approach to inter-layer bond strengthening in extrusion based polymer additive manufacturing. *Journal of Manufacturing Processes*, 24, 179-185. doi:10.1016/j.jmapro.2016.08.007
- [5] Crump, S. (1992). U.S. Patent No. 5,121,329. Washington, DC: U.S. Patent and Trademark Office.
- [6] Sweeney, C. B., Zahner, B., Stockton, A., & Teipel, B. (2019). Directed electromagnetic energy applicator for high strength additive manufactured parts. *SAMPE Journal*, 55(5), 18-25.
- [7] Seppala, J. E., Han, S. H., Hillgartner, K. E., Davis, C. S., & Migler, K. B. (2017). Weld formation during material extrusion additive manufacturing. *Soft Matter*, 13(38), 6761-6769. doi:10.1039/c7sm00950j

- [8] Tofangchi, A., Han, P., Izquierdo, J., Iyengar, A., & Hsu, K. (2019). Effect of Ultrasonic Vibration on Interlayer Adhesion in Fused Filament Fabrication 3D Printed ABS. *Polymers*, 11(2), 315. Doi:10.3390/polym11020315
- [9] Turner, B. N., Strong, R., & Gold, S.A. (2014). A review of melt extrusion manufacturing processes: I. Process design and modeling. *Rapid Prototyping Journal*, 20(3), 192-204. doi:10.1108/rpj-01-2013-0012
- [10] Partain, S. C. (2007). Fused deposition modeling with localized pre-deposition heating using forced air (PhD thesis). Montana State University-Bozeman, College of Engineering.
- [11] Harris, M., Potgieter, J., Archer, R., & Arif, K. M. (2019). In-process thermal treatment of polylactic acid in fused deposition modeling. *Materials and Manufacturing Processes*, 34(6), 701-713. doi:10.1080/10426914.2019.1566611
- [12] (n.d.). Retrieved May 18, 2020, from <https://reprap.org/mediawiki/images/2/22/FFF.png>
- [13] Rodriguez, J. F., Thomas, J.P., & Renaud, J.E. (2001) Mechanical behavior of acrylonitrile butadiene styrene (ABS) fused deposition materials. *Experimental investigation. Rapid Prototyping Journal*, 7(3), 148-158. doi:10.1108/13552540110395547
- [14] Morales, N. G., Fleck, T. J., & Rhoads, J. F. (2018). The effect of interlayer cooling on the mechanical properties of components printed via fused deposition. *Additive Manufacturing*, 24, 243-248. doi:10.1016/j.addma.2018.09.001
- [15] Kim, Y. H., & Wool, R. P. (1983). A theory of healing at a polymer-polymer interface. *Macromolecules*, 16(7), 1115-1120. doi:10.1021/ma00241a013

- [16] Gennes, P. G. (1971). Reptation of a polymer chain in the presence of fixed obstacles. *The Journal of Chemical Physics*, 55(2), 572-579.
doi:10.1063/1.1675789
- [17] Ahn, S., Montero, M., Odell, D., Roundy, S., & Wright, P.K. (2002). Anisotropic material properties of fused deposition modeling ABS. *Rapid Prototyping Journal*, 8(4), 248-257. doi:10.1108/13552540210441166
- [18] Yan, Y., Zhang, R., Hong, G., & Yuan, X. (2000). Research on the bonding of material paths in melted extrusion modeling. *Materials & Design*, 21(2), 93-99.
doi:10.1016/s0261-3069(99)00058-8
- [19] Wang, C. C., Lin, T., & Hu, S. (2007). Optimizing the rapid prototyping process by integrating the Taguchi method with the Gray relational analysis. *Rapid Prototyping Journal*, 13(5), 304-315. doi:10.1108/13552540710824814
- [20] Sweeney, C. B., Lackey, B. A., Pospisil, M. J., Achee, T. C., Hicks, V. K., Moran, A. G., Teipel, B. R., Saed, M. A., & Green, M. J. (2017). Welding of 3D-printed carbon nanotube-polymer composites by locally induced microwave heating. *Science Advances*, 3(6), 1-6. doi:10.1126/sciadv.1700262
- [21] Es-Said, O. S., Foyos, J., Noorani, R., Mendelson, M., Marloth, R., & Pregger, B. A. (2000). Effect of layer orientation on mechanical properties of rapid prototyped samples. *Materials and Manufacturing Processes*, 15(1), 107-122.
Doi:10.1080/10426910008912976

- [22] Kishore, V., Ajinjeru, C., & Duty, C. E. (2016). Infrared preheating to enhance interlayer strength of components printed on the big area additive manufacturing (BAAM) system (May 23-26, Long Beach, CA, 1-14). Society for the Advancement of Material and Process Engineering.
- [23] Kishore, V., AjinJeru, C., Nycz, A., Post, B., Lindahl, J., Kunc, V., & Duty, C. (2017). Infrared preheating to improve interlayer strength of big area additive manufacturing (BAAM) components. *Additive Manufacturing*, 14, 7-12.
doi:10.1016/j.addma.2016.11.008
- [24] Sood, A. K., Ohdar, R. K., & Mahapatra, S. S. (2012). Experimental investigation and empirical modeling of FDM process for compressive strength improvement. *Journal of Advanced Research*, 3(1), 81-90. Doi:10.1016/j.jare.2011.05.001
- [25] Li, L., Sun, Q., Bellehumeur, C., & Gu, P. (2002). Investigation of bond formation in FDM Process. *Solid Freeform Fabrication Proceedings* (Vol. 403, pp. 400-407)
- [26] HOMEPAGE | SOLIDWORKS. (n.d.). Retrieved May 3, 2020 from <https://www.solidworks.com/>
- [27] Thingiverse.com. (n.d.). Digital Designs for Physical Objects. Retrieved May 03, 2020, from <https://www.thingiverse.com/>
- [28] YouMagine – Where makers collaborate on 3D designs. (n.d.). Retrieved May 03, 2020, from <https://www.youmagine.com/>
- [29] Cura Lulzbot Edition. (2019, November21). Retrieved May 03, 2020 from <https://www.lulzbot.com/cura>
- [30] (n.d.). Retrieved May 18, 2020, from <https://www.pronterface.com>

- [31] Lulzbot Taz 5 User Manual. (2015). Loveland, CO: Aleph Objects. Retrieved May 03, 2020 from <http://download.lulzbot.com/TAZ/5.0.1/documentation/Manual/Manual.pdf>
- [32] (n.d.). Retrieved May 18, 2020, from https://reprapworld.com/products/extruder/brands/e3d/volcano/e3d_volcano_harden_steel_nozzle_1_20_mm_1_75_mm/
- [33] Ceramic Reflective IR Lamps “Good as Gold”. (n.d.). Retrieved May 18, 2020 from www.andresonthermal.com
- [34] The Omega Infrared Emitter. (n.d.). Retrieved May 18, 2020, from https://www.heraeus.com/media/media/hng/doc_hng/products_and_solutions_1/infrared_emitters_and_systems/omega_infrared_emitter.pdf
- [35] (n.d.). Retrieved May 18, 2020, from https://www.heraeus.com/en/hng/products_and_solutions/infrared_emitters_and_systems/infrared_special_emitters/infrared_special_emitters.html
- [36] Stratasys Materials Testing Procedure (Publication). (2019). Eden Prairie, MN: Stratasys.
- [37] ISO/ASTM International. (2015). ISO/ASTM 638:2014(D), Standard Test Method for Tensile Properties of Plastics (ISO/ASTM 628:20145(D)). Retrieved from <https://compass-astm-org.libproxy.txstate.edu/>
- [38] ISO/ASTM International. (2017). ISO/ASTM 790:2017(D), Standard Test Methods for Flexural Properties of Unreinforced and Reinforced Plastics and Electrical Insulating Materials (ISO/ASTM 790:2017(D)). Retrieved from <https://compass-astm-org.libproxy.txstate.edu/>

- [39] ECOMAX® PLA. (n.d.). Retrieved June 17, 2020, from <https://www.3dxttech.com/general-purpose-filaments/ecomax-pla/>
- [40] Sodergard, A., & Stolt, M. (2002). Properties of lactic acid based polymers and their correlation with composition. *Progress in Polymer Science*, 27(6), 1123-1163. doi:10.1016/s0079-6700(02)00012-6
- [41] ThermaX® PEKK-C. (n.d.). Retrieved May 18, 2020, from <https://www.3dxttech.com/ultra-performance-filaments/thermax-pekk-c/>
- [42] Kepstan by Arkema Technical Data Sheet – 6000 Series. (2013, March). Retrieved May 18, 2020, from <https://www.arkema.com/export/shared/.content/media/downloads/products-documentations/incubator/arkema-kepstan-6000-tds.pdf>
- [43] Stratasys Antero 800NA Data Sheet (Publication). (2020). Eden Prairie, MN: Stratasys.
- [44] ThermaX™ PEI, Made using ULTEM™ 1010. (n.d.). Retrieved May 18, 2020, from <https://www.3dxttech.com/high-performance-filaments/thermax-pe-made-using-ultem-1010/>
- [45] Product Data Sheet & General Processing Conditions RTP 2100 Polyetherimide (PEI). (2005, January 06). Retrieved May 18, 2020 from <http://web.rtpcompany.com/info/data/2100/RTP2100.htm>
- [46] Stratasys Ultem 1010 Resin Data Sheet (Publication). (2020). Eden Prairie, MN: Stratasys.
- [47] ThermaX™ PEEK [NATURAL]. (n.d.). Retrieved May 18, 2020, from <https://www.3dxttech.com/ultra-performance-filaments/thermax-peek-natural/>

- [48] Stocker, S. (2020, June 11). Re: PEEK Annealing [E-mail to the author].
- [49] Product Data Sheet & General Processing Conditions RTP 2200 LF Polyetheretherketone (PEEK). (2005, September 27). Retrieved May 18, 2020 from <http://web RTP company.com/info/data/2200/RTP2200LF.htm>
- [50] 3DXTECH Advanced Materials Technical Data Sheet: ThermaX™ PEEK 3D Printing Filament, TDS Rev 3.0 (Publication). (n.d.).
- [51] Rahman, K. M., Reese, R., & Iletcher, T. (2015). Mechanical properties of additively manufactured PEEK components using fused filament fabrication. Houston, TX: ASME 2015 International Mechanical Engineering Congress Exposition IMECE2015. doi:10.1115/IMECE2015-52209
- [52] ISO/ASTM International. (2013). ISO/ASTM 792:2013(D), Standard Test Methods for Density and Specific Gravity (Relative Density) of Plastics by Displacement (ISO/ASTM 792:2013(D)). Retrieved from <https://compass-astm-org.libproxy.txstate.edu/>
- [53] All About Density of PLA. (2020, February 26). Retrieved July 4, 2020, from <https://all3dp.com/2/pla-density-what-s-the-density-of-pla-filament-plastic/>
- [54] PEKK. (n.d.). Retrieved July 04, 2020, from <https://filament2print.com/gb/advanced/899-pek.html>
- [55] PEI (ULTEM 1010). (n.d.). Retrieved July 04, 2020, from <https://filament2print.com/gb/advanced/892-pei-ultem-1010.html>
- [56] Materials – Large Scale 3D Printing. (n.d.). Retrieved July 4, 2020, from <https://www.cosineadditive.com/en/materials>